Aspects of Dose Optimisation and Diagnostic Efficacy Relating to Dental Cone Beam Computed Tomography

Margarete McGuigan

A thesis submitted to the University of Dublin, Trinity College in fulfilment of the requirements for the degree of Doctor of Philosophy

Division of Oral & Maxillofacial Surgery, Medicine, Pathology & Radiology
School of Dental Science
Trinity College Dublin

2023

Declaration

I declare that this thesis has not been submitted as an exercise for a degree at this or any other University and it is entirely my own work. I agree to deposit this thesis in the University's open access institutional repository or allow the Library to do so on my behalf, subject to Irish Copyright Legislation and Trinity College Library conditions of use and acknowledgement. I consent to the examiner retaining a copy of the thesis beyond the examining period, should they so wish (EU GDPR May 2018).

—————————————

Margarete McGuigan

SUMMARY

The increasing acceptance of cone beam computed technology (CBCT) as a standard form of dental diagnostic imaging is based upon its ability to produce multiplanar cross-sectional ('3-dimensional') images at resolution levels that, while not as high as conventional radiographs, overcomes anatomical overlap and distortions characteristic of two dimensional (2D) radiology. CBCT imaging is achieved at relatively low doses compared with conventional computed tomography (CT). The recent promotion of new hybrid devices incorporating 2D and 3D imaging has increased CBCT use in both the primary dental care setting and specialist practice, not only as a pre-operative diagnostic imaging tool but also for post-operative outcome assessment (e.g. surgical, implant and endodontic). However, extensive persuasive marketing, has largely downplayed concerns of increased patient dose, estimated to be between 10–100 times (small field of view [FOV]) that of a standard periapical radiographic exposure, hence significantly increasing radiation detriment. Therefore, it is essential to understand the image quality (IQ) determinants for CBCT, in order to fully appreciate the potential for dose optimisation, and to facilitate the establishment of low dose strategies for dental applications. This is particularly relevant for tasks deemed to require higher resolution and doses, such as endodontic imaging. In order to balance radiation risk, the potential benefits of CBCT imaging must be verified, which only be achieved by analysing the evidence base on the diagnostic efficacy of CBCT relating to the particular diagnostic task.

The overarching aim of this thesis is to identify a strategy in which radiation dose can be reduced for a specific diagnostic task, while maintaining images of diagnostic quality, and to demonstrate any potential impact of CBCT imaging on treatment outcome for this diagnostic task. Initially, the literature on optimisation and diagnostic efficacy relating to CBCT imaging was reviewed to identify important questions as well as gaps in knowledge in this area. Thereafter, the first study aimed to identify a dose as low as diagnostically acceptable and a threshold level of image quality (IQ) for CBCT imaging of root canal anatomy, using the second mesiobuccal (MB2) canal of extracted maxillary first molars (M1M), of varying complexity. The impact of experience on the diagnostic efficacy of observers was also assessed. Using two CBCT scanners, the aim was also to establish if an objective IQ parameter could act as a transferable IQ metric

in order to simplify the process of optimisation for a diagnostic task. Subsequently, after an exploration of IQ metrics and IQ determinants in the CBCT imaging chain, the second aim was, using regression analysis, to identify the IQ metric(s) that have a statistically significant relationship with successful achievement of the diagnostic task of root canal identification. A further aim was to identify which of these IQ determinants had a statistically significant relationship with achieving this diagnostic task. A final aim of this thesis was, using 3D-printed M1M teeth, to identify if supplemental CBCT imaging could potentially improve outcome after endodontic access cavity preparation in M1Ms. This was achieved by analysing changes in tooth substance removed, procedural time taken and root canals located, in relation to location of the MB2 canal, compared with the use of conventional (intraoral periapical [IOPA]) and clinical methods alone; thereby justifying the increased dose associated with CBCT imaging.

This is the first study to address optimisation of CBCT imaging of root canal anatomy, and it was demonstrated that a similar threshold dose for this diagnostic task could be identified for two scanners. This optimised dose was achieved using standard protocols instead of high resolution scans and applied to simple - moderate MB2 canal complexity. Increasing dose to enhance visualisation of more complex canal anatomy was ineffective. The IQ metric, contrast-noise-ratio (CNR) was not demonstrated to be a transferable measure of IQ for this diagnostic task. Further investigation of the relationship between objective and subjective IQ identified CNR as the significant predictor of successfully achieving the diagnostic task of root canal identification when adjusting for the other evaluated core IQ metrics, using logistic regression. The imaging variables: x-ray tube voltage, x-ray tube current, degree of rotation and native pixel array were demonstrated to have a significant effect on successfully achieving the diagnostic task of root canal identification. In addition, experienced observers significantly increased the likelihood of successfully identifying root canal anatomy. The final "with or without" study using 3D printed teeth, demonstrated that additional preoperative CBCT imaging significantly reduced tooth volume removed, procedural time and increased the number of MB2 canals located for standard anatomies and more experienced operators. Within the limitations of the model, these findings potentially

translate to improved patient outcome for non-surgical endodontics but ideally require validation from a prospective clinical trial.

Acknowledgements

Table of Contents

List of Figures

List of Tables

LIST OF ABBREVIATIONS

3D	Three-dimensional
2D	Two-dimensional
AAE	American Association of Endodontists
AAOMR	American Academy of Oral and Maxillofacial Radiology
AAP	American Academy of Periodontology
AEC	Automatic exposure control
ALADA	As low as diagnostic acceptable
ALADAIP	As low as diagnostically acceptable being indication-oriented and patient specific
ALARA	As low as reasonably achievable
AAOMR	American Academy of Oral and Maxillofacial Radiology
CBCT	Cone beam computed tomography
CCD	Charge-coupled device
CTDI	Computed tomography dose index
CEJ	Cementoenamel junction
CMOS	Complementary metal oxide semiconductor
CNR	Contrast-to-noise ratio
COS	Core outcome set
CSR	Confidence scale rating
CT	Computed tomography
CTDI	CT dose index volume
DA	Diagnostic accuracy
DAP	Dose-area product
DICOM	Digital Imaging and Communications in Medicine
DIMITRA	Dentomaxillofacial paediatric imaging: an investigation towards low-dose radiation induced risks
DMFR	Dentomaxillofacial radiology
DOM	Dental operated microscope
DRL	Dose reference level
E	Effective Dose
EADMFR	European Academy of DentoMaxilloFacial Radiology
EAO	European Association for Osseointegration
ESE	European Society of Endodontology

EURADOS	European Radiation Dosimetry
FGDP	Faculty of General Dental Practice
FPD	Flat panel detector
FOV	Field of view
FWHM	Full width half maximum
GDP	General Dental Practitioner
GSDF	Grey scale display function
Gy	Gray
HPA	Health Protection Agency
H_T	Equivalent dose
IAEA	International Atomic Energy Agency
ICRP	International Commission on Radiological Protection
IOPA	Intraoral periapical
IQ	Image quality
kV	Kilovoltage
LED	Light emitting diode
LNT	Linear non-threshold
LSF	Line spread function
LP/mm	Line pairs per millimetre
M1M	Maxillary first molar
mA	Milliamperage
MAR	Metal artifact reduction
mAs	Tube current exposure - time product
MB2	Second mesio-buccal canal
MEDLINE	Medical Literature Analysis and Retrieval System Online
MeSH	Medical Subject Headings
mGy	Milligray
µGy	Mircogray
Md	Median
MPE	Medical Physics Expert
MPR	Multi-planar reconstruction
MPV	Mean pixels value
MSCT	Multi-Slice Computed Tomography
MTF	Modulation transfer function

NRPB	National Radiological Protection Board
PCD	Peri-cervical dentine
PHE	Public Health England
PMMA	Polymethyl methacrylate
PSF	Point spread function
PSP	Phosphor storage plates
PTFE	Polytetrafluoroethylene
R	Programming language for statistical computing and graphics supported by R Foundation for Statistical Computing
RCT	Randomised controlled trial
ROC	Receiver operating characteristic curve
ROI	Region of interest
SD	Standard deviation
SI	Le système international d'unités
SEDENTEXCT	Safety and Efficacy of a New and Emerging Dental X-ray Modality
SMPTE	Society of Motion £icture and Television Engineers
SPSS	Statistical Package for the Social Sciences
Sv	Sievert
µSv	Microsievert
mSv	Millisievert
TAT	Tooth autotransplantation
TFT	Thin-film transistors
TLD	Thermoluminescent dosimeter
TMJ	Temporomandibular joint
U	Uniformity
UK	United Kingdom
USA	United States of America
W_R	Radiation Weighting Factor
W_T	Tissue Weighting Factor

Chapter 1

Literature review:

Adapted from MCGUIGAN MB, DUNCAN HF, HORNER K: An analysis of effective dose, optimisation and its impact on image quality and diagnostic efficacy relating to dental cone beam computed tomography (CBCT). Swiss Dent J 128(4): 297-316 (2018) PMID: 29589667.

1.1 INTRODUCTION

Since its origins in the 19th century, dentomaxillofacial radiology (DMFR) has relied on 2D imaging, with more recent advancements in radiographic film and digital radiography offering lower doses and faster image production. Conventional 2D radiographs, however, are limited by superimposition, distortion, magnification and misrepresentation of structures (SCARFE & FARMAN 2008) with planar 2D interpretation of the 3D maxillofacial anatomy creating a superimposed image, which prevents optimal visualization due to overlying structures (KILJUNEN ET AL. 2015). The introduction in medicine of computed tomography (CT), later followed by cone beam computed tomography (CBCT) (ROBB 1982) heralded the clinical progression from 2D to 3D images generated by computer enabled reconstruction of the acquired data.

Dental CBCT was introduced commercially in Europe in 1999 (MOZZO ET AL. 1998, ARAI ET AL. 1999) and since its inception has become an increasingly popular imaging modality, with a recent report identifying 203 commercially available CBCT models (from 47 manufacturers) (GAÊTA-ARAUJO ET AL. 2020). Rapid advances in detector technology and computer software systems able to handle large volumes of data have propelled the evolution from initial basic prototypes into faster, more sophisticated imaging tools targeted at specific clinical applications (e.g. small volume scanners used in endodontics: Accuitomo 3D; Morita Corporation, Kyoto, Japan). Furthermore, it is likely that the recent availability of compact and affordable hybrid devices that constitute 87% of all models identified has increased its accessibility and use in a primary dental care setting (GAÊTA-ARAUJO ET AL. 2020). CBCT certainly offers a significant benefit over conventional CT imaging by allowing high resolution 3D visualization of the maxillofacial skeleton with adjustable field of views (FOV) sizes and concomitant reduction in patient dose (SCHULZE ET AL. 2004). This 3D visualization offers a wide range of potential applications within dentistry, primarily aimed at examination of the hard tissues as well as the various sinuses and air cavities of the maxillofacial region (DE VOS ET AL. 2008); however, CBCT appears to be of limited value for soft tissue evaluation due to limited low contrast resolution (SCARFE & FARMAN 2008). Common dental CBCT applications include implant planning, maxillofacial surgery, endodontics and orthodontics (ALAMRI ET AL, 2012); but use must be tempered by the understanding that

the effective dose of CBCT is significantly higher than traditional intra oral periapical radiography (IOPA) and panoramic radiography (ROBERTS ET AL. 2009). CBCT image quality is also limited by a relatively large degree of noise and artefacts on imaging of high density tissues and metal objects due to scatter, beam hardening and photon starvation (SCHULZE ET AL. 2011). Given the explosion of higher dose CBCT imaging in dentistry, there is certainly an evolving need for robust, evidence-based directives and guidelines on selection criteria and specific dose optimisation protocols in key procedures (HORNER ET AL. 2013, HORNER ET AL. 2015). The widespread and increasing use of CBCT in dental practice (DÖLEKOĞLU ET AL. 2011, BERG ET AL. 2014, HOL ET AL. 2015) has raised other concerns, with a shift in reporting responsibilities from radiologists to dentists who may not be appropriately trained to interpret all the structures visible on the CBCT scan (PARASHAR ET AL. 2012). As a result, the European Academy of DMFR (EADMFR) has highlighted the lack of dental undergraduate (and perhaps postgraduate) training in this novel evolving technology and has recommended appropriate training in justification, acquisition and interpretation of CBCT imaging (BROWN ET AL. 2014).

CBCT offers clear advantages in 3D visualisation and diagnostic accuracy (MATZEN ET AL. 2013, ROSEN ET AL 2015), which are reflected in guidelines advocating its use in specific clinical applications (EUROPEAN COMMISSION 2012, AAE & AAOMR 2015, OENNING ET AL. 2018, ESE 2019, MATZEN ET AL. 2019). Notably, questions remain as to what quantifiable impact 3D imaging has in modifying diagnosis, treatment planning and outcome when compared with conventional radiography. As health care professionals, we must consider if the benefit of CBCT imaging outweighs the associated radiation risks for each individual patient and for society.

Consequently, the aims of this review include, understanding radiation risk, which also requires a knowledge of quantification of dose and an appreciation of dosimetry techniques and their limitations. Reduction of this risk through processes of justification and optimisation will be addressed. Primarily, the parameters that can influence CBCT dose will be explored in conjunction with measures and protocols to aid the operator in achieving dose optimisation while investigating what impact this has on image quality for a range of diagnostic tasks. Finally, the impact of CBCT on decision-making and treatment outcome will be accessed and gaps in our knowledge highlighted.

1.2 MATERIALS AND METHODS

This chapter is based on a review published in the Swiss Dental Journal (MCGUIGAN ET AL. 2018). A comprehensive MEDLINE search up to May 2017 was conducted using various medical subject headings (MeSH) in combination with 'and' or 'or'. The major MeSH terms searched were 'Radiography, Dental', 'Tomography, X-Ray' and 'Diagnostic Imaging' and 'Radiographic Image Enhancement' in combination with a series of related subheadings. In addition, the following terms were added 'optimisation' and 'CBCT'. Bibliographies of all relevant papers and previous review articles were hand-searched. Any relevant work published in the English language and presenting pertinent information related to this review was considered for inclusion. Titles were generally excluded if they were conference reports or if aspects of CBCT were discussed that were not the subject of the current review. For the purpose of the thesis, the same MEDLINE search was updated to May 2022 and adaptions made to the text.

1.3 RESULTS

Optimisation is a process for ensuring that the likelihood and magnitude of exposures and the number of individuals exposed are as low as reasonably achievable, with economic, societal and environmental factors taken into account (IAEA 2022). In practical terms, optimisation in CBCT involves quantification of the radiation dose and risk for patients, while assessing the impact on image quality for specific diagnostic tasks. In order to fully consider CBCT optimisation, this review will analyse the literature on dose and risk as well as the impact of optimisation on image quality and diagnostic efficacy of CBCT.

1.3.1 Radiation damage and protection

Each radiological exposure involves interaction of body tissues with ionizing radiation and therefore carries the potential of permanent alteration in cellular DNA with the ultimate risk of latent tumour formation and hereditable effects. This chance happening is described as a stochastic effect, where the magnitude of risk is believed to be proportional to the radiation dose; notably there is no threshold dose below which these effects will not occur (IRCP 2007). Furthermore, risk is sex and age dependent,

being greatest for children (10-year-old, 3x higher risk than 30-year-old) and up to 40% more for females than males (IRCP 1990, EUROPEAN COMMISSION 2012).

Practitioners should be aware of the potential effects of ionizing radiation and understand the increased doses attributable to CBCT imaging, this reinforcing the importance of strict adherence to the IRCP principles of justification and optimisation (IRCP 2007). Indeed, the preliminary process of justification can be the most effective means of dose reduction particularly for young children and adolescents. Guidance documents and position statements provide a framework for selection criteria to ensure CBCT scans are prescribed appropriately, ensuring a net potential benefit to the patient. Therefore, in general, guidelines do not advocate CBCT as a routine imaging tool but only when an alternative reduced dose imaging technique is diagnostically insufficient (HORNER ET AL. 2009, EUROPEAN COMMISSION 2012, DULA ET AL. 2015, FGDP [UK] 2018, ESE 2019); however, routine use of CBCT has been recommended by some (DRAGO & CARPENTIERI 2011, NOFFKE ET AL. 2011) but not all groups in implant dentistry. Valid guideline documents should be extracted from the evidence base rather than relying solely on expert opinion and general consensus; however, a relatively recent review (HORNER ET AL. 2015) identified only two evidence based guidance documents at the time of publication (EUROPEAN COMMISSION 2012, AWMF 2013). This review (HORNER ET AL. 2015) highlighted the need for more rigorous and consistent reporting of guidelines, free of potential bias, facilitated by the use of the AGREE 11 instrument (Appraisal of Guidelines for Research & Evaluation 11). That said, it is recognized that evidence based guidelines can only reflect the validity of the research that exists. The inherent difficulties of achieving studies at higher hierarchical levels of Diagnostic Efficacy are discussed subsequently.

Optimisation of diagnostic medical exposures means, keeping the exposure of patients to the minimum necessary to achieve the desired diagnostic objective (IAEA 2022). Broad guideline documents serve to direct the practitioner in achieving this goal of minimizing patient exposure while achieving the diagnostic information required. Optimisation involves a range of factors, from maintenance and selection of equipment most suited to clinical/imaging needs of patient base, selection of the appropriate exposure and imaging parameters (**Table 1.1**), limitation of the exposed volume, use of shielding devices and establishing diagnostic reference levels (DRL) (HPA 2010, EUROPEAN

COMMISSION 2012). The inherent difficulty of creating a standardized optimisation protocol in CBCT imaging relates to the range of clinical protocols and diversity of available CBCT systems. The clinician's expectation of high resolution and "visually pleasing" CBCT images, perhaps without due consideration of dose implications, has prompted the adoption of a modification of the ALARA principle. The concept of 'as low as diagnostically acceptable' (ALADA) acknowledges the link between dose and image quality and encourages the minimum exposure possible for the specific diagnostic task (WHITE ET AL. 2014). The ALADA principle evolved from the drive to increase radiation protection in paediatric populations associated with the increased awareness of their sensitivity to diagnostic radiation (HALL & BRENNER 2008, THEODORAKOU ET AL. 2012, PAUWELS ET AL. 2014a, WHITE ET AL. 2014, HIDALGO RIVAS ET AL. 2015). This principle has been adapted further to consider the specific diagnostic indication, ALADAIP (As Low as Diagnostically Acceptable being Indication-oriented and Patient-specific [OENNING ET AL. 2018]).

	EXPOSURE AND IMAGE PARAMETERS				
	↑kV	↑mAs	↓FOV	↓Voxel Size	↑No of Projections
Dose	↑	↑	↓	↑ is device dependent	↑
Spatial Resolution	X	X	X	↑	↑
Contrast	↓	X	↑	X	X
Noise	↓	↓	↓	↑	↓
Artefacts	↓ beam hardening	X	↑ truncation artefact	X	X

TABLE 1.1 Effects of exposure and image quality parameters on dose and image quality. ↓: decrease, ↑: increase, X: not affected. This table reports influence of each factor independently but in reality some variables will be inter-related.

1.3.2 What do we understand by patient dose?

Patient dose monitoring is an essential part of quality assurance (QA) to ensure doses are kept as low as reasonably achievable and allow comparison to DRLs (EUROPEAN COMMISSION 2004). DRLs do not indicate the desired dose level for a specific diagnostic task but instead define a reference dose or threshold above which operators should investigate the potential for dose reduction measures (YU ET AL. 2009). Dosimetry is also essential to study the radiation–induced risk of different types of diagnostic imaging examinations enabling comparison of imaging modalities/devices which can influence directives on justification and dose reduction strategies.

Absorbed dose (D_T), describes the amount of energy absorbed from the radiation beam per unit mass at a site of interest. The SI unit for this is the gray (Gy) representing one joule per kilogramme but the milligray (mGy) is more appropriate in the context of diagnostic imaging (WHITE & PHAROAH 2013). Although useful for quality control purposes (IRCP 2007), radiation absorbed dose gives no indication of stochastic

risk. A complicating factor when considering 'dose' of radiation is that different types of radiation have different biological effectiveness, in terms of their potential to cause damage. Particulate radiation (high-energy protons, neutrons, alpha particles) cause greater damage than X-rays. Thus an absorbed dose of 1 mGy from X-rays would give less damage to tissues than 1 mGy from high energy proton radiation. The differing radiobiological effectiveness of different types of radiation is taken into account by attributing a radiation weighting factor (W_R) to the absorbed dose, resulting in the concept of equivalent dose (H_T), which can be calculated as: D_T x radiation weighting factor (W_R). Fortunately, the W_R of X-rays is 1, but the SI unit of equivalent dose is changed from the Gy to the sievert (Sv).

Effective dose (E) (recommended by The International Commission on Radiological Protection (IRCP 2007) is a more relevant index when considering patient dose. It enables a measure of radiation risk from different exposures of ionizing radiation to various body tissues/organs which exhibit a range of radiosensitivities. Specifically, it is calculated as a product of the equivalent doses to the irradiated tissues and the tissue weighting factor (W_T) (which reflects the degree of sensitivity of each of the tissues to radiation and relative contribution to overall risk). These weighted doses are then summed to deliver the effective dose, which is typically expressed in millisieverts (mSv) or microsieverts (µSv). $E = \sum W_T \times H_T$. Importantly, effective dose allows an approximate comparison of radiation–induced risk among different types of examinations. Thus, it becomes possible to compare the radiation-associated risk of, for example, an intraoral radiograph with a chest radiograph or a CT scan of the abdomen.

The most recent tissue weighting factors are provided by the IRCP (IRCP 2007) which revised the existing figures from 1990 (IRCP 1990). Particularly relevant to dental imaging, new tissue weighting factors for salivary glands, oral mucosa, lymph nodes and brain were included (EUROPEAN COMMISSION 2012). This updating of tissue weighting factors results in a 10% increase in the weighting ascribed to tissues located in the maxillofacial region. Being a relatively recent imaging modality, most CBCT dosimetry research studies have used the updated tissue weighting factors but, along with the variation in CBCT device parameters, it is worth considering these issues when comparing dose estimations from different studies.

1.3.3 How is dose quantified?

In order to compare radiation risk between different types of examination, effective dose is considered the most appropriate metric. Since effective dose cannot be measured directly in vivo, it is only possible to quantify it in laboratory studies or by computer modelling. Traditionally, ascertaining the dosimetry necessary for the calculation of effective dose involved the use of anthropomorphic phantoms constructed from materials that have comparable X-ray attenuation characteristics to human tissue. Multiple thermoluminescent dosimeters (TLDs) are distributed throughout the phantom (position dependent on tissues to be evaluated) to allow for accurate measurement of absorbed dose. Notably, no standards have been set as to the number or locations of the TLDs, often leading to low reproducibility of this technique (LUDLOW ET AL. 2006, PAUWELS ET AL. 2012a, LUDLOW ET AL. 2015). This fact, compounded by the use of a range of phantoms have resulted in studies that are not readily comparable and highlights the need for standardized method of dose measurements to enable comparison between studies (PAUWELS ET AL. 2012a).

Computed dose simulations using virtual phantoms have been developed. These virtual phantoms potentially negate the need for the laborious task of repeated dosimetry on standard adult or paediatric phantoms, which do not allow for consideration of population variation in size (KOIVISTO ET AL. 2012, MORANT ET AL. 2013, ALJAWHARA ET AL. 2020). This technique allows simulation of the interaction of radiation with matter and provides a quick way of modelling the multitude of potential variations within imaging systems and patients. It has been widely used in radiotherapy dosimetry but has also been used in a small number of dental CBCT studies (STRATIS ET AL. 2016, EZELDEEN ET AL. 2017, MARCU ET AL. 2018, OENNING ET AL. 2019). Appraisal of the use of virtual phantoms with Monte Carlo simulation of exposure, as a dependable replacement for anthropomorphic phantoms, suggests that further development of virtual phantoms is necessary (ZHANG ET AL. 2013).

Neither laboratory studies using phantoms nor complex computer modelling, have direct use in clinical situations. For measuring dose in clinical facilities, particularly for dose audits, alternative measures are needed from which effective dose can be estimated. In the context of dental CBCT, examples of these include dose area product (DAP), also known as kerma area product (KAP). This is a simple, less laborious

technique for indirectly estimating effective dose. DAP is defined as the air collision kerma integrated over the beam area. It can be measured using a DAP meter (calibrated ionisation chamber that measures dose and beam size at a fixed point). Additionally, DAP can be available via machine output data (determined computationally, based on the x-ray tube output and field size settings), however these data can be unreliable and calibration is required (AL-OKSHI ET AL. 2017). Measured DAP values can then be converted to effective dose using conversion factors (KIM ET AL. 2014, MAH ET AL. 2021). There are conflicting opinions as to the accuracy of this dose index in the calculation of effective dose. DAP has been recommended for establishing achievable doses and, possibly, diagnostic reference levels and is described as relating 'reasonably well' with effective dose (HOLROYD & WALKER 2010, EUROPEAN COMMISSION 2012). However, the central point of the scan is not always in the centre of the clinical area of interest and patient dose measurements could be either underestimated or overestimated. It has been demonstrated that within a small field of view (FOV), although effective doses exhibited a three-fold change over three separate locations, DAP remained unchanged (LUDLOW 2009). Additionally, an average of 35% absolute error in calculation of the effective dose resulted when using DAP, even when using conversion factors specific for FOV size, arch location and patient type (KIM ET AL. 2014). Furthermore, it was concluded that since imaging factors (FOV size and positioning) govern the actual distribution of dose throughout the patient, generally it would not be possible to link DAP values to patient effective doses (PAUWELS ET AL. 2012a). Accepting its limitations (LARSSON ET AL. 1996, LUDLOW & IVANOVIC 2008) and being aware that its precision as a measure of risk is questionable (LUDLOW ET AL. 2015), it was reported that DAP could be used to assess dose reduction strategies and compare the results from different CBCT units (LOFTHAG-HANSEN 2010, GOULSTON ET AL. 2016). Furthermore, according to the ICRP recommendations (ICRP, 2015), effective dose quantity (mSv), is not the dose descriptor of choice in CBCT dosimetry due to the wide variation in conversion factors.

Interestingly, use of dose height product (DHP) in place of area resulted in statistically improved accuracy in the estimation of effective dose, with a reduction in absolute error to 19% from 35% evidenced with DAP (LUDLOW ET AL. 2015). Ludlow theorized that DHP may correlate more with effective dose than DAP due to the nature of the vertical distribution of radiosensitive organs. Therefore, an increase in height of

the FOV results in new and potentially radiosensitive tissues being brought into the area of direct exposure, while an increase in beam width, merely results in an increased dose to tissues that are already being exposed. It was concluded that the use of DHP as a means of estimating effective dose merits further investigation (LUDLOW ET AL. 2015). CT dose index volume (CTDI) is the international assessment metric used to measure the radiation output of CT scanners. Studies have revealed that CTDI measurement methodology does not accommodate the cone shaped beam of CBCT and the larger FOVs (MORI ET AL. 2005).

It has been established that owing to its unique exposure geometry (eliciting a dose distribution which can be asymmetrical and exhibits a strong dose gradient outside the primary beam), CBCT requires a specific dose index that copes with differences in FOV, diameter, positioning and varying degrees of rotation arc (PAUWELS ET AL. 2012c). Alternative dose indices have been explored by the SEDENTEXCT team but further work is necessary to establish if such indices are appropriate for establishing DRLs (EUROPEAN COMMISSION 2012).

1.3.4 What are the reported CBCT doses and how does it compare with conventional radiography?

The effective dose ranges quoted for CBCT reflect the range of devices and imaging protocols (collimation of the cone beam, detectors, exposure factors, image quality parameters), in addition to the location of the radiation field with respect to the radiosensitive organs, which leads to a considerable difference in absorbed dose for all organs in the head and neck region (PAUWELS ET AL. 2012a, THEODORAKOU ET AL. 2012, BORNSTEIN ET AL. 2014, PAUWELS ET AL. 2014a, LUDLOW ET AL. 2015, ALJAWHARA ET AL. 2020). As a result of this diversity between devices it is not possible in the field of CBCT to establish a single average effective dose when making comparisons to conventional 2D radiography and multi-slice CT (MSCT) (PAUWELS ET AL. 2012a). Effective dose for CBCT has been quoted in tens to several hundred µSv, demonstrating a twenty-fold range (EUROPEAN COMMISSION 2012, PAUWELS ET AL. 2012a, PAUWELS ET AL. 2014a, LUDLOW ET AL. 2015). If effective dose calculations are categorised by FOV size (**Section 1.3.3**), dose ranges have been demonstrated using a broad selection of devices as: small FOV: 19-44 µSv, medium FOV: 28-265 µSv and large FOV: 68-368 µSv (PAUWELS ET AL. 2012a, AL-OKSHI

ET AL. 2021). These figures clearly demonstrate the impact of FOV size of which FOV height is believed to be the key determinant of effective dose (PAUWELS ET AL. 2014a). An intraoral periapical radiograph (IOPA) effective dose is quoted as less than 1.5 µSv when morantall parameters are fully optimized (LUDLOW ET AL. 2008). Reported effective dose ranges for panoramic radiography are 2.7-24.3 µSv and less than 6 µSv for cephalometric radiography (EUROPEAN COMMISSION 2012), this confirming the fact that radiation dose and risk is considerably greater for CBCT than conventional radiography. It is generally accepted that effective doses for CBCT are well below those for common MSCT protocols, with a range of dose being reported as 280-1410 µSv (EUROPEAN COMMISSION 2012). However, CBCT images with a large FOV and high exposure factors can have comparable dose ranges with low-dose MSCT protocols (LOUBELE ET AL. 2009, SUOMALAINEN ET AL. 2009, KYRIACAOU ET AL. 2011, ALJAWHARA ET AL. 2020).

The effective dose from a dental CBCT exposure is mainly defined by the absorbed dose of the remainder organs (38%), salivary glands (25%), thyroid gland (19%) and red bone marrow (14%) (MORANT ET AL. 2013). If the effective dose of a small FOV upper anterior scan (19 µSv) is compared with a lower molar scan (40 µSv), the observed difference in effective dose can be attributed to the increased absorbed dose, particularly of the salivary glands and thyroid gland associated with a mandibular scan (PAUWELS ET AL. 2012a). This variation clearly demonstrates the impact of FOV position relative to the radiosensitive organs on patient dose.

When appropriate child settings are selected, effective doses for children and adolescents (measured in paediatric and adolescent phantoms) have been reported as similar to effective doses measured in adult phantoms; the lowest effective doses reported resulted from small FOV and 'small patient' settings (THEODORAKOU ET AL. 2012). In the paediatric phantom, equal contributions to effective dose come from the remainder organs, salivary and thyroid glands. Other studies have reported that where imaging protocols remained constant (adult setting), the highest absorbed dose was measured in all locations in the small child phantom and the lowest in the adult phantom which attenuated more radiation due to its increased diameter (AL NAJJAR ET AL. 2013, CHOI & FORD 2015). An increasing number of paediatric CBCT scans are being performed with indications including impacted teeth, orthodontics and dentomaxillofacial development, highlighting the need for appropriate justification and

dedicated paediatric protocols optimized for the imaging task (CHOI & FORD 2015, HIDALGO RIVAS ET AL. 2015).

1.3.5 Risk considerations related to CBCT

Effective dose was developed for use in radiation protection to provide a measure of overall risk of stochastic effects from diagnostic radiation exposure. However, with regards to CBCT imaging, it is generally measured in a standard phantom, estimating risk for an average sized adult reference patient. This does not reflect the risk of the individual patient who varies in size and mass with a concomitant variation in dose (MARINE ET AL. 2010, CASSOLA ET AL. 2011). This has implications particularly for children, being physically smaller, with more tissue (e.g. brain and thyroid now closer to dental area) in the primary beam and subject to scatter radiation; therefore, absorbed dose to the head and neck regions will be higher if appropriate 'child settings' are not used (BORISIVA ET AL. 2008, THEODORAKU ET AL. 2012, AL NAJJAR ET AL. 2013). Furthermore, this increased risk is compounded by age (owing to their larger proportion of dividing cells and a longer remaining lifespan to express stochastic effects) and gender sensitivity (female risk > male risk) to potential stochastic effects from radiation (IRCP 1990). It was concluded that since effective dose is not individual-specific, it is not a suitable quantity for individual patient risk estimation but is considered a useful indicator of relative risk when comparing a range of examination protocols or differing imaging modalities (LUDLOW ET AL. 2015). Interestingly, a method to estimate patient-specific dose and cancer risk from CT examinations has been developed by combining a validated Monte Carlo program with patient-specific anatomical models (LI ET AL. 2011).

There is continuing debate about the level of risk associated with diagnostic imaging and the validity of the linear-no-threshold model (LNT) of extrapolating cancer risk from higher doses to lower levels of exposure (IRCP 2007, TUBIANA ET AL. 2009). The uncertainty lies with the inherent limitations associated with the studies available for risk analysis of low doses (PAUWELS ET AL. 2014a). Such data includes the Life Span Study of atomic bomb survivors, which serves as a model for determining cancer risk for low doses (PRESTON ET AL. 2007). Additionally, epidemiological studies on the cancer risk of CT scan exposures to the maxillofacial region suggest that increased risks associated with doses applicable to CT are not hypothetical and are independent of extrapolations

and modelling. These studies have demonstrated a significant increase in brain cancer and leukaemia among the scanned subjects, the increased incidence being associated with increasing dose and young age at the time of exposure (PEARCE ET AL. 2012, MATTHEWS ET AL. 2013). These studies support the LNT hypothesis of a proportional increase in cancer risk and heritable defects concomitant with any exposure of radiation above zero. Of note, other dose-risk models exist which are diverse from the LNT hypothesis (e.g. radiation hormesis and supra-linear models) while others adhere to the principles of the LNT hypotheses while involving a dose-rate effectiveness factor (DDREF) to compensate for the potentially lower biological effectiveness of low doses. However current literature appears to support the LNT hypothesis (IRCP 2007, BARRET ET AL. 2015).

When considering risk specifically associated with CBCT, it has been estimated that the lifetime attributable risk (LAR) for cancer induction is between 2.7 and 9.8 per million examinations (PAUWELS ET AL. 2014a). Children exhibit the highest cancer risk in this spectrum due to their increased radiosensitivity, which highlights the importance of an understanding of this increased risk by operators and referrers and implementation of a more rigorous application of the ALARA principle (HORNER ET AL. 2009). These LAR figures were calculated by applying established correlation factors (PAUWELS 2012a & 2012b) to measured skin doses on patients receiving CBCT scans to estimate patient organ dose. Individual effective dose was then calculated using tissue weighting factors (IRCP 2007). Finally, lifetime attributable cancer risk was calculated from gender and age specific risk factors reported in the Biological Effects of Ionizing Radiation (BEIR) V11 report (National Research Council of the National Academies 2006).

1.3.6 Technical and imaging parameters that influence dose optimisation

The technical principles and details of CBCT design have been reviewed in detail (SCARFE & FARMAN 2008, NEMTOI ET AL. 2013, KILJUNEN ET AL. 2015, PAUWELS ET AL. 2015a, KAASALAINEN ET AL. 2021). The aim of the current review is to analyse the manner in which technical specifications, optimum selection of exposure and image quality parameters can minimize radiation and risk to the patient, while maintaining image quality and diagnostic accuracy. This aim adheres to the principle of optimisation stipulated by the IRCP (IRCP 2007).

CBCT imaging is accomplished using a rotating gantry (similar to a panoramic system) to which an x-ray source and opposing detector are fixed in a c-shaped arm arrangement (PAUWELS ET AL. 2015a). Scanning can be performed in a standing (most common but susceptible to patient movement), sitting or supine position (space-demanding) according to device design or patient requirements. Each unit has a device specific stabilization method to minimise patient motion which can degrade image quality (DONALDSON ET AL. 2013, SPIN-NETO & WENZEL 2016). The fundamental principle of x-ray production is similar for two- and three- dimensional imaging modalities, the x-ray tubes differing mainly in the size of the exit window (i.e. collimation), the range of exposure factors and the amount of beam filtration (PAUWELS ET AL. 2015a). Dental CBCT utilizes a cone- or pyramid-shaped X-ray beam, which is directed at the required FOV, the X-ray source and detector rotating around a rotation fulcrum fixed within the centre of the region of interest. Rotation times range most commonly between 10 and 40 seconds, during which the X-ray exposures (at certain degree intervals) result in several hundred 2D projections (raw data) being acquired by the detector. These images have been described as similar to lateral and posterior-anterior cephalometric images, each slightly offset from the other (SCARFE & FARMAN 2008). Only one rotation sequence is required to acquire sufficient data for image reconstruction as the beam incorporates the entire FOV. This differs from medical CT which uses a fan shaped beam in a helical movement and acquires only individual slices of the FOV at a time (**Figure 1.1**).

1.3.7 Exposure settings

Assuming all other scan factors remain equal, the dose associated with each CBCT scan is determined by tube operating potential ('voltage'), measured in kilovolts (kV), and tube current-exposure time product, measured in milliampere.seconds (mAs). These parameters are initially determined by the manufacturer, perhaps with an emphasis on delivering images of high quality rather than dose optimisation. Some CBCT models have pre-set exposure settings for differing clinical applications (e.g. endodontic mode) and for patients of different sizes, thus enabling a degree of dose and image optimisation. Other devices enable the operator to select the kV, mA and exposure time within a specified range allowing the user the possibility of reducing dose for a smaller patient/child or for a particular diagnostic task. This necessitates operator knowledge

and experience and demands evidence-based guidance regarding the impact of exposure parameters on image quality for specific diagnostic tasks. Collaboration of the clinician with a medical physicist and engineer can facilitate further optimisation. The use of automatic exposure control (AEC) has been introduced to a limited degree in CBCT imaging. The aim of AEC is to automatically modify the tube current to accommodate attenuation differences due to patient size, shape and anatomy, for example when the mAs is varied depending on the density distribution of a scout image (KALENDER ET AL. 1999). In CT, AEC has been found to lead to a significant dose reduction and could negate the need to manually adapt the kV and mA according to patient size (PAPADAKIS ET AL. 2008). However, a recent European Radiation Dosimetry (EURADOS) working group survey confirmed that AEC in dental CBCT imaging is generally not used or available across the responding surveyed sites (SIISKONEN ET AL. 2021).

1.3.7.1 Current-exposure time product

For the CBCT devices currently available, tube current ranges from 1-120 mA but tube current values typically selected for 3D imaging are 2-15 mA (KAASALAINEN ET AL. 2021). Both the tube current and exposure time (seconds) determines the quantity of X-ray photons produced which reach the detector. When other exposure factors are kept constant, a linear relationship exists between current exposure-time product (mAs) and patient dose i.e. increasing mAs causes a proportional increase in dose. With regards to image quality, an increased mAs decreases image noise by increasing signal at the detector but, since the beam penetration remains the same, contrast is unaffected.

1.3.7.2 Tube voltage

Typical tube voltages in existing CBCT scanners vary most commonly between 60-90 kV (full range 50-120 kV), the full range often reflecting the options available for 2D imaging in hybrid devices, this being the case for tube current also (KAASALAINEN ET AL. 2021). As tube voltage increases, the mean energy/penetrating power but also the quantity of the photons in an X-ray beam increases and, overall, radiation dose is increased (other factors being constant). However, unlike current exposure-time product the relationship between tube voltage and dose is not linear. Higher kV values increase the detector signal due to the increased photon count and a decreased

absorption ratio. In respect to image quality, at a higher kV the difference in X-ray attenuation between tissues of differing density is decreased, which can result in a decreased image contrast (**Table 1.2**). Conversely, a lower kV can lead to increased image contrast with regards to the hard tissue of maxillofacial region (DRAGE ET AL. 2010). However, this dynamic of increased contrast at lower beam energies is not fully translatable to CBCT due to the complementary information of projectional data from many angles (PAUWELS ET AL. 2014b). Nevertheless, there is the potential to decrease the voltage and thus dose while maintaining image contrast, which is especially pertinent for smaller patients/children where less penetrating X-rays (80 kV or less) are required (YU ET AL. 2009). A reduced kV is associated with increased noise; however, the compensating effect of better contrast maintains the contrast-to-noise ratio (CNR) (KARMAZYN ET AL. 2013). With the greater attenuation associated with larger patients and accompanying increase in noise, a greater tube voltage has been recommended (SEIGEL ET AL. 2004).

Certainly, optimisation by kV and mA reduction below the manufacturer's recommendations has been investigated with maintenance of image quality (objective and subjective), facilitating diagnostic accuracy and significant dose reductions (**Table 1.3, Fig. 1.1**). Unfortunately, the effect of changing one or both of the exposure factors is not straightforward. An objective image quality study recommended that a low dose protocol should constitute reduction of the tube current-exposure time product (depending on the clinical application), while keeping the tube voltage constant at 90 kV (highest kV in device studied) as this achieved the highest CNR at low dose levels (PAUWELS ET AL. 2015b). The inference of Pauwel's study (2015b) being that the increase in noise for a given mAs reduction would be less than that seen with kV reduction. Later studies by the same group have suggested identifying the optimal tube voltage for a given diagnostic task and subsequently determining the minimally acceptable current-time exposure product, employing the use of fast-scan modes (PANMEKIATE ET AL. 2018). However, another study (same CBCT scanner used), assessing image quality relating to the anterior maxilla in a paediatric skull phantom, found that dose reductions (50% less than manufacturer's recommendations) could be achieved with a reduction in X-ray tube voltage (80 kV) and indeed for a range of combinations of kV and mAs (HIDALGO RIVAS ET AL. 2015). Optimizing kV and mAs settings is difficult and involves appropriate

balancing, where sufficient image quality is achieved dependent on imaging task at the lowest dose possible and the need for more studies in this area has been highlighted (EUROPEAN COMMISSION 2012).
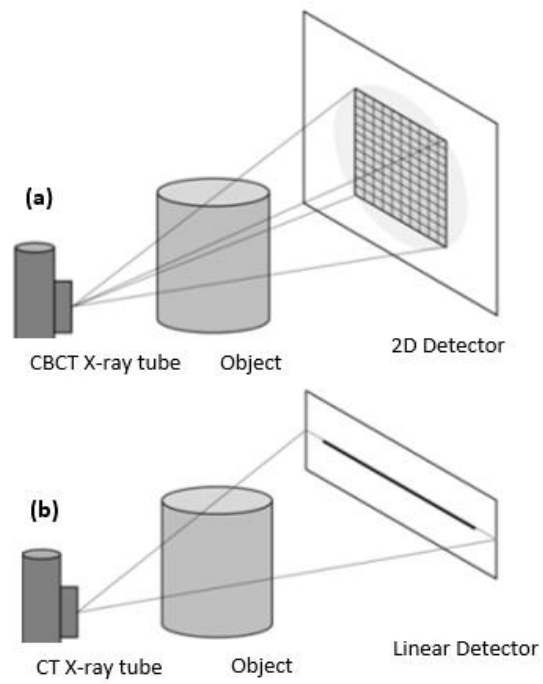
FIGURE 1.1 Cone beam geometry of CBCT **(a)** compared to the fan shaped beam of medical CT **(b).**

IMAGE QUALITY CHARACTERISTIC	DEFINITION	DETERMINING FACTORS	CHARACTERIZED BY:
Spatial resolution	Ability to discriminate small structures in an image. Especially relevant where depiction of fine detail is critical for diagnosis. Spatial resolution is approx. one order of magnitude lower than that of PR (periapical radiography).	Nominal detector pixel size, fill factor, detector motion blur, grey-level resolution, reconstruction technique applied, patient movement, scatter, imaging parameters (Table 1.1)	Traditionally, assessed visually in line-pairs per millimetre ($lp\ mm^{-1}$). Considering movement and scatter effects, a realistic spatial resolution of $\geq 1\ lp\ mm^{-1}$ has been suggested (HORNER ET AL. 2015) Automated assessment: Modulation Transfer Function (MTF) – the ability of the system to transfer signal of a given spatial frequency. It is a metric for the objective measurement of spatial resolution in X-ray based tomographic modalities
Contrast	Ability to distinguish tissues or materials of differing densities. Contrast resolution of CBCT is limited by scattered radiation and FPD related artefacts (saturation, dark current and bad pixels). CBCT soft tissue contrast is lower than MDCT.	Dynamic range of detector, bit depth of reconstructed images, exposure factors (see Table 1)	Contrast to noise ratio (CNR) – combines contrast and noise and is a metric of imaging performance with respect to large structures of varying attenuation.
Noise	Scattered radiation that is recorded by pixels on the detector contributes to image degradation. Scatter α total mass of tissue contained within the primary X-ray beam, increasing with object thickness and field size. Additional sources: **Quantum noise**: statistical variations in the homogeneity of the incident X-ray beam **Electronic noise**: caused by the conversion and transmission of the detector signal	Exhibits an interdependent relationship with spatial resolution i.e. factors that improve one (e.g. voxel size) degrades the other.	CNR: can be enhanced by changing some parameters during scanning procedure such as the FOV, mAs, kV and projection number. However, high-density materials such as metals can cause beam hardening and streak artefact which leads to a decrease in the CNR.

Artefacts	**Inherent Artefacts:**		
	-Scatter	-Capture of scattered photons.	-Increased noise, streak artefacts.
	-Partial volume averaging	-Selected voxel size is larger than size of object being imaged.	-'Step appearance' in image or homogeneity of pixel intensity.
	-Cone-beam effect	-Divergence of the X-ray beam means that structures at the top or bottom of the image field or only exposed when x-ray source is on the opposite side of the patient.	-Streaking artifacts and greater peripheral noise.
	Procedure-related Artefacts:		
	-Undersampling	-Too few basis projections or incomplete scanning trajectory.	-Mis-registration of data by reconstruction software (aliasing) resulting in increased image noise and appearance of fine striations radiating from the edge of image- "moire" pattern.
	Scanner related Artefacts:		
	-Circular artefact	-Imperfections in scanner detection or poor calibration	-Circular or ring streaks.
	Introduced Artefact: -Cupping and extinction artefact	-Both of these artefacts are as a result of beam hardening (absorption of lower energy photons in preference to higher energy photons as the beam passes through a given material and is more pronounced for denser materials i.e. metal)	-Distortion of metallic structures due to differential absorption. -Streaks and dark bands between two dense objects.
	-Patient motion artefact	-Patient motion causes mis-registration of data, the smaller the voxel size the more marked the effect of patient movement.	-Double contours in the reconstructed image.

TABLE 1.2 Image quality characteristics. FPD: flat panel detector, MDCT: multi-detector computed tomography.

STUDY	DIAGNOSTIC TASK	EXPOSURE FACTORS ALTERED	REFERENCE STANDARD	DOSIMETRY	RECOMMENDATION OF LOW-DOSE PROTOCOL	PRINCIPLE CONCLUSIONS
KWONG ET AL. 2008	-Diagnostic quality of images assessed via questionnaire.	-kV -mA	-No standard	-Not recorded	-Not described	-Images at reduced kV and mA generally maintained DA -High observer variation in quantifying image quality
BROWN ET AL. 2009	-Orthodontic linear accuracy (LA) study	-Exposure time	-Dry human skull measurements	-Not recorded	-Not described	-Reduced exposure time (projections) did not reduce DA
SUR ET AL. 2010	-Implant planning- identification of relevant anatomic landmarks	-mA -Exposure time by using 180° and 360° rotations	-Reference exposure 80kVp, 8mA, 360° rotation	-Not recorded	-Not described	-Reducing rotation at 4mA provided acceptable image quality, image quality at 2mA provided acceptable image quality only with 360° scans.
DURACK ET AL. 2011	-Detection of simulated external inflammatory resorption (ERR)	-Exposure time by using 180° and 360° rotations	-Reference exposure 90kVp/3mA/17.5s, 360° rotation	-Not recorded	-Not described	-Reducing rotation from 360° to 180° with small FOV reduced exposure time but not DA.
LENNON ET AL. 2011	- Detection of simulated periapical bone loss	- Exposure time by using 180° and 360° rotations	-No standard	-Not recorded	-Not described	-Reducing rotation from 360° to 180° reduced exposure time but not DA -Wide range of interobserver variation.

AL-EKRISH 2012	-Implant planning/dimensional accuracy	-Exposure time (3 different times)	-Dry human skull measurements	-Not recorded	-Not described	-Reliability and dimensional accuracy remain the same with the chosen reductions in exposure time
HASHEM ET AL. 2013	-LA of simulated external inflammatory resorption	-Exposure time with 180° and 360° rotations	-Dry porcine hemi-mandible measurements	-Not recorded	-Not described	-Reducing rotation from 360° to 180° produced equally accurate measurements.
WALTRICK ET AL. 2013	-Implant planning/LA and visibility of mandibular canal	-Exposure time by using 3 different resolution settings	-Dry human skull measurements	-Not recorded	-Not described	-All of the protocols produced an image adequate for measurements and mandibular canal visualisation.
YADAV ET AL. 2015	-Detecting arthritic change in the TMJ	-Exposure Time with 180° and 360° rotations	-Dry human skulls with simulated soft tissue and artificial joint lesions.	-Not recorded	-Not described	-Images were equally diagnostic at 180° and 360° rotations (other exposure factors remained identical)
HIDALGO RIVAS ET AL. 2015	Evaluation of impacted maxillary canines and possible adjacent resorption in paediatric skull phantom. Objective measure of image quality	-kV

-mA | Reference image data sets using highest and lowest exposures possible with device being used. | -DAP Meter | -80Kv 3Ma | LDP (Acc) could achieve up to a 50% dose reduction while maintaining sufficient IQ for evaluation of impacted maxillary canines. Optimum CNR at lower tube voltage than maximum |

AL-OKSHI ET AL. 2017	Assessment of periodontal space at apical third of root, MBC and CEJ. Objective measure of image quality	-kV -mA -Trajectory arc – 180°, 360°	No Standard	-DAP Metre	-80Kv/5Ma/360 or 17.5 s	CNR and visualization of periodontal structures were not compromised at this lower dose protocol. 180° rotation degraded image quality.
EZELDEEN ET AL. 2017	Planning and tooth replica fabrication (TAT) and follow up on three different CBCT devices	-kV, mA and time Altered via selecting a range of pre-defined protocols (18) on 3 CBCT machines.	Reference CBCT scanning protocol validated for accurate tooth and bone segmentation.	Monte Carlo dose simulations for 3 paediatric models.	Pre-defined low dose protocols specific to device.	Use of device specific pre-defined low dose protocols can achieve considerable ED reductions while maintaining image quality for TAT.
EL SAHILI ET AL 2018	Implant planning using human cadavers	-mA -Exposure time Altered via selecting a pre-defined protocols: high/low dose	High dose protocol CBCT dataset	Device DAP	Pre-defined low dose protocols specific to device.	Reducing mA and exposure time did not affect ability to identify key landmarks in implant planning
BRASIL ET AL 2019	Paediatric indications using two paediatric anthropomorphic phantoms	- kV - mAs	No objective reference standard Subjective comparisons used	Not recorded	High kV ≥ 95 (for device used), reduce mAs according to diagnostic task	Identification of an optimal kV, minimising noise and artefacts, allows selection of minimal mAs for the patient specific diagnostic task

TABLE 1.3 Selected representative studies demonstrating exposure factor reductions that maintained images of diagnostic quality in a range of diagnostic tasks.
MBC: marginal bone crest, CEJ: cementoenamel junction, ED: effective dose, TAT: tooth autotransplantation, CNR: contrast-to-noise ratio, LDP: Low dose protocol

FIGURE 1.2 The effect of exposure factors (kV, mAs) and choice of exposure parameter (voxel size) on image quality is demonstrated by exposing 16 region of a dry skull using a ProMax 3D Classic (Planmeca Oy, Finland) CBCT scanner. From exposure A-C, kV, mAs are reduced and voxel size is increased by selecting smaller patient settings and moving from high resolution to ultra-low dose (ULD) settings. Although the image sharpness is reduced it remains diagnostically acceptable with the identification of the MB2 still possible (Exposure C.), illustrating the principle of optimisation.

1.3.7.3 Field of view

The dimensions of the field of view (FOV) are dependent largely on the size and shape of the detector, the beam projection geometry and the ability to collimate the beam (SCARFE ET AL. 2008). The FOV is either cylindrical or spherical and collimation of the primary X-ray beam using adjustable lead shields limits exposure to the anatomical area of interest, thus avoiding unnecessary exposure. CBCT devices can be categorized according to the dimensions of the FOV. Some devices offer a single fixed FOV, with the majority offering a few pre-set options of FOV, particular to a specific indication. Other devices allow freely adjustable FOVs within certain limitations with another option being the stitching together of adjacent 3D volumes to achieve a larger FOV. The drawback of stitching being that the overlapped area is imaged twice, doubling the exposure to such areas. FOVs (described as diameter [D] x height [H] in cm²) can range from small (<10cm in field height, e.g. D x H: 4x4 cm² suitable for imaging a localized dentoalveolar area (1-3 teeth) and 8 cm x 8 cm²- suitable for imaging the dentate areas of the maxilla and mandible) to medium (10-15 cm in field height). Large FOVs (>15 cm field height) are required for full craniofacial imaging (up to dimensions of 26 x 26 cm²). However it is evident from the literature that FOVs are not always categorised using the same criteria as above, with a recent meta-review highlighting the necessity for a

general consensus on classification of FOV dimensions to allow comparison of effective doses (AL-OKSHI ET AL. 2021)

Reducing the FOV size (specifically field height) is the most straightforward method of reducing patient radiation dose and is a key factor in CBCT optimisation (DAVIES ET AL. 2012, PAUWELS ET AL. 2012a, THEODORAKOU ET AL. 2012, BORNSTEIN ET AL. 2014, PAUWELS ET AL. 2014a, LUDLOW ET AL. 2015). Nevertheless, with the diversity of devices and scan options, an approximate ten-fold variation in dose for an equivalent FOV was reported between the units studied (BORNSTEIN ET AL. 2014). FOV size and collimation in addition to diagnostic image quality are key determinants in the diagnostic application of a CBCT device (HIRSCH ET AL. 2008, LOUBELE ET AL. 2009). In relation to image quality, an increase in FOV results in a relatively greater amount of scatter reaching the detector and thus is accompanied by a relative increase in noise/artefacts and a reduction in contrast.

Larger FOVs have implications for the thyroid gland, especially for children. This radiosensitive organ has a significant contribution to effective dose (17-20% - Adults, 30-37% - children) (IRCP 2007) and can be exposed to scatter (contribution of internal scatter is uncertain) and possibly to the primary beam in dental CBCT. Use of thyroid shields has demonstrated a thyroid dose reduction in children (17-42%) and adults (20-49%) (TSIKLAKIS ET AL. 2005, QU ET AL. 2012, HIDALGO-RIVAS ET AL. 2015). Thyroid shielding is not mandatory in the EU as it was concluded that the thyroid gland is not normally in the primary beam during dental CBCT scans (HPA 2010, EUROPEAN COMMISSION 2012). However, it is advised that a decision should be made locally with the aid of a medical physics expert concerning large FOV scans, if it is likely the thyroid lies in or close to the primary beam (www.bir.org.uk/patientshielding). Notably, in the USA, dentists are advised to use thyroid shielding routinely for all dental radiography and for CBCT so long as this does not interfere with the examination (https://www.thyroid.org, http://www.imagegently.org). However, if the thyroid shield lies within the X-ray beam, even if outside the displayed FOV, it will attenuate the beam and produce artefacts on CBCT scans. Furthermore, if an AEC is used, at least in theory, a thyroid shield may reduce the dose to the receptor sufficiently to increase automatically the exposure. A recent publication presenting a consensus of multidisciplinary European organisations, including dental, concluded that thyroid contact shielding 'may be used' for CBCT when

it is outside the field of view of the scan, but with a strong recommendation that a Medical Physics Expert (MPE) is consulted first (HILES ET AL. 2022).

1.3.7.4 Filtration

Filtration serves to limit patient exposure to lower energy photons, which will contribute to skin dose but not to image formation. Therefore, highly filtered X-ray beams have an increased mean energy, reduced entrance exposure and suffer less from beam hardening, but can be associated with loss of contrast (LOFTHAG-HANSEN ET AL. 2008, ROBERTS ET AL. 2009, LUDLOW 2011). CBCT scanners typically utilize aluminium filtration (2.5-21 mm) with additional copper filtration being increasingly common. Dose reductions associated with additional copper filtration in selected CBCT devices have been reported (LUDLOW & IVANOVIC 2008, QU ET AL. 2010, LUDLOW 2011, KOIVISTO ET AL. 2012, KAASALAINEN ET AL. 2021). In reality, clinicians using CBCT have no easy means of changing filtration, which would require the input of a medical physics expert and an equipment engineer. Even then, this would be challenging without cooperation from equipment manufacturers.

1.3.7.5 Detector

The X-ray detector samples the attenuated beam in its trajectory. The incoming X-ray photons are converted by X-ray detectors to an electrical signal. Almost all modern CBCT scanners utilize indirect flat panel detectors (FPD) consisting of a pixel array of hydrogenated amorphous silicon thin-film transistors (TFT) or complementary metal oxide semiconductors (CMOS). In both cases a layer of scintillator material [gadolinium oxysulfide or caesium oxide] converts X-ray photons to light photons. Subsequently, the light is detected on the photodiodes and read from the entire detector array to compile a raw-data digital image (KILJUNEN ET AL. 2015). FPDs offer higher spatial and contrast resolution, greater dynamic range and reduced peripheral distortion compared with the earlier generation image intensifiers and charged coupled devices (CCD) technology, which have gradually been superseded (BABA ET AL. 2004, NEMTOI ET AL. 2013, PAUWELS ET AL. 2015a). Involvement of a medical physics expert at installation is deemed essential to optimize the detectors parameters with regards to dose and image quality (EUROPEAN COMMISSION 2012).

1.3.8 Image quality parameters

1.3.8.1 Exposure frequency: continuous v pulsed exposure

A minority of CBCT units utilize continuous X-ray exposure i.e., exposure time equals scan time. However, constant exposure during signal integration contributes to patient dose but not to image formation as most detectors are unable to record X-ray exposure during the acquisition process. To avoid this unnecessary exposure the majority of current CBCT units have a pulsed/intermittent X-ray emission to coincide with detector activation, ensuring that there is no exposure being made between projections. Pulsed emission systems not only result in a reduced dose but also may exhibit improved spatial resolution owing to a reduced motion effect (PAUWELS ET AL. 2015a). A small number of CBCT models have been reported to use both pulsed and continuous depending on the scanning mode (KAASALAINEN ET AL. 2021).

1.3.8.2 Rotation arc

Of the currently commercially available devices, the rotation angle varies between 180° and 540°, the majority of scanners having a single fixed rotation angle (most commonly 180°) with some devices enabling selection of a variable rotation arc according to scan protocol (HORNER ET EL. 2013, NEMTOI ET AL. 2013, KAASALAINEN ET AL. 2021). A shorter scan arc results in a reduced scan time and hence dose (lower total mAs) with a 180° arc resulting in an approximately 50% dose reduction compared to a 360° arc. Images produced by partial rotation have been associated with increased reconstruction artefacts (SCARFE & FARMAN 2008, BECHARA ET AL. 2013) and particularly those acquired with restricted FOVs (COSTA ET AL. 2019). Additionally, while it would be expected that this reduced mAs would be accompanied by increased noise and reduced image quality, studies demonstrate that for particular diagnostic tasks image quality and diagnostic accuracy can be maintained (LENNON ET AL. 2012, BECHARA ET AL. 2013 COOK ET AL. 2015, TADINADA 2017). This finding implies that manufacturers' recommendations for exposure factors are too high for these tasks.

1.3.8.3 Number of projections

The number of acquired projection images ('basis images') during the scan arc movement is determined by the rotation time, frame rate (number of projection images

per second), the completeness of the trajectory arc and the speed of the rotational movement (SCARFE & FARMAN 2008). A greater amount of projection data generally necessitates a longer scan time, with greater potential for patient movement and consequently a higher patient dose. Enhanced image quality accompanies this increased projection data; providing more information to reconstruct the image, allowing for greater spatial and contrast resolution and an increased signal-to-noise ratio and decreased metallic artefacts (PAUWELS ET AL. 2013). However, minimizing the number of projections appropriately can result in reduced patient dose (via ↓mAs) and still be consistent with diagnostic images (KUSNOTO ET AL. 2015). Furthermore, it is reported that increasing exposure does not improve the appearance of metal artefacts sufficiently to justify the increased radiation exposure (PAUWELS ET AL. 2013). Notably, iterative reconstruction algorithms show promise in overall image quality improvement and artefact reduction (SCHULZE ET AL. 2011, NIEBLER ET AL. 2019).

1.3.8.4 Voxel size

Voxels (the individual volume elements) produced in formatting the volumetric data set, dictates the spatial resolution of a CBCT image (SCARFE & FARMAN 2008). Voxel size can be selected on most dental CBCT systems according to the particular diagnostic task. Overall, voxel sizes of CBCT equipment have been reported to range from 0.05 mm to 0.6 mm, with the more recent availability of these smallest voxel sizes being attributed to improved image reconstruction algorithms, image noise reduction, and patient movement correction methods (GAÊTA-ARAUJO ET AL. 2020). The smaller the voxel size, the higher the spatial resolution (**Fig. 1.1**) and therefore smaller voxel sizes are generally selected when a high level of detail is required e.g. endodontic purposes (LIEDKE ET AL. 2009, KAMBOROĞLU & KURSUN 2010, MELO ET AL, 2010, MARET ET AL. 2012). However, voxel dimensions primarily depend on the pixel size on the area detector and smaller pixels capture fewer X-ray photons which result in more image noise. This may require a compensatory increase in radiation dose to achieve a sufficient signal-noise ratio to achieve this improved diagnostic image quality (via ↑ mAs or basis images). Some devices allow the operator to control exposure factors used with different resolutions, while others automatically dictate exposure factors accompanying particular voxel sizes in order to keep noise relatively constant. Notably, a study reported that the patient

dose was doubled on selection of the high resolution from standard on a particular CBCT unit (LUDLOW & WALKER 2013). In the pursuit of dose optimisation, the lowest resolution (larger voxel size) option should be selected where the nature of the diagnostic task permits (EUROPEAN COMMISSION 2012). It was reported that the effect of voxel size on diagnostic outcome has not yet been systematically demonstrated (SPIN-NETO ET AL. 2013a). While there appears to be a trend of increased diagnostic accuracy relating to smaller voxel sizes for conditions such as root fracture and external root resorption (BRAGATTO ET AL. 2016, WANDERLY ET AL. 2017, GUO ET AL. 2019), it has also been established that larger voxel sizes do not necessarily mean lower diagnostic accuracy for a range of diagnostic tasks including those requiring fine detail (ÖZER 2011, MA ET AL. 2016, SONMEZ ET AL. 2018, KEHRWALD ET AL. 2022). Conflicting results may be related to the use of different devices used and varying methodology (KEHRWALD ET AL. 2022). Therefore, as previously identified (SPIN-NETO ET AL. 2013a), it is still not possible to suggest general protocols for all diagnostic tasks and further standardised studies are required to establish accurate guidelines in this area.

It is apparent from the aforementioned that the image quality (ability of CBCT images to display the required anatomical features and/or pathologies) and consequent dose of CBCT imaging is influenced by a number of variables (**Table 1.1**). Such variables include the individual device (e.g. detector, filtration, FOV capabilities etc.), the exposure parameters (kV, mAs) and image quality parameters (voxel size/resolution, basis images [dependent on rotation arc, exposure frequency]). These variables can be inter-related and therefore selection of the optimal combination of scanning parameters to reduce dose can prove a challenge to the operator with very little in the way of practical guidance. While general recommendations on dose-optimisation exist (HPA 2010, EUROPEAN COMMISSION 2012, AMERICAN DENTAL ASSOCIATION COUNCIL ON SCIENTIFIC AFFAIRS 2012, WHITE ET AL. 2014, DIMITRA [OENNING ET AL. 2018]), reviews of the literature have highlighted the need for more specific guidance on how optimisation can be achieved for specific diagnostic tasks in the full range of dental disciplines (GOULSTON ET AL. 2016, YEUNG ET AL 2019, VAN ACKER ET AL. 2020, KAASALAINEN ET AL. 2021). Nevertheless, it is accepted that establishment of diagnostic task specific protocols may prove difficult due to wide range of CBCT devices and capabilities. The development of low dose protocols in a range of diagnostic applications has gone some way in beginning to

achieve optimisation (HIDALGO RIVAS ET AL. 2015, AL-OKSHI ET AL. 2017, YALDA ET AL. 2022) as could device specific low dose pre-set options (EZELDEEN ET AL. 2017, OENNING ET AL. 2019).

1.3.9 Image quality

In keeping with the ALADA principle, the image quality attained should be sufficient to achieve the specific diagnostic task, but at the minimum exposure possible. The operator must be aware that the acceptable level of image quality and the radiation dose may vary according to the particular diagnostic task and indeed the anatomical region investigated/position of the pathology (LOFTHAG-HANSEN ET AL. 2011, NEVES ET AL. 2012). Image quality is described in terms of spatial resolution, contrast, noise and presence of artefacts (**Table 1.2**) but on a simple level can be assessed relative to achieving the diagnostic task e.g. visualisation of a periapical radiolucency, identification of the second mesiobuccal canal (MB2). A number of parameters impact on image quality; tube current, tube voltage, FOV, voxel size, number of projections and type of detector (MARET ET AL. 2012, SPIN-NETO ET AL. 2013a, PAUWELS ET AL. 2015a). As previously established, there is a great array of CBCT devices available commercially, exhibiting a range of technical specifications, doses and image quality capabilities (HATCHER 2010, NEMTOI 2013). In order to achieve optimisation of these devices it is essential to use a standardized approach to assessing image quality (PAUWELS ET AL. 2011). Image quality can be assessed using subjective and objective methods.

1.3.9.1 Subjective evaluation

This is considered as the benchmark when assessing image quality in relation to achieving a specific diagnostic task. It involves the standardized presentation of images (anthropomorphic phantoms, human skulls or jaws) to a specified number of observers who are provided with a scale to grade their ability to identify the presence of anatomical structures or/and grade the sufficiency of the image quality for a particular task e.g. root resorption, implant planning and periapical diagnosis. (ALQERBAN ET AL. 2011, DURACK ET AL. 2011, ESPOSITO ET AL. 2011, LOFTHAG-HANSEN ET AL. 2011, SHELLEY ET AL. 2011). This technique is limited by its inherent subjectivity, (inter-observer, intra-observer, case-sample variability, and the use of non-standardised skull and jaw models, which limits comparison (TAPIOVAARA 2008, LOFTHAG-HANSEN ET AL. 2011). Furthermore,

findings are often limited to the CBCT device investigated due to the large diversity in image quality between scanners (PAUWELS ET AL. 2012d).

1.3.9.2 Objective evaluation

This involves quantitative measurement (on physical test objects) of physical factors such as spatial resolution, contrast resolution, image density/pixel intensity, image noise and artefacts, on the basis that they equate to clinical image quality using test phantoms (WATANABE ET AL. 2011). Identifying the need for a standardized phantom appropriate for dental CBCT, the SedentexCT project developed a quality control phantom (SedentexCT IQ phantom) which enables reproducible measurement of these technical image quality parameters on any CBCT device and thus is utilized for assessing device performance and quality control (PAUWELS ET AL. 2011, BAMBA ET AL. 2013, LUDLOW & WALKER 2013, DE LAS HERAS GALA ET AL. 2017).   Other devices have been developed, including the QUART DVTkp test tool (Quart GmbH, Germany).   While objective evaluation is essential for quality assurance (QA) of CBCT devices and these physical indices are germane, there is no direct means by which to relate them to clinical diagnostic accuracy (MARTIN ET AL. 1999, MÅNSSON 2000, WATANABE ET AL. 2011).   Studies have shown a significant association of physical factors (modulation transfer function [MTF] and/or CNR]) with subjective image quality and related this to the ability to achieve a specific diagnostic task (CHOI ET AL. 2015, HIDALGO RIVAS ET AL. 2015, AL-OKSHI ET AL. 2017).   Choi and co-workers (2015) demonstrated that a better physical image quality (higher MTF and CNR value) was required to achieve the clinical task of periapical diagnosis compared with implant planning in the mandible, the findings corresponding in part to a study on subjective image quality in relation to diagnostic task (LOFTHAG-HANSEN ET AL. 2011).   However, both of these studies' findings were not related to dose measurements.

1.3.10 Is there evidence that ALADA is practicable in a range of dental diagnostic tasks?

Optimised exposure protocols can be achieved while maintaining adequate image quality and thus diagnostic accuracy for a range of clinical tasks (EUROPEAN COMMISSION 2012, GOULSTON ET AL. 2016). These results relate to the diagnostic task investigated using specified CBCT scanner(s) and that technical specifications limit translation to all CBCT scanners. As previously discussed, it has been established that size and position of FOV relative to the radiosensitive organs and the scanned individual have a substantial impact on dose optimisation (DAVIES ET AL. 2012, PAUWELS ET AL. 2012a, THEODORAKOU ET AL. 2012, PAUWELS ET AL. 2013). Nonetheless, several *in vitro* studies specifically demonstrate that a reduction in exposure factors (kV, mA, exposure time - also altered through rotation time or voxel size/resolution) can be consistent with sufficient image quality to enable diagnosis in a range of clinical applications (**Table 1.3**). Furthermore, some of these studies included dose measurements, recommending low dose protocols or threshold doses for their respective diagnostic tasks (HIDALGO RIVAS ET AL. 2015, AL-OKSHI ET AL. 2017, MCGUIGAN ET AL. 2020, YALDA ET AL. 2022). One low dose protocol established a 50% dose reduction from the manufacturer's recommended protocol (HIDALGO RIVAS ET AL. 2015), which highlights the difficulty for practitioners in optimizing exposures. Other studies demonstrated the limitations of lower exposures relating to specific sites or pathology location (LOFTHAG-HANSEN ET AL. 2011, NEVES ET AL. 2012), reporting that although 180° rotations produced diagnostic images for maxillary implant planning, this was not the case for mandibular implant planning or periapical diagnosis (LOFTHAG-HANSEN ET AL. 2011). In the same way, Neves et al. (2012) suggested a reduced dose scanning protocol produced images of diagnostic quality for detection of external root resorption (ERR) with the caveat that the position of root resorption may affect the ability to diagnose at lower exposures.

Generally, studies have reported that image quality is consistently degraded with reduced exposure factors (SUOMALAINEN ET AL. 2009, LUCKOW ET AL. 2011, PARSA ET AL. 2013). The most commonly investigated diagnostic task with regard to optimisation of exposure factors was that of implant planning, perhaps reflecting the almost ubiquitous use of CBCT in this dental application. Oddly, considering that children have a significantly increased radiation risk, there is more limited literature regarding

optimisation of exposure factors in orthodontic diagnostic tasks, while in the available studies it has been highlighted that orthodontic scanning in a child phantom resulted in on average an effective dose 36% greater than in the adult phantom (LUDLOW & WALKER 2013). Other orthodontic studies found that reduced exposure time and/or number of projections was consistent with maintenance of diagnostic accuracy (BROWN ET AL. 2009, COOK ET AL. 2015, KOSNOTO ET AL. 2015).

In conclusion, it is evident that radiation doses that are significantly reduced from the manufacturer's recommendations can be achieved (via reduced kV, mA or time, number of projections) while maintaining acceptable image quality and applied for certain diagnostic tasks and particular devices (**Table 1.3**). Nonetheless, it has been emphasized that radical reductions in dose are futile if image quality degrades to the point of being non-diagnostic, thereby necessitating a repeat scan (LUDLOW & WALKER 2013). Evidentially more research is needed, perhaps in collaboration with industry to further assist practitioners in this important area. Furthermore, moving forward inclusion of guidance on use of low-dose protocols as part of position statements from a range dental disciplines would be instrumental in disseminating the importance and practical application of optimisation.

1.3.11 How valid is the research on dose optimisation on image quality?

The majority of studies relating optimisation to image quality are *in vitro* and thus of low hierarchal evidence-based standing (MARSHALL & SYKES 2011, YEUNG ET AL. 2019). Variations in CBCT device setting and properties make it impossible to reliably compare dose estimations from different studies. A systematic review of the literature on CBCT imaging in the oral and maxillofacial region highlighted inconsistent reporting on device settings and properties concluding, that a specific list of CBCT device parameters (e.g. exposure time, FOV, detector type, rotation arc etc.) should be documented to enable comparison (DE VOS ET AL. 2009). Unfortunately, this policy has not been universally adopted, but is reiterated in a more recent literature on optimisation (EUROPEAN COMMISSION 2012, GOULSTON ET AL. 2016). These reviews highlight, among other issues, the need for international compliance on a standardized method of accurately measuring patient dose using a standard commercially available phantom and the use of consistent reference standards when diagnostic accuracy is measured.

1.4 DIAGNOSTIC EFFICACY

1.4.1 Does CBCT have a greater diagnostic efficacy than conventional techniques?

The final section of this review analyses the evidence comparing the diagnostic efficacy of CBCT and conventional techniques for specific clinical tasks. If it is accepted that the diagnostic accuracy of CBCT is superior to conventional techniques for certain diagnostic tasks, albeit at a higher dose to the patient, can this enhanced accuracy deliver a net benefit to the patient as evidenced by an impact on diagnosis, clinical decision-making and treatment outcome?

Critical appraisal of the literature on CBCT imaging efficacy is best facilitated by a hierarchal classification model, which categorizes six ascending levels of diagnostic efficacy (FRYBACK & THORNBURY 1991). The levels start with the simple goal of procuring the most accurate image and ascends to the complex target of improving patient outcome and societal impact with the aim of effecting evidence-based changes in patient care and health policy (**Table 1.4**). The lower tiers (Levels 1 and 2) focus on image quality (NATIONAL COUNCIL ON RADIATION PROTECTION AND MEASUREMENTS 2005, KRUPINSKI ET AL. 2007) and diagnostic accuracy of CBCT (GHAEMINIA ET AL. 2009, MATZEN ET AL. 2013, PATEL ET AL. 2016, YI ET AL. 2017). Such technical and diagnostic efficacy studies constute the bulk of evidence in the literature and are less time consuming and expensive than study designs required at higher levels of efficacy; however, even these research domains are considered incomplete (EUROPEAN COMMISSION 2012, PETERSSON ET AL. 2012, KRUSE ET AL. 2015, ROSEN ET AL. 2015, HORNER ET AL. 2020, ROSEN ET AL. 2022). While these principally lab-based studies are essential in establishing accuracy and report that CBCT exhibits higher sensitivity and specificity than intra-oral radiography for several diagnostic tasks (PETERSSON ET AL. 2012, ROSEN ET AL. 2015, NIKOLIC-JAKOBA ET AL. 2016, SALINEIRO ET AL. 2017, AMINOSHARIAE ET AL. 2018), albeit often in the absence of a relevant reference method (PATEL ET AL. 2012, URABA ET AL. 2016), they do not provide any evidence of impact on patient care. Critically, accuracy studies should use a non-radiographic reference standard, which is an exact reflection of the true situation (MILEMAN & VAN DEN HOUT 2009) and could include histology (DE PAULA-SILVA ET AL. 2009, KRUSE ET AL. 2017) or intrasurgical visualization (GHAEMINIA ET AL. 2009, QIAO ET AL. 2014). *Ex vivo* simulation studies on dry skulls (DURACK ET AL. 2009, BRAUN ET AL. 2014) utilize direct

visualisation/measurement as a reference, however it is questionable whether artificially created lesions represent either the true topography or borders of resorption or periodontal lesions (PETERSSON ET AL. 2012). Furthermore, considering the effect of patient movement on image quality, these studies are even further removed from the *in vivo* reality (SPIN-NETO ET AL. 2013b, 2015, 2016, 2018, SPIN-NETO & WENZEL 2016).

On the contrary, other reports conclude that there is insufficient evidence of superior diagnostic accuracy of CBCT over intra-oral imaging for a range of diagnostic tasks including vertical root fracture detection (CORBELLA ET AL. 2014, CHANG ET AL. 2016). These findings were attributed not just to the heterogeneous nature of the included studies, with high levels of bias, but also to the impact of artefacts created by radiopacity of root canal filling materials and intracanal post restorations (BRULLMAN & SCHULZE 2015). Specifically, systematic reviews with meta-analysis have reported reduced diagnostic accuracy using CBCT in detection of VRF in endodontically treated teeth and teeth with intracanal post restorations (MA ET AL. 2016, TALIWAR ET AL. 2016), where presence of streak artefacts reduced specificity. Similarly, reduced diagnostic accuracy was reported for periapical lesion detection with CBCT in surgical endodontic retreatment cases, where 40% of teeth identified by CBCT as having a periapical lesion proved not to have periapical inflammation histologically (KRUSE ET AL. 2017). In a later study by the same author (KRUSE ET AL. 2018), it was also theorized that these reduced diagnostic accuracy parameters associated with root filled teeth (not evident in the study's findings with non-root filled teeth), may relate not only to artefacts associated with the obturant but also possibly due to a widened periodontal ligament reaction to the root filling that occurs even where no pathology exists (TORABINEJAD ET AL. 2018).

Levels 3 and 4 evaluate whether an imaging modality can give rise to a change in diagnostic thinking or patient management and therefore begin to consider impact on patient's health. Before-and-after studies are frequently used to investigate the impact of diagnostic and therapeutic choices at levels 3 and 4 (GUYATT ET AL. 1986, FRYBACK & THORNBURY 1991, MEADS & DAVENPORT 2009). The number of studies published at this level are much reduced compared to technical and diagnostic efficacy studies and the need for more research in these higher levels has been repeatedly highlighted (EUROPEAN COMMISSION 2012, BORNSTEIN ET AL. 2014, ROSEN ET AL. 2015, NIKOLIC-JAKOBA ET AL. 2016, HORNER ET AL. 2020). Level 3 evidence suggests that CBCT does have an impact on diagnostic

thinking efficacy in more complex and challenging cases with regards to implant placement and endodontics but cannot be justified for routine use (EE ET AL. 2014, MOTA DE ALMEIDA ET AL. 2015, SHELLEY ET AL. 2015, AL-SALEHI & HORNER 2016). However, these studies have their limitations, including retrospective designs, selection bias, recall bias of operators and type of operator used, e.g. Al-Salehi and Horner used general dental practitioners (GDPs), which may mean the results may not be applicable more widely to other groups such endodontists, especially as the cases in their study were patients referred to specialists (AL-SALEHI & HORNER 2016). Additionally, in an orthodontic study on impacted canines, CBCT did increase accuracy in diagnosis, especially for more critical information such as the labiopalatal position of the canine cusp tip (HANEY ET AL. 2010). Albeit, it was accepted that most impacted teeth can be accurately diagnosed/ localized with conventional radiographs, nonetheless, there are undoubtedly cases which benefit from CBCT imaging (BJERKLIN & ERICSON 2006).

Therapeutic efficacy studies (Level 4) revealed a range of CBCT-impact on therapeutic decisions, perhaps influenced by study design (e.g. case selection method, teeth numbers, observer numbers/experience) and/or diagnostic task investigated. An endodontic study (24 teeth) revealed there was no significant difference in lesion size recorded or treatment strategy for periapical lesions in non-complex cases between periapical radiography (PR) and CBCT imaging (BALASUNDARUM ET AL. 2012). Although the numbers of subjects enrolled in the study are small, it does highlight that if CBCT does not actually alter the treatment plan, then the increased diagnostic accuracy of CBCT in recognizing apical periodontitis is of no real benefit (DE PAULA- SILVA ET AL. 2009, PATEL ET AL. 2012, VENSKUTONIS ET AL. 2014). It could be argued that the increased sensitivity of CBCT does diagnose AP lesions of smaller dimensions that would otherwise go undiagnosed and untreated by PR, this constituting an increased therapeutic efficacy; however, this is not clear as the possibility of reduced specificity of CBCT in diagnosing AP has been reported *in vivo* (POPE ET AL. 2014). Pope's (2014) study reports on error in interpretation of the healthy periapex on CBCT scans and the inherent flaw of applying PR interpretation of health and disease to CBCT, thereby risking overdiagnosis (MOYNIHAN ET AL. 2012 KRUSE ET AL. 2015, TORABINEJAD ET AL. 2018). Furthermore, a study referred to previously and categorised as having low levels of bias (ROSEN ET AL. 2022) has

identified that this increased sensitivity and concomitant reduced specificity can lead to overdiagnosis and overtreatment as verified with histopathology (KRUSE ET AL. 2018)

Other endodontic studies and periodontal studies have demonstrated a significant impact of CBCT imaging on treatment planning choices in complex cases (EE ET AL. 2014, MOTA DE ALMEIDA ET AL. 2014, VENSKUTONIS ET AL. 2014, PATEL ET AL. 2016, PARKER ET AL. 2017, RODRÍGUEZ ET AL. 2017, WOEBLER ET AL. 2018). The general consensus from these studies is that the increased diagnostic information from 3D cross sectional imaging provided by a CBCT scan compared with 2D conventional radiography had a substantial impact on treatment planning of high difficulty cases (e.g. resorption, surgical cases). An orthodontic study showed that CBCT imaging evoked a change in treatment plan from conventional imaging but only in a minority of cases (27%), concluding that the additional diagnostic information did not translate to a significant change in treatment plan (HANEY ET AL. 2010). Implant studies reported a significant change in treatment plan with CBCT imaging for more challenging cases (narrower implants selected in the anterior mandible with CBCT) and high risk anatomical regions (posterior jaw-longer implants selected using panoramic images) (SHELLEY ET AL. 2015, GUERRERO ET AL. 2014b); however, when all cases were considered a significant change in treatment plan between the two imaging modalities was not demonstrated. In general, these studies reflect the majority of current guidelines/position statements across the dental disciplines, which highlight that use of CBCT is not recommended routinely, but is only advisable in more complex cases where conventional radiography does not elucidate the diagnostic information required (EUROPEAN COMMISSION 2012, HARRIS ET AL. 2012, AAOMR 2015, FGDP [UK] 2018, ESE 2019). Notable exceptions to this conservative approach to CBCT prescription do exist (DRAGO & CARPENTIERI 2011, NOFFKE ET AL. 2011, TYNDALL ET AL. 2012), with routine use of cross-sectional imaging in dental implant planning and treatment advocated, based on a reduced risk of neurosensory and neurovascular injury (ZIJDERVELD ET AL. 2008, RENTON ET AL. 2012, ROEDER ET AL. 2102, JACOBS ET AL. 2014). This routine CBCT use has been questioned by other groups who elicited opposing conclusions from the literature, highlighting the lack of evidence-based guidance in most national and international guidelines on implant dentistry and described their recommendations as largely expert opinion and consensus driven (BORNSTEIN ET AL. 2014, HORNER ET AL. 2015). Regarding management of mandibular third molars, a recent review

(MATZEN & BERKHOUT 2019) identified that CBCT did change the treatment plan in a small percentage of cases (GHAEMINIA ET AL. 2011, MATZEN ET AL 2013), however, for the majority of mandibular third molars, the selected treatment plan was the same as that selected using panoramic radiographs.

Ultimately, if clinicians are exposing patients to diagnostic ionizing radiation which is of significantly higher dose than that of the existing diagnostic imaging modality of choice, the new imaging modality should demonstrate a positive impact on patient outcome (Level 5-Patient outcome efficacy), preferably in a cost-effective manner (Level 6-Societal efficacy). Randomized controlled trials (RCTs) are the optimal study design to assess these levels of accuracy (FRYBACK & THORNBURY 1991). Generally, RCTs are expensive and time consuming, often resulting in low subject numbers and underpowered studies (ROEDER ET AL. 2012). Furthermore, they can be ethically difficult or impossible to perform with regards to diagnostic imaging modalities (MILEMAN & VAN DEN HOUT 2009) and it has been argued that due to their longitudinal nature and the fast pace of CBCT technology development, their results can be redundant even before publication (KIM ET AL. 2011). Perhaps not surprisingly there are very few studies published which assess patient outcome efficacy (Level 5). Three studies investigating surgical extraction of impacted mandibular third molars (GUERRERO ET AL. 2014a, GHAEMINIA ET AL. 2015, PETERSEN ET AL. 2016) failed to demonstrate any beneficial impact of CBCT over panoramic imaging on patient related outcomes (i.e. neurosensory disturbances and other post-operative complications). Although, it should be recognized that the studies were small, with an inadequate sample size for a comparative prospective study (ROEDER ET AL. 2012). On reviewing the more recent literature regarding mandibular third molar extraction, an EADFMR position paper (MATZEN & BERKHOUT 2019) concluded that CBCT imaging does not appear to be a superior predictor of post-operative sensory disturbance when compared with panoramic imaging. In fact, absence of bony separation viewed on CBCT imaging had a low predictive value, no higher than some of the seven signs identified for panoramic radiographs (ROOD & SHEBAB 1990). Secondly, using evidence from a meta-analysis of RCTs (CLÉ-OVEJERO ET AL 2017) and other high quality studies (SANMARTÍ-GARCIA ET AL. 2012), the review identified that pre-operative CBCT does not reduce the frequency of post-operative sensory disturbances, operation time, needs for analgesics, nor post-

operative complications when compared with conventional imaging. The conclusion was that CBCT imaging of the mandibular third molar has no positive impact on patient outcome and should not be applied as a routine diagnostic method before removal of mandibular third molars. Therefore, CBCT imaging should only be applied when the surgeon has a very specific clinical question in an individual patient case that cannot be answered by conventional (panoramic and/or intraoral) imaging. In reality this may result in a pattern of imaging prescription that correlates with the clinician's experience. Conclusions on the impact of CBCT imaging on patient outcome subsequent to third molar extraction is based on high levels of evidence, including RCTs with high numbers of patients using definitive outcome measures. Conversely, although the endodontic literature is replete with CBCT-related publications, only two studies that assessed endodontic patient outcome could be identified by a recent review (ROSEN ET AL. 2022), both of which were categorized as low quality studies, making it impossible to assess the validity of their findings (KURT ET AL 2014, YANG ET AL. 2016). One of the additional difficulties in endodontic outcome studies is the absence of a core outcome set that can be used to definitively assess outcome in a homogenous manner.

Societal efficacy studies (Level 6) aim to prove that implementation of this diagnostic imaging modality is an efficient use of societal resources and can provide medical benefits to society. There is a paucity of RCTs investigating societal efficacy. One prospective RCT reported on the absolute and relative costs of a CBCT scan compared with that of a panoramic examination undertaken for third molar surgery, identifying a 3-4 times greater cost associated with CBCT than panoramic imaging but there was no significant difference in resources consumed between the imaging groups, either surgically or post-surgery (PETERSEN ET AL. 2014). The same group also published an epidemiological study in Denmark (PETERSEN ET AL. 2015), which highlighted the higher economic implications of potential routine use of CBCT in extraction of mandibular third molar teeth. Importantly, this study actually considers the radiation risk implications associated with this potential policy change (calculation of cancer incidence – 0.46 per year) which is necessary when contemplating societal efficacy. Other Level 6 studies are descriptive; a cost analysis study noted that a demonstrated cost-effectiveness of CBCT imaging in one healthcare system cannot necessarily be translated to another (CHRISTELL ET AL. 2012). A periodontal case series reported that CBCT based treatment decisions for

maxillary molars with furcation defects can lead to time and cost benefits when compared with conventional radiography in a Swiss dental health setting (WALTER ET AL. 2012), although that study was not a rigorous economic evaluation. The economic evaluations required in level 6 studies can be performed in conjunction with level 3 or 4 studies when RCTs are considered to be unfeasible. Such a study was previously carried out (CHRISTELL ET AL. 2018). They were able to calculate the incremental cost-effectiveness ratio (ICER), a measure of the average additional cost per treatment decision that was changed as a result of using CBCT imaging for the assessment of maxillary canines as part of orthodontic treatment. Based on the cost analyses performed, it was concluded that CBCT as an additional diagnostic measure is only justified when more invasive therapies are planned and considering the potential increased radiation risk associated with additional imaging, cases should be judged on an individual basis. Again, this conclusion is open to subjective interpretation.

Overall, the ways in which diagnostic efficacy may alter patient diagnosis, management and potentially treatment outcome for a specific diagnostic task can vary according to a range of factors. These may include the technical efficacy of the CBCT scanner used and the selected exposure parameters, such as voxel size (SPIN NETO ET AL. 2013a). Additionally, monitor resolution and post-acquisition adjustments; contrast, brightness and magnification (PAUWELS ET AL. 2015a) and ultimately the subjective interpretation of the observer, all impact on the detection accuracy of a given condition (HORNER ET AL. 2020).

In conclusion, there is still a lack of studies exhibiting the impact of CBCT at higher levels of efficacy (EUROPEAN COMMISSION 2012, PITTAYAPAT ET AL. 2014, MATZEN & WENZEL 2015, ROSEN ET AL. 2015, NIKOLIC-JAKOBA ET AL. 2016, MATZEN & BERGOUT 2019, HORNER ET AL. 2020, ROSEN ET AL. 2022). Unfortunately, regardless how compelling the results of the technical and diagnostic accuracy efficacy studies, this literature is not indicative of any translational benefit of CBCT to patient's treatment and outcome or indeed to society.

LEVEL OF DIAGNOSTIC EFFICACY	DEFINITION AND PARAMETERS MEASURED
1.Technical Efficacy	Evaluates technical quality of imaging modality: i.e. noise, contrast, resolution, presence of artefacts and includes dose and dimensional accuracy.
2. Diagnostic Accuracy Efficacy	Evaluates accuracy of imaging modality in establishing a correct diagnosis when compared with the reference or 'gold standard' technique: sensitivity, specificity, predictive values, ROC curves.
3.Diagnostic Thinking Efficacy	Evaluates the ability of the imaging modality to improve diagnostic decisions. Evidenced in before-and-after studies where an alternative diagnostic conclusion is made with new imaging modality when compared with diagnosis made using the existing conventional imaging modality.
4.Therapeutic Efficacy	Evaluates the impact that the imaging modality has on the choice of treatment. Evidenced in clinical studies (before-and-after) by observing for changes in treatment strategies where the new imaging modality scan is or is not supplied.
5.Patient Outcome Efficacy	Evaluates the impact of the imaging modality on patient outcome. Has this new diagnostic technique lead to an improved treatment strategy with a concomitant improved outcome for the patient e.g. reduction in post-operative complications? This is assessed via randomized controlled trials (RCT's) comparing patient outcome using new technique compared with existing 'gold standard'.
6.Societal Efficacy	Assesses the cost-benefit ratio of the imaging modality to society as a whole.

TABLE 1.4 Hierarchal model of classification of diagnostic accuracy (FRYBACK & THORNBURY 1991). ROC: receiver operating characteristic curve.

1.5 CONCLUSIONS

- Conventional radiography is limited by the inability to describe the 3D anatomy of teeth and their related structure. It has therefore been recommended that CBCT be used in select cases in which conventional radiography cannot supply satisfactory diagnostic information.

- CBCT is often a more sensitive diagnostic tool than conventional radiography but delivers a significantly greater patient dose. Therefore, unless the benefit to the patient can be justified there is a risk of overexposure. Furthermore, there is concern that with increased diagnostic sensitivity there is a loss of specificity which may result in over-representation of disease, which highlights a need for establishing 'the limits of normal' particular to CBCT, in order to correctly diagnose pathology.

- The clinician in practice prescribes, exposes, analyses and reports on the CBCT image. Therefore, appropriate training in justification, acquisition and interpretation is paramount.

- The evidence base highlights the lack of evidence that use of CBCT imaging has a significant impact on decision-making and treatment outcome, therefore, the clinician remains unsupported in their justification of CBCT imaging.

- With an awareness of the potential stochastic radiation risks of CBCT, being particularly pertinent to the young, judicious case selection is essential to ensure that the benefits–risk ratio remains in favour of the individual patient. Guidelines constructed from the best available evidence serve to aid the clinician's justification. Unfortunately, these available guidelines are of varying quality with the majority being based on expert opinion. It is important that a more critical systematic approach is adopted in the formulation of new guidelines

- It is accepted in CBCT that FOV height and relation of the FOV to the radiosensitive organs are the main determinants of effective dose. Additionally, optimisation of exposure and imaging parameter factors can achieve significant dose reductions while maintaining image quality for a range of diagnostic tasks,

but this is not necessarily translatable to all devices. Further development of low dose protocols in key diagnostic areas would greatly aid the clinician.

- Despite the lack of evidence on the efficacy of CBCT, its use is expanding rapidly in dental practice. It is a lucrative, industry-driven business sold on the basis of improved, attractive and high quality imaging. Critical evaluation of manufacturer's advice and default protocols necessitates appropriate undergraduate and postgraduate training and knowledge of the evidence base regarding CBCT imaging.

The current literature on CBCT imaging reveals the need for consistent and standardized testing and reporting to allow effective comparisons of dose calculations and optimisation techniques on image quality. Diagnostic accuracy studies do not always reflect the clinical situation and inconsistent reference standards make ready comparison between results impossible. Notably, higher hierarchal level studies are rare, with few studies of high quality, assessing clinical outcome efficacy. Nevertheless, for the purpose of establishing robust guidelines for appropriate use of CBCT, research in the future should be directed at higher level clinical studies.

1.6 AIMS & OBJECTIVES

As was concluded from the literature review, there are outstanding challenges to be addressed regarding the use of CBCT imaging, to ensure adherence of both the principles of optimisation and justification. Specifically, there is a need for low dose protocols in key diagnostic areas to aid the clinician in optimisation. Additionally the review highlighted the lack of evidence that use of CBCT imaging has a significant impact on the higher levels of diagnostic efficacy such as outcome efficacy. Therfore the principle aims of this thesis are are to identify a strategy in which radiation dose can be reduced for a specific diagnostic task, while maintaining images of diagnostic quality, and to demonstrate any potential impact of CBCT imaging on treatment outcome for this diagnostic task. Consequently the overall objectives of this thesis are:

(1) To identify a threshold dose for imaging of fine detailed structures in endodontics as represented by the diagnostic task of MB2 root canal identification while maintaining images of diagnostic quality.

(2) To quantify the objective image quality at this threshold dose and by performing this using two scanner types, to gain some insight into the transferability of the results obtained which could facilitate the process of optimisation.

(3) To examine the impact of anatomy complexity on establishing this threshold dose and examining the impact of operator experience on diagnostic efficacy.

(4) To explore optimisation strategies by examining the relationships between IQ metrics and IQ determinants and the diagnostic task of root canal. Specifically, using regression analysis to identify those that have a statistically significant relationship with successful achievement of the diagnostic task of root canal identification.

(5) To investigate if supplemental CBCT imaging can potentially be demonstrated to improve outcome after endodontic access cavity preparation in M1Ms using a with or without sudy on 3D-printed teeth, thereby justifying the increased dose associated with CBCT imaging.

Chapter 2

An investigation into dose optimisation for imaging root canal anatomy using cone beam CT

2.1 INTRODUCTION

The use of CBCT as a diagnostic aid in a range of dental disciplines is not routinely indicated, but can be justified when conventional radiography is insufficient for the specific diagnostic task (EAO 2012, EUROPEAN COMMISSION 2012, HARRIS ET AL. 2012, AAE & AAOMR 2015, EUROPEAN COMMISSION 2012, FGDP [UK] 2018, ESE 2019). Nevertheless, CBCT use is becoming increasingly prevalent in primary care, where there is potentially less supervision and a range of training and experience among its users (BROWN ET AL. 2014). CBCT can provide acceptable image quality over a wide range of exposures; therefore, the risk of over-exposing the patients, without any improvement in diagnostic image quality exists (KÖRNER ET AL. 2007).

As initially discussed in section **1.3.1**, an awareness of the need to 'tailor' dose according to the specific diagnostic indication, while also considering patient type, has now prompted the evolution from the dose optimisation strategy ALADA toward ALADAIP (DIMITRA Project: Position Statement 2018). Selection criteria guidelines and general dose optimisation guidance serves to aid the practitioner in the appropriateness of CBCT exposure (HPA 2010, EUROPEAN COMMISSION 2012, ESE 2018, MATZEN & BERKHOUT 2019). The pertinence of employing low dose protocols has recently been highlighted (YEUNG ET AL. 2019), with protocols achieving significant dose reductions suggested in the dental disciplines of paediatric dentistry (OENNING ET AL. 2019), orthodontics (HIDALGO RIVAS ET AL. 2015), tooth autotransplantation (TAT) (EZELDEEN ET AL. 2017), periodontology (AL-OKSHI ET AL. 2017) and implant dentistry (ALAWAJI ET AL. 2018). In the process of optimisation, both the acceptable clinical level of the image quality and the radiation dose may differ according to diagnostic tasks (LOFTHAG-HANSEN ET AL. 2011). Although such studies have provided evidence to assist in optimisation efforts for the particular scanner models used, there is no evidence that the objective image quality measurements can be transferred to a different manufacturer's CBCT equipment or even to different models from the same manufacturer. Thus there is a need to identify a threshold level of objective image quality for a specific diagnostic task that might be readily transferable to a different scanner, avoiding the time-consuming assessments used in these research studies.

Within endodontics, limited volume, high resolution CBCT is indicated where the diagnostic yield from conventional radiography is inadequate, such as in cases of complex/atypical anatomy, resorption, perforation and complicated endodontic surgery (EUROPEAN COMMISSION 2012, AAE & AAOMR 2015, ESE 2019). Complex and atypical anatomy is of particular relevance as evaluation of tooth complexity is subjective and because the success of treatment depends on location, negotiation and chemo-mechanical debridement of the entire root canal system prior to filling (CHANG ET AL. 2013, WITHERSPOON ET AL. 2013, KARABUCH ET AL. 2016). Recognised differences in M1M root canal morphology exist due to the anatomic variations of the second mesiobuccal (MB2) canal (WEINE ET AL. 1969, VERTUCCI ET AL. 1984) within which there is an inherent range of complexity (CLEGHORN ET AL. 2006, BRISEÑO MARROQUÍN ET AL. 2015). Of all dental applications of CBCT, endodontics is the one for which a high level of image quality is invariably required (EUROPEAN COMMISSION 2012). Imaging the MB2 root canal anatomy of upper first molars represents a good clinical test of image quality needs of an endodontist. High resolution settings are often selected in such situations, although it is essential to recognise that this is only achieved by changing exposure parameters in ways that increase patient dose, so optimisation of exposures is especially relevant to endodontic practice.

Clinically, image quality is ultimately subjective, being based on whether the diagnostic task can be achieved in the opinion of the reporting clinician. Because of inter- and intra-clinician variability in assessment of radiological images, it is important to relate such subjective assessments to objective measurements of image quality, such as CNR, with the purpose of identifying if minimally acceptable values exist for specific diagnostic tasks that could potentially aid in the process of dose optimisation (PAUWELS ET AL. 2014b). Validated methods of assessing objective and subjective image quality using a SedentexCT phantom and anthropomorphic phantoms respectively have been used in the pursuit of optimizing doses for specific diagnostic tasks (HIDALGO RIVAS ET AL. 2015, AL-OKSHI ET AL. 2017, ALAWAJI ET AL. 2018) but not for identification of root canal anatomy for endodontic purposes. As high resolution protocols may be indicated for CBCT imaging to assess complex root canal anatomy where the diagnostic yield from conventional imaging has proved insufficient for treatment planning (EUROPEAN COMMISSION 2012), in addition to studying the impact of altering tube voltage and tube

current-exposure time product, this study planned to investigate the effect of available scanning protocols including high resolution and 180° scans on achieving this clinical task.

2.2 AIMS & OBJECTIVES

The principle aim of this study is to identify a threshold dose for CBCT which is as low as diagnostically acceptable for adequate imaging of MB2 root canal anatomy of M1Ms and additionally, to quantify the objective image quality at this threshold dose. By performing this using two scanner types, some insight into the transferability of the results would be obtained. Additional aims included investigating the impact of anatomy complexity on establishing this threshold dose and examining the impact of operator experience on diagnostic efficacy. Consequently the overall objectives of this thesis are:

1. To determine the radiation dose, as measured by DAP, for a range of combinations of tube voltage and tube current-exposure time product in CBCT using two different scanners: Accuitomo 170 (J. Morita, Kyoto, Japan) and ProMax 3D Classic (Planmeca, Helsinki, Finland) at the smallest available voxel size of each scanner.

2. To determine objectively the image quality, as measured by CNR at the exposure combinations used in 1. using a commercially available image quality phantom for CBCT.

3. To manufacture an anthropomorphic phantom containing maxillary molar teeth with a range of complexity of MB2 canal morphology and to image it using the two scanners for the range of exposure combinations used in 1. and 2.

4. To measure the diagnostic efficacy of observers, of differing experience level, in identifying the MB2 canal anatomy using the CBCT images obtained in 3., along with recording their subjective image quality assessment of the images.

5. To identify, for each scanner, the combination of exposure parameters giving the lowest achievable dose, consistent with an adequate level of diagnostic efficacy and without observing a significant loss of subjective image quality.

6. To use the information to suggest a threshold level of objective image quality and radiation dose for each CBCT scanner when used for imaging root canal anatomy and to compare the concordance between the two scanners in the objective image quality threshold.

2.3 MATERIAL AND METHODS

2.3.1 Sample selection and preparation

Ethical approval for the use of pooled extracted teeth in this study was obtained from St. James' Hospital/Tallaght University Hospital (SJH/TUH) Joint Research Ethics Committee (Reference number 2019-02 Chairman's Action [05]). M1Ms were selected from a bank of extracted teeth. After extraction the teeth were washed with water and the adherent tissue removed gently, before being immersed in a 2% sodium hypochlorite solution (Milton solution, Proctor & Gamble Ireland, Dublin, Ireland) for 24 hours prior to storage in a sterile saline solution until ready to use. Inclusion requirements included M1Ms (as identified by their coronal and root anatomic-morphological appearance) of normal external anatomy, a mesio-distal crown diameter of 10 mm ± 0.2 (JORDAN ET AL. 1992), three mature distinct roots with closed apices, absence of root fracture, caries or resorption, a complete pulpal floor and no evidence of previous root canal treatment. The 12 left maxillary molars which visually appeared at this point to fit these criteria were imaged using the ProMax 3D Classic CBCT scanner to confirm the inclusion characteristics and subsequently three left maxillary molars of varying MB complexity were provisionally selected.

2.3.1.1 MicroCT analysis

In order to confirm the presence of a MB2 canal and identify the root canal system complexity of the MB root, these three left maxillary molars were subjected to further analysis using a microCT scanner (µCT 40 SCANCO Medical AG, Brüttisellen, Switzerland) (**Figure 2.1**). MicroCT analysis was completed at 70 kVp, 114 mA, 8 W with a spatial resolution of 20 µm. For each tooth, a microCT 3D model of the root canal system was constructed with 3D IPO image processing language (version 5.15, Scanco Medical, Brüttisellen, Switzerland). The reconstructed microCT 3D models of the root canal systems and 2D slices (n = 502 per tooth) were viewed independently by two endodontists (defined as individual who has completed a three-year full time training in endodontics) who by consensus, confirmed the teeth as M1Ms. In order to facilitate comparison between the three teeth, the diameter of the main trunk of the MB2 canal was measured. The maximum width of the MB2 canal in the coronal third was; T6 - 760

µm; T7 - 710 µm; T8 - 735 µm and the minimum diameter, which was either in the middle or apical third of the root was; T6 - 200 µm; T7 - 145 µm; T8 - 163 µm. Subsequently, the canal number, configuration and complexity of the MB2 canals of each of the three maxillary molars were determined and classified accordingly.

FIGURE 2.1 MicroCT scanner: 40 SCANCO Medical AG, Brüttisellen, Switzerland used to obtain microCT 3D model of the root canal system.

Specifically, the root canal systems of three representative M1Ms were classified into simple, moderate and complex morphology as seen in **Figure 2.2a-c**. The 'root canal system' was defined as arising from an orifice(s) in the pulp floor, continuing through the canal(s) to the apically positioned foramen (or foramina) (AHMED ET AL. 2017). The maxillary molar positioned in the skull in the first molar position was named T6, (**Figure 2.2a**). The MB2 root canal system of T6 originated from one orifice in the pulpal floor, before the MB1 and MB2 canal splits 1-2 mm apical to the pulp floor in the coronal third of the root. The MB2 canal re-joined the MB1 canal in the coronal aspect of the mid-third of the root before terminating in one foramen. This is a common anatomical variation that is relatively easy to manage and was therefore classified to be of simple complexity. The M1M in the second molar position in the skull was named T7 (**Figure 2.2b**). The MB2 root canal system of T7 originated from two orifices in the floor

of the pulp chamber and terminated just short of the MB1 in the apical third of the root. Tooth T7 exhibited an added anatomical feature of an anastomosis between the MB1 and MB2 in the mid-root area and, as a result T7, was considered to be of simple to moderate complexity. The M1M occupying the third molar position in the skull was called T8 (**Figure 2.2c**). The MB root canal system of T8 exhibited three separate MB canals (MB2 and MB3 [within the MB2 complex]), with multiple connections between the MB2, MB3 canals and MB1 canal in the middle third of the root. Consequently, T8 was classified as having complex anatomy, being categorized as high difficulty with respect to diagnosis and treatment (AAE 2006).
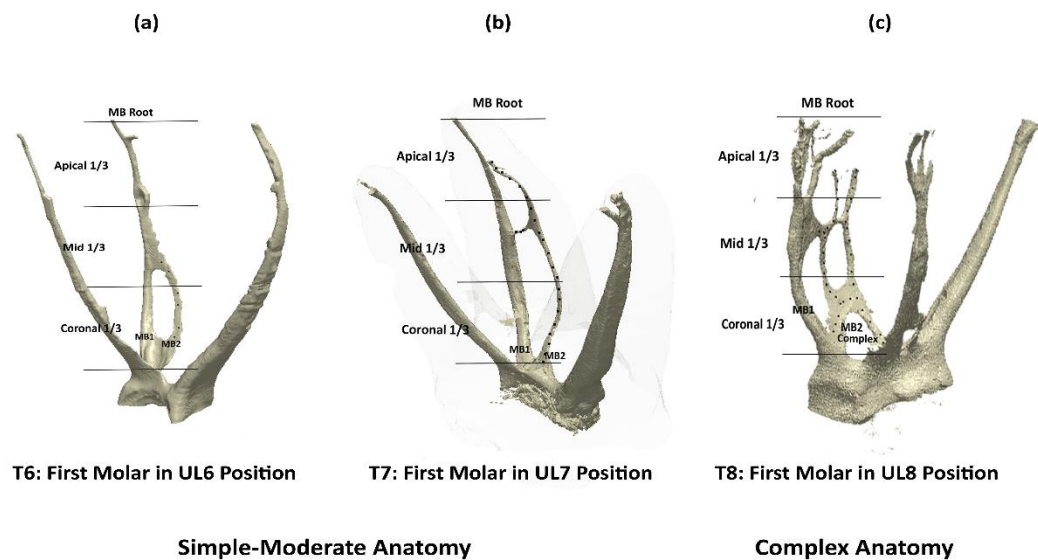
FIGURE 2.2. MicroCT 3D models of the root canal systems of the three maxillary molars: **(a)** T6 **(b)** T7 (simple-moderate anatomy) and **(c)** T8 (complex anatomy) constructed with 3D IPO image processing language (version 5.15, Scanco Medical, Brüttisellen, Switzerland).

2.3.2 CBCT scanners and selected exposure parameters

Two scanners were selected to perform CBCT imaging: Accuitomo 170 and ProMax 3D Classic. The smallest available voxel size and FOV option applicable to each scanner were selected according to the manufacturers' guidelines for endodontic imaging:

- Accuitomo 170 (Accuitomo): 40 mm (D) x 40 mm (H): 80 µm
- ProMax 3D Classic (ProMax): 50 mm (D) x 50 mm (H): 100 µm

There were 33 different scanning protocols for the Accuitomo: manually selected X-ray tube voltages of 70, 80, 90 kV and X-ray tube current selections included 3, 5, 7 and 9 mA. These combinations were completed using a full rotation 360° at normal (17.5

seconds) and high resolution (30 seconds) settings and then again at 180° (9 seconds). For the ProMax scanner the same X-ray tube voltages 70, 80, 90 kV were manually used, with X-ray tube currents of 3, 5, 7.1 and 9 mA, which were the closest possible options to the Accuitomo that could be manually selected. This resulted in 12 exposure combinations for the ProMax scanner. Rotations of 180° and high resolution options altering time alone were not features of the ProMax scanner available. These combinations represent a wide range of exposures, including those employed in clinical practice and recommended in manufacturer protocols for endodontic imaging.

2.3.3 Dose measurements

Dose measurements were performed on each CBCT scanner for the chosen exposure settings. DAP values (μGycm^2) were obtained using a DAP meter sensor (**Figure 2.3**) with an active area of 7cm (VacuDap; VacuTech Messtechnik GmbH, Dresden, Germany) positioned at the centre of the X-ray tube window; completely intercepting the radiation field (4x4cm: Accuitomo and 5x5 cm: ProMax) for all combinations of tube voltage and current-time exposure product. For the Accuitomo this resulted in 33 DAP values (as exposures at 9 mA were not possible at high resolution setting) and 12 DAP values for the ProMax. To assess consistency of the units, the DAP values were repeated and recorded four times for 80 kV, 5 mA at normal and high resolution where applicable and the coefficient of variance calculated.

FIGURE 2.3 DAP meter used to obtain DAP values at the exit of the X-ray beam.

2.3.4 Image quality: Objective measurement

To assess objective image quality, contrast resolution was measured using the SedentexCT IQ phantom (Leeds Test Objects, Boroughbridge, UK): 162 mm (H) x 160 mm (D) along with the corresponding polytetrafluoroethylene (PTFE) insert, consisting of five rods of PTFE of differing diameters (1, 2, 3, 4 and 5 mm) embedded in polymethylmethacrylate (PMMA). The PTFE insert was selected as being representative of dental hard tissue (HIDALGO RIVAS ET AL. 2015, AL-OKSHI ET AL. 2017)

The insert was positioned in the upper left molar region in the phantom (as per position of experimental teeth in skull) and the remaining phantom columns in the SedentexCT IQ were filled with PMMA inserts (**Figure 2.4**). The dedicated dental CBCT phantom was mounted on a rigid tripod and positioned as per standard patient set-up. In total all inserts were scanned individually at all exposure protocols for Accuitomo (x33) and ProMax (x12).
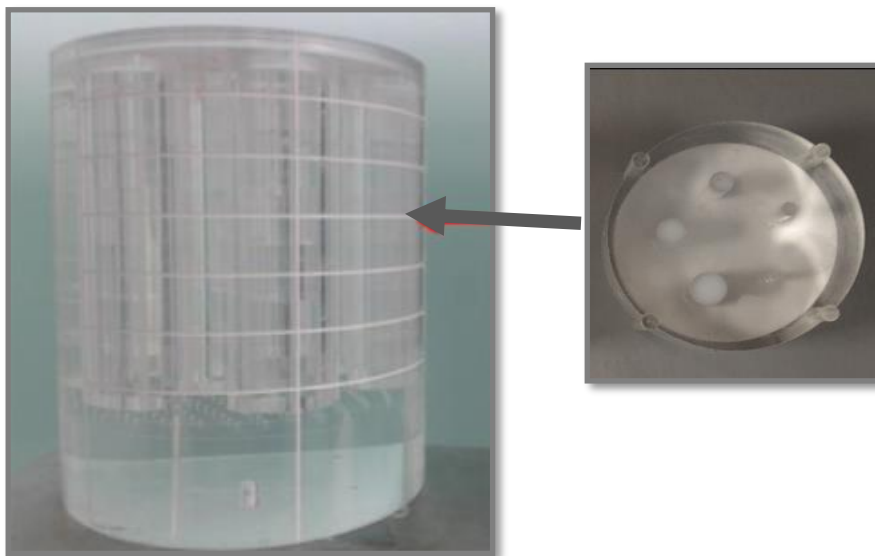
FIGURE 2.4 SedentexCT phantom (left) and PTFE (insert (right) placed in phantom and scanned to measure objective image quality.

2.3.4.1 Calculating CNR

To assess contrast resolution and calculate CNR for all the imaging protocols, the PTFE insert was scanned individually for every exposure protocol for both the Accuitomo (x33) and the ProMax (x12), as described above. The resulting 45 data sets were individually exported as DICOM files into Image J software v. 145s (National Institute of Health, Bethseda, USA). Axial images were analysed at a 16-bit scale. On these images

a circular region of interest (12 mm²) was drawn on the 5 mm diameter rod of the PTFE insert (**Figure 2.5a**) and another in the background PMMA (**Figure 2.5b**) thereby enabling pixel value calculation of each material. Beginning at the centre of the 5 mm rod and moving upwards (to avoid possible interference in pixel values created by the air gap between the test insert and the blank PMMA) measurements were performed on five consecutive axial images.
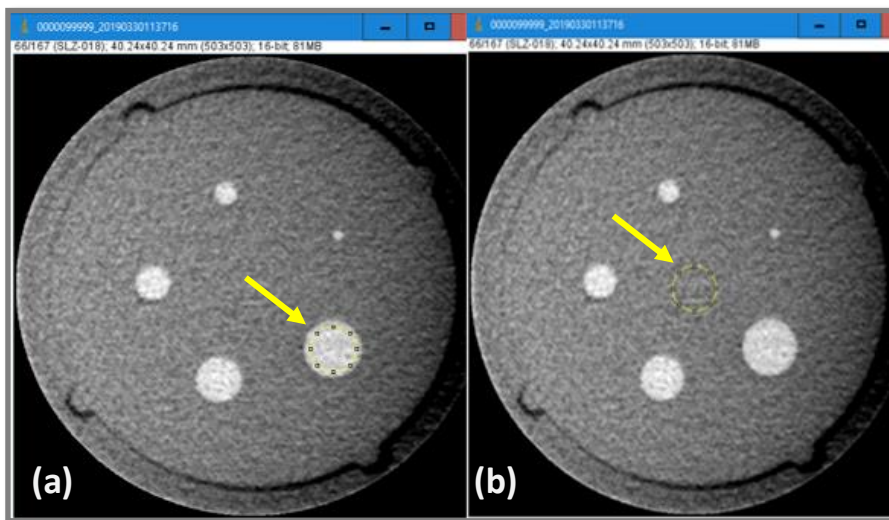
FIGURE 2.5 Images from ImageJ software of the scanned PTFE test insert enabling evaluation of the pixel values in the centre of the PTFE 5mm rod **(a)** and in the background PMMA **(b)**.

For each scanning protocol the mean and standard deviation (SD) of the pixel values from the five slices were recorded for the PTFE rod and background material and CNR calculated using the formula:

$$CNR = \frac{(MPV_{insert} - MPV_{background})}{\sqrt{(standard\ deviation^2{}_{insert} + standard\ deviation^2{}_{background})/2}}$$

2.3.5 Image quality: Subjective measurement

The three selected left maxillary molars were mounted in a dried adult skull (obtained from the Anatomy Department of Trinity College Dublin) from which the existing molars had been carefully extracted by sectioning the roots to avoid damage to surrounding bone. Mounting of the three teeth selected for the study involved careful osteoplasty of the alveolar bone using a stainless steel rosehead bur in a slow-speed handpiece to acquire a best possible fit, prioritising the buccal roots' position. The three study teeth were maintained in place with a modelling wax, which lacked radiopacity. The skull and implanted teeth were positioned in a head-shaped polystyrene container, specifically designed to house the skull morphology along with cervical spine (C1-C4) and immersed in water to simulate soft tissue density (**Figure 2.6**). This anthropomorphic phantom is a validated method, designed and used in previous studies (SHELLEY ET AL. 2011, HIDALGO RIVAS ET AL. 2015) designed to replicate the clinical scenario as much as possible with the skull and cervical spine (C1-C4) also being soaked in water for 48 hours before imaging to ensure water had displaced air from all trabecular spaces.

The container design facilitated fixation to a tripod stand and allowed positioning as for a patient set-up with initial scout images confirming centring of the FOV on the upper left molar region. The phantom was then exposed to all 33 scanning protocols as described for the Accuitomo scanner, this being completed in one session ensuring imaging consistency. This same protocol was repeated exactly for all 12 scanning combinations described for the Promax scanner.
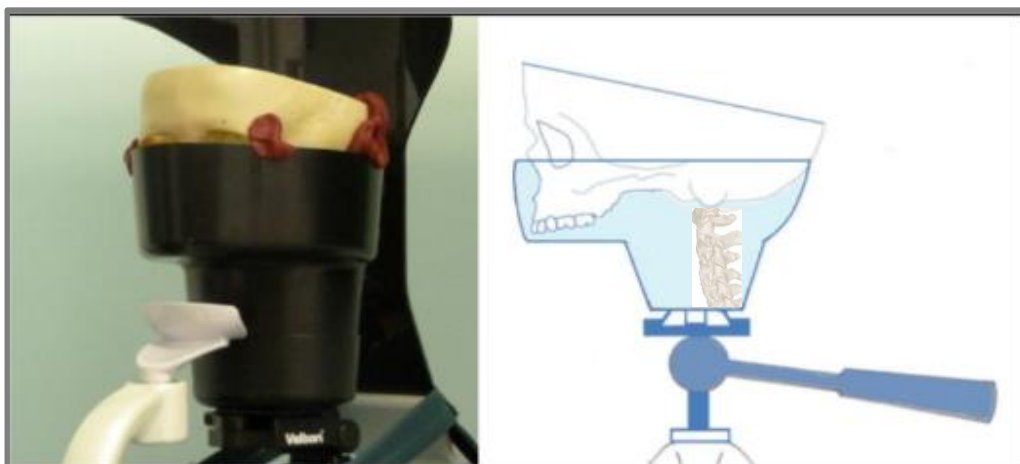
FIGURE 2.6 Positioning of anthropomorphic phantom in CBCT scanner (left), diagrammatic image of skull in water bath to simulate soft tissue (right).

2.3.6 Image evaluation

Including both scanners, there were 45 CBCT datasets available for observation, additionally 9 datasets (20%) were randomly selected and duplicated within the study sample to assess intra-observer variability, the observer being blinded to the duplicates. The resulting 54 datasets were randomized (via a downloaded internet programme: https://app.studyrandomizer.com/); volume acquisition parameters anonymized and each allocated a number 1-54.

Images were viewed with the viewing software provided by the manufacturer; Accuitomo datasets using i-Dixel One Volume Viewer software (Morita, Japan) and the ProMax datasets viewed using Planmeca Romexis software (Helsinki, Finland). Evaluation of the images was facilitated using a new Acer V176LBMD 17" HD Ready Monitor, with luminance of 250cd/m², dynamic contrast ratio of 100000000:1 and resolution of 1280x1024 pixels. These technical specifications are within the range indicated by the Health Protection Agency (HPA) as required for diagnostic purposes of dental CBCT images (HPA 2010). The monitor was DICOM-calibrated to comply with the DICOM GSDF (Greyscale Standard Display Function) standard (GRIMSTEAD & AVIS 2009). Evaluation of the monitor using a test pattern (Society of Motion Picture and Television Engineers test pattern [SMPTE]) was carried out to determine that each distinct greyscale levels could be appreciated and the elements of the resolution test patterns could be individually resolved.

Subjective evaluation of image quality was performed by nine observers; three radiologists, three endodontists and three junior hospital dentists (JHDs). The observers were informed that the purpose of the study was to evaluate the effect of differing acquisition parameters on identification of MB2 canal anatomy in M1Ms. All observers had exposure to CBCT image interpretation and software. Nonetheless, due to their differing skill sets, range of CBCT interpretation experience and familiarity with the two viewing software systems utilized in the study, a standardized interactive tutorial was given prior to the observation and reinforced with a printed document. Viewing conditions for all observers were consistent. Ambient room lighting was recorded using an illuminance metre and ensured that this was less than 50 lux. Observers were able to adjust contrast and brightness as required and to rotate and tilt the volumetric data

using the three orthogonal reconstructions (axial, coronal and sagittal) (**Figure 2.7**). No time restriction was placed on the period of observation.
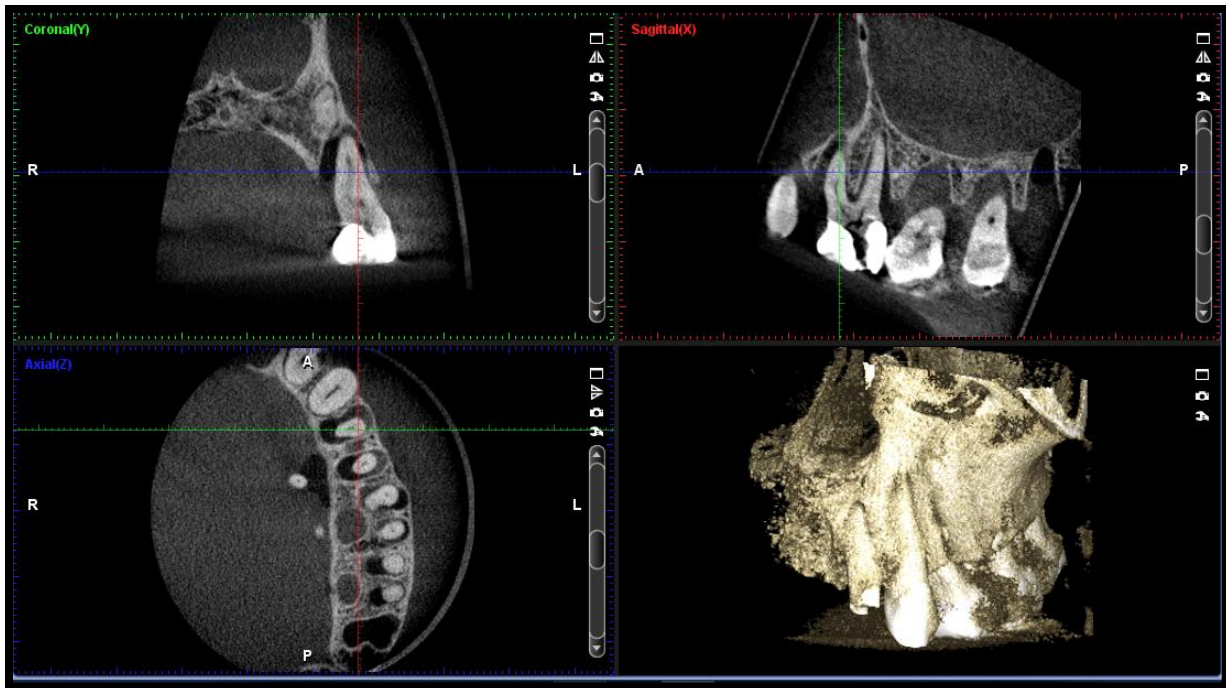
FIGURE 2.7 ProMax 3D Classic volume (viewed with Romexis software) of the three implanted maxillary molars which were evaluated in all three orthogonal planes to identify the presence and extent of the MB2 canal at the exposure parameters of that image set (80Kv, 5mA).

Each observer completed a seven-part questionnaire (summarised **Table 2.1**) which they answered using a five-point Likert rating scale of agreement for each of the three M1Ms, circling the number which corresponded to their answer. Questions (Q's): 1-5 related to the visibility of the MB2 anatomy in the coronal, mid and apical thirds of the tooth and Q6 related to the confidence the observer had in the diagnostic acceptability of the volume. A final required task involved tracing the extent of the MB2 canal that they could definitively identify from the image set for each of the three teeth, over the included microCT images of the molar anatomy. These tracings of the anatomy were then measured using a calibrated acetate overlay and a resulting percentage of the MB2 anatomy identified (recorded as a percentage of the total length as seen on microCT) and assigned to each of the three maxillary molars per volume. To assess repeatability of this technique, five randomly chosen datasets were selected to repeat the measurements.

The observers had been familiarized with the questionnaire as part of the instruction tutorial.

2.3.6.1 Pilot study

The questionnaire was piloted by two endodontists and two JHDs (three of which participated in the study), they evaluated ten randomly chosen datasets and their feedback on the instructions and questionnaire was used to refine the final documents.

Can you identify a **separate** second mesiobuccal canal (MB2) in the root anatomy for each maxillary first molar: **Q1**- At level of pulp floor? **Q2**- Within coronal third? **Q3**- Within mid-third? **Q4**- Within apical-third?	**0= No - Complete Confidence** **1= No - Partial Confidence** **2= Unsure** **3= Yes - Partial Confidence** **4= Yes – Complete Confidence**
Q5- If identified, is the MB2 canal continuously visible from its perceived origins coronally to its termination?	
Q6- Are you confident that this volume is diagnostically acceptable?	
Q7- For each volume 1-54, can you trace over the microCT depiction of the MB2 canal anatomy that you can **definitively identify** from the image set for the first molar teeth in positions UL6, UL7, UL8 with the provided red pen.	

TABLE 2.1 Summary of questionnaire with a rating scale to reflect the confidence the observers had in their response.

2.3.7 Data analysis

Diagnostic acceptability (Q6) responses for each of the 45 datasets (excluding repeats) were examined and if the percentage of observers recording a scan as diagnostically acceptable (i.e. agreed or strongly agreed options) fell below 67% (i.e. 6 out of 9 observers), it was considered a negative result and was excluded from further analysis.

Assessment of pilot study results identified target levels for specific subjective imaging tasks: identification of the overall proportion (%) of MB2 root canal identifiable and secondly for both confidence in the presence of the canal at the different levels of the root (Qs 1-4, **Table 2.1**) and in identification of canal continuity (Q5, **Table 2.1**).

On analysis of percentage of MB2 root canal anatomy identified by each observer for each of the three M1Ms at every diagnostic exposure protocol in the pilot study, a target subjective image task was provisionally set as identifying 95% of the MB2

canal anatomy. This task included identification of the canal at the level of the pulp chamber floor and the coronal third of the MB root, which by consensus was deemed most relevant from an endodontist's perspective.

Employing the confidence scale ratings from questionnaires for diagnostic exposure protocols from the pilot study, the median of the observers' confidence scale rating (CSR) responses for the identification of the MB2 canal for Q's 1-4 at the level of the pulpal floor and in the coronal, middle and apical thirds of the root were identified for each of T6, T7 and T8. Similarly, the median CSR responses related to Q5: identification of a continuous MB2 canal from perceived origin to termination, were established. Using these data, a second target subjective image task of achieving median CSRs of 3.5 was set from the pilot study. This corresponded to greater than or equal to 95% MB2 canal anatomy identification, achieving close to complete confidence in identifying the MB2 canal in all thirds of the root canal and identifying the MB2 canal continuously from origin to its termination.

These combined subjective image tasks were used to indicate the CNR values necessary to achieve the diagnostic task of root canal identification and from which the corresponding threshold exposure factors and DAP values could be identified.

2.3.7.1 Statistical analysis

Statistical analysis was performed using IBM SPSS Statistics (Version 24.0; IBM Corporation, Chicago, USA). Intra observer and inter observer agreement of subjective image quality assessment was calculated using Cohen's Kappa test (K) using the scale for strength of agreement described by Altman (ALTMAN 1990) (**Table 2.2**).

Value of K	Strength of agreement
≤ 0.20	Poor
0.21 - 0.40	Fair
0.41 - 0.60	Moderate
0.61 - 0.80	Good
0.81 - 1.00	Very good

TABLE 2.2 Altman's (1990) strength of agreement scale to facilitate interpretation of Kappa values.

Intra observer agreement was calculated for each of the observers by considering their responses for Q's 1-5 (identification of root canal anatomy) in the questionnaire and also separately for Q6 (diagnostic acceptability of the datasets). To facilitate the analysis, the responses to the six questions were dichotomized, with values 4 and 5 considered as a positive result while 1, 2 and 3 were considered as negative result (GIJBELS ET AL. 2001, HIDALGO-RIVAS ET AL. 2015). Inter observer agreement was evaluated for Q's 1-6 separately. The proportion of acceptable/unacceptable images identified by the JHDs and senior staff (endodontists and radiologists) was calculated. Contingency tables and a Chi-squared test was used to determine statistical significance of the difference in proportions of these two groups with statistical significance set at $p<0.05$.

2.4 RESULTS

2.4.1 Dose measurements

DAP values for the ProMax (**Table 2.3a**) and Accuitomo (**Table 2.3b**), demonstrate expected variations according to exposure settings. DAP value reproducibility for the ProMax scanner, based on four measurements at 80 kV and 5 mA resulted in a (SD) of ± 0.96 mGy cm². For the Accuitomo, reproducibility at 80 kV and 5 mA for both standard and high resolution settings had a resulting SD ± 1.07 and ± 1.39 mGy cm² respectively.

DAP Values (mGy cm²)			
Tube Current		Tube operating potential (kV)	
mA	**mAs**	**70**	**80**	**90**
3.2	**38.4**	49.5	90.3	135.3
5	**60**	77.1	139.4	209.3
7.1	**85.2**	107.6	195	294
9	**108**	134.4	244.6	373.3

TABLE 2.3a Dose-area product (DAP) values recorded using the ProMax 3D Classic scanner, expressed in mGy cm² for all combinations of tube operating potential (kV) and tube current-exposure time product (mAs [mAs = mA x time]) used in this study. All scans were performed using a full rotation of 200° at an exposure time of 12 second.

DAP Values (mGy cm²)												
Tube Current				Tube operating potential (kV)								
mA	**mAs**			**70**			**80**			**90**		
	180°	**S**	**HR**	**180°**	**S**	**HR**	**180°**	**S**	**HR**	**180°**	**S**	**HR**
3	**27**	**52.5**	**92.4**	54.3	106.4	187.5	72.3	143.8	251.2	90.5	181.7	316.8
5	**45**	**87.5**	**154**	88.5	174.9	306.7	118.0	233.9	409.5	147.1	294	517.5
7	**63**	**122.5**	**215.6**	120.9	240.7	426.3	163.2	324.4	568.9	203.2	405.1	714.4
9	**81**	**157.5**	**277.2**	154.6	304.6	N/A	207.9	410.5	N/A	257.6	520.2	N/A

TABLE 2.3b. Dose-area product (DAP) values recorded using the Accuitomo 170, expressed in mGy cm² for all combinations of tube operating potential (kV) and tube current-exposure time product (mAs) used in this study. All standard (S: 17.5 seconds) and high resolution scans (HR: 30.8 seconds) were performed using a full rotation of 360° with a third set of scans performed at a reduced rotation of 180°. N/A: setting not permitted by the scanner

2.4.2 Image quality: Objective measurement

Figure 2.8a & b relate CNR values to DAP values for the ProMax and Accuitomo scanners respectively. This approximates to a second order polynomial relationship. **Figure 2.8b** demonstrates that high resolution settings achieve comparatively lower CNR values than the standard and 180° scans for the Accuitomo at equivalent DAP. CNR values are notably lower for the Promax compared with the Accuitomo at equivalent kV and mA protocols (**Figure 2.8a & b**).
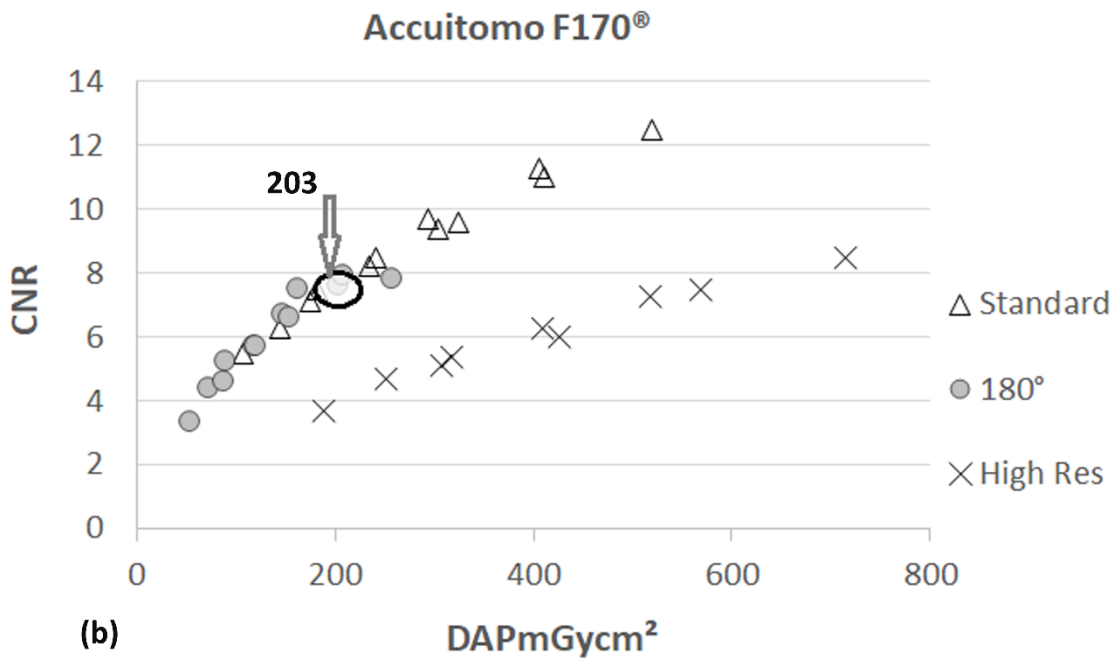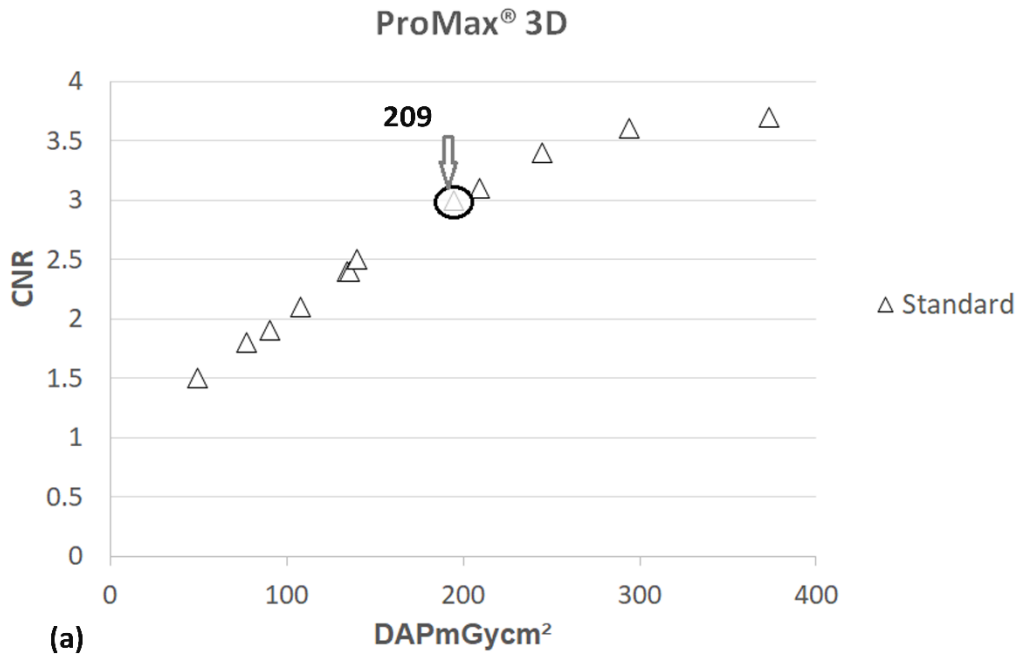
FIGURE 2.8 Contrast-to-noise ratio (CNR) values plotted against dose-area product (DAP) values for **(a)** ProMax 3D Classic and **(b)** Accuitomo 170. Additionally, the DAP values corresponding to the CNR value necessary to achieve the combined subjective image tasks for root canal identification are highlighted.

2.4.3 Image quality: Subjective measurement

Kappa values for intra observer agreement are detailed in **Table 2.4**. JHDs demonstrated fair-moderate strength of agreement (κ = 0.31-0.56), while senior staff (radiologists and endodontists) exhibited good-very good strength of agreement (κ = 0.65-1) for questions relating to identification of root canal anatomy and continuity of the canal (Q1-5) as well as the diagnostic acceptability of the datasets (Q6). Inter observer agreement for questions relating to root canal anatomy identification (Q2-5) and diagnostic acceptability (Q6) ranged from moderate to good (κ = 0.45-0.58). Levels of agreement were only fair for Q1: identification of the MB2 canal at the level of the pulp chamber floor (κ = 0.27).

Observer Code	END1	END2	END3	RAD1	RAD2	RAD3	JHD1	JHD2	JHD3
Kappa Values: Q's 1-5	0.65	0.69	0.71	0.67	0.73	0.69	0.50	0.51	0.56
Kappa Values: Q6	0.73	1	0.76	1	1	0.76	0.31	0.55	0.53

TABLE 2.4 Intra observer agreement of the nine observers (END=Endodontist, RAD= Radiologist, JHD= Junior hospital dentist) for Q's 1-5 (root canal anatomy identification and continuity) and Q6 (diagnostic acceptability), measured using Kappa.

The proportion of datasets judged as being of acceptable/unacceptable image quality (Q6) by the radiologist and endodontists were similar, being 84%/16% and 81%/19% respectively, but differed from the judgments of JHDs; 67%/33%. Using the Chi square test, a significant difference was identified (p=0.043) with JHDs classifying significantly more images as undiagnostic compared with senior staff.

   Tables 2.5a & b show the results of the subjective image quality assessments for ProMax and Accuitomo respectively at each exposure protocol and corresponding DAP value. Four scans taken using the ProMax and four using Accuitomo were categorized as undiagnostic and excluded from further analysis.

(a)

mA	mAs	...		

(a) DAP Values				
Tube Current		Tube Voltage (kV)		
mA	mAs	70	80	90
3.2	38.4	49.5	90.3	135.3
5	60	77.1	139.4	209.3
7.1	85.2	107.6	195	294
9	108	134.4	244.6	373.3

(b) DAP Values											
Tube Current			Tube Voltage (kV)								
	mAs			70			80			90		
mA	180°	S	HR	180°	S	HR	180°	S	HR	180°	S	HR
3	27	52.5	92.4	54.3	106.4	187.5	72.3	143.8	251.2	90.5	181.7	316.8
5	45	87.5	154	88.5	174.9	306.7	118.0	233.9	409.5	147.1	294	517.5
7	63	122.5	215.6	120.9	240.7	426.3	163.2	324.4	568.9	203.2	405.1	714.4
9	81	157.5	277.2	154.6	304.6	N/A	207.9	410.5	N/A	257.6	520.2	N/A

TABLE 2.5 For ProMax 3D Classic **(a)** and Accuitomo 170 **(b)** Dose-area product (DAP) values and associated exposure protocols of datasets that observer assessment identified as being:

Undiagnostic: ▮

Diagnostic: ▯

Diagnostic and achieving 'combined target subjective image tasks': ▯

On analysing the percentage of MB2 root canal anatomy identified by each observer for the 37 diagnostic datasets, for simple-moderately complex anatomy, senior staff consistently identified a marginally increased percentage (0-7.2%) of MB2 root canal anatomy than junior staff; the difference was not evident at the highest DAP values for both scanners (**Appendix I**). This trend between junior and senior staff was repeated for complex anatomy, but with margin of difference increasing (1.9-18.1%); however, for complex anatomy, increasing the DAP values did not reduce the differences between junior and senior staff in the percentage of canal identified. Agreement within both groups was greatly reduced for complex anatomy, as reflected by their greatly increased SD values.

Repeatability assessment of the recording of the percentage of canal identified using the five repeat volumes (15 teeth) demonstrated that while 10 teeth showed no difference from the original recording, five teeth exhibited a small variation ranging from 1-1.7%.

2.4.4 CNR values necessary to achieve diagnostic task of root canal identification

Figure 2.9a & b highlight that the percentage of MB2 canal anatomy identified increased along with CNR values. The target subjective image task of identifying ≥ 95% of the MB2 canal anatomy corresponded to a CNR of 3 for simple to moderate anatomy (T6, T7) for the ProMax and a markedly different CNR of 7.6 for the Accuitomo scanner. The target subjective image task was not achieved at any DAP value for complex anatomy (T8).
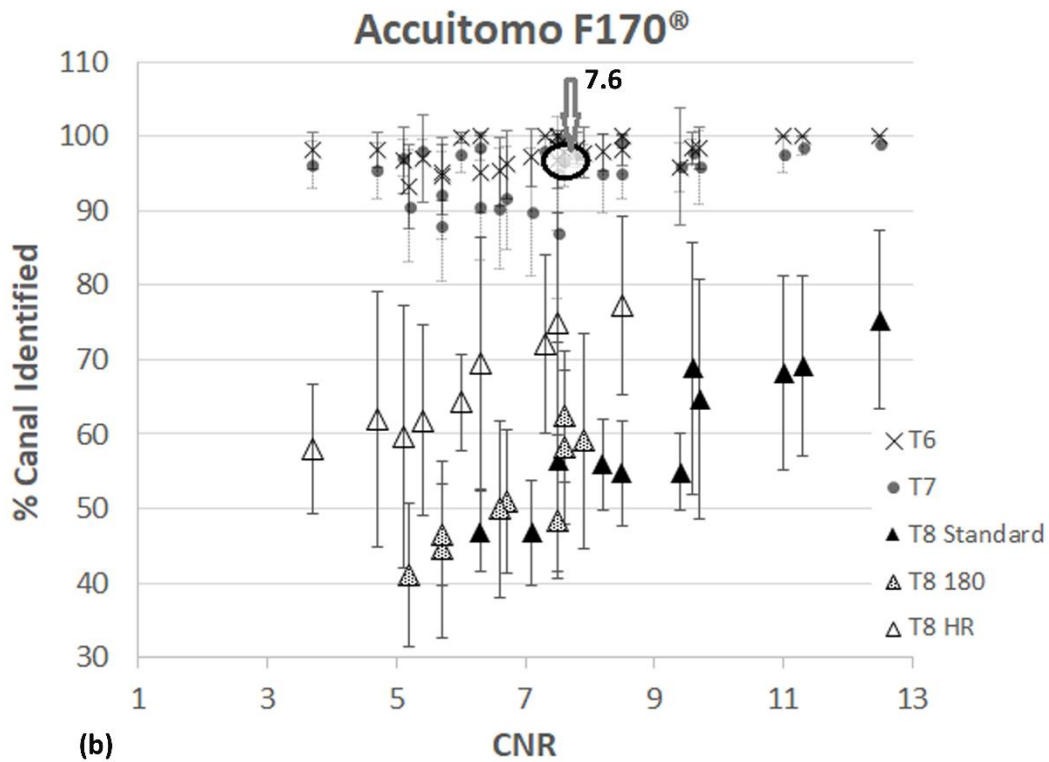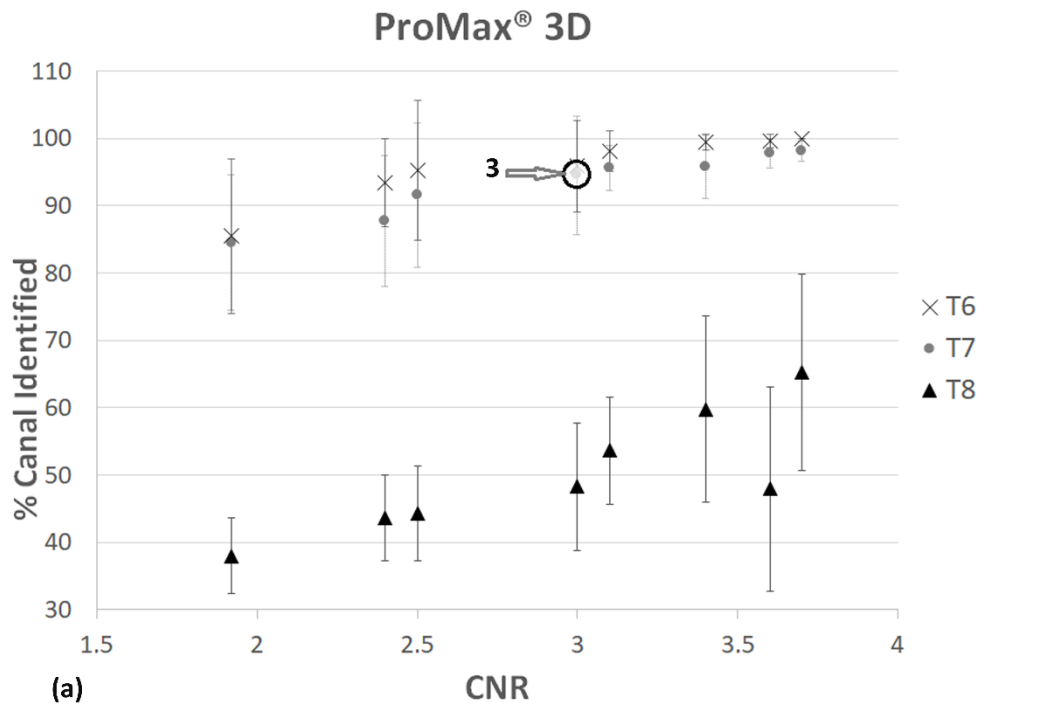
FIGURE 2.9 Mean percentage of MB2 canal anatomy identified by all observers related to contrast-to-noise ratio (CNR) values, calculated for each exposure protocol judged as diagnostically acceptable for **(a)** ProMax 3D Classic and **(b)** Accuitomo 170. Regarding simple-moderate anatomy, a CNR of ≥ 3 and ≥ 7.6 were necessary to achieve the subjective task (i.e. identifying ≥ 95% MB2 canal anatomy) for the ProMax 3D and Accuitomo 170 respectively.

The second subjective task of achieving median CSR's ≥ 3.5 for Q's 1-4 and Q5 were related to CNR for both scanners and are depicted in **Figure 2.10a-d**. With the ProMax scanner; for simple-moderate anatomy, achieving median CSR responses of ≥ 3.5 occurred at a CNR of 3 for both identifying the MB2 canal in all thirds of root canal anatomy (Q's 1-4) and for identifying it as continuous from perceived origin to termination (Q5) and at 3.6 and 3.7 respectively for complex anatomy (**Figure 2.10a & b**). For the Accuitomo scanner, median CSR responses of ≥ 3.5 for both tasks Q1-4 and Q5 for simple-moderate anatomy corresponded to a CNR value of 7.5 and 7.3 respectively and at 8.5 and 11.3 values for complex anatomy (**Figure 2.10c & d**).
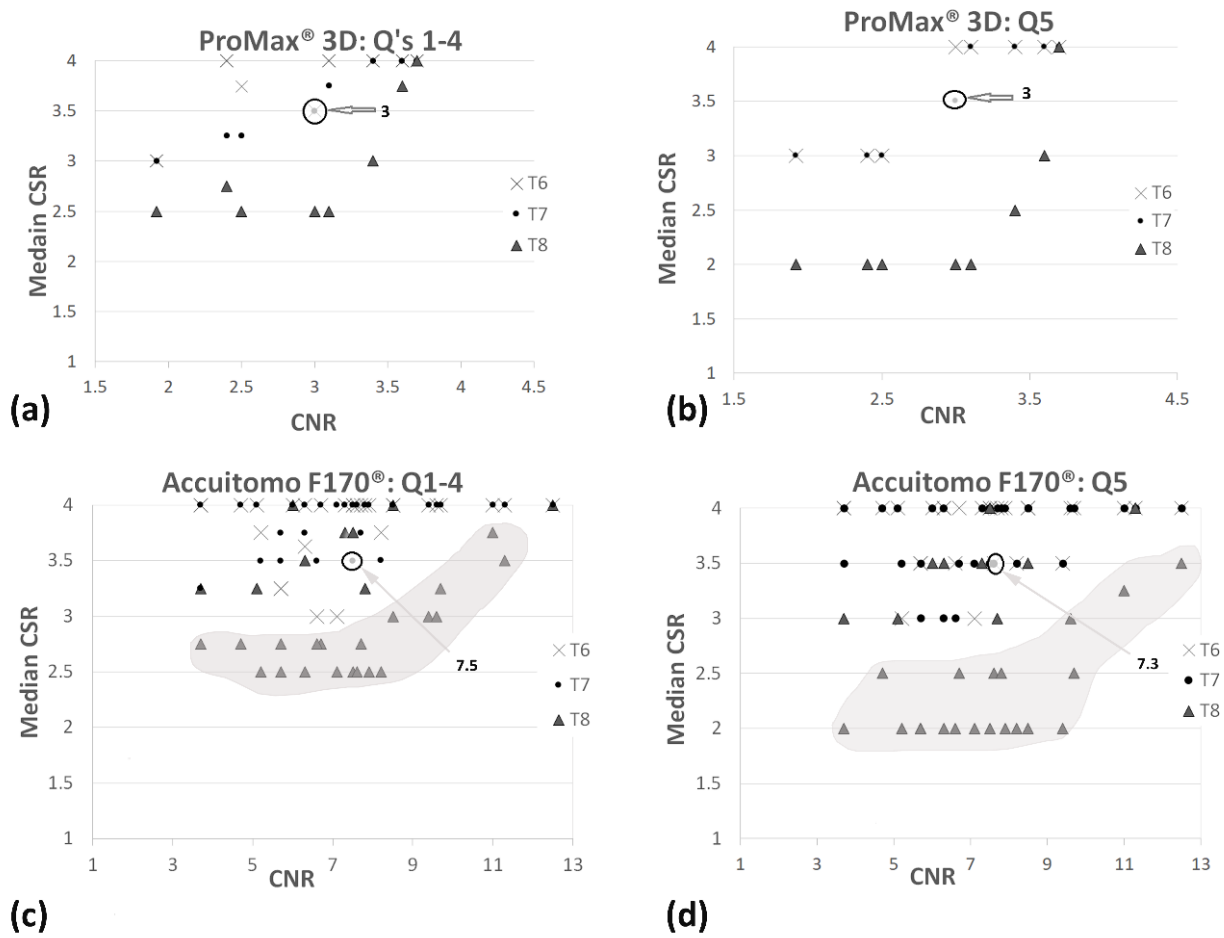
FIGURE 2.10 Median of the observer confidence scale ratings (CSRs) related to contrast-to-noise ratio (CNR) for Qs 1-4 **(a)** and Q5 **(b)** for ProMax 3D Classic and Q1-4 **(c)** and Q5 **(d) for** Accuitomo 170. Regarding simple-moderate anatomy, achievement of the second subjective task (median CSRs of ≥ 3.5) was possible at a CNR of 3 for the ProMax 3D for both Qs 1-4 and Q5 and 7.5 and 7.3 respectively for the Accuitomo 170. Shaded areas outlined in **(c)** and **(d)** highlight the trend of markedly lower median CSRs scored with complex anatomy compared with simple-moderate anatomy.

2.4.5 Identifying DAP and exposure protocols that correspond with threshold CNR values

As shown in **Figure 2.8a &b**, the DAP values necessary to achieve the combined subjective image tasks for simple-moderate MB root canal complexity (T6, T7), were 209.3 and 203.2 mGy cm² for Promax 3D and Accuitomo scanners respectively. For complex anatomy (T8), this subjective image task was not achieved, even at the highest DAP values for both scanners.

For M1Ms exhibiting simple-moderate root canal complexity, **Table 2.5a & b** summarise the exposure protocols and resultant DAP values that were considered undiagnostic, diagnostic and those which were at or above the 'threshold dose' to achieve the combined 'target subjective image quality tasks'. For the ProMax the threshold dose (≥209.3 mGy cm²), included 90 kV protocols of 5mA and above and one 80 kV/ 9 mA protocol (**Table 2.5a**). For the Accuitomo, the threshold dose (≥ 203.2 mGy cm²) was achieved for a range of protocols (**Table 2.5b**). Only three 180° scan protocol at the higher range of the kV and mA protocols were identified as achieving these combined 'target subjective image quality tasks'. Conversely all high resolution Accuitomo scans reached this level of subjective image quality, except at the lowest kV and mA experimental selection. These tables do not include complex anatomy (T8) as the combined subjective task was not achieved at any experimental DAP value.

2.5 DISCUSSION

This purpose of this study was to ascertain whether a threshold level of image quality, and hence an optimised dose level, could be established for the accurate identification of root canal anatomy using CBCT imaging, a diagnostic task which is believed to necessitate high image detail and an associated increase in patient dose compared with less demanding diagnostic tasks (BAUMAN ET AL. 2011, MALOUL ET AL. 2011). By measuring DAP values at a range of exposure protocols and carrying out parallel subjective and objective image quality assessments, it was anticipated that the impact of varying exposure settings could lead to the identification of a threshold dose and CNR value as well as identification of a practical strategy for the reduction and optimisation of radiographic exposures within endodontics.

Furthermore, by carrying out the investigations using two commercial CBCT scanners, an analysis of whether the threshold level of objective image quality for this specific diagnostic task could be transferred to a different scanner was carried out. Protocols achieving significant dose reductions in other dental disciplines have been established (HIDALGO RIVAS ET AL. 2015, AL-OKSHI ET AL. 2017, EZELDEEN ET AL. 2017, ALAWAJI ET AL. 2018, OENNING ET AL. 2019) involving dose measurement, objective and subjective assessment, but not in endodontics and none of these have investigated the transferability of objective image quality measurements between scanners. Additionally, this study also examined the impact of anatomy complexity on establishing a threshold dose for this diagnostic task and the effect of operator experience on diagnostic efficacy. One previous study has investigated the relationship between objective and subjective image quality and the potential for transferability of findings between different CBCT scanners, recording observer findings of various anatomical features in a human skull phantom (PAUWELS ET AL. 2015b). These included 'pulp canal' assessments, but were in the form of a general overview of all teeth in a skull phantom rather than a detailed endodontic assessment. They did not find evidence that minimally acceptable image quality values were applicable to multiple CBCT models, but did not specifically consider the root canal visualisation, focusing on implant planning, root pathology and sinus pathology.

CBCT imaging of root canal systems prior to endodontic management is indicated in cases in which anatomically challenging morphology is predicted and for which a combination of conventional radiography and potential clinical investigation with a dental operating microscope cannot indicate the orifice, portals of exit or extent/continuity of the canal (ESE 2019) Identification and negotiation of more complex anatomy is important, as failure to locate anatomy reduces chemo-mechanical debridement and results in excessive dentine removal, which can lead to potential clinical complications including root fracture and perforation (TSESIS & FUSS 2006), as well as an increased risk of root canal treatment failure and possible tooth loss (DE CHEVIGNY ET AL. 2008). The MB root of a M1M is recognised as having the most predictably complex root canal anatomy in adult, teeth (WOLCOTT ET AL. 2005, CHANG ET AL. 2013) and therefore was used within the current study as a 'model' to

investigate the effect of reducing dose on the diagnostic task of root canal identification in teeth with a range of root complexities.

The need for dose reduction strategies within the discipline of endodontics and specifically canal anatomy identification is particularly pertinent. While it is difficult to currently ascertain the incidence of CBCT use for this indication, it appears that routine endodontic preoperative CBCT scans of teeth are being suggested for a more accurate assessment of root canal anatomy (PATEL ET AL. 2019), which is not in keeping with current guidelines on dental CBCT imaging (EUROPEAN COMMISSION 2012)

This diagnostic task-based study ultimately relied on subjective analysis of the CBCT images. In order to reproduce the clinical situation as accurately as possible, the skull and cervical spine set up was used to replicate the normal attenuation and scatter by a human head (SHELLEY ET AL. 2011). However, like other optimisation studies in the literature (HIDALGO RIVAS ET AL. 2015, AL-OKSHI ET AL. 2017, EZELDEEN ET AL. 2017, ALAWAJI ET AL. 2018, OENNING ET AL. 2019), it does not replicate the impact of patient movement on image quality, which can be particularly pertinent for high resolution settings with extended scan times (SPIN-NETO & WENZEL 2016). Similarly, in this study the first molar and adjacent teeth had not been restored with metal restorations and were not previously root canal treated, which can both produce artefacts throughout the FOV that can negatively impact on image quality and thus on canal visualisation (BECHARA ET AL. 2012a & b).

Assessing the impact of differing exposure protocols on root canal anatomy identification necessitated selection of M1Ms with differing root canal anatomies, reflecting a spectrum of both complexity and difficulty with respect to diagnosis and treatment. To exclude the impact of MB2 canal width, it was ensured that all MB2 canals exceeded 100 μm at their narrowest point, this figure was extrapolated from the literature on CBCT detection of vertical fractures (BRADY ET AL. 2014, GUO ET AL. 2019) which has shown that defects above a minimum width of ≥100 μm could be predictably appreciated and diagnosed with CBCT imaging.

Anatomical variations in the MB root canal system vary in both incidence and complexity (VERTUCCI 1984, BRISEÑO-MARROQUÍN ET AL. 2015) with recognised variations

considered in this study encompassing additional, accessory and connecting canals, anastomoses and canal divisions. The three selected molars in this study all displayed a MB2 canal, but with variations in origin, length, anastomoses, divisions and as a result, complexity of the MB2 canal. T6 was classed as having simple anatomy as this canal variation (type II Vertucci) is the most common in the MB root (MARTINS ET AL. 2019). T7 was classed as representing a simple-moderate complexity, being type II Vertucci, with an incidence of 25-45% (GUO ET AL. 2014, BRISEÑO-MARROQUÍN ET AL. 2015) but with an added anastomosis between MB1 and MB2, which is reported to occur in 2.9% of cases (BRISEÑO-MARROQUÍN ET AL. 2015). Although these anastomoses cannot be instrumented, their visualization is relevant to alert the clinician regarding potential reservoirs of bacteria and need for enhanced irrigation. T8, possessing several variations and classified as complex (a variation of type VIII Vertucci), has a reported incidence of 1.3% and 0.2-12% (SERT ET AL. 2004, AHMAD & AL-JADAA 2014). Obviously the selected sample of MB2 root anatomical configurations is not exhaustive; however, in combination with two CBCT scanners and range of exposure protocols it was not considered feasible to include a greater selection of teeth, not least because of observer time commitment requirements.

No validated tool for subjective assessment of root canal identification at a range of exposure protocols exists; the development of the seven-part questionnaire and subsequent assessment of the results took into account methodology from other previously published studies reporting on the measurement of image quality in diagnostic radiology (MARTIN ET AL. 1999, HIDALGO RIVAS ET AL. 2015, AL-OKSHI ET AL. 2017). This design approach was used in conjunction with a discussion amongst the researchers and the pilot study results. Use of a five-point rating scale for observer assessments is a validated tool for assessing image quality in diagnostic radiology (GIJBELS ET AL. 2001). This scale permits the observers to have a wider scope in which to record their answer, rather than being limited only to a positive/negative response, an approach utilized/validated in other subjective image quality studies (GIJBELS ET AL. 2001, HIDALGO RIVAS ET AL. 2015). This facilitates assessment of the degree of certainty and uncertainty and the option of being unsure to be reflected in elements of the analysis (median CSR responses). Additionally,

dichotomization of the data was necessary for other aspects (identification of diagnostic/undiagnostic data) with 0, 1, 2 responses being classified as a negative response and 3, 4 as a positive response. Unsure (=2) was noted as a negative response leaving just two positive options (=3, 4) ensuring that a positive response was documented only when the observer recorded as such.

Nine observers (three radiologists, three endodontists and three JHDs) were enlisted to perform subjective image quality assessments under standardized conditions in order to reflect the varying experience and skill set of a range of operators, who would realistically be carrying out this diagnostic task in primary/tertiary, clinical/referral practice. Although, the number of observers was in keeping with other image quality assessment studies, there is no clear guidance on how many observers are needed in imaging studies (OBUCHOWSKI 2004). Larger numbers of observers would reduce the impact of subjectivity; however, recruiting greater number of observers was not possible.

Identifying a 'target subjective image task' involved analysing the endodontists opinion of the volume of root canal identification necessary to fulfil the diagnostic task, balanced with clinical relevance. A consensus of opinion between the three endodontists established that the position of the MB2 orifice relative to the floor of the pulp chamber was particularly important, as this would dictate the volume of dentine required to be removed prior to potential canal location. Additionally, whether the canal was readily visible in the coronal third of the root was also clinically relevant, as it would be unlikely that the operator would search for a canal beyond the coronal third of the root, due to the potential complication of perforation and weakening of the root structure (TSESIS & FUSS 2006). Percentage of root canal identified was assessed from tracing over the microCT 'truth' and not from being asked to simply draw that part of the MB2 canal that they could definitively identify. It is of course possible that the availability of the 'diagnostic truth' might have led to higher proportions of root canal length by observers than were genuinely seen by them, but the strategy was considered to be the only practicable way forward but the strategy was considered to be the only practicable way forward.

After analysis of the pilot study results and discussion with three 'study' endodontists, a provisional figure of 95% of the MB2 canal identified was chosen as a 'target subjective image task'. It was observed from the pilot study data that when the observers identified ≥ 95% canal anatomy, that the MB2 canal was also always successfully identified at the level of the pulp floor and in the coronal third of the MB root, these two objectives being deemed by endodontists to be particularly clinically relevant to this diagnostic task. The target subjective image task of 95% was reassessed after analysis of the completed study results and it was identified that this same pattern was evident. Similarly, analysis of the pilot study results also elicited a further subjective image target of achieving median CSRs ≥ 3.5 (questionnaire scale 0-4), which reflected the observer's confidence in continuously identifying the canal in all thirds of the tooth and was established with 95% canal identification as the combined 'target subjective image tasks'.

Randomly selecting and repeating 20% of datasets within the study sample was used as the method to assess intra observer variability, resulting in 54 of data sets (including duplicates). It could be argued that a means of reducing recall bias further would be to include a greater number of teeth but this would have increased the number of datasets and time required from observers to an impractical level. For the three JHDs, although statistically significantly lower than those of the specialists, intra observer reliability was still classifiable as "moderate" for all questions except for one observer for the question (relating to overall image quality, not specific to root canal visualisation), which was only 'fair'. It might be argued that the lower intra observer reliability of the junior clinicians was not sufficient for a research study. Their inclusion was, however, considered worthwhile in being representative of the real world, in which use of CBCT is not limited to specialists.

Although pairwise comparison for observer results for questions relating to root canal identification and diagnostic acceptability (Q's 2-5 and 6) revealed moderate to good inter observer agreement, agreement was only 'fair' for identification of the MB2 canal at the level of the pulp chamber floor (**Table 2.4**). Differing perceptions as to whether this

referred to a common orifice for MB and MB2 or a separate orifice for MB2 could potentially explain this as would observer perception of the pulpal floor.

Undiagnostic scans were removed prior to analysis, being identified as those scans which at least six out of the nine observers did not record as diagnostic (67%). This was keeping with majority based image quality acceptance that been utilized in optimisation studies (HIDALGO RIVAS ET AL. 2015). The percentage of scans identified as undiagnostic by JHDs was significantly greater than that by the senior staff (p=0.043). This is likely to be due to the influence of experience and training that radiologists and endodontists possess with regard to diagnostic skills compared with recently qualified graduates. Notably, it has been suggested that the inexperienced operator is also more likely to request a CBCT scan (MATZEN & WENZEL 2015), highlighting less confidence with diagnostic skills in general and perhaps a familiarity and reliance on new technologies.

DAP was used to establish dose of each of the scanning protocols for both scanners; it is practically easy to achieve, relates relatively well to effective dose and has been recommended for establishing DRLs (EUROPEAN COMMISSION 2012). It is understood that DAP has the potential limitation of being over or underestimated (LOFTHAG-HANSEN 2010) nonetheless, DAP is still advocated and utilized for comparing dose between machines and assessing dose reduction strategies (LOFTHAG-HANSEN 2010, AL-OKSHI ET AL. 2017, ALAWAJI ET AL. 2018).

A range of physical phantoms has been employed to facilitate dental CBCT objective image quality assessment (LOUBELE ET AL 2008, SUOMALAINEN ET AL. 2009, WATANABE ET AL. 2011) The SedentexCT phantom was used in the current study, as it was designed specifically for dental CBCT and is successful in assessing basic image quality parameters (PAUWELS ET AL. 2011, BAMBA ET AL. 2013). The SedentexCT phantom is the size of an adult human head and is constructed from PMMA on the basis that this material simulates the average attenuation of the soft tissues of the human head, taking into account that there are also high attenuation structures (e.g. mandibular cortical bone and tooth enamel) in addition to the low attenuating contribution of air cavities (sinuses and oral cavity); this is reported to result in detector photon fluences similar to the human head (SUOMALAINEN ET AL. 2009,

PAUWELS ET AL. 2013) Therefore, the objective image parameters measured using the selected inserts can be related to the scanners' clinical performance.

CNR is an objective measure of technical image quality and an effective means of assessing performance and constancy of a CBCT device (PAUWELS ET AL. 2011). CNR can be easily interpreted and has been widely used to assess the impact of tube voltage and tube current-exposure time product on image quality and therefore is considered an appropriate tool in optimisation strategies (KALENDER 2009, KLINTSTRÖM ET AL. 2014) CNR was assessed using a PTFE insert (this particular insert approximating bone density), with previous related clinical diagnostic studies confirming that the PTFE insert generated CNR values which had a significant relationship with bone tissue (HIDALGO RIVAS ET AL. 2015, EZELDEEN ET AL. 2017). While other software exists for evaluation of physical parameters on IQ phantoms for dental CBCT, Image J was employed in this study as it is readily accessible and its effectiveness has been validated in several similar studies (PAUWELS ET AL. 2011 & 2013)

The results demonstrated that CNR increased with increasing DAP and hence with tube voltage and tube current (**Figure 2.8a & b**). Differences in CNR have been identified as largely influenced by the noise element of the equation (BECHARA ET AL. 2012c, PAUWELS ET AL. 2014b). Increasing mAs decreases the image noise by increasing signal at the detector but, since the beam penetration remains the same, contrast is unaffected. Higher kV values increase the detector signal due to the increased photon count and energy, resulting in a proportional fall in photoelectric effects and an increase in Compton scatter. In 2D radiography, reducing tube voltage within diagnostic range leads to an increased difference in attenuation between tissues of varying density and therefore increased image contrast, the opposite being the case when tube voltage is increased. In contrast, with CBCT imaging, the pure signal that reaches the detector does not solely determine contrast due to the additional information from the projectional data at many angles. Therefore, for CBCT imaging in this otherwise fixed scanning set up, contrast over the range of exposures exhibited relatively little variation (as could be identified from the pixel/grey value data) whereas noise varied with exposure protocol (as identified from the SD of grey values

consistently decreasing with increased tube voltage and tube current) causing noise to be the major contributor to CNR.

When compared to standard protocols, 180° scans resulted in CNR values at the lower end of the range (**Figure 2.8b**), this being related to decreased basis images and a concomitant increase in noise. For each kV and mA protocol, high resolution setting selection delivered CNR values only marginally greater than 180° scans and markedly lower than standard protocols. Moreover, when considering equivalent DAP, CNR values of high resolution settings were distinctly lower than both standard and 180° protocols. This can be attributed to the fact at high resolution setting the pixel array changes from a 2x2 array (i.e. four for standard setting) to an individual pixel (i.e. one for high resolution setting), thereby reducing the signal by one quarter, increasing noise and resulting in a decreased CNR values. Additionally, the small FOV (4x4cm) reduces photon fluence further, allowing noise to dominate. Accuitomo CNR values for standard protocols were considerably higher than for the equivalent protocols using the ProMax scanner. This may be related to the differing voxel size and/or differing technologies e.g. detector efficiency.

The evaluation of clinical image quality by observers is unavoidably subjective, as can be seen from inter observer agreement levels, whereas physical parameters can largely be measured in a reliable and repeatable manner; however, there is no direct way of translating these physical parameters to clinical image quality. This study defined a combination of subjective image tasks for the diagnostic task of root canal identification and identified the objective image quality, in this case CNR that achieved these tasks for two different scanners. Regarding the ProMax, achieving all components of the combined 'target subjective image task' elicited identical CNR values (3) and similar CNR values for the Accuitomo (7.3, 7.5, 7.6), this being for M1Ms exhibiting simple-moderate root canal complexity. This indicates that for the same scanner, these clinically relevant and necessary tasks to achieve root canal identification all consistently demanded the same or similar CNR level, indicating that CNR is a relevant measure of objective image quality in the task of canal identification. For both CBCT models, on relating CNR to the subjective measurements of image quality, similar patterns of improved subjective image quality with

increased CNR were evidenced in the scatter plots (**Figures 2.9a& b and 2.10 a-d**), albeit the relationship between CSRs and CNR for the Accuitomo was less clear cut (**Figures 2.10c & d**). However, it has to be concluded that in this study the CNR values identified to achieve the diagnostic task were not the same, or even similar, for the two CBCT models and therefore indicates that a reference CNR value for this diagnostic task cannot be applied between CBCT models. This can likely be attributed to differing technologies such as tube filtration, detector efficiency, FOV, filtering or voxel size of both scanners. Relating CNR alone to subjective image quality has some limitations in that it does not account for spatial resolution and, as can be seen from **Figure 2.9b**, focusing on the complex anatomy, there is a pattern of lower CNR high resolution scans achieving similar levels of canal identification to CNR standard protocols, which perhaps may be attributable to enhanced spatial resolution of these high resolution protocols. Therefore, in agreement with other studies, the relationship between objective measurements of image quality (in this case CNR) and subjective image quality is complex, with it being difficult to definitively relate one to the other in order to devise optimisation strategies (BECHARA ET AL. 2012C, PAUWELS ET AL 2015, AL-OKSHI ET AL. 2017, OENNING ET AL 2019).

For M1Ms exhibiting simple-moderate root canal complexity, the threshold DAP values necessary to achieve the combined subjective image tasks were similar for both scanners (209.3 and 203.2 mGy cm² for Promax and Accuitomo scanners respectively) and lower than the recently published National Diagnostic Reference Level (NDRL) for adult CBCT (based on maxillary molar preoperative implant assessment) in the UK of 265mGy cm² (PHE 2019) and much lower than the Finnish NDRL (specifically for CBCT examination aimed at assessment of tooth's periapical region and root canal morphology) of 550 mGy cm² (STUK 2016). This study suggests that there is scope for optimisation of patient dose in CBCT used in endodontic practice. Nonetheless, it is recognised that these study data are not clinical data and exclude the impact of movement and restoration artefact and that clinical studies would still be required. Furthermore, **Table 2.5b** highlights that standard protocols, except at the lower mA settings, achieved the diagnostic task while avoiding large DAP values that can be associated with high resolution scans.

The tables do not include complex anatomy (T8), as the target of 95% canal identification was not achieved at any experimental DAP value. This study suggests that factors other than diameter of a structure can impact on its visibility on CBCT scans. Rotating the 3D reconstructions of the MB2 canals of the selected molars, identified T8 as exhibiting the most curved MB2 canal structure, resulting in the canal 'weaving in and out' of a coronal and sagittal slices and altering position in axial slices. These features were complicated further by the presence of isthmuses and reduced observer ability to confidently identify its path. It could be concluded that in perceived complex cases, as judged from clinical perception or preoperative 2D radiography, increasing tube voltage and current-time exposure product, and resultant patient dose (maximum experimental DAP values achieving canal identification of 65% [ProMax] and 77% [Accuitomo]), could not be justified on the basis that it seemed probable that there was no likelihood of potentially improving diagnostic or clinical outcome.

2.6 CONCLUSIONS

- For the diagnostic task of root canal anatomy identification as 'modelled' by the M1M, MB2 canal, a representative threshold dose of just over 200mGy cm² was identified for the ProMax and Accuitomo scanners, lower than published NDRLs.

- Achieving the individual subjective image tasks for root canal identification required a consistent CNR value within each scanner. However, the markedly different CNR values identified for the two CBCT models suggest that it not possible to determine a single threshold level of objective image quality that could be universally applicable to other CBCT models.

- Experience and expertise was shown to have a significant impact on the diagnostic efficacy of observers in the diagnostic task of root canal identification.

- Ultimately all dose reduction strategies are scanner specific and in practice needs to be achieved with the advice of a medical physics expert.

- The results suggested that selection of standard protocols instead of high resolution scans is a practical means of reducing patient dose and that increasing dose to enhance visualisation of the most complex anatomy was ineffective.

- As with all *ex vivo* optimisation studies, these findings must be interpreted with caution. The *ex vivo* design, with a limited number of teeth, without patient movement or the presence of restorations, along with the subjective criteria for image quality and the complex inter relationship between subjective and objective image quality, all mean that there are significant limitations. Clinical studies are still required, presenting considerable challenges to researchers in terms of testing different exposure protocols.

Chapter 3

Investigation into the relationship between objective IQ metrics and determinants of IQ and the diagnostic task of root canal anatomy identification

3.1 INTRODUCTION

Clinically acceptable levels of image quality are dependent on the specific diagnostic task and are influenced by the IQ metrics of the scan (e.g. CNR, noise, spatial resolution). These IQ metrics reflect the selected exposure and imaging parameters in addition to the reconstruction process and specifications of the CBCT model (PAUWELS ET AL. 2012d). Quantifying these IQ metrics and relating them to clinically acceptable levels of image quality, could potentially indicate the IQ metric(s) that have a statistically significant relationship with successfully achieving that diagnostic task, thus facilitating optimisation of image quality. Furthermore, understanding how differing exposure protocols, and other variables in the imaging chain, influence each IQ parameter could facilitate optimisation of dose for that specific diagnostic task.

In **Chapter 2**, the IQ metric CNR was related to the diagnostic task of MB2 canal identification and resulted in similar patterns of improved canal identification as CNR increased, for both CBCT models, Accuitomo 170 (Accuitomo) and ProMax 3D (ProMax). Additionally, threshold CNR values were identified for both scanners, above which the diagnostic task was consistently achieved. It was concluded that CNR was a relevant objective IQ measure for the subjective task of MB2 canal identification in M1M teeth. However, it was also identified that the high resolution protocols with lower CNR values (below the threshold value identified for the Accuitomo) also achieved the diagnostic task, this finding being potentially attributed to the enhanced spatial resolution of these protocols. Clearly, therefore, CNR alone is insufficient to use as a metric in guiding optimisation strategies. The purpose of this study was to identify the association with other IQ metrics, to investigate their relative importance in achieving this diagnostic task and to explore all the determining factors affecting these metrics and indeed the diagnostic task of root canal identification (**Table 3.2**).

In this study, IQ metrics that are commonly used in research to characterize the quality of a CBCT image were assessed objectively in terms of spatial resolution, CNR and noise. Other IQ parameters that relate to the performance evaluation of CBCT systems and more commonly used for quality control (QC) purposes regarding CBCT include uniformity

(U), geometrical precision, voxel density values and artefact behaviour (ABOUEI ET AL. 2015, DE LAS HERAS GALA ET AL. 2017). A principal advantage of CBCT technology is its relatively high spatial resolution, largely the result of FPD technology and isotropic data, which is of particular importance in clinical dental applications (BRULLMAN & SCHULZE 2015). Notably, it has been reported that certain diagnostic tasks, such as periapical diagnosis, demand higher spatial resolution in addition to CNR values, compared with implant planning in the mandible (CHOI ET AL. 2015). This present study and others in this thesis used an endodontic-model and specifically MB2 canal identification as it is representative of the finest submillimetre detail required in dental imaging, and is assumed to demand higher spatial resolution which is generally associated with an increase in patient dose.

Spatial resolution substantially depends on the technical characteristics of the scanner, such as focal spot dimension, source-object-detector distances and detector specifications (matrix size, detector element size, number and spacing of detector elements), which can change over time (SMITH 2003). The number of projections, reconstruction process (voxel size, interpolation, filtering) and artefacts also impact on spatial resolution (GOLDMAN 2007, PAUWELS ET AL. 2012d, PAUWELS ET AL. 2015a) (**Table 1.1 & 1.2**). Measurement of spatial resolution provides a quantitative evaluation of the size of the smallest object that can be resolved in the acquired volumetric dataset and the Nyquist theorem indicates that for a fine structure, e.g. 100 µm to be reproduced accurately it must be sampled by pixels of 50 µm (twice the frequency). Studies show that theoretical spatial resolution, calculated from the number of pixels per square millimetre, differs greatly from that quantified during tests to measure this IQ metric (BRULLMAN & D'HOEDTT 2011). This disparity between ideal and spatial resolution measurements can also be explained by a number of other factors; pixel cross talk, partial volume averaging, image processing and noise (BRULLMAN & SCHULZE 2015, WILLEMINK ET AL. 2018). Image quality depends on the accuracy of the X-ray projection signal, which is acquired by a two-dimensional array of pixel cells in the detector. If the signal of X-ray photons is spread out to neighbouring pixels (crosstalk) and not discretely sampled by each pixel but spread over a number of pixels, a decrease of spatial resolution may result (ENGEL ET AL. 2006, WILLEMINK ET AL. 2018).

Additionally, partial volume averaging artefact occurs when tissues of broadly different absorption are captured on the same voxel (e.g. buccal bone and air) producing a beam attenuation proportional to the average value of these tissues. This is a limitation in resolution of small structures such as thin bone (MOLEN 2010). The influence of partial volume averaging is reduced by selection of the smallest voxel size possible (native pixel array), however, the reduced photon fill of the smaller pixels, receiving a reduced signal, allows noise to dominate which also can reduce spatial resolution. The signal acquired by flat panel detectors is pre-processed and, subsequently, additionally processed by pixel binning and/or noise reduction, generally resulting in the projection images having a higher actual resolution than that of the reconstructed volumes (BRULLMAN & D'HOEDTT 2011).

Smaller voxel sizes often necessitate longer scan times (to increase number of projections for reconstruction) which will increase the likelihood of patient movement. If there is patient movement (also contributed to by heartbeat and respiration amplitude) during the scan of more than the voxel size, then after the movement, grey values from neighbouring anatomy instead of the correct anatomy are back projected into the volume (DE KINKELDER ET AL. 2011, ZHANG ET AL. 2011, SPIN-NETO ET AL. 2013b). This results in motion blur and in reduced spatial resolution (BRULLMAN & SCHULZE 2015). Evidently, the smaller the voxel size, the smaller the movement necessary to move the patient structures out of the 'correct' voxels (SCHULZE ET AL. 2011); therefore, the higher the nominal resolution, the more likely motion artefacts are to appear. Decreasing scan time and hence frame acquisitions, to reduce the risk of motion artefact, can lead to undersampling which again reduces spatial resolution and the ability to resolve fine structures.

The subjective assessment of distinguishing line-pairs per millimetre (lp mm^{-1}), a function of the contrast between the line and background, has been largely replaced by technical, and more objective, measures of spatial resolution: MTF and full width half maximum (FWHM) (NAKAHARA ET AL. 2016). All real objects can be decomposed into sine waves of different amplitudes, frequencies, and phases and computation in spatial frequency domain is easier than in the spatial domain, which is achieved in the calculation of MTF (SMITH 2003). MTF is a graphical description of the spatial resolution characteristics

of an imaging system and measures change in the amplitude of sine waves. It can be evaluated by imaging a thin wire or a slanted edge to attain the point spread function (PSF) or Line Spread Function (LSF) (BRULLMAN & SCHULZE 2015). The Fourier transform of the PSF/LSF yields the MTF which measures how spatial frequencies pass through the system and has been described as a measure of contrast transfer from an object to an image (SCHULZE & DOERING 2019). The limiting spatial resolution (in the form of the smallest size of high contrast objects that can still be adequately imaged by the X-ray device) is usually associated with the frequency at which the MTF falls to a defined level (usually 10%) of its maximum value, with studies showing a fair agreement between visually discernible lp mm^{-1} and the frequency at 10% modulation (BRULLMAN & SCHULZE 2015).

Spatial resolution can also be expressed by FWHM, which is evaluated using the PSF insert and calculating the FWHM of a series of one-dimensional line profiles through the metal wire in the axial plane. FWHM is the width of the spectrum curve which is measured between two points on the y-axis that are half the maximum amplitude (SMITH 2003, ABOUIE ET AL. 2015, YALDA 2019). The SedentexCT PSF insert consists of a 0.25mm in diameter wire. Literature has suggested that a more accurate method of recording FWHM would be acquired using a wire diameter smaller than the smallest voxel size of both scanners and would therefore be completely captured within a voxel (NAKAYA ET AL. 2012, TRAN ET AL. 2021).

Noise is the result of fluctuation of photons hitting the detector manifesting as graininess and compromising the visibility of low-contrast tissue. The main sources of noise are quantum noise, electronic noise and noise introduced during the reconstruction process (**Table 1.2**). The noise levels in scans vary greatly between machines, each machine's settings, environment, and reconstruction algorithms affecting the image's noise (MIRACLE & MUKHERJI 2009). Noise levels can be reduced by increasing the exposure settings; scanning time, tube amperage, and kilovoltage peak and by using 2x2 and larger binning sizes, thereby maximizing the signal-to-noise ratio (SNR). During the reconstruction stage, it is also possible to use smoothing filters to reduce noise. The acceptable noise level for dedicated dental CBCT is normally higher than in conventional CT or other CBCT applications, because the high contrast between the studied tissues (teeth, bones and soft

tissue) cancels out the effect of the high noise. Noise appears as fluctuations in pixel values, with the SD indicating the magnitude of these random fluctuations, the larger the SD, the higher the image noise and such a measurement can be made using regions of interest (ROIs) on a scan of a PMMA insert.

On a practical level, image quality is determined primarily by the lesion-to-background contrast, which is believed to relate more strongly to CNR than to image noise (KALENDER 2008). Previous studies have demonstrated an association between CNR and achieving the diagnostic task (CHOI ET AL. 2015, AL-OKSHI 2017, WANG 2020, YALDA ET AL. 2022). Contrast in radiographic imaging indicates the ability to differentiate various material types which have different attenuation coefficients. Image contrast is determined by many factors such as the contrast of physical objects or materials, exposure factors, the bit depth of the reconstructed image, and the display settings (e.g. window level) in the image visualization stage (**Table 1.2**). Furthermore, scatter degrades contrast, with CBCT having up to 15 times higher scatter levels than that of medical CT (MOLEN 2010), however, scatter can be reduced with smaller FOV selection and peripheral FOV positions (PAUWELS ET AL. 2016), often applicable in dental imaging. Specifically, variations of this IQ metric are an indicator of changes in tube performance, as low-contrast resolution is linked to the peak-voltage (kVp) of the X-ray tube and consequently to patient dose (DE LAS HERAS GALA ET AL. 2017). While FPD technology offers excellent spatial resolution, contrast resolution suffers, however, due to increased X-ray scatter and the reduced temporal resolution and dynamic range (BECHARA ET AL. 2012C).

It is clear that there is some inter-dependence between these different IQ metrics, with noise being a principal determinant of contrast resolution and hence CNR, and also impacting to a lesser extent on spatial resolution. Furthermore, it is apparent that there are a range of variables influencing these IQ metrics and in turn the patient dose required to achieve adequate image quality. Therefore, the first aim of this study was to build on the work presented in **Chapter 2**, by undertaking an investigation into the relationships between IQ metrics using a regression analysis and to identify those that have a statistically significant relationship with successful achievement of the diagnostic task of root canal

identification. The hope is that this information might assist in optimisation strategies and help in selection of exposures that are as low as diagnostically acceptable. While IQ parameters allow objective measurements, the underlying determinants of IQ consist of a multiplicity of factors in the imaging chain. A second aim, therefore, was to explore these variables in the imaging chain that are expected to have an impact on root canal identification and to identify which of these predictor variables have a statistically significant relationship with achieving the diagnostic task.

3.2 OBJECTIVES

Using the data (detailed in **Chapter 2**) collated from nine observers, identifying 45 exposure protocols as diagnostically acceptable or not acceptable for the diagnostic task of root canal identification (MB2 canal) in M1Ms, the following objectives were defined:

1. To quantify the following IQ metrics: CNR, MTF, noise, FWHM for each of the 45 exposure protocols used to image the M1Ms.

2. To perform a regression analysis, using a logistic regression model, to identify the IQ metric(s) and the imaging chain determinants of IQ (the independent variables) that are associated with successful achievement of the diagnostic task of root canal identification (the dependent variable) by analysing the relationships between these independent variables.

3.3 METHODS AND MATERIALS

3.3.1 Assessment of subjective image quality

The method was that described in **Chapter 2**, **Section 2.3.5**; so, to summarize: an anthropomorphic phantom with three mounted upper left M1Ms, was scanned at the exposure protocols listed in **Table 3.1** using both the Accuitomo (voxel size: 80 µm) and the ProMax (voxel size: 100 µm). Subjective evaluation of image quality of the resulting CBCT datasets was performed by 9 observers; 3 radiologists, 3 endodontists and 3 JHDs, specifically regarding identification of MB2 root canal anatomy in the M1Ms. The observers were asked to record confidence in their ability to, identify the MB2 canal in the coronal, mid and apical section of the root respectively and identify it as continuous, from a Likert scale (1 = lowest to 5 = highest), for each M1M for all dataset exposure protocols. Subsequently, the observers were then asked to trace these sections of the MB2 canal that they could definitively identify on scrolling through each of the datasets, over the provided microCT images of the M1M anatomies (**Section 2.3.6**). The resulting percentage of the MB2 anatomy identified for each of the three maxillary molars per volume was recorded. From analysis of the pilot data (**Section 2.3.6**), a combined subjective image task was set at: identifying ≥ 95% canal identification (including identification of the coronal third MB2 canal) and a median confidence scale rating of ≥ 3.5. Analysis of the completed study data revealed that achieving median scale ratings of ≥ 3.5 corresponded with 95% MB2 canal identification (**Section 2.3.7**). Each exposure protocol dataset was thereafter classified either as being of sufficient or insufficient image quality to achieve the diagnostic task of root canal identification.

Tube current (mA)	Tube Voltage (kV)								
	70			80			90		
	180°	S	HR	180°	S	HR	180°	S	HR
3	✓	✓ ✓	✓	✓	✓ ✓	✓	✓	✓ ✓	✓
5	✓	✓ ✓	✓	✓	✓ ✓	✓	✓	✓ ✓	✓
7	✓	✓ ✓	✓	✓	✓ ✓	✓	✓	✓ ✓	✓
9	✓	✓ ✓	N/A	✓	✓ ✓	N/A	✓	✓ ✓	N/A

TABLE 3.1 Study exposure protocols: Accuitomo (voxel size: 80 μm): Red Tick and the ProMax (voxel size: 100 μm): Black tick. kV: Kilovoltage, mA: Milliampere
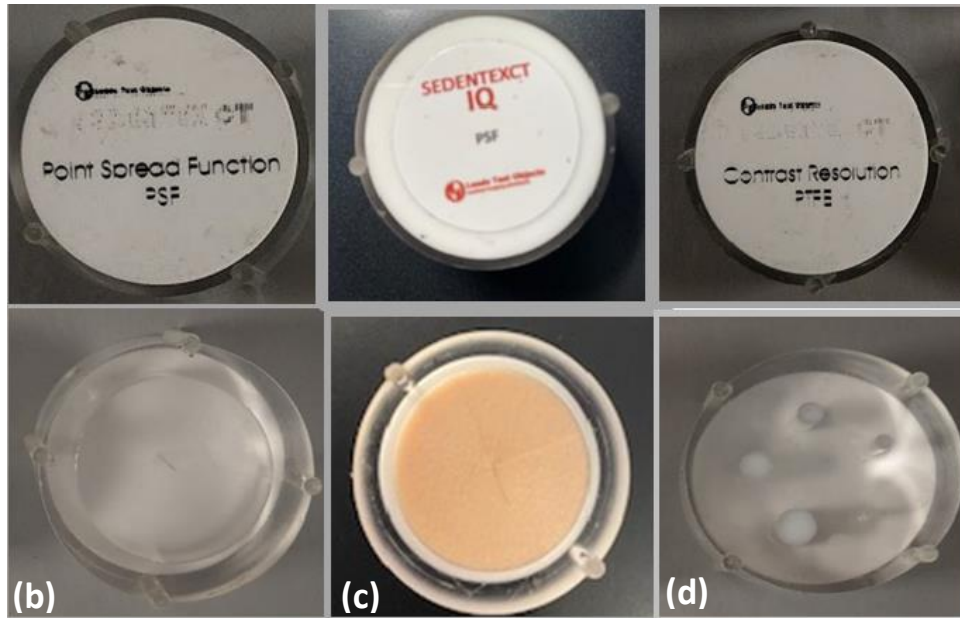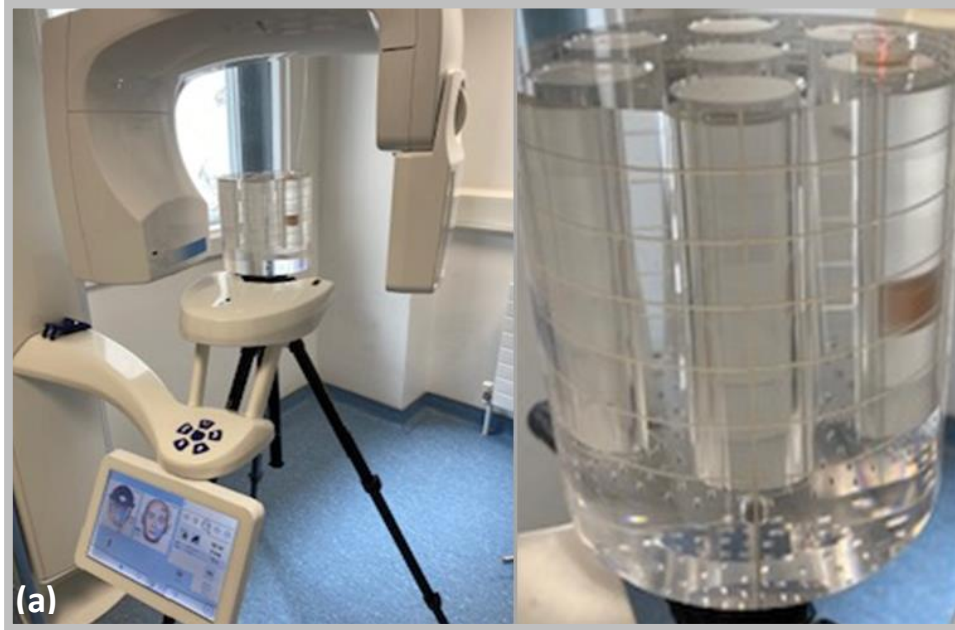
FIGURE 3.1 a) SedentexCT phantom and tripod set up for the 12 protocols for the ProMax scanner. **b)** PSF insert - 0.25 mm diameter **c)** PSF insert - 0.075 mm diameter **d)** PTFE

3.3.2 Assessment of objective IQ metrics

The SedentexCT IQ phantom was used to assess the objective IQ metrics of CNR, noise, MTF and FWHM for both CBCT scanners. This dedicated dental phantom is a head-sized cylinder 162mm (H) x 160mm (D) made of PMMA with a density of 1.20 ±0.01 gcm^3 to simulate human tissue. In this study, it was placed on a tripod, levelled with a spirit level, and positioned using lasers to align the phantom within the FOV (**Figure 3.1a**). IQ assessment was obtained by scanning the phantom containing each selected insert (35 mm [D] x 20 mm [H]), positioned in turn (**Figure 3.1b-d**), approximating the upper left molar position, using the protocols listed for both scanners (**Table 3.1**).

3.3.2.1 Quantifying spatial resolution:

Spatial resolution was assessed using the quantitative objective measurements MTF and FWHM.

MTF: Specifically, 10% MTF was assessed as this is associated with limiting spatial resolution. This was facilitated by using the PSF insert, which contains a 0.25-mm diameter stainless steel wire suspended in air parallel to the z-axis (**Figure 3.1b**). The insert was positioned in the SedentexCT IQ phantom approximating the upper left first molar position and scanned centrally within the FOV using the same 45 exposure protocols for both the Accuitomo and ProMax scanner detailed in **Table 3.1**. The resulting 45 data sets from the insert scans were individually exported as DICOM files into Image J software. Ten adjacent central axial images were selected, a ROI (30 x 30 pixels) placed centrally around the wire (**Figure 3.2**) and analysed at a 16-bit scale. The MTF 10% was calculated from 1-D PSF using the fast Fourier transform method, by means of the open source Spice CT plugin (https://imagej.nih.gov/ij/plugins/spice-ct/SPICE_CT.jar). The generated MTF 10% was averaged for the ten readings and recorded for all exposure protocols for both scanners.
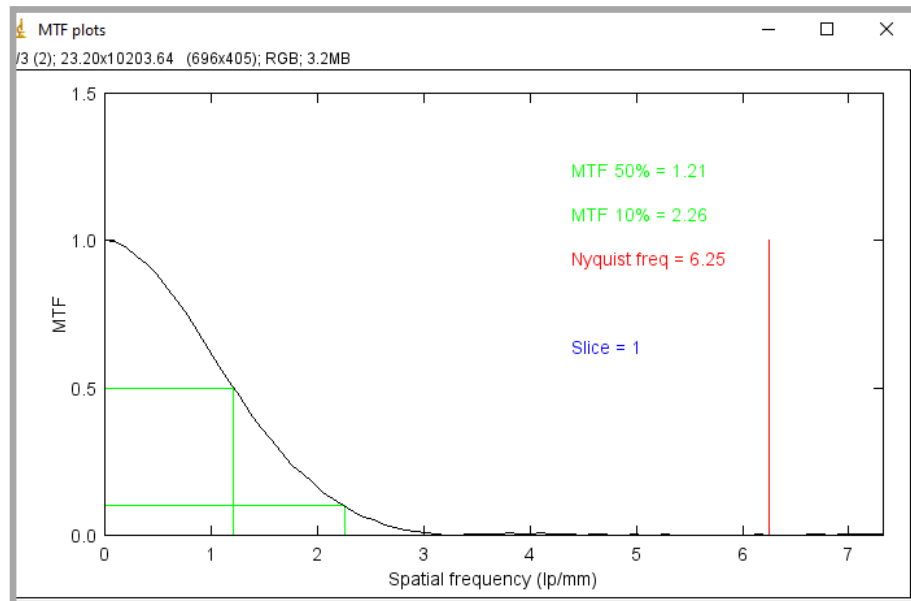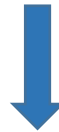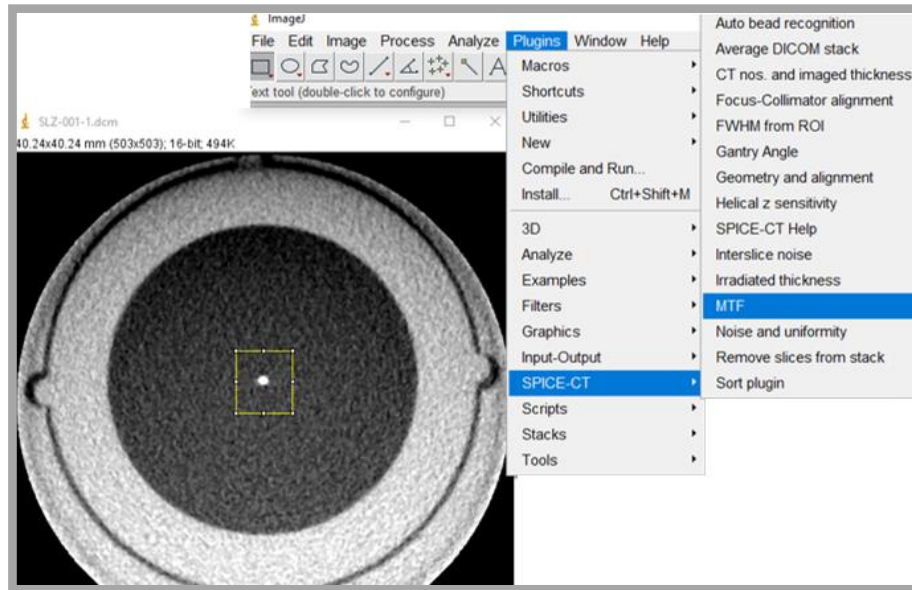
FIGURE 3.2 Calculation of MTF: DICOM files exported into ImageJ of the scanned PSF inserts enabled calculation of 10% MTF using open source SPICE-CT plug-in.

FWHM: The DICOM files from the PSF insert (0.25 mm) scans were again individually imported into Image J. Ten central axial slices were selected and a ROI was placed (30 x30 pixels) to record the background pixel value. The central image of the wire was magnified, the minimum window width set and the maximum window level set at the point the central magnified image disappeared and the pixel value noted (**Figure 3.3a-c**). The pixel value at half maximum was then calculated using the equation:

$$\frac{Pixel\ Value\ (maximum) - Pixel\ Value\ (background)}{2} + Pixel\ Value\ (background)$$

The 'measure' tool was then used to measure the distance in mm between the two points at half maximum of the metal wire line profile (**Figure 3.3d**), with the average of the ten values generating FWHM. Calculation of FWHM was repeated as described above from scans (all 45 exposure protocols for both scanners) of a second PSF insert, containing a 0.075 mm diameter stainless steel wire (**Figure 3.1c**). This was based on suggestions from the literature (NAKAYA ET AL. 2012).

96
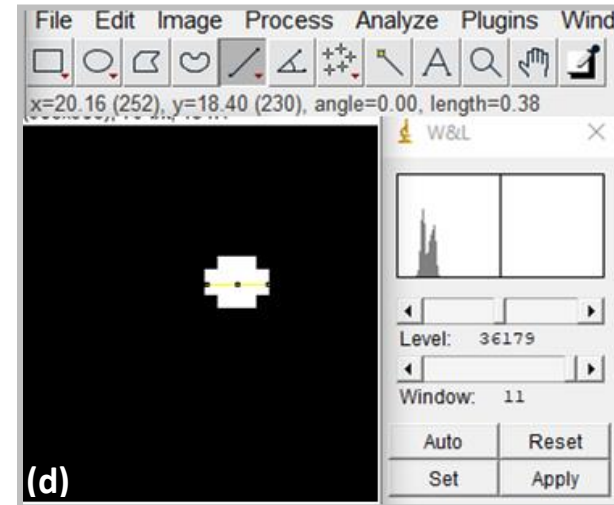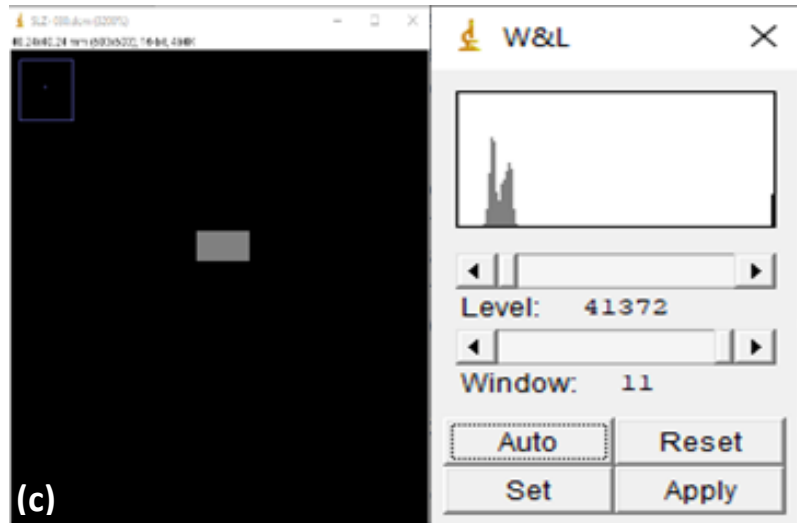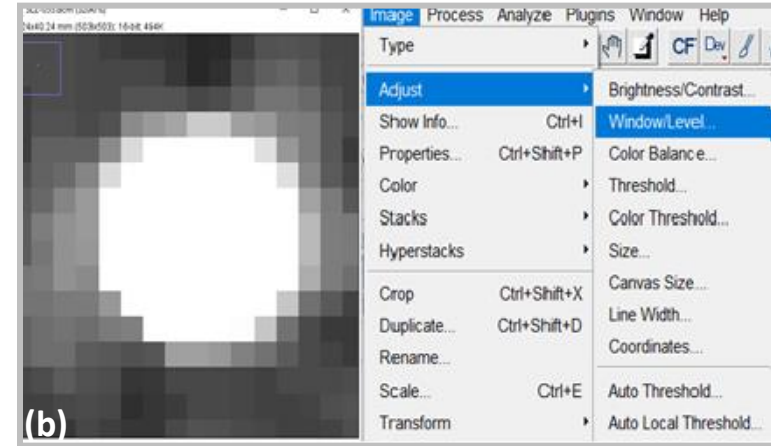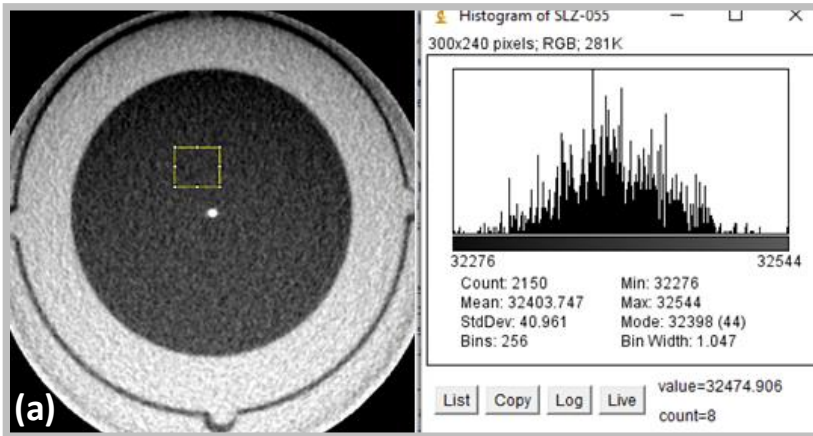
FIGURE 3.3 Calculation of FWHM: DICOM files from scanned PSF insert exported into ImageJ, enabling **(a)** evaluation of background pixel value, **(b & c)** Magnification of image and setting of maximum window level and minimum window width **(d)** The 'measure' tool used to measure the distance in mm between the two points at half maximum of the metal wire line profile.

3.3.2.2 Quantifying CNR and noise

Both CNR and noise were assessed using a PTFE insert, consisting of five rods of PTFE of differing diameters (1, 2, 3, 4 and 5 mm) embedded in PMMA. PTFE was used as it is considered representative of dental hard tissue (**Figure 3.1d**). The insert was placed in the SedentexCT IQ phantom as described **Section 2.3.4** and scanned using the 33 selected exposure protocols for Accuitomo and 12 protocols for the ProMax as detailed in **Table 3.1**.

CNR: CNR was quantified by exporting the 45 data sets as DICOM files into Image J software and the histograms generated from ImageJ (**Figure 3.4**) enabled evaluation of the mean and SD of pixel values of the PTFE rod centre and PMMA background, which were then used to calculate CNR as described in **Section *2.3.4.1.***

Noise: This was measured as the average of the SD's of the pixel value (**Figure 3.4**) within a ROI (12 mm²), taken in the central region of the PMMA section of the PTFE insert, and using five consecutive axial slices either side of the central slice.

3.3.2.3 Reproducibility of IQ metrics

Reproducibility of IQ parameters were assessed from the average SD's of the repeated measurements for each of the IQ metrics. This deviation represents the intrascan reproducibility of the phantom and measuring methods.
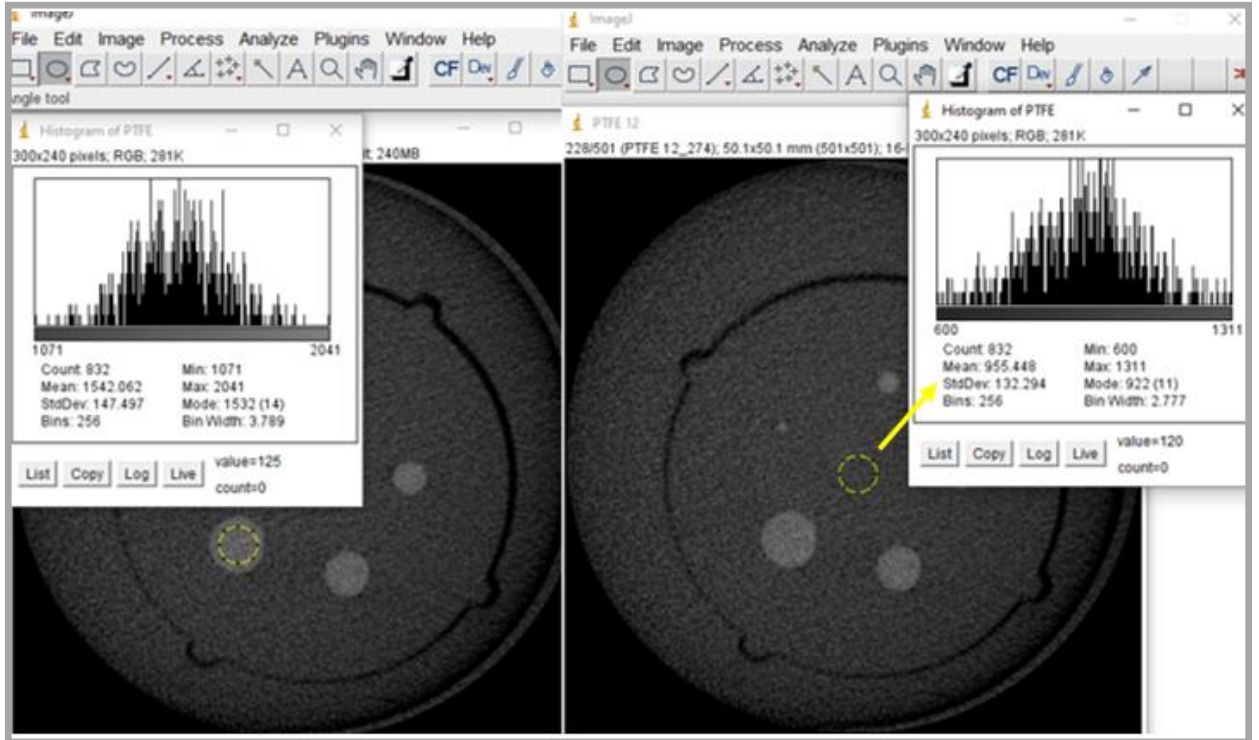
FIGURE 3.4 Histograms generated from exported DICOM files into ImageJ of the scanned PTFE test insert (PTFE rod and PMMA background) enabling calculation of CNR and noise (yellow arrow - standard deviation of PMMA background pixel value).

3.3.3 Exploration of the determinants of IQ that impact on root canal identification

The possible variables that can influence the visibility of root canal anatomy on CBCT imaging, from patient factors or anthropomorphic phantom set up in this experiment, right through the imaging chain to the observation of the acquired dataset are described in **Table 3.2**. While some of these independent variables were fixed (e.g. most aspects of the anthropomorphic model, many equipment factors), others were altered in the study, and could therefore be considered in the regression analysis as potential predictors of successful achievement of the diagnostic task. Variables that showed collinearity had to be excluded from statistical analysis, also all those variables that varied only because the difference in machine specifications/type could only be grouped together under the variable, machine type.

		Varied in the study	Type of variable
Patient anatomical factors	Anatomical: • Physical thickness of bone • Bone density • Root canal dimensions and configurations	No No **Yes** (varied with M1M)	Continuous
Other patient variables	• Movement • Artefact from adjacent structures, including high attenuation objects (restorations; implants; radiation protective barriers, etc.)	No No	
X-ray quantity	• mAs	**Yes**	Continuous, but limited settings
X-ray quality (spectrum characteristics)	• Beam spectrum shape • Maximum X-ray energy • Mean X-ray energy • Operating potential • Exposure Type • Focal Spot • Filtration	No **Yes** **Yes** **Yes** **Yes: Acc**: DC Continuous **Pmx**: Pulsed (Varied with machine type) No: Both 0.5 mm **Yes:** **Acc**: ≥ 3.1 mm Al **Pmx**: 2.5 mm Al + 0.5 mm Cu	Continuous, at three settings
X-ray field size	• Height • Diameter • Source-to-object distance (SOD)	**Yes** (Varied with machine type) **Yes** (Varied with machine type) **Yes** (Varied with machine type)	**Acc**: 4x4 cm **Pmx**: 5x5 cm **Acc**: 740-840 mm **Pmx**: 517.5 mm

TABLE 3.2 Exploration of determining variables in the imaging process that may impact on root canal identification. M1M: Maxillary first molar, Acc: Accuitomo, Pmx: ProMax, mAs: tube current-exposure time product.

Number of projections	• Half rotation, standard or Hi Res	**Yes** (Acc)	**Acc**: 180°= 256 360°= 512 Hi Res= 600 **Pmx**: 200° = 275
X-ray absorbed dose-area-product	• DAP	**Yes**	Continuous: **Acc**: 33 settings **Pmx**: 12 settings
X-ray detector characteristics	• Detector type • Detector pixel dimensions • Native pixel array	No **Acc**: 127 μm **Pmx**: 127 μm **Yes**: HiRes: **Acc** only	
Image reconstruction	• Reconstruction algorithm? • Voxel dimensions	No: Feldkamp* **Yes** (varied with machine type)	**Acc**: 80 μm **Pmx**:100 μm
Image display	• Monitor size and pixel dimensions • Magnification used • Contrast/ brightness (i.e. grey scale histogram) • Room lighting etc.	No (same monitor screen throughout) Not definable: Adjusted freely Not definable: Adjusted freely No – fixed	
Operator Variables	• Visual acuity • Experience	No – not measured Yes: JHD/Senior staff	

TABLE 3.2 Continued: Exploration of determining variables in the imaging process that may impact on root canal identification. Acc: Accuitomo, Pmx: ProMax, JHD: Junior hospital dentist, Senior staff: Endodontists and Radiologists

3.3.4 Statistical analysis

Statistical analysis was performed using IBM SPSS Statistics (Version 24.0; IBM Corporation, Chicago, USA). Binary logistic regression analysis was performed to identify firstly which of the IQ metrics CNR, MTF, FWHM or noise (continuous independent variables) were statistically significant predictors of successful achievement of the diagnostic task of root canal identification (dichotomous dependent variable). Additionally, logistic regression was used to identify which of the IQ determinants considered in **Table 3.2** had a statistically significant association with this diagnostic task. To ensure the data could be analysed using binary logistic regression, checks were made to ensure all assumptions were met.

3.4 RESULTS

3.4.1 Subjective image quality assessment

The exposure protocols that achieved the diagnostic task of root canal identification *i.e.* attained the combined target subjective image task (**Section 2.3.7**) are listed in **Table 3.3**. These results refer only to standard anatomy results (T6, T7). For complex anatomy (T8), the combined target subjective image task was not achieved at any exposure protocol for either scanner (**Figure 2.9a & b**). As the identification ≥ 95% of MB2 canals largely equated with achieving a median CSR ≥ 3.5, all plotting of IQ metrics have been related solely to percentage of canal identified for interpretation and ease of display purposes. As described previously (**Section 2.4.3**), for questions relating to the identification of root canal anatomy, intra observer agreement ranged from good to very good for senior observers (radiologists and endodontists) and fair to moderate for the JHDs.

	Accuitomo						ProMax			
	CNR	Noise	MTF	FWHM	FWHM		CNR	Noise	MTF	FWHM
180° kV/mA				0.25mm	0.075mm					0.25mm
70/3	3.3	154.88	1.97	0.48	0.39					
70/5	4.6	111.34	1.94	0.48	0.37					
70/7	5.7	91.62	1.94	0.48	0.33					
70/9	6.6	76.42	1.93	0.48	0.31					
80/3	4.4	103.7	1.98	0.40	0.34					
80/5	5.7	82.84	1.97	0.40	0.31					
80/7	7.5	66.22	1.97	0.40	0.39					
80/9	7.9	62.14	1.97	0.40	0.38					
90/3	5.2	86.88	1.99	0.40	0.36					
90/5	6.7	65.28	1.98	0.40	0.37					
90/7	7.6	56.32	1.98	0.40	0.36					
90/9	7.8	53.64	1.95	0.45	0.30					
Standard										
70/3	5.5	98.38	1.94	0.47	0.30		1.5	410	1.28	0.60
70/5	7.1	73.08	1.96	0.40	0.31		1.8	338	1.31	0.60
70/7	8.5	63.74	1.97	0.40	0.35		2.1	276	1.32	0.60
70/9	9.4	53.94	1.97	0.40	0.37		2.4	242	1.28	0.60
80/3	6.3	75.98	1.98	0.40	0.38		1.9	300	1.35	0.60
80/5	8.2	57.16	1.96	0.40	0.37		2.5	243	1.37	0.60
80/7	9.6	52.88	1.93	0.40	0.31		3	207	1.36	0.60
80/9	11	46.4	1.95	0.40	0.31		3.4	236	1.33	0.60
90/3	7.5	68.45	1.93	0.47	0.38		2.4	250	1.43	0.60
90/5	9.7	48.1	1.94	0.40	0.36		3.1	197	1.4	0.60
90/7	11.3	43.12	1.93	0.40	0.33		3.6	160	1.43	0.60
90/9	12.5	40.24	1.93	0.40	0.31		3.7	194	1.39	0.60
High Res										
70/3	3.7	137.52	2.21	0.47	0.31					
70/5	5.1	101.26	2.28	0.40	0.32					
70/7	6	83.66	2.20	0.32	0.30					
80/3	4.7	100.04	2.28	0.32	0.30					
80/5	6.3	72.32	2.20	0.39	0.29					
80/7	7.5	61.84	2.24	0.39	0.30					
90/3	5.4	80.32	2.33	0.39	0.26					
90/5	7.3	60.74	2.29	0.38	0.24					
90/7	8.5	52.3	2.24	0.39	0.28					

TABLE 3.3 Image quality metrics for ProMax and Accuitomo at all exposure protocols.

Achieved Diagnostic Task of Root Canal Identification: | Yes | | No |

3.4.2 Objective IQ metrics

3.4.2.1 Spatial Resolution

MTF: MTF 10% appears to be unrelated to DAP (**Figure 3.5a**). 10% MTF values ranged from 1.93 - 1.99 for 180° and standard protocols and 2.2 - 2.33 for high-resolution protocols for the Accuitomo scanner (**Table 3.3**). A range of MTF values achieved the diagnostic task, however protocols with an MTF above 2.21 achieved the diagnostic task consistently, with these higher MTF values being reserved for the high resolution scans (**Fig 3.6a**). For the ProMax scanner MTF 10% ranged between 1.28 and 1.43 (**Table 3.3**) with no obvious threshold value above which the diagnostic task was achieved (**Figure 3.6b).**

FWHM: FWHM appears to be unrelated to DAP (**Figure 3.5b**).

0.25 mm wire - For the Accuitomo scanner FWHM values ranged from 0.32-0.48. The higher resolution scans exhibited some of the lower FWHM values of this range and the standard and 180° scans had similar distribution of values of 0.40-0.48 (**Table 3.3**). For the Accuitomo a range of FWHM values achieved the diagnostic task, but protocols with a FWHM value < 0.4, achieved the diagnostic task consistently (**Figure 3.6c**). The ProMax scanner showed no variability, recording a constant FWHM value of 0.6 for all exposure protocols and therefore no threshold value for achieving the diagnostic task was evident (**Table 3.2, Figure 3.6d**).

0.075 mm wire - For the Accuitomo scanner FWHM values ranged from 0.24-0.39, the high-resolution scans again recording the lower end of this range of FWHM values (**Table 3.3**). FWHM values could not be quantified for the ProMax scanner with the 0.075 diameter wire as the central pixel values of the wire did not differ sufficiently from the background pixel to allow measurement of FWHM (**Figure 3.8**).

3.4.2.2 CNR and noise

CNR: CNR increased with DAP (**Figure 3.5c**). Values for the Accuitomo scanner ranged from 3.3–7.9 for 180° scans and a similar range of 3.7–8.5 for high-resolution scans, with standard scans recording the highest CNR values ranging from 5.5–12.5 (**Table 3.3**). While a range of CNR values achieved the diagnostic task, a threshold value CNR value of

7.6 was identified, above which the diagnostic task was consistently achieved (**Figure 3.7a**). For the ProMax scanner CNR values ranged from 1.5–3.7, the diagnostic task being achieved consistently above a CNR value of 3 (**Figure 3.7b**).

Noise: Noise was shown to decrease with DAP (**Figure 3.5d**). Values, only at the lower end of the respective ranges, achieved the diagnostic task for standard and 180° scans for the Accuitomo and also for ProMax scanner (**Table 3.3, Figures 3.7 b-c**). In comparison, the diagnostic task was achieved almost for the full range of noise values for the high-resolution scans. Specifically, a noise value of ≤ 95 and < 207 for the Accuitomo and ProMax respectively achieved the diagnostic task consistently.

3.4.3 Reproducibility of measurements

The average intrascan SD's of the repeated measurements for each of the IQ metrics for both machines were; MTF: ±0.08, FWHM (0 .25mm): ±0.02, FWHM (0.075mm, Accuitomo only): ±0.28 CNR: ±0.35, noise: ±3.41. The highest intrascan deviation was evident for noise. Measurement of FWHM (0.25mm) showed the highest intrascan reproducibility but there was a disparity between the two diameters of wire, with the FWHM (0.075mm) showing much greater intrascan variability.
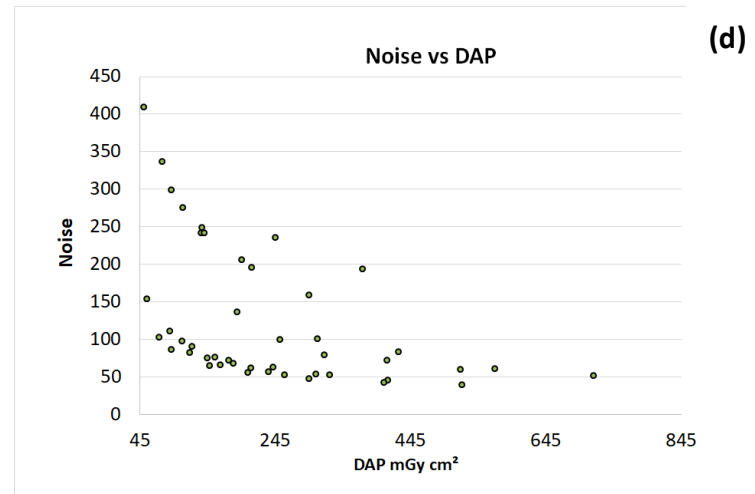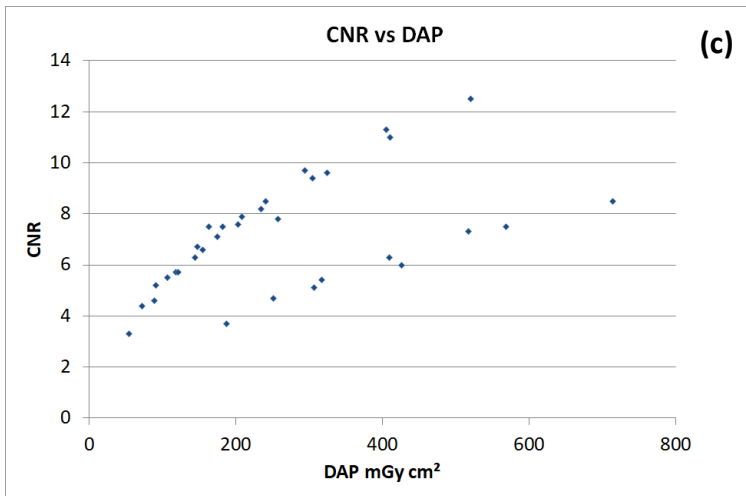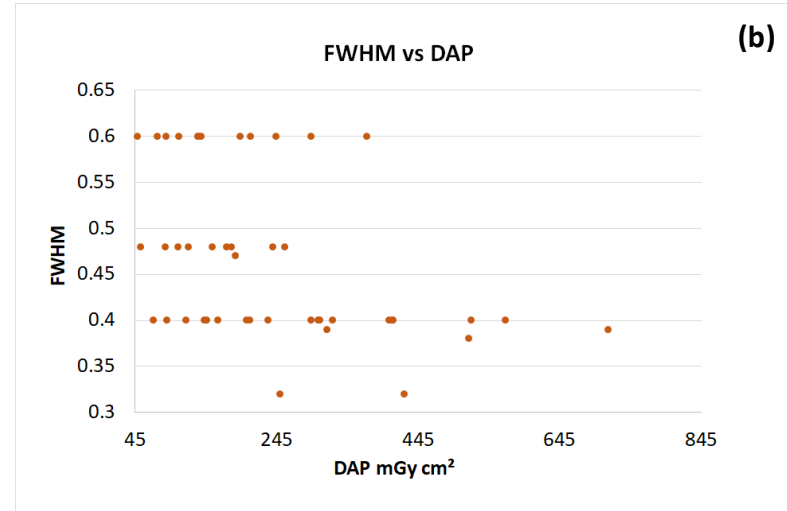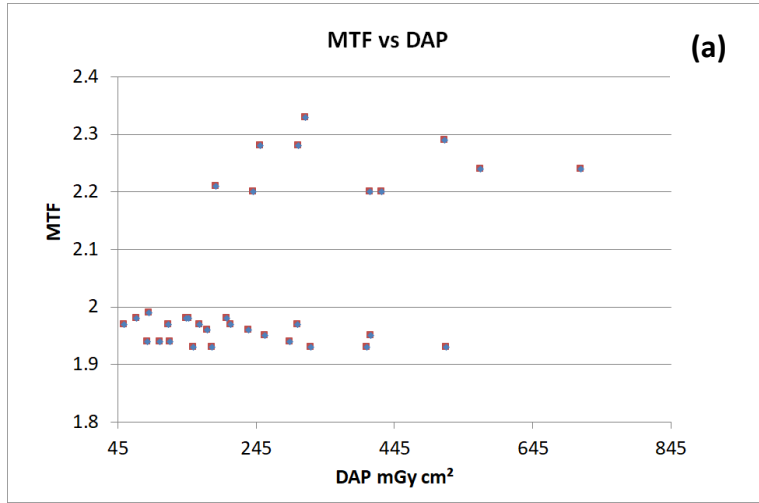
FIGURE 3.5 Relationship of IQ metrics: **(a)** MTF **(b)** FWHM **(c)** CNR **(d)** Noise, to DAP (mGYcm²)
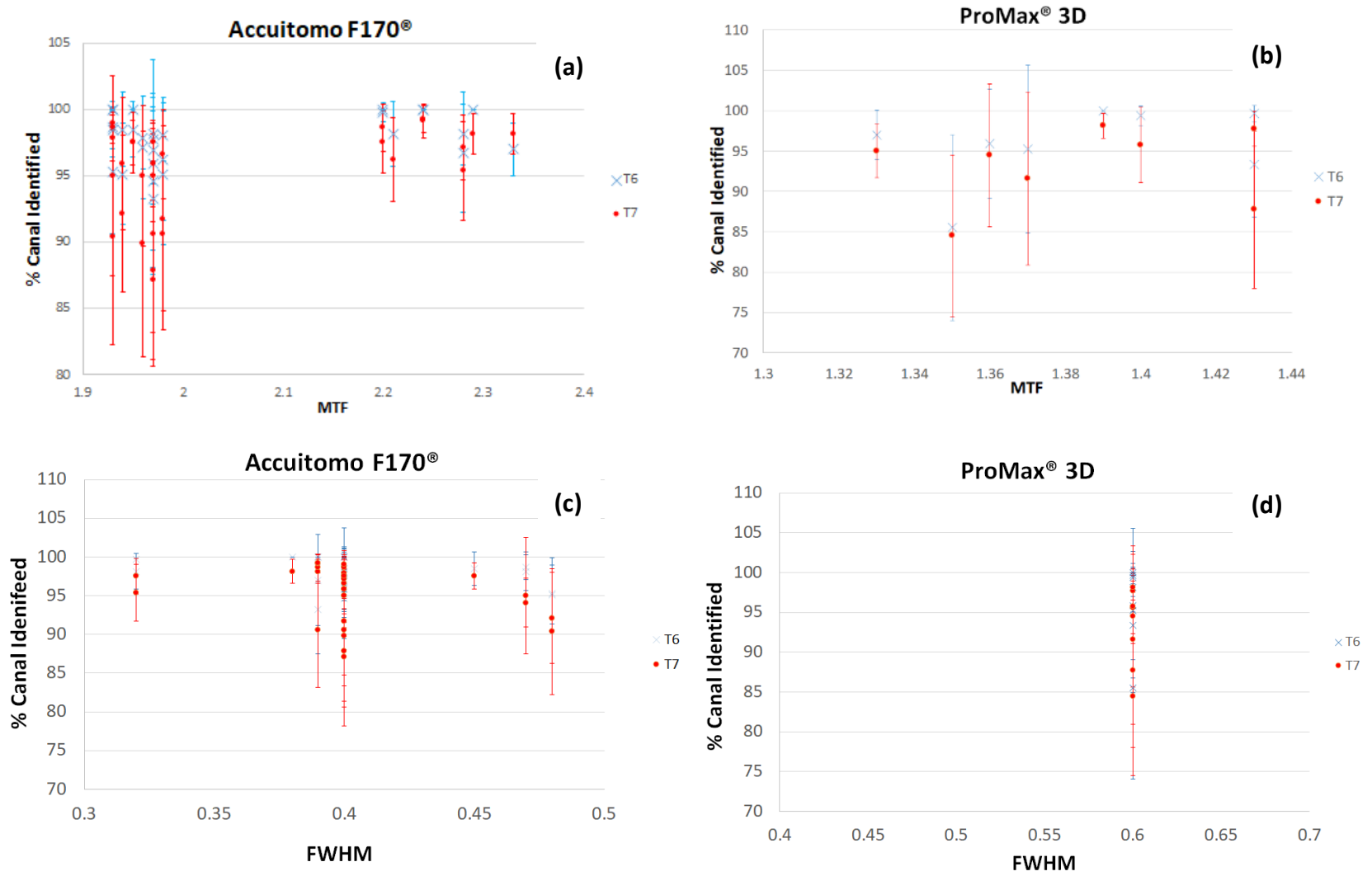
FIGURE 3.6 Relationship of MTF and FWHM values to achieving the diagnostic task of root canal identification for Accuitomo **(a, c)** and ProMax **(b, d)** scanners.
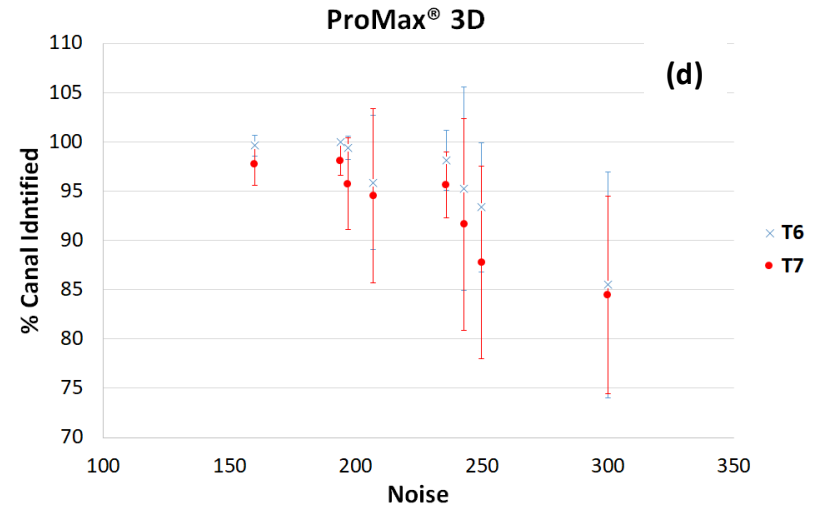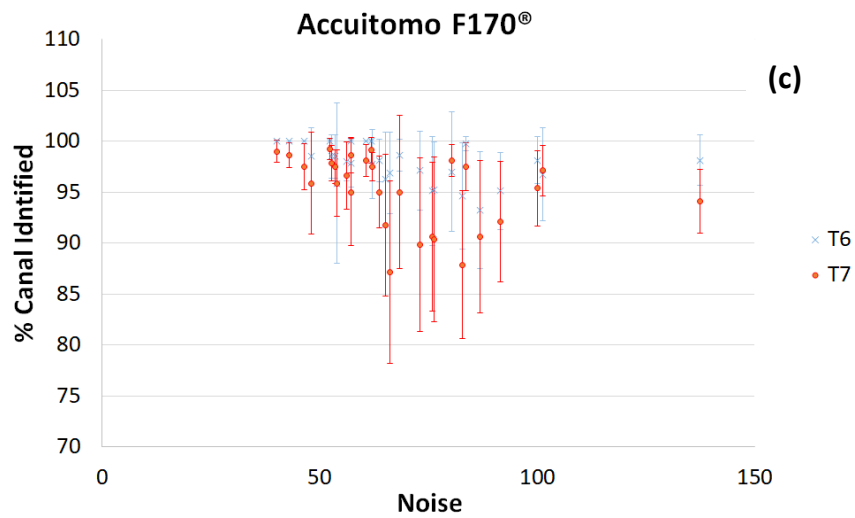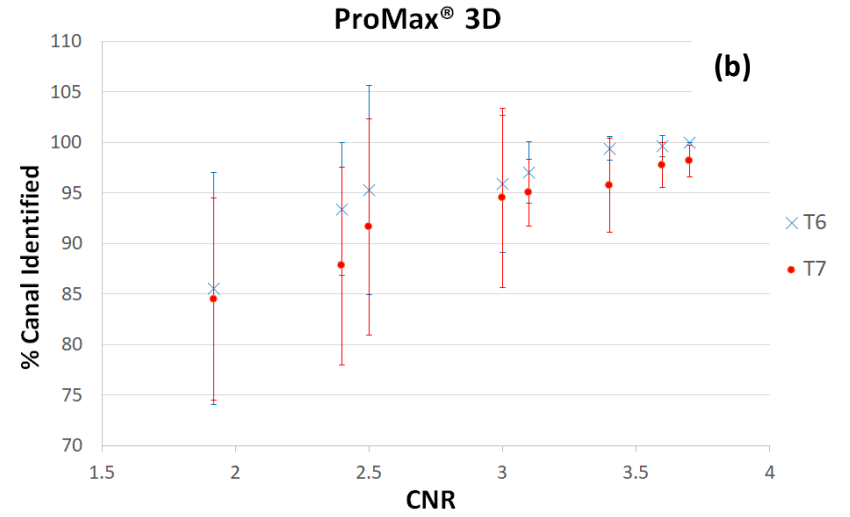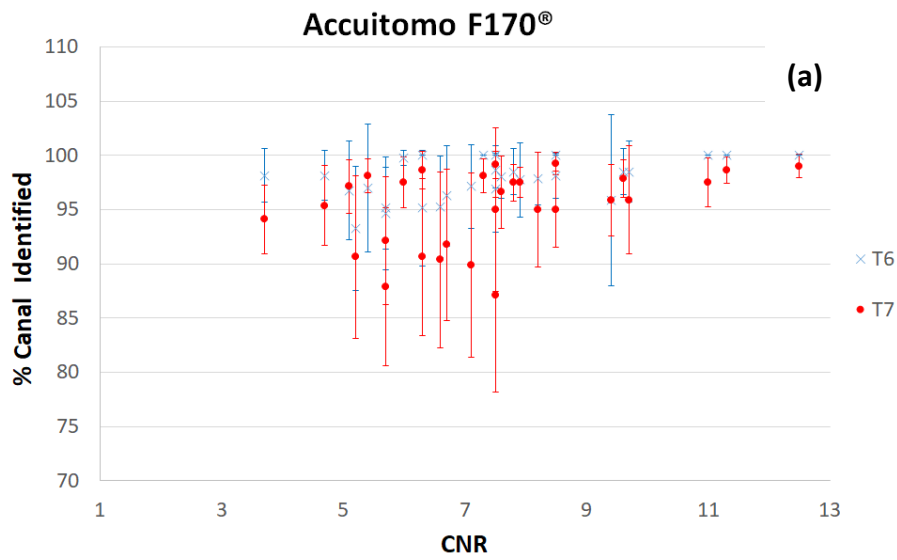
FIGURE 3.7 Relationship of CNR and noise to achieving the diagnostic task of root canal identification for Accuitomo **(a, c)** and ProMax scanners **(b, d).**
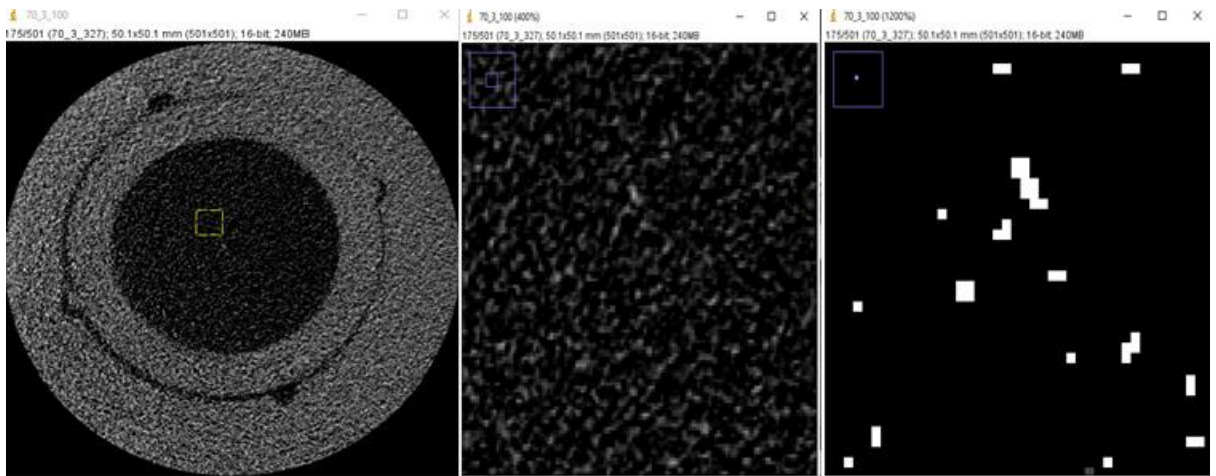
FIGURE 3.8 ProMax scan slice of 0.075 mm PSF insert in Image J: On magnification of image, poor distinction between background pixel value and wire pixel value.

3.4.4 Logistic Regression

3.4.4.1 IQ Metrics

Preliminary statistical analysis showed that multi-collinearity was present, relating to noise and FWHM (0.25mm), this was demonstrated by a tolerance value approaching 0.1 and a high variation inflation figure (VIF) greater than 5 (**Table 3.4**). On removing noise and FWHM as independent variables in the regression the VIF reduced to nearer 1. SPSS output did not produce a casewise plot as no outliers in the data were discovered. The model was statistically significant, $\chi 2$ (2, N = 45) = 14.35, *p* =.001, demonstrating that the model could distinguish between protocols that did and did not achieve the diagnostic task. The model explained between 27.3% (Cox & Snell R square) and 36.4% (Nagelkerke R square) of the variance in the dependent variable and correctly classified 71% of cases. Findings indicate (**Table 3.5a**) that when CNR and MTF are considered separately they both have a statistically significant effect on successfully achieving the diagnostic task of root canal identification albeit the larger confidence intervals for MTF suggest that this finding for MTF should be viewed with caution. However, when both variables are considered in the same model (**Table 3.5b**) and when adjusting for MTF, CNR still had a significant effect on successfully achieving the diagnostic task, increasing the odds of doing so by a factor of 1.68 (95% CI 1.13 – 2.51), when all other features remained the same.

	Collinearity Statistics			
	Tolerance	VIF	Tolerance	VIF
CNR	.26	3.79	0.63	1.56
MTF	.27	3.63	0.63	1.56
Noise	.12	7.87	-	-
FWHM	.97	10.33	-	-

TABLE 3.4 Test for collinearity among the independent variables. VIF = Variance inflation Factor

(a)			95% CI for OR		(b)		95% CI for OR	
	P	OR	Lower	Upper	*P*	Adjusted OR	Lower	Upper
CNR	.002	1.696	1.210	2.302	.011	1.684	1.129	2.513
MTF	.033	9.214	1.192	71.240	.941	.900	.057	14.280

TABLE 3.5 Logistic regression predicting the likelihood of achieving the diagnostic task: **(a)** odds ratios when CNR and MTF are considered separately **(b)** adjusted odds ratios when both CNR and MTF are considered. OR = Odds ratio, *p* = *p* value

3.4.4.2 IQ determinants

Variables that differed exclusively with machine type (**Table 3.2**), included exposure type, filtration, FOV, source-to-object distance (SOD), pixel dimension and voxel dimension. These variables could therefore, not be considered separately and were jointly considered under the category of machine. The assumption of multi-collinearity was not met for the remainder of the variables; tooth, tube current-exposure time product: mAs, X-ray tube voltage: kV, degrees of rotation/ number of basis images, pixel binning (1x1, 2x2) and operator experience. On substituting tube current-exposure time product with tube current and time as separate variables, the same problem remained. Accordingly, the model was run with the variables; X-ray tube voltage, X-ray tube current, pixel binning, rotation, machine type and operator and preliminary analysis showed the assumption of multi-collinearity was met (**Table 3.6**). The model was statistically significant, χ2 (9, N = 180) = 165.99, *p* <.0001, demonstrating that the model could distinguish between protocols that did not achieve the diagnostic task. The model explained between 60.2% (Cox & Snell R square) and 80.5% (Nagelkerke R square) of the variance in the dependent variable and correctly classified 87.8% of cases. As shown in **Table 3.7** all of the predictor variables except machine type significantly contributed to successfully achieving the diagnostic task of root canal identification.

Specifically, adjusting for other variables, an increasing kilovoltage, 80 kV (OR = 5.52, 95%CI [1.48, 23.97]) and 90 kV (OR=22.72, 95% CI [5.14, 134.920]) was associated with an increased odds ratio of successfully achieving the diagnostic task when compared with 70kV. Similarly, an increasing tube current, 5 mA (OR= 9.2, 95% CI [1.99, 54.92]), 7 mA (OR= 25.54, 95% CI [5.06, 177.95]) and 9 mA (OR= 67.24, 95% CI [10.29, 350.56]) was also associated with an increased odds ratio of successfully achieving the diagnostic task when compared with 3 mA.

The odds of successfully achieving the diagnostic task was 64.72 [95% CI (12.50, 335.03] times greater with single pixel read-out than with 2x2 pixel read-out. Additionally, increasing rotation degrees, 360° [OR = 32.29, 95%CI (3.26, 330.97)] and 200° [OR=10.77, 95% CI (5.14, 53.95] was associated with an increased odds of successfully achieving the diagnostic task when compared with 180°.

Successful achievement of the diagnostic task was 6.62 times more likely [95%CI (2.53, 17.37)] for senior observers (endodontists and radiologists) than junior observers (JHDs). However, machine type did not have a statistically significant effect on successfully achieving the task. When looking at the association of the predictor imaging variables with the outcome variable, independently (**Table 3.7a,** left column), the same significant/non-significant associations existed. However, when adjusting for the other variables (**Table 3.7**, right column) the odds ratios and confidence intervals were greatly inflated when adjusting for the other variables (**Table 3.7b,** right column).

	Tolerance	VIF
kV	1.000	1.000
mA	.966	1.035
Pixel Binning	.697	1.435
Rotation	.596	1.677
Machine Type	.757	1.322
Operator	1.000	1.000

TABLE 3.6 Test for collinearity among the independent variables. VIF = Variance inflation factor

(a)	P	OR	95% CI for OR Lower	95% CI for OR Upper	(b)	P	Adjusted OR	95% CI for OR Lower	95% CI for OR Upper
kV=90	.000	7.000	3.133	15.640		.000	22.718	5.139	134.922
kV=80	.002	3.267	1.537	6.942		.003	5.515	1.479	23.967
kV=70	Reference Category					Reference Category			
mA=9	.000	7.800	2.930	20.765		.000	67.243	10.286	350.560
mA=7	.000	7.286	2.955	17.692		.000	25.544	5.056	177.950
mA=5	.004	3.545	1.492	8.425		.001	9.230	1.990	54.921
mA=3	Reference Category					Reference Category			
Pixel Bin: 1x1	.000	7.125	2.622	19.363		.001	64.716	12.501	335.034
2x2	Reference Category					Reference Category			
Rotation:360°	.000	10.263	4.477	23.525		.000	32.29	3.264	330.974
200°	.054	2.333	.980	5.554		.004	10.769	2.150	53.946
100°	Reference Category					Reference Category			
Machine Type Acc	.084	1.800	.924	3.507		.509	1.389	.523	3.689
Pmx	Reference Category					Reference Category			
Operator: Senior Staff	.003	2.849	1.363	4.546		.000	6.620	2.523	17.372
JHDs	Reference Category					Reference Category			

TABLE 3.7 Logistic regression predicting the likelihood of achieving the diagnostic task: **(a)** odds ratios when predictor variables are considered separately **(b)** adjusted odds ratios when all included predictor variables are considered. OR = Odds ratio, p = p value <.05

3.5 DISCUSSION

The dose optimisation strategy ALADAIP (As Low as Diagnostically Acceptable being Indication-oriented and Patient-specific) highlights the importance of tailoring dose for a specific diagnostic task (OENNING ET AL. 2018). Therefore, an awareness of the most significant IQ metric in achieving a diagnostic task would certainly be of value when adopting this key radiation principle. This investigation aimed to find which of the core IQ metrics; CNR, noise, MTF and FWHM, that encapsulate the objective IQ of the acquired CBCT datasets, was a significant predictor of successfully achieving the diagnostic task of root canal identification. An additional aim was to explore the impact of all identifiable determining factors on this diagnostic task given the differing machines and imaging parameters.

3.5.1 Spatial resolution IQ metrics: Determining factors

The SedentexCT IQ phantom and inserts facilitates evaluation of the different aspects of the imaging chain in a standardised and reproducible mode and has been used to assess the correlation between objective IQ metrics and clinical diagnostic tasks (PAUWELS ET AL. 2012d, YEUNG ET AL. 2019). Encased in the PMMA phantom, which approximates the attenuation of the human head, the peripherally placed inserts replicated the peripheral position of structures of interest in dentomaxillofacial imaging of (e.g. teeth, jaw bones, sinuses). This is particularly relevant for the small FOVs used in this study as it has been shown that the size and position of a FOV can affect the image quality relating to the 'exomass effect' (BYRANT ET AL. 2008, PAUWELS ET AL. 2011). The methods of quantifying the IQ metrics were selected to remove subjectivity as much as is possible.

MTF values were calculated using a 30x30 pixel ROI, this is within the range deemed large enough to include the entire object response without including extraneous noise and artefact (KAYUGAWA ET AL. 2013). The MTF 10% values for the Accuitomo and ProMax (1.28-2.33 cycles per millimetre) were in keeping with the range reported (0.5 – 2.3 cycles per millimetre, median 2.1 cycles per millimetre) in a meta-analysis involving numerous machines with differing parameters (BRULLMAN & SCHULZE 2015). These ranges however, refer to theoretical spatial resolution emanating from

experimental conditions, without patient movement or normal patient scatter. The literature reports that there is a fair agreement with MTF 10% and lp mm^{-1} and that CBCT spatial resolution is, in reality, closer to 1 lp mm^{-1}, yielding a resulting visibility of details of only 0.5 mm (HORNER ET AL. 2013, BRULLMAN & SCHULZE 2015).

The MTF values were higher for the Accuitomo (voxel size: 80 μm) than the ProMax (voxel size: 100 μm), and is consistent with previous studies reporting higher MTF values with smaller voxel size (SUOMALAINEN ET AL. 2009, WATANABE ET AL. 2011, CHOI ET AL. 2019). Albeit, the literature has reported no significant correlation between MTF 10% and voxel size (ABOUEI ET AL. 2015, SCHULZE & DOERING 2019) for reasons (**Section 3.1**) such as errors in the imaging chain and implications of the Nyquist theorem, with voxel size described as only a rough indicator of available spatial resolution (BRULLMAN & D'HOEDTT 2011, BRULLMAN & SCHULZE 2015). This difference in spatial resolution may indeed be due to other factors that differed between the two machines. Across all settings, MTF 10% values were higher than that of the ProMax, this could also be attributed to the greater number of basis images associated with the larger rotation angle and exposure time. However, the ProMax had a greater number of basis images (rotation: 200°/exposure: 12 seconds) and yet recorded lower MTF 10% values than the Accuitomo 180° setting (180°/9 seconds). Furthermore, MTF 10% exhibits no relationship with dose (**Figure 3.5a**). The markedly lower noise values of the Accuitomo and consequently improved CNR may impact on MTF, being a function of contrast. Given that MTF is a system-level performance metric, differences in machine specifications (**Table 3.2**) may have had an influence. Both machines were identical with regards to focal spot size, (0.5 mm), pixel size (127 μm) and filters used in reconstruction. However, the Accuitomo (512 projections) had a higher number of projections than the ProMax for the standard setting which would enhance spatial resolution. Additionally, the he Accuitomo had a larger SOD (740-840 mm) than the ProMax (517.5 mm). This larger SOD can lead to sharper images owing to reduction of focal spot blur, the shorter SOD giving a higher geometric magnification (TRAN ET AL. 2021). In reality, identification of machine specifications provided in the instructions for use (IFU) cannot provide a comprehensive insight or understanding into the level of image quality attained by a given CBCT model, but is also established by undisclosed manufacturer customizations and adjustments.

FHWM was an additional IQ metric used to characterise spatial resolution, again involving imaging of a fine wire insert, with the acquired image being the PSF of the system. Unlike MTF, FWHM does not relate to the subjective observer measurement of lp mm^{-1}. Measurements of FWHM using the 0.25 mm steel wire in this study were also somewhat consistent with other reported studies, in so far as there were little to no differences evident in values for the range of protocols within the same FOV and protocols reconstructed at the same voxel size (PAUWELS ET AL. 2011, ABOUEI ET AL. 2015). Specifically, studies have reported decreases in FWHM values (enhanced spatial resolution) with increasing tube current-exposure time product from low to high dose protocols in the same device, the exception being where these protocols were reconstructed at the same or similar voxel sizes (PAUWELS ET AL. 2011). Furthermore, it was reported that FWHM values were almost the same within each FOV (ABOUEI ET AL. 2015). In reality, FWHM is unaffected by the product of X-ray tube current and exposure time and is precisely assessed at higher doses in X-ray systems to suppress noise. Exposure time has an indirect effect on FWHM as it impacts on the number of projections and consequently on the reconstruction algorithm (BUSHBERG ET AL. 2020). Reflecting normal clinical protocols for imaging individual teeth for endodontic purposes, only the smallest voxel size and FOV within each machine were selected, therefore FWHM was not a particularly discerning IQ metric in this study. Specifically, there was no change in FWHM for the ProMax protocols, and minimal change for the Accuitomo, although its high-resolution protocols (largest number of projections, native pixel array) did record the lowest FWHM values (increased spatial resolution) but FWHM showed no relationship with dose (**Figure 3.5b**). As with MTF, studies have shown that while there was some consistency between FWHM values and voxel sizes of the CBCT datasets, values did not significantly correlate with reconstructed voxel size (PAUWELS ET AL. 2011, ABOUEI ET AL. 2015). Additional factors, such as the difference in voxel values for the steel wire and the surrounding air, and the presence of small streak artefacts have also been demonstrated to influence PSF and thus the recorded spatial resolution (PAUWELS ET AL. 2011).

The 0.075 mm stainless steel wire was additionally used to calculate FWHM as it is smaller than the voxel size of both machines and theoretically could characterise the point spread function more accurately (NAKAYA ET AL. 2012, TRAN ET AL. 2021). It was

shown that in fact, for the ProMax protocols, the weak signal produced from minimal attenuation by the thinner wire was swamped by the random noise. Although, the signal from the higher current-time product protocols was stronger, measurement of FWHM was prohibited at all exposure protocols. It could be theorised that a wire of a higher atomic number element (e.g. tungsten 74, or gold 79) would have circumvented this problem. FWHM was recorded for the thinner wire for the Accuitomo for all settings, it can be seen from the results (**Table 3.3**) that there were was more variability in the range of values, with high resolution scans achieving the smallest FWHM values. It was noted that there was greater intrascan deviation in the readings for the 0.075 mm wire than the 0.25 mm wire (**Section 3.4.3**) particularly for the lower tube current-exposure time product settings, this being perhaps related to undersampling (WATANABE ET AL. 2010).

3.5.2 CNR and noise: Determining factors

On relating noise to dose for both machines it is evident (**Figure 3.5d**), that noise levels can be reduced by altering the exposure settings, including increasing the scanning time, tube current, and tube voltage. The results show that the ProMax noise levels were higher for the equivalent tube voltage and tube current standard setting of the Accuitomo, this may be related to the longer exposure times of the Accuitomo, its smaller FOV (negligible difference between scanners), filters, reconstruction algorithms, smoothing filters, detector efficiency or even machine environment (PAUWELS ET AL. 2015a). In fact, the Accuitomo demonstrated superior control over noise, considering the ProMax higher noise levels when compared with the high resolution settings, despite the noise elevating effects of the native pixel array and the smaller voxel size.

CNR, being a quantitative measurement of low-contrast resolution, indicates the system's ability to differentiate a signal from the background and relates more strongly to image quality than noise (KALENDER 2009). The factors determining CNR are considered in detail in Chapter 2 (**Section 2.5.3).** To summarize, complementary information of projectional data rather than signal at the detector dictates contrast in CBCT imaging and thereby diminishes the effects of X-ray tube voltage on contrast (PAUWELS ET AL. 2014b). Thus, contrast, which remains relatively stable in this study's fixed scan set up (phantom composition), is relatively independent of exposure factors;

however, CNR is largely driven by noise and thus CNR demonstrates a positive relationship with tube current-exposure time product and hence DAP (**Figure 3.5c**). Consequently, Accuitomo CNR values were superior to those of the ProMax, even for the high resolution settings, where the CNR dropped relative to the machines standard and 180° settings.

3.5.3 Logistic Regression

3.5.3.1 IQ metrics

FWHM and noise were removed from the logistic regression model due the high degree of correlation with the other independent variables MTF and CNR. Such multi-collinearity occurs when independent variables are effectively a measure of the same element and have to be removed from the model as they would reduce the precision of the estimated coefficients and weaken the statistical power of the regression model. Of the IQ metrics measured, CNR was shown to be significantly associated with successfully achieving the diagnostic task of root canal identification and agrees with other studies reporting the positive relationship between CNR and the identification of anatomical landmarks and achieving diagnostic tasks (CHOI ET AL. 2015, PAUWELS ET AL. 2015b, MCGUIGAN ET AL. 2020, WANG ET AL. 2020). The regression model did not identify spatial resolution, as quantified by MTF, as having a statistically significant relationship with the diagnostic task of root canal identification when adjusting for CNR. On confirmation of the correlation between FWHM and MTF, FWHM was removed, as it was evident from graphical display (**Figures 3.6 c & d**) that FWHM did not show a clear relationship with achieving the diagnostic task. Contrary to this finding, one identified study concluded that FWHM provided the most suitable link with the subjective assessment of identifying anatomical landmarks (OENNING ET AL. 2019). However, this study reported that this finding applied only when protocols involving a range of different voxel sizes were being compared, and indeed that CNR is more relevant when the voxel size is fixed, as was the case in this study for each machine.

3.5.3.2 IQ determinants

Regarding exposure factors, the regression model demonstrated, as expected, that the odds of successfully achieving the diagnostic task were significantly increased with

higher levels of kV and mA compared to a lower baseline level (**Table 3.7**). Native pixel array compared to 2x2 pixel binning and 360° and 200° rotation compared to 180° also significantly increased the odds of successfully identifying the root canal anatomy. However, it is impossible to extricate native pixel array properties of the high-resolution setting from the effects of increased tube current-exposure time product associated with increased time and basis images that accompanies this setting for the given exposure protocol. It should be mentioned that, while these identified variables are significant and they do have an effect on the response variable, the large confidence intervals associated with the adjusted odds ratios mean these results have to be viewed with caution. Causes of large confidence intervals may possibly be due to a small sample size or due to the combination of variables in the model. Calculation of sample size (10k/p: k = number of independent variables, p= proportion of –ve or +ve cases in the population) did indicate 133 cases were required, this number being exceeded in this study (180). Other means of statistically analysing the data were investigated (linear mixed effects, fixed effects model) but model assumptions were not satisfied.

The odds ratios for the variables, machine type and operator did exhibit narrow confidence intervals. Machine type did not prove to have a statistically significant effect on successfully achieving the diagnostic task in this study despite the superior CNR, noise, MTF values, in addition to the higher DAP values and smaller voxel size of the Accuitomo F170®. Furthermore, these variations were accompanied by the hardware differences identified between the two machines (**Table 3.2**). These differences in value highlights that IQ metrics are device dependent and not readily comparable. Interestingly, MTF being a measure of spatial resolution and voxel size, albeit considered under the umbrella of machine type, did not prove to have a significant effect on this task (BRULLMAN & SCHULZE 2015). It would be presumed that an IQ metric or imaging variable that enhanced the ability to differentiate small structures as separate entities would prove to be a significant factor in this diagnostic task. However, it has been well established that larger voxel sizes do not necessarily mean lower diagnostic accuracy for diagnostic tasks requiring fine detail, with a meta-analysis of studies reporting no impact of voxel size on the detection of vertical root fracture (MA ET AL. 2016). Notably, a recent study did identify an impact of voxel size on vertical root

fracture diagnosis but only when comparing broadly different voxel sizes (250/160 μm and 250/80 μm), (GUO ET AL. 2019).

Operator experience was demonstrated to have a statistically significant effect on successfully achieving the diagnostic task, which is in agreement with other studies that reported on the impact of operator expertise/experience and variance, on achieving a diagnostic task using CBCT (PARKER ET AL. 2017, WOLF ET AL. 2020). The benefits of increased operator experience may relate not solely to enhanced interpretive skills, but also to proficiency in making full use of zooming tools and maximising windows in order to achieve a 1:1 ratio of image pixel to monitor pixel which allows optimal presentation of the scan images. The Acer V176LBMD 17" HD Ready Monitor (Acer UK, London) used in this study had a resolution of 1280 x 1024 pixels, with machine FOV and voxel sizes (ProMax® 3D: 50 mm (D) x 50 mm (H): 0.1 mm, Accuitomo: 40 mm (D) x 40 mm (H): 0.08 mm) resulting in each scan slice for both machines being 500 x 500 image pixels. Therefore, viewing in the multiplanar formatting (2x2) view would require a minimum resolution height of 1000 x 1000 pixels. However, if considering the screen pixels occupied by the graphic user interface, this would necessitate a monitor height in excess of the 1024 pixels available in order to show each slice at a 1:1 ratio of scan voxels with monitor pixels. This could only be achieved in this study set up through use of zooming tools or maximizing windows. Therefore, magnification of image may have had an indirect impact on successfully achieving the diagnostic task. While all observers, not proficient in viewing the software of each system, were given a standardized interactive tutorial prior to observation, a potential limitation of the study was not to record whether the operators actually availed of magnification in their observations so its impact could have been assessed. The benefits of large-size and high resolution monitors are thus apparent (PAUWELS ET AL. 2015a). Higher diagnostic accuracy has been associated with medical grade monitors (ORGILL ET AL. 2019) although not exclusively so (ISIDOR ET AL. 2009). The technical specifications of the monitor used in this study were within the range indicated by the UK Health Security Agency (UKHSA) as required for diagnostic purposes of dental CBCT images (Health Protection Agency, 2010). In this study a DICOM-calibrated consumer grade display was used for the subjective assessment of the CBCT datasets and a standardised ambient room lighting recorded of less than 50 lux (HELLÉN-HALME ET AL., 2012). Studies have concluded that

DICOM-calibrated consumer grade monitors have been shown to be capable of displaying luminance image quality (MCILGORM ET AL. 2013) and facilitating diagnostic accuracy for a range of diagnostic tasks (KALLIO-PULKKINEN ET AL. 2015) comparable with that achieved with a DICOM-calibrated medical grade monitor.

CNR is a measurement of low-contrast resolution and indicates the system's ability to differentiate a signal from the background and accordingly, between tissue types. This study shows that CNR is a significant IQ metric in successfully identifying root canal anatomy. CNR is largely dictated by noise and thus driven by exposure settings and time, this being confirmed by the findings that higher tube voltage, tube current and rotation angle (above study baseline) significantly increased the odds of achieving the diagnostic task. From an optimisation perspective it is useful to establish the relationship between IQ metrics and exposure parameters, with a specific diagnostic task, in order to prioritise those most relevant at an optimised dose. **Chapter 2** confirmed how a threshold CNR can be established (for a given machine) for the diagnostic task of identification of root canal anatomy, above which the diagnostic task was consistently achieved. This study provides further support for this strategy and the potential clinically for identifying the exposure protocols that can achieve this threshold CNR level at the minimum patient dose, while being aware of the over estimation of diagnostic accuracy in *ex vivo* studies.

Additional limitations of this study included the wide confidence interval for the dose related variables, it was hypothesized this may be due to the sample size although the requirement for sample size were met. Possibly some interaction between degree of rotation and pixel binning may have caused this issue. It would be of interest to repeat this study with a wider variation of machines that could allow clearer isolation of imaging variables that varied exclusively with machine in this study. Additionally, imaging a greater variety of M1Ms anatomy would allow a more insightful assessment of the impact of tooth anatomy on successful completion of the diagnostic task to be assessed. In this study tooth type/anatomical variation was not included in the list of possible variables as T8 did not achieve the task at any exposure protocol. Inclusion of T8 would have caused issues of convergence in the regression model (ALLISON 2008) as all observations for the variable would be the same (0 - did not achieve the task). A wider variation of machines and/or teeth would obviously increase scan numbers to be

observed which may create issues of observer recruitment as has been reported (YALDA ET AL. 2022). Albeit, this increase could be counteracted by restricting the range of exposure protocols e.g. removing the lowest (those that were already identified as diagnostically unacceptable) and highest DAP protocols. Ultimately a clinical study, allowing impact of motion blur from patient movement in addition to artefacts from restorations, particularly existing endodontic treatment (KRUSE ET AL. 2019) would provide more clinically relevant data rather than use of data from an ex-vivo model (**Section 2.5.1**). The issue of course with a clinical study, apart from the obvious ethical issues that exists with all optimisation studies, is the absence of the reference standard as a micro CT could not be completed on a tooth *in vivo*, although there is at least the theoretical possibility of using teeth which are planned for extraction (e.g. some third molars or other ectopic teeth).

3.6 CONCLUSIONS

- The IQ metric shown to have a statistically significant effect on successfully achieving the diagnostic task of identification of root canal anatomy is CNR.

- Imaging variables; X-ray tube voltage, X-ray tube current, degree of rotation and native pixel array were demonstrated to have a statistically significant effect on successfully achieving this diagnostic task, albeit with wide confidence intervals.

- Skilled, experienced observers significantly increased the odds of successfully identifying root canal anatomy.

- Measurement of spatial resolution using FWHM in not a discerning IQ metric when the acquired scans have the same voxel size and FOV.

- Assessing FWHM with a wire diameter (0.075 mm) smaller than the voxel size (80 µm) was not successful for both machines due to the resulting weak signal.

Chapter 4

The impact of CBCT on endodontic access cavity preparation and associated outcomes in maxillary 3D printed first permanent molars

4.1 INTRODUCTION

CBCT offers the advantages of cross-sectional imaging and, for some diagnostic tasks, superior diagnostic accuracy, compared with conventional radiographic techniques (SCARFE & FARMAN 2008). This benefit is reflected in clinical guidelines that advocate its use for specific clinical applications (HARRIS ET AL. 2011, EUROPEAN COMMISSION 2012, AAE & AAOMR 2015, PATEL ET AL. 2019, HORNER ET AL. 2020). Uncertainty remains, however, as to whether this enhanced accuracy translates into positive impacts on patient outcome, classified as level 5 (**Section 1.4.1; Table 1.4**) of Fryback and Thornbury's imaging efficacy classification model (FRYBACK & THORNBURY 1991), which would thereby help to justify the higher doses associated with this imaging modality.

A general paucity of literature demonstrating a positive impact of CBCT imaging on patient outcome exists across the spectrum of dental disciplines and notably in the endodontic literature. This is, in part, due to the fact that that investigation of diagnostic efficacy at the higher levels of the hierarchical model (FRYBACK & THORNBURY 1991), is difficult to achieve in the absence of randomised control trials (RCT). These are ethically challenging and may be impossible to perform with regards to diagnostic imaging modalities (MILEMAN & VAN DEN HOUT 2009) and furthermore often result in poor reproducibility, high-bias and ultimately low quality studies, which are inadequately powered (ROEDER ET AL. 2012). A recent review (HORNER ET AL. 2020) identified 26 systematic reviews (involving *in vivo* and *ex vivo* studies of adult patients) of CBCT diagnostic efficacy, of which 12 related to endodontology. Only one of these 12 endodontic systematic reviews (ROSEN ET AL. 2015) reported on diagnostic efficacy studies higher than diagnostic accuracy efficacy (level 2, of the hierarchical model [FRYBACK & THORNBURY 1991]), with only one article having findings relating to patient outcome (KURT ET AL. 2014). This systematic review by Rosen and co-workers (ROSEN ET AL. 2015) was recently updated to consider only high-level-evidence studies (ROSEN ET AL. 2022), but only identified one further article relating to patient outcome (YANG ET AL. 2016).

The identified patient outcome studies (KURT ET AL. 2015, YANG ET AL. 2016) did report positive findings and potential justification of CBCT with regard to the impact on surgical and non-surgical endodontic treatment outcome but these findings have to be

judged in context of their methodological quality. Both outcome studies were identified as having high levels of bias (met no more than five of the quality criteria [REITSMA ET AL. 2009]). Yang et al. (2016) carried out a prospective clinical study reporting that CBCT, in addition to ultrasonics and use of a dental operated microscope (DOM), aided negotiation of all 16 calcified (mid and upper third sclerosis) molar root canals. However, it was a single-arm intervention study (or a case-series), small patient numbers (13) with the absence of a power calculation, control group; therefore, it was described as a low quality study, making it impossible to assess the validity of its findings. Kurt et al. 2015 performed a randomized control trial to compare the impact of CBCT with conventional imaging on molar periapical surgery (40 patients). No significant difference was shown between treatment success rates using CBCT imaging and conventional imaging but a significantly shorter procedural time was reported with CBCT imaging. This study was criticized as it showed verification bias (outcome being assessed by the actual index test), incorporation bias in addition to uninterpretable results. The evidence of CBCT impact on endodontic outcome is limited to these two studies, which appear to be of limited quality. Of the other high-evidence-level studies (levels 3 and 4) identified in the review (ROSEN ET AL. 2022) only two were considered to have a low risk of bias and these and other relevant studies are considered in **Section 1.4**. The predominance of high bias, lower-evidence-level studies highlights most of all, perhaps, the difficulty in designing and executing studies to provide the robust evidence that the clinician needs to satisfy themselves that CBCT will influence decision making, treatment strategy and treatment outcome.

A positive impact on patient outcome efficacy, (level 5 of the imaging classification model) (FRYBACK & THORNBURY 1991) in non-surgical endodontics, must primarily demonstrate an improvement in the long-term retention of the tooth, achieved by treating or preventing apical periodontitis. The management of necrotic pulp tissue and apical disease is achieved by effective chemo-mechanical debridement of the entire root canal system after location and instrumentation of all root canals present, with the ultimate aim of optimal reduction/elimination of microbial biofilm in the root canal system (ESE 2006). Long-term retention of the tooth was considered by consensus as the most critical outcome for non-surgical root canal treatment in the development of the ESE S3-level clinical practice guidelines (DUNCAN ET AL. 2021), while

another specific outcome measure, cited in these guidelines as important, was 'tooth function (fracture, restoration longevity)' (DUNCAN ET AL. 2021). Resistance to root fracture is multifactorial and requires preservation of the structural integrity of the tooth after endodontic access cavity and root canal preparation has been completed (LANG ET AL. 2006). Additional factors including dentine age (AROLA & REPROGEL 2005), the use of root canal irrigants (KAFANTARI ET AL. 2019) and type of medicaments used (ANDREASEN ET AL. 2002), which have been shown *in vitro* to affect the physical properties of dentine. Loss of marginal ridge (REEH ET AL. 2009, EL-HELALI ET AL. 2013) and lack of cuspal coverage of endodontically treated posterior teeth (SORENSEN & MARTINOFF 1984) are well reported causes of reduced fracture resistance, in addition to the compounding effects of masticatory forces (CHAN ET AL. 1998). Furthermore, residual tooth volume and the presence of cracks, have been demonstrated to influence restoration and tooth survival (AL-NUAIMI ET AL. 2017, AL-NUAIMI ET AL. 2020, BHUVA ET AL. 2021, LIN ET AL. 2022). The concept of minimally invasive endodontics dictates that non-surgical endodontics should cause the least amount of change to the dental hard tissues in order to preserve the strength, stiffness, function, and longevity of the endodontically treated tooth (TANG ET AL. 2010, GLUSKIN ET AL. 2014). While ultimately, the total volume of residual tooth substance has been identified as being linked to tooth survival (AL-NUAIMI ET AL. 2017, AL-NUAIMI ET AL. 2020), specifically maintaining the structural integrity and dentine volume of the peri-cervical area of the tooth (defined as the area approximately four millimetres above and below the alveolar crest) has been identified as being critical to fracture resistance and long-term survivability (CVEK 1992, KATEBZADEH ET AL. 1998, CLARKE & KHADEMI 2010). Indeed, the thinness of the cervical area was a significant factor in the determining the occurrence of root fracture clinically of immature incisor teeth (CVEK 1992). Thus, minimising the dimensions of the access cavity while achieving adequate root canal access is an important objective. It can be hypothesised that the availability of CBCT, providing cross-sectional imaging of the tooth, would assist in achieving this objective.

Root canal anatomy varies enormously from tooth to tooth and from patient to patient. Any study attempting to quantify the efficacy of a diagnostic technique such as CBCT is faced with a choice of which teeth to study. The results of studies on, for example, endodontics of maxillary central incisors might be expected to be different to those on teeth with more complex root canal systems for which cross-sectional imaging

might offer greater benefits. Molar endodontics is usually seen as being complex and identifying the location of the MB2 canal in maxillary first molar (M1M) teeth would generally be seen as particularly challenging for clinicians. The evidence suggests that a greater number of MB2 canals could be located clinically (78%: using experienced endodontists and a dental operating microscope), than were identified on CBCT imaging (69%: using separate pair of evaluators, a suspected MB2 canal was classified as absent [HIEBERT ET AL. 2017]). However, in cases where clinical methods cannot locate the MB2 canal, supplemental CBCT imaging has been shown to have a significant impact on the incidence of locating the MB2 canal (HIEBERT ET AL. 2017, PARKER ET AL. 2017). Regarding preservation of dentine, guided-endodontics, which uses a 3D printed stent generated by CBCT, to clinically locate the canal orifice, has been shown to reduce tooth substance removal in incisor teeth with sclerosed canals (BUCHGREITZ ET AL. 2019, CONNERT ET AL. 2019) as well as extracted maxillary molars (SATO 2020). However, guided-endodontics adds both time and expense and is not commonly used in molar endodontics, and it has not yet been shown if CBCT imaging alone (without a stent) had any impact on tooth substance removal when locating all four root canals in M1Ms.

Position statements from European and American Endodontic organizations have stated that CBCT imaging of teeth prior to root canal treatment is indicated in cases where anatomically challenging morphology is predicted or when a combination of planar radiography and clinical investigation with a dental operating microscope cannot locate the orifice, portals of exit or extent/continuity of the canal, (AAE & AAOMR 2015, ESE 2019). Identification and negotiation of more complex anatomy is important, as failure to locate all the root canal anatomy in a tooth reduces the efficacy of chemo-mechanical debridement and increases risk of persistent disease, endodontic failure and potentially tooth loss (WOLCOTT ET AL. 2005, TSESIS & FUSS 2006, CHANG ET AL 2013). Conversely, extensive searching to locate root canals can result in excessive dentine removal, particularly in the mesio-buccal (MB) root area, which can lead to potential complications including reduced resistance to root fracture, perforation and compromised restoration (DE CHEVIGNY ET AL. 2008, GLUSKIN ET AL. 2014, BHUVA ET AL. 2021), leading to potential tooth loss (STUDEBAKER ET AL. 2018). Previously, it has been suggested that CBCT imaging may improve the ability to locate root canals in teeth with challenging anatomy (HIEBERT ET AL. 2017, RODRÍGUEZ ET AL. 2017). A positive impact of CBCT

imaging on patient outcome, relating to second mesiobuccal (MB2) canal location, could be determined by a reduction in tooth substance loss, increased canal identification and reduced procedural time. Reduced procedural time may have an impact on the patient-centred outcome, cost-effectiveness (SCHWENDICKE & GÖSTEMEYER 2016).

To test a hypothesis that the availability of CBCT imaging might lead to patient or societal benefits, the ideal research design would be a RCT. As described in **Chapter 1** of this thesis, RCTs are challenging to perform to an excellent standard. Unlike new drug therapies, there are no comparable frameworks for requiring evidence of improvements in outcome efficacy. New diagnostic methods, particularly imaging, are therefore often introduced into practice without clinical trial evidence (KNOTTNERUS ET AL. 2002). Furthermore, clinician and patient recruitment could be challenging for a RCT on an established diagnostic imaging method because of a perception that some patients would be 'deprived' of access to the best techniques. 'Before-after' study designs have been used as one method of identifying changes in clinical practice (Level 3 and 4 of Fryback & Thornbury's hierarchy) but can also be applied to patient outcomes studies (Level 5 or 6). In its traditional sense, the 'before-after' design would involve measuring some aspect of diagnostic thinking, treatment or outcome before and after introduction of a new imaging method, so permitting the identification of any changes resulting from it. As highlighted, this research design has several weaknesses that mean changes in the measured parameter 'after' introduction of the new method might not actually be due to the new imaging technique itself (ROHLIN ET AL. 2020). An alternative method is to test the impact of the new method in parallel rather than in series, in a 'with-without' design (ROHLIN ET AL. 2020). It is impossible to treat a patient twice for the same purpose simultaneously, so this method is applicable to clinical 'vignettes' or scenarios, in which clinicians are presented with clinical and diagnostic information (e.g. history and examination information, photographs, diagnostic test results) about a patient with, and then without, the addition of the new imaging information. An extension of this design can be proposed for dental or surgical purposes by manufacturing a model of a patient upon which the procedure can be performed. Such a method was used in the context of dental implant placement (SHELLEY ET AL. 2011). A

key aspect of this design is that the model should be as close to a clinical situation as possible.

Therefore, due to the ethical challenges of clinical trials and logistical impossibility of comparing outcome measures within the same tooth to establish the benefits of CBCT imaging compared with conventional radiography, this study utilized 3D printed reproductions of extracted first permanent molar teeth in a clinical scenario with laboratory simulation. The development of an accurate 3D printed replicate facilitates experimental standardization and realistic clinical simulation (LIANG ET AL. 2018, CONNERT ET AL. 2019, MAGNI ET AL. 2021).

The aim of this 'with-without' study using 3D printed M1M teeth was to identify if supplemental CBCT imaging can potentially improve outcome after endodontic access cavity preparation in M1Ms, by analysing changes in tooth substance removed, procedural time taken and root canals located, specifically in relation to location of the MB2 canal, compared with the use of conventional (IOPA) and clinical methods alone; thereby justifying the increased dose associated with CBCT imaging.

4.1.1 Null hypotheses

The null hypotheses of this 'with or without' study design, were that provision of additional CBCT imaging would result in:

1. No difference in the volume of tooth substance removed.

2. No difference in time taken to complete access cavity preparation (procedure time).

3. No differences in the outcome measurement (1-2) when adjusting for experience level, session number, magnification, tooth type.

4. No change in the proportion of canals located and specifically, MB2 canals located.

5. No impact on operator confidence and reported 'helpfulness' on location of the MB2 canal.

4.2 OBJECTIVES

1. For participants, over two randomised sessions (with washout period), to locate and establish coronal patency of the palatal, disto-buccal, MB1 and MB2 canals in three different bespoke 3D-printed M1M teeth with the preoperative aid of either IOPA imaging alone or IOPA supplemented with CBCT imaging. Each tooth would have distinct MB2 canal morphologies and location challenges.

2. To quantify the volume of tooth substance removed and specific access cavity dimensions subsequent to procedure outlined in 1., in both sessions.

3. To measure the time taken to complete endodontic access cavity preparation and attempt location of all four canals in both sessions.

4. To analyse the number of canals located after both sessions.

5. To measure operator confidence and perceived 'helpfulness' of both imaging techniques in achieving MB2 canal location outlined in 1.

6. To assess any impact of operator experience, the session number, magnification and tooth type on tooth substance removal and time taken for endodontic access cavity preparation and canal location, using conventional and CBCT imaging.

4.3 MATERIALS AND METHODS

4.3.1 Teeth selection

Ethical approval for the use of pooled extracted teeth in this study had previously been obtained from St. James' Hospital/Tallaght University Hospital (SJH/TUH) Joint Research Ethics Committee (Reference number 2019-02 Chairman's Action [05]). M1Ms were selected by the author from a bank of extracted teeth, collected for this study. After extraction, the teeth were washed with water and the adherent tissue gently removed, before being immersed in a 2% sodium hypochlorite solution (Milton, Milton International, Nantes, France) for 24 hours prior to storage in a sterile saline solution (Henry Schein, Dublin, Ireland). Inclusion requirements were based on preliminary visual and radiological examination. Visual inclusion criteria were the external anatomical features, a mesio-distal crown diameter of 10mm ± 0.2 (JORDAN ET AL. 1992), three mature distinct roots with closed apices, and absence of root fracture. Radiological criteria were the presence of a pulp chamber and absence of extensive tertiary dentine deposition, as seen on using conventional radiography. Ten teeth were identified in this way. Subsequently, CBCT imaging (ProMax 3D Classic, CBCT scanner) was used to refine the selection of teeth, with the intention of obtaining a range of MB2 features; this limited the ten M1Ms that visually appeared to fit the inclusion criteria, to three left M1Ms and one right M1M (provisionally three study and one practice tooth) representing differing MB2 bucco-palatal and apico-coronal positions, MB2 orifice width, and possessing a visible MB2 canal in the coronal aspect of the root canal.

4.3.1.1 MicroCT analysis

In order to confirm MB2 anatomical features, microCT analysis of the four selected M1Ms (µCT 40 SCANCO Medical AG, Brüttisellen, Switzerland) was performed in the core facility in the Bioengineering Building, TCD. The teeth were positioned in turn with the occlusal surface (pulpal floor) parallel to the horizontal plane and imaged at 70 kVp, 114 mA, 8 W with a spatial resolution of 20 µm. DICOM files were imported into ITK-SNAP (free software, Version 3.8, http://www.itksnap.org), allowing visualisation and navigation through all three orthogonal planes of the reconstructed microCT 3D images of the tooth/root canal systems **(Figures 4.1a-c: 1-3)**. Additionally, the hard tooth

structure and, separately, the pulp chamber and root canal anatomy of each M1M were segmented in ITK-SNAP (process described in detail **Section 4.3.2.1**) and the Standard Tessellation Language (STL) files imported into Meshmixer (free software, version 3.5, http://www.meshmixer.com) to allow analysis of and interaction with the 3D structures. The resulting segmented meshes (**Figures 4. 1a-c: 4 - 5**), in addition to the reconstructed images of the tooth/root canal systems (**Figures 4. 1a-c: 1-3**), were viewed by two independent endodontists not taking part in the study itself. Endodontists were defined as individuals who had completed a three-year full time equivalent training in endodontics. The endodontists were asked to describe canal numbers in each tooth, canal continuity, and the bucco-palatal and apico-coronal positions of the MB2 orifice relative to the pulp chamber floor.

The two independent endodontists confirmed that teeth X, Y and Z were left M1Ms and the practice tooth was a right M1M, each exhibiting four canals including a continuous MB2 canal, while all differed with regards to the position and origin of the MB2 orifice (**Figure 4.1a-c, Table 4.1**). The investigator scrolled using the (↓) cursor through the 2D axial slices (**Figure 1a-c**) from the pulpal floor in an apical direction, noting the bucco-palatal and apico-coronal location of the MB2 canal orifice (**Table 4.1**). The origin was recorded as the position at which the MB2 orifice first became identifiable as a separate canal in the axial slices (**Table 4.1**). The endodontists identified the MB2 orifice of Tooth Z as being the most technically challenging to locate. It had the smallest coronal diameter; its origin was located almost 1 mm apical to the floor of the pulp chamber and was close to the MB1 orifice. Tooth X and Y had different MB2 origins in the bucco-palatal plane compared with tooth Z (**Table 4.1**). After assessment all four teeth (X, Y, Z and the practice tooth) were selected for 3D printing. Prior to printing, the four teeth were accessed to ensure the canals were in fact present as visualised on the microCT scans and were negotiable.

	Bucco-palatal Position of MB2 Orifice Reference Point: Direct line: Mid MB1-P Direct line: Mid MB1-MB2	Apico-coronal Position of MB2 Orifice	Approximate Diameter of MB2 Orifice at level first identified (mm)
X	Mesial: Mid MB1-P Mid MB1-MB2: 2.38 mm	At floor of pulp chamber, appears simultaneously with MB1, DB, P	0.61
Y	Mesial: Mid MB1-P Mid MB1-MB2: 1.01 mm	Just below main body of floor of pulp chamber, appears simultaneously with MB1, DB	0.53
Z	Mesial: Mid MB1-P Mid MB1-MB2: 0.63 mm	Finally separates from the MB1 main orifice 0.84 mm below the main pulp body floor (measured in sagittal view).	0.21

TABLE 4.1. Classification of features of MB2 canal for Tooth X, Y, and Z.   MB1: First mesiobuccal
canal, MB2: Second Mesiobuccal Canal, DB: DIstobuccal canal, P: Palatal canal.

FIGURE 4.1a Tooth X: MicroCT images reconstructed in ITK-SNAP from DICOM files **(1-3).** Segmented meshes reconstructed in Meshmixer from STL files of the pulp chamber and root canal anatomy **(4)** and the entire hard tooth structure using toggle visibility **(5).** ITK-SNAP: software application used to segment structures in 3D medical image. DICOM: Digital Imaging and Communications in Medicine.
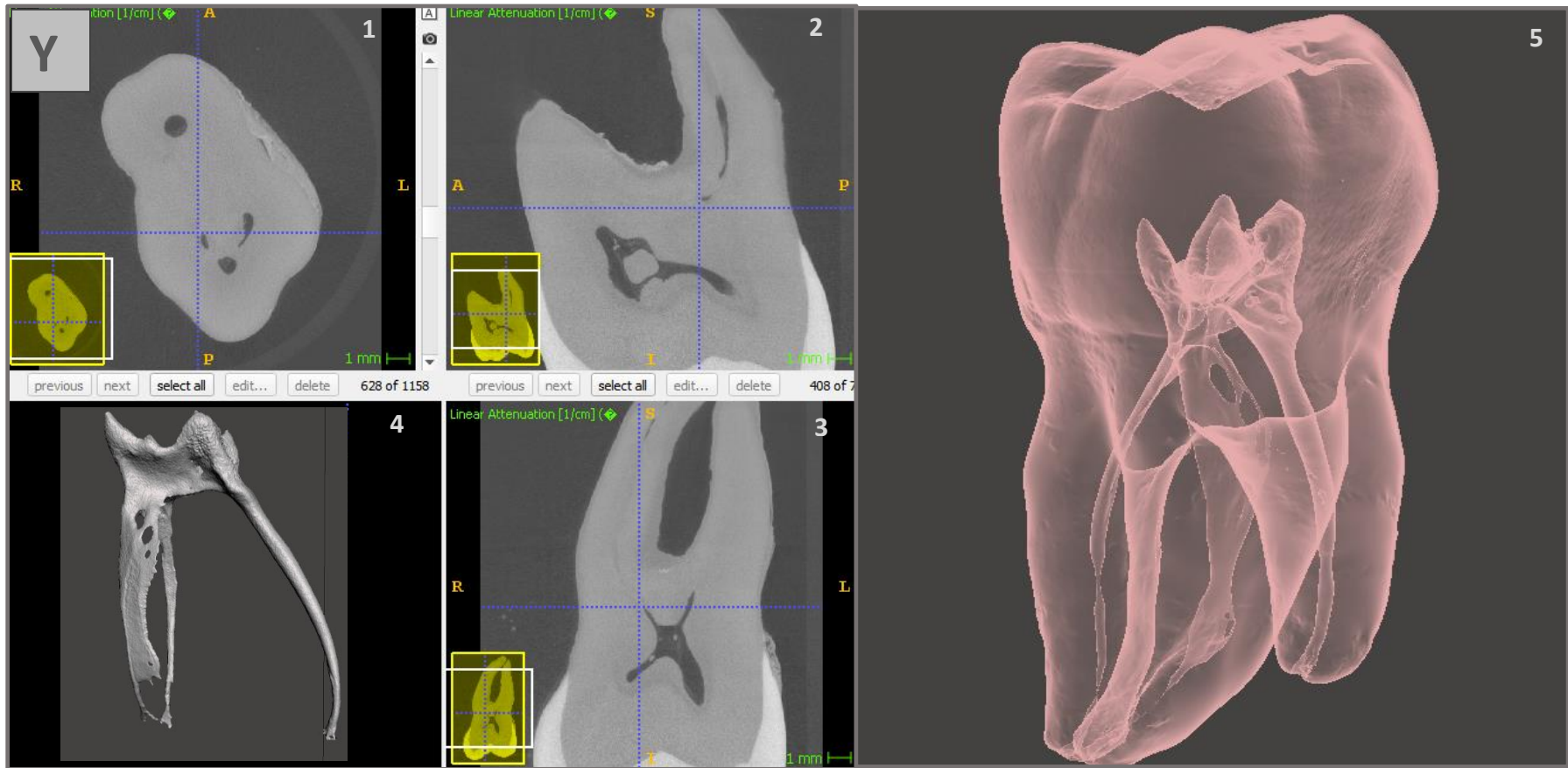
FIGURE 4.1b Tooth Y: MicroCT images reconstructed in ITK-SNAP from DICOM files **(1-3).** Segmented meshes reconstructed in Meshmixer from STL files of the pulp chamber and root canal anatomy **(4)** and the entire hard tooth structure using toggle visibility **(5).** ITK-SNAP: software application used to segment structures in 3D medical image. DICOM: Digital Imaging and Communications in Medicine.
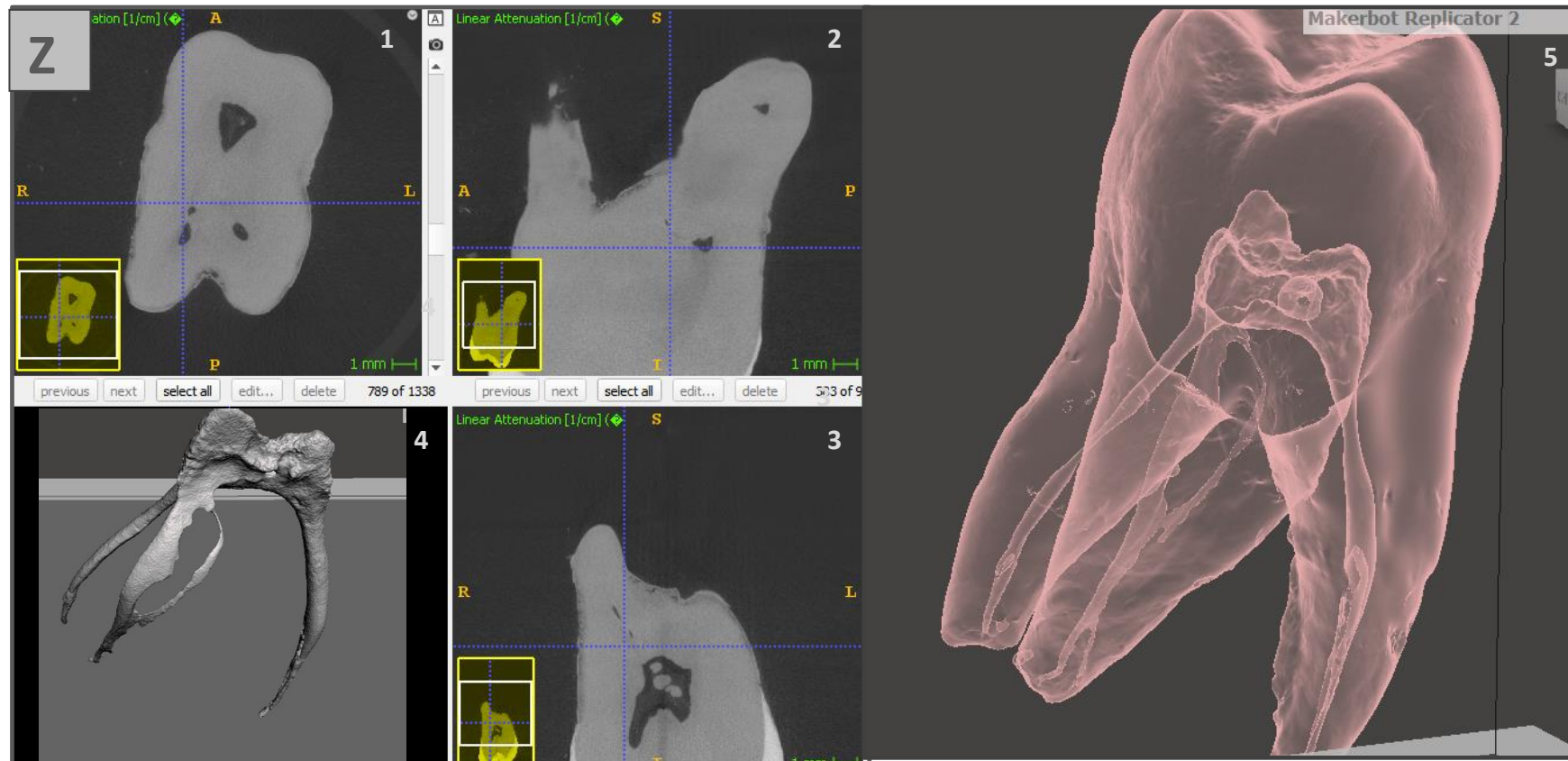
FIGURE 4.1c Tooth Z: MicroCT images reconstructed in ITK-SNAP from DICOM files **(1-3).** Segmented meshes reconstructed in Meshmixer from STL files of the pulp chamber and root canal anatomy **(4)** and the entire hard tooth structure using toggle visibility **(5).** ITK-SNAP: software application used to segment structures in 3D medical image. DICOM: Digital Imaging and Communications in Medicine.

4.3.2 3D printing of M1M replicas

4.3.2.1 3D printing workflow

Segmentation of the M1M images (imported as DICOM files into ITK-SNAP) was required to facilitate 3D printing of the teeth. Digital image segmentation is the process (**Figure 4.2a-f**) whereby the selected structure of interest, in this case the hard tissue structure of the tooth, is delineated using thresholding according to pixel value (**Figure 4.2b**). A label is assigned to every pixel in the image region of interest, with pixels sharing the same characteristics, having the same label. Labelling was executed in all three orthogonal planes and results were visualized as a three-dimensional rendering or mesh. The segmented meshes were imported as STL files into Meshmixer to facilitate preparation for printing. The mesh of a tooth is a complex geometry represented by several million constituent triangles. In this form, the mesh cannot be processed by the computer programs necessary for the printing process, as the number of triangles is proportional to rendering speeds and memory requirements. A decimation algorithm in Meshmixer was applied to the mesh, specified as a percent reduction (50%) of the original mesh, reducing the number of triangles (to < 1 million triangles) while preserving the original topology and good adherence to the original geometry. Subsequently, the outer surface of the crown/root was smoothed to remove any defects that would potentially interfere with printing (**Figure 4.3**). Finally, the STL files were imported into Blender (free software, version 2.9, http://www.blender.org) to check STL files for printability and any further editing where necessary.
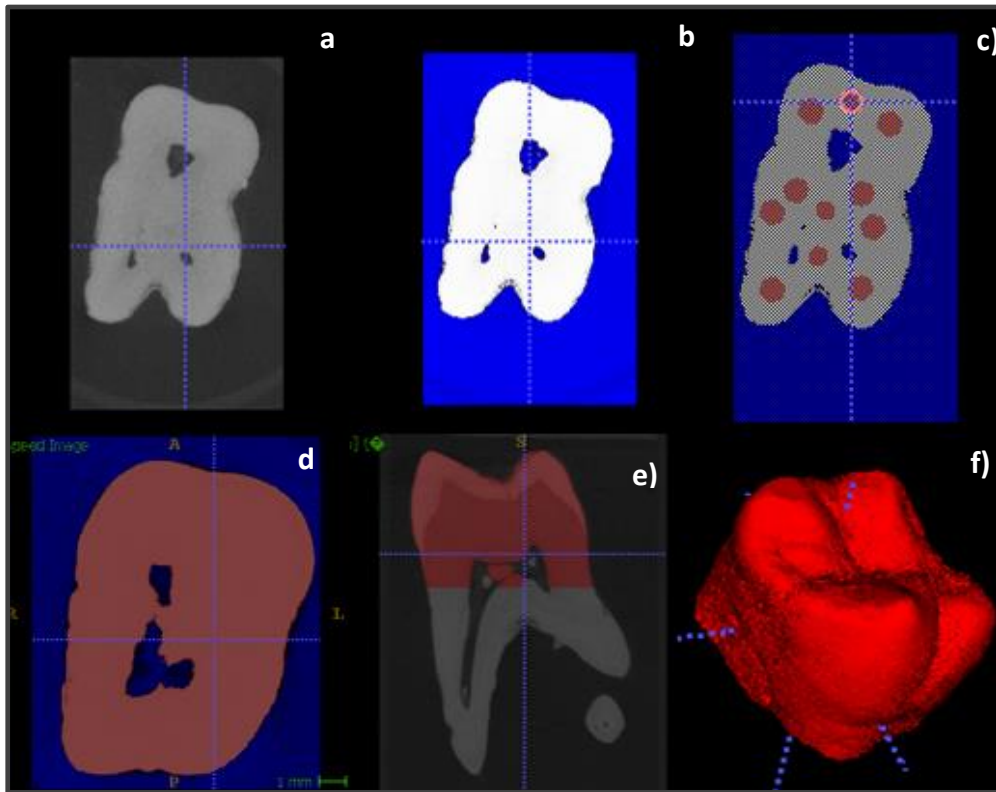
FIGURE 4.2 Illustration of segmentation process of M1M crown using ITK-SNAP semi-automatic segmentation: **a)** Definition of the region of interest (axial view), **b)** thresholded image: upper and lower threshold values adjusted so that structure to be segmented (crown structure) is white and sharply delineated from the blue area that is not to be segmented (pulp chamber). **c)** Labelling: 3D bubbles placed inside of the crown of tooth (evolution after 30 iterations), **d)**, **e)** axial and then sagittal view of finished evolution of crown structure (after 325 iterations), **f)** mesh of crown obtained after automatic segmentation. Meshes were produced for the entire tooth for each M1M. M1M: First Maxillary Molar

ITK-SNAP: software application used to segment structures in 3D medical images.
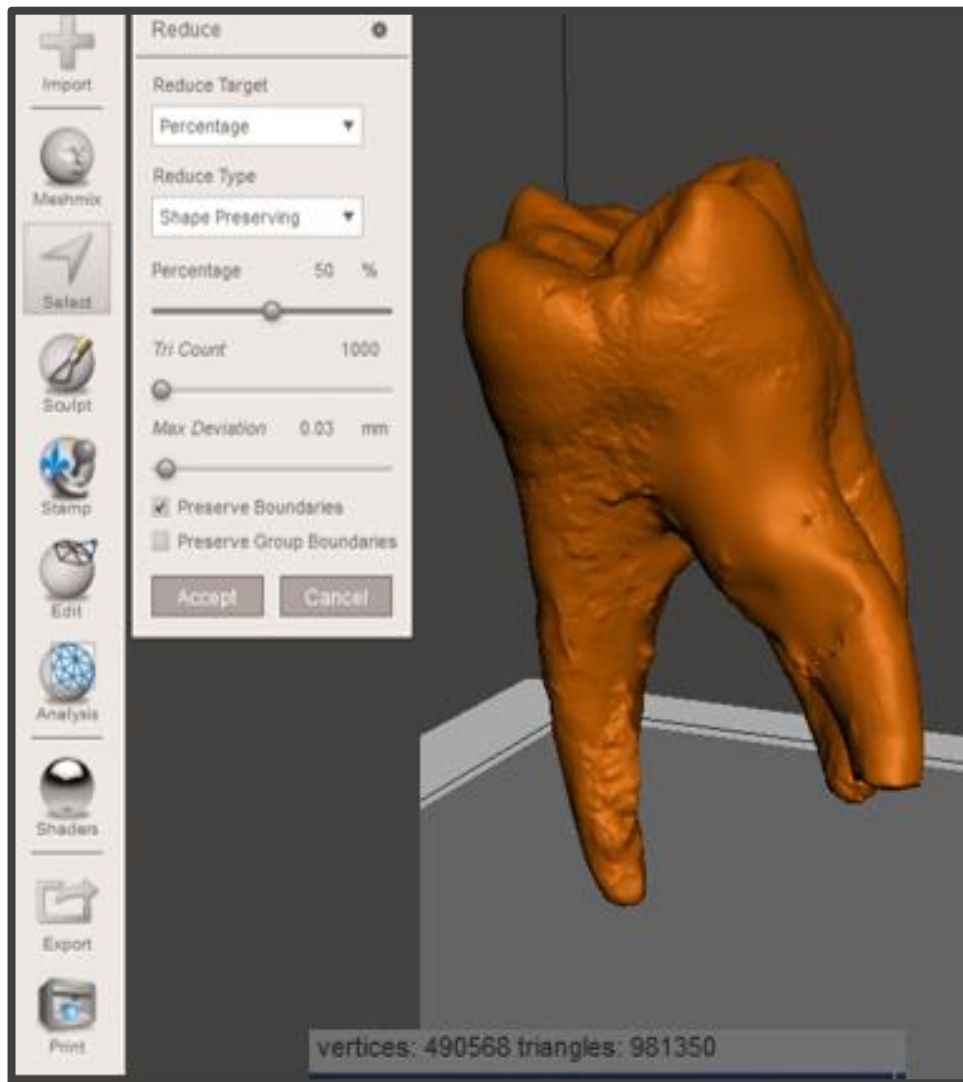
FIGURE 4.3 Decimation of mesh in Meshmixer: The structure of interest is demarcated (in brown) and percentage reduction of triangles is selected. 50% reduction applied, reducing mesh triangles to just < 1 million triangles which can be readily processed by relevant programs for printing. Additionally, a smoothing and analysis function was applied to remove rough/uneven surface and to remove surface defects. Meshmixer: 3D modeling software to create, analysis and optimize 3D models.

In order to print the four selected M1Ms (labelled: X, Y and Z and practice) with the fine detailed canal morphology required, polyjet printing technology was necessary; however, it was not available in TCD. As a result, STL files were sent to collaborators (Prof. Gabriel Krastl, Dr. Julia Ludwig, Würzburg Dental Hospital, Germany) with access to a polyjet printer (**Figure 4.4**). The materials used were Objet 30 Prime, Materials: Vero White Plus (VWP) with SUP705 (support material), Stratasys Ltd, Minneapolis, MN). A preliminary first batch of ten of each tooth type was printed for use in the subsequent feasibility study.

4.3.3. Feasibility study

Two endodontists, who had previously analysed the microCT datasets for M1M suitability, were allocated samples of each of the four M1Ms (X, Y, Z, practice), and asked to access the first batch of 40 printed study teeth, to check if all canals were accessible. The endodontists confirmed that for tooth X, all four canals were negotiable and distinct and that the tooth required no alterations, but stated that the other M1M's (Y, Z, practice) required modification as the MB2 canals were not all consistently negotiable after the 3D printing process. The STL files of teeth Y and Z were reimported into Blender software, to enable modifications to the MB2 canals. Minor enhancement of these MB2 canals, in areas with the narrowest of dimensions using the Blender tool (delineated in orange, **Figure 4.5**), prior to reprinting, proved sufficient for tooth Y and Z, producing teeth which were checked and the MB2 was consistently negotiable. The practice tooth required greater modifications, departing further from its original anatomy, so it was confirmed as a non-study tooth to allow operators to practice and become accustomed to the texture of the teeth.

FIGURE 4.4 Laserjet printer used to print 3D teeth: Objet 30Prime (Stratasys Ltd, Minneapolis, MN, used for printing M1M's (Würzburg Dental Hospital, Germany). M1M: First Maxillary Molar.
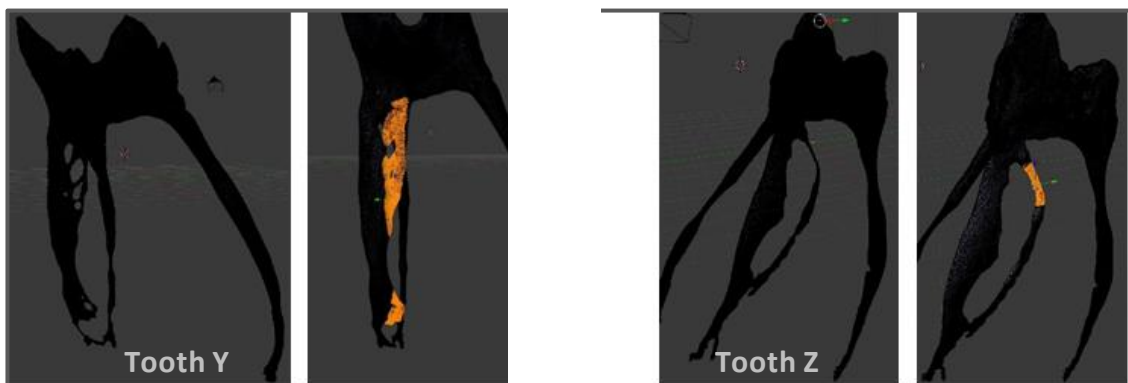
FIGURE 4.5 Blender software modifications (orange) to MB2 canal fin for Tooth Y and to the narrowest point of MB2 just below MB2 canal orifice.
MB2: Second Mesiobuccal Canal. Blender: Open-source 3D computer graphics software toolset for printing 3D models.

After the modified batch of teeth were reprinted, a further, more developed, feasibility study was undertaken by the same non-study endodontists during which they completed the endodontic access cavity, prior to locating and instrumenting all four canals in each M1M type. The purpose of this second feasibility study was to confirm if all canals were consistently present, continuous and accurately reflected the micro-CT datasets with regards to bucco-palatal and apico-coronal location of canal orifice and relative dimensions of the canal orifices. Additionally, they were asked to qualitatively describe the characteristics of the printed teeth as compared with real teeth, specifically with regards to similarity to the texture and hardness of dentine during access opening, canal gauging and canal instrumentation. These details would later be included in the pre-operative instructions as a guide to prepare the operators. The feasibility study feedback concluded that teeth X, Y and Z teeth were suitable for the study and presented different challenges with respect to the location of the MB2. The practice tooth was used to familiarise the operator with drilling and instrumenting of this particular 3D printed teeth resin material.

4.3.4 Preparing clinical simulation mock-up

4.3.4.1 Imaging

To reproduce the clinical scenario as closely as possible, imaging of the selected study teeth (X, Y, Z) was facilitated by using an anthropomorphic phantom as used in previous studies (SHELLEY ET AL. 2011, HIDALGO RIVAS ET AL. 2015, MCGUIGAN ET AL. 2020). This consists of skeletal material suspended in head-shaped polystyrene container, with air displaced by water to mimic soft tissues. This involved soaking a skull and cervical spine (C1-C4) in water for 48 hours before imaging; this was in order to ensure water had displaced air from all trabecular spaces. Thereafter, the selected teeth were in turn mounted into the upper left first molar socket of the maxilla, a procedure that involved careful osteoplasty of the alveolar bone using a stainless steel water-cooled rosehead bur in a slow-speed handpiece to acquire the best possible fit. The study teeth were retained with the aid of modelling wax which has a radiopacity greater than air and less than that of water. The anthropomorphic phantom was imaged using the Planmeca dental intraoral unit and, for CBCT imaging, the ProMax 3D Classic at the optimised adult settings used clinically for each unit in DDUH X-Ray Department.

- Conventional Imaging: 66 kV operating potential, 8 mA tube current, 0.32 seconds exposure time, rectangular collimation (30x40mm beam), focus-to-skin distance (FSD) 200 mm.

Two intraoral periapical radiographs were taken of each of the three study teeth, one using the paralleling technique and the second at a 30 degrees angle to the first, shifting the tubehead in the horizontal plane to provide a parallax view (**Figure 4.6**).

- CBCT Imaging: 50 mm (D) x 50 mm (H) field of view: 100 µm voxel, 90 kV operating potential, 5 mA tube current, 12 second exposure time.

A CBCT scan was completed of each of the three teeth in the anthropomorphic phantom (**Figure 4.6**).
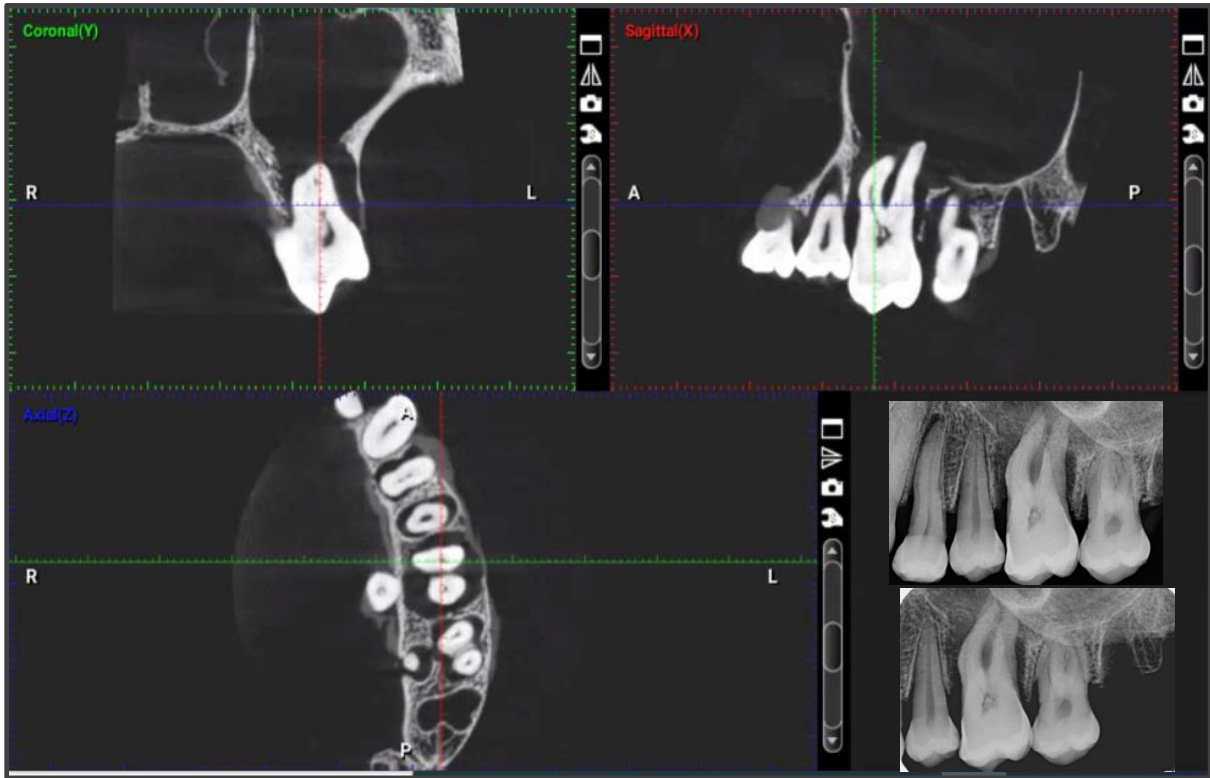
Figure 4.6 Tooth Z: Imaging provided to operator: CBCT dataset image and inset: parallax IOPA's: parallel image (upper), 30° to the parallel image (lower). IOPA: Intraoral periapical CBCT: Cone beam computed tomography.

4.3.4.2 Simulated dental arch preparation

Nine magnetised plastic arch trays were adapted (**Figure 4.7**) to enable secure retention in the Frasaco dental manikin head (Frasaco Gmbh, Tettnang Germany). The manikin head was inserted into the individual dental units in the DDUH clinical skills laboratory. In the DDUH, the clinical skills lab uses identical stations, dental light, headpieces and set-up in order to accurately replicate the clinical experience and enhance training.

To replicate the orientation of the M1Ms and the adjacent upper left premolars and second molar on the IOPAs and CBCT image dataset, an acrylic jig was created around the upper left quadrant for the set-up of teeth X, Y and Z (**Figure 4.8**). The plastic arches were lined with carding wax and Frasaco plastic teeth were placed from 17 (upper right second molar) to 23 (upper left canine) position, simulating their position in the upper arch (**Figure 4.9**).

The acrylic jig was removed from the skull and placed in the simulated upper magnetised plastic arch and pressed into carding wax, in order to record and replicate the orientation of the M1M as imaged (**Figure 4.9a**). The jig was carefully prised open on one side and the M1M was replaced with its printed replica, which was embedded in the carding wax.

The abutment teeth were each in turn replaced with commercially available printed teeth, being positioned in turn into the carding wax. The arch tray was then filled with a polysilicone laboratory putty Affinis (Coltène/Whaledent, Altstätten, Germany) to secure the teeth firmly in place and simulated acrylic gingival tissue placed around the M1M and abutment teeth (**Figure 4.9b**).

Prior to access cavity preparation, in order to facilitate volume removal assessment (**Figure 4.12, Section 4.3.5.1**), a low shrinkage resin-based composite (Filtek LS, 3M ESPE, Minneapolis, USA) imprint was made of each of the 3D printed M1M teeth, which was cured with a LED Curing light (Elipar DeepCure-S, 3M ESPE, Minneapolis, USA), labelled and stored for later use.

To complete the clinical simulation, the dental arch, including the M1M, was inserted into the manikin head with an opposing lower arch (**Figure 4.10a**). A clamp, rubber dam and metal frame were used to isolate the tooth in the same manner as a normal clinical endodontic set up (**Figure 4.10b**). A separate simulated dental arch was prepared for each of the three M1M (X, Y, Z) study teeth for each participant at both

sessions. All three teeth at both sessions were assigned an electronic patient name and clinical chart on the patient database normally used at DDUH (SALUD; Two-Ten Health Ltd., Dublin, Ireland) through which the imaging could be retrieved, resulting in six experimental patient charts.

FIGURE 4.7 Frasaco dental care training manikin head with magnetised receiving plate (left), adapted magnetised plastic arch tray with holes drilled to accommodate metal projections (right).

FIGURE 4.8 Acrylic jig constructed on skull.
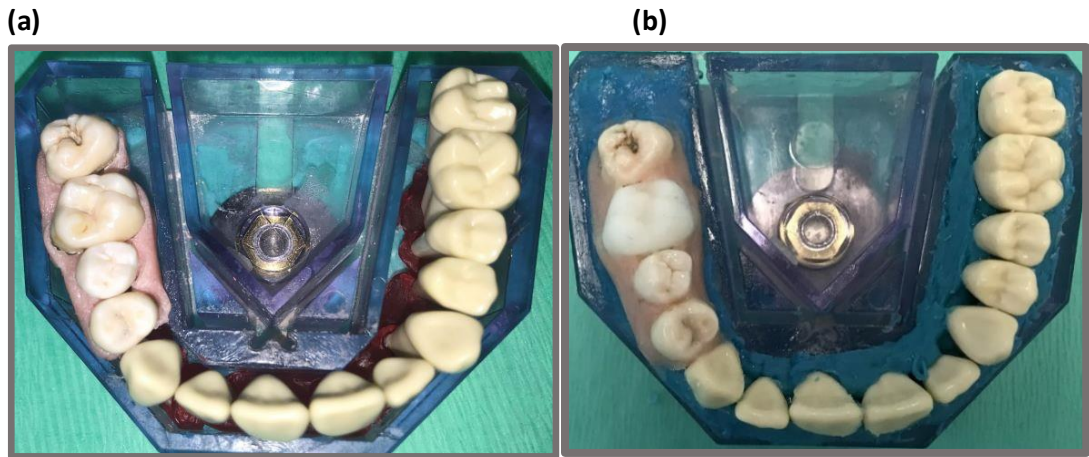
FIGURE 4.9 a) Jig in place in mock up arch. **(b)** Printed teeth stabilised with polysilicone material
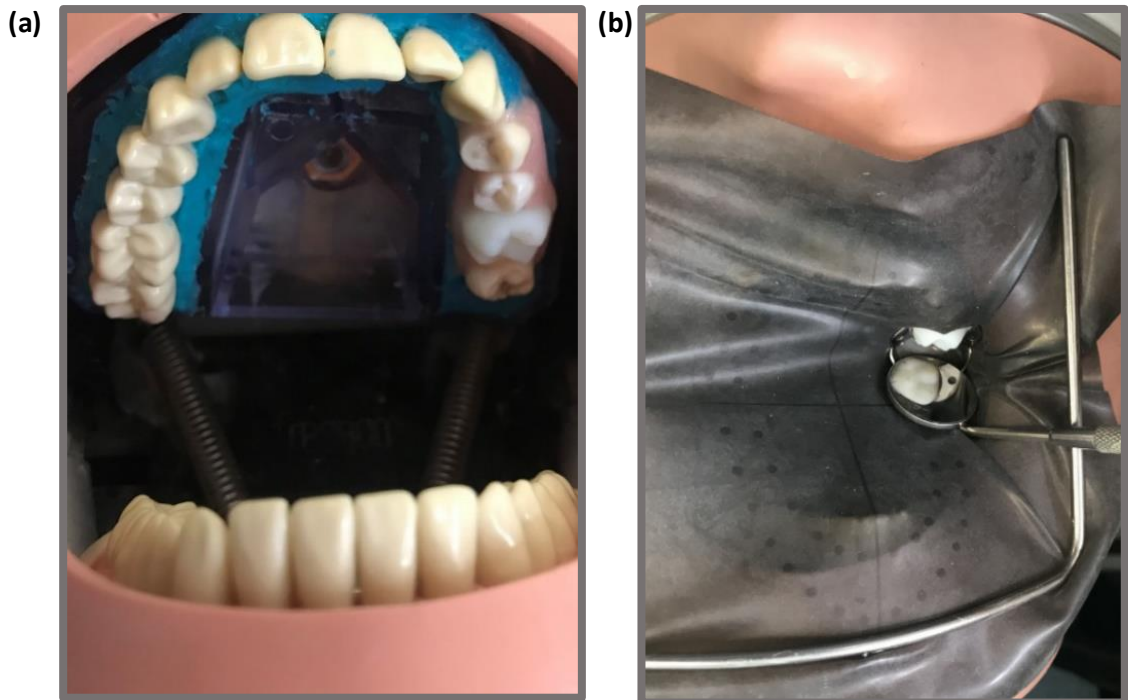
FIGURE 4.10 (a) Mock up arch in manikin with opposing arch. **(b)** Endodontic isolation of 26 (upper left first molar).

4.3.5 Pilot study

Prior to commencing the study proper, a pilot study was completed by two endodontists, who had not previously examined the teeth and were not participants in the study proper. The final experimental protocol is explained in depth for Session 1 and 2 in **Section 4.3.8**. The pilot study was carried out in an identical manner to the planned study (**Figure 4.11**), with all 3 M1Ms instrumented in two sessions (random allocation to either IOPA only or, IOPA + CBCT). The purpose of the pilot study was three-fold: to highlight any potential methodological errors, troubleshoot practical problems and use the resulting data to create a power calculation.
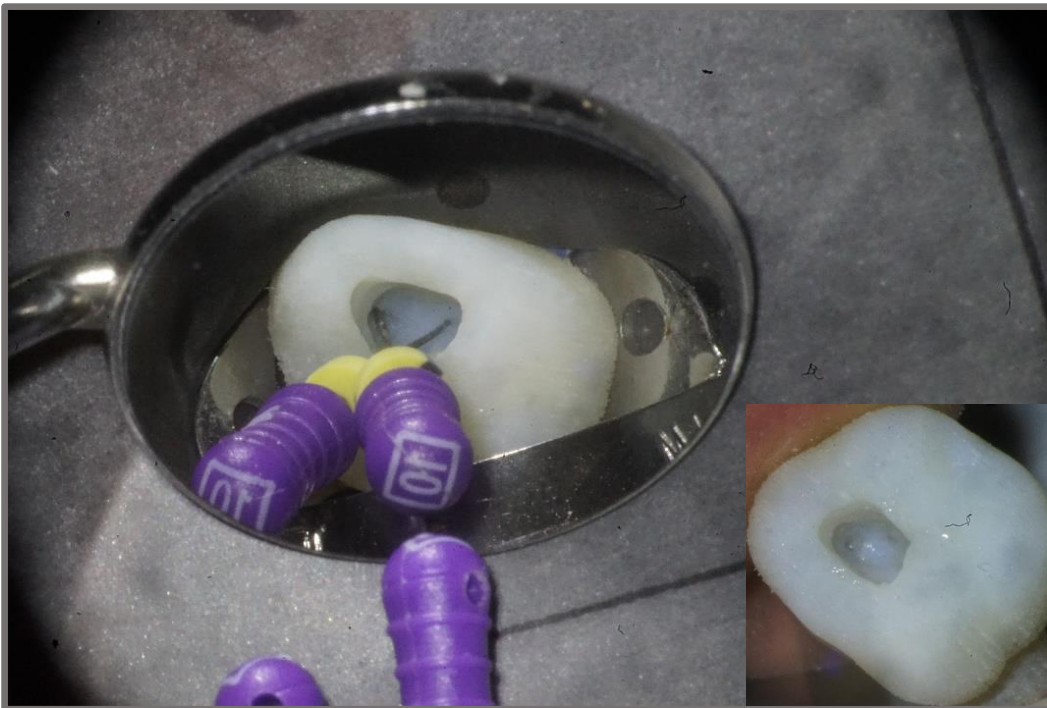
FIGURE 4.11 Access cavity and canal location completed in pilot study using size 10 K-handfiles (Flexofile, Dentsply-Maillefer), and with files removed (inset image), displaying a blue hue evident in pulp chamber.

4.3.5.1 Assessing volume removed

The endodontic access cavities from each M1M included in the pilot study were volumetrically assessed to demonstrate reliability and repeatability of the measurement technique and the software to be used for volumetric assessment in the study. The accessed M1Ms from the pilot study teeth were stabilised in wax and CBCT scanned using identical exposure protocols (50 mm [D] x 50 mm [H] field of view: 75 μm voxel, 90 kV operating potential, 10 mA tube current, 14.9 second exposure time) and the DICOM files imported into ITK-SNAP to allow volumetric evaluation of the access cavities. This technique has been previously validated as a method of assessing volume in airways and cysts (ALMUZIAN ET AL, 2018, GOMES ET AL, 2020). Additionally, the process was trialled by scanning an air-filled syringe (50 mm [D] x 50 mm [H] field of view: 75 μm voxel, 90 kV operating potential, 10 mA tube current, 14.9 second exposure time) at two different volumes with a small intervening difference, this resulted in a discernible difference in volume being recorded in ITK-SNAP (**Appendix II**). Each M1M needed to be prepared before scanning by sealing the orifice of each located canal with an injected flowable composite (Clearfil, Kuraray, New York, USA) whilst rigorously ensuring removal of any excess from the pulp chamber with fine and superfine microbrushes performed under a dental operating microscope (Zeiss, Oberkochen, Germany). Additionally, the composite imprint of each printed M1M constructed prior to the endodontic access procedure (**Section 4.3.4.2**), was repositioned on top of the M1M, to provide a definite seal to the access cavity, replicating its original occlusal topography (**Figure 4.12 a-c**). A check, in all orthogonal planes in ITK-SNAP was completed of the canal orifice seals, ensuring that they sealed the orifice and that there was an absence of excess material. Similarly, the accuracy of the cavity occlusal seal was checked. If problems were identified, the seals were removed and repeated until accurate. The access cavity was then segmented in ITK-SNAP, with the canal orifice seals and composite imprint preventing the segmentation bubble spreading outside the confines of the cavity so to ensure an accurate and reproducible reading of volume removal. Extrusion of the segmentation bubble outside the cavity in any orthogonal plane was again an indication to repeat the sealing process. The resulting volume was extracted from volume statistics accessible from the drop-down menu in ITK SNAP. Each volume measurement was repeated three times, the mean calculated and

standard deviation of the result recorded: SD± 0-0.09 (**Appendix III**). The segmented

access cavity volume was then imported into Meshmixer software as STL files and the

greatest depth, bucco-palatal width and mesio-distal width were recorded (**Figure 4.13**).
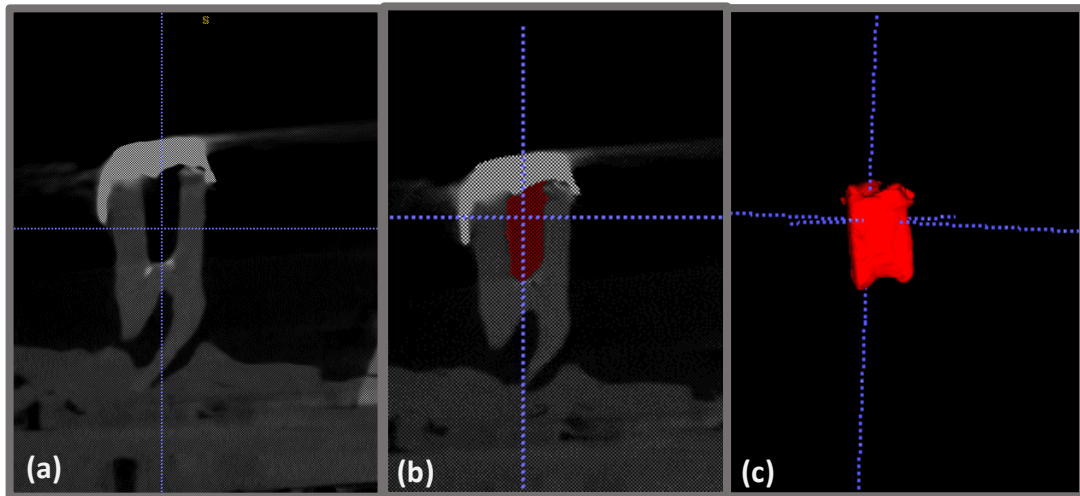
FIGURE 4.12 DICOM files of CBCT scanned image of 3D printed tooth, post access cavity preparation, imported into ITK-SNAP. **(a)** Demonstrates composite imprint and seal of canal orifices in that orthogonal plane which functioned to stop segmentation bubble extending outside the confines of the cavity **(b)** Segmentation bubbles completely merged to fill access cavity. **(c)** Segmented cavity preparation from which volume of tooth substance removal was evaluated. DICOM = Digital Imaging and Communications in Medicine. ITK-SNAP = software application used to segment structures in 3D medical images.
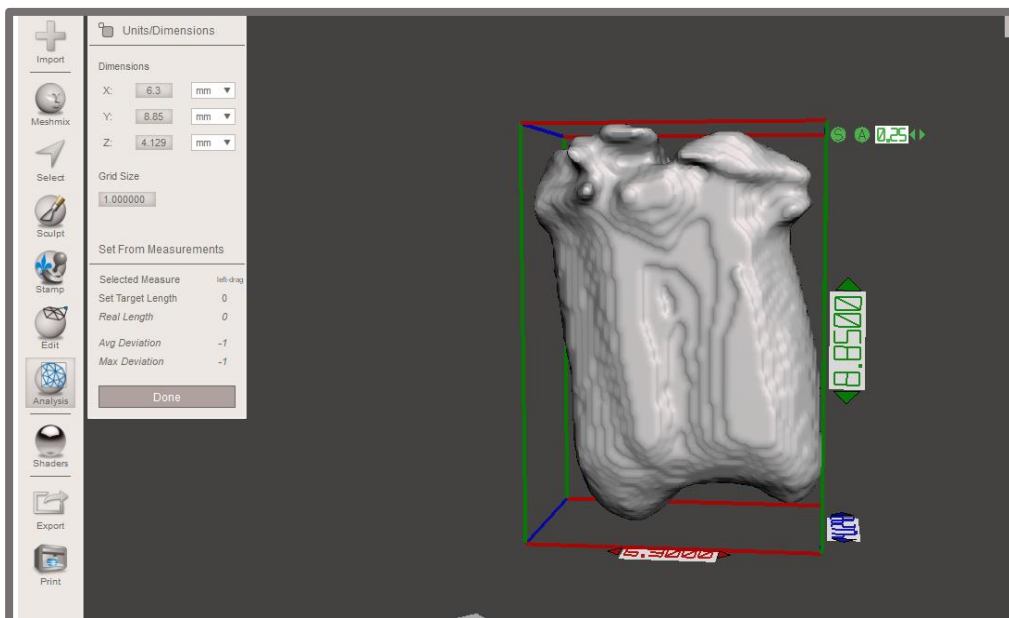
FIGURE 4.13 STL files imported into Meshmixer software to enable measuring of greatest depth, bucco-palatal width and mesiodistal width of cavity preparation. Meshmixer: 3D modeling software to create, analysis and optimize 3D models.

155

4.3.6 Sample size

The power calculation was based on the primary outcome: volume removed (mm³), which was established after analysis of pilot study data (**Appendix IV**). Similar themed studies were available in the literature (IKRAM ET AL. 2009, CONNERT ET AL 2019, SATO 2020); these provided guidance regarding the volume of tooth substance removal during endodontic access as well standard deviation among operators. However, these previous studies, although investigating the volume of tooth substance removed with the aid of CBCT imaging, related only to guided endodontics: i.e. a jig provided a guided access pathway for the operator and therefore the results only partially reflected the aims and methods of this study. Nevertheless, a mean reduction 63.2 mm³ (± 12.2) was shown for maxillary molars. Pilot study data from 2 operators (volume of tooth substance removed during endodontic molar access with conventional imaging alone as compared with additional CBCT imaging) (**Section 4.3.5**) suggested a mean reduction of 7.7 mm³ with CBCT imaging and a standard deviation ±9.9 **(Appendix IV)**. Using an online sample size calculator for comparing paired differences: http://statulator.com/SampleSize/ss2PM.html, it was ascertained that a minimum sample size of 16 would be required to achieve a power of 80% and a level of significance of 5% (two sided). The aim of the study was also to recruit three tiers of experience regarding endodontic and CBCT knowledge/skills/competence; however, the primary measure was overall volume removed regardless of experience. Therefore, a total sample size of 18 operators was selected (6 in each experience level). A separate calculation was not made on the secondary outcome measures of time and number of canals identified.

4.3.7 Sample

In total, 23 potential operators were invited to partake in this study and 18 operators eventually recruited for this study, reflecting a range of endodontic experience. This included three groups: six endodontists (completed postgraduate qualification in endodontics and current practice limited or largely limited to endodontics), six postgraduate dentists (qualified 2-4 years and completed endodontic rotations under supervision of endodontist for at least one year) and six general practitioners (practice including simple/uncomplicated molar endodontics). Since this study was completed

in a Dental Hospital, both practicality and laboratory indemnity purposes necessitated recruiting Hospital employees, either full time or part-time, to populate these groupings. The postgraduates were all full-time members of staff, the endodontists were both full-time members and part-time teachers with the general practitioners all being part-time teaching members of staff. The three sub-groups of operators are hereafter referred to as Experience Groups: ET (Endodontist), PG (Postgraduates) and GP (General Practitioners).

4.3.8 Study protocol

The operators were informed that the aim of the study, using 3D printed M1M teeth, was to identify the impact of additional CBCT radiographic imaging in the diagnostic task of root canal location. As detailed in sample (**Section 4.3.7**), the operators possessed a range of awareness, knowledge and competence with regards to CBCT image interpretation and manipulation of CBCT viewing software. ETs were experienced and competent both in interpretation and interaction with a range of viewing software. The PGs generally had some limited experience and knowledge of interpretation and interaction with Romexis viewing software (available in DDUH) while GPs varied, with some familiar with CBCT interpretation, but others only aware of CBCT interpretation. Generally, GPs had limited experience in interaction with viewing software. In order to familiarise the operators with the Romexis (Planmeca, Helsinki, Finland) viewing software system utilized in the study, a standardized interactive tutorial was given prior to engaging in the study, which was reinforced with a printed document for the participant to keep. Endodontic access of the three printed M1Ms was completed on two separate occasions (session 1 and 2), with the two sessions occurring eight weeks apart to allow 'wash-out' and reduce recall. Each operator was randomly assigned either intraoral periapicals (IOPAs) alone or IOPA and additional CBCT datasets of each of the M1Ms to be accessed at each session. Specifically, using an online list randomisation generator allocation: https://www.random.org/lists/, three out of six operators in each experience group was randomly selected to be provided with IOPAs in session one and three with CBCT datasets and IOPA's in session one, with the opposite scheduled for session two (**Table 4.2**). Standardised and optimised viewing

conditions were established for all operators viewing the preoperative imaging. Additionally, each operator completed a five-part questionnaire (**Table 4.3**).

		ET						PG						GP				
	1	2	3	4	5	6	1	2	3	4	5	6	1	2	3	4	5	6
S1	IOPA+CBCT			IOPA			IOPA+CBCT			IOPA			IOPA+CBCT			IOPA		
S2	IOPA			CBCT+IOPA			IOPA			CBCT+IOPA			IOPA			CBCT+IOPA		

TABLE 4.2 Randomisation of preoperative assignment of conventional or CBCT and conventional imaging between S1: session 1 and S2: session 2, within each experience group. IOPA Intraoral periapical CBCT: Cone beam computed tomography.

SESSION 1 & 2: BEFORE TASK COMPLETION FOR EACH TOOTH		
Q.1	Can you identify an MB2 Canal from imaging provided?	<u>Y/N</u>
Q.2	How confident are you from using the available imaging data that you could actually locate the MB2 canal?	1= No confidence 2= Slight confidence 3= Moderate Confidence/Unsure 4= High confidence 5= Complete confidence
SESSION 1 & 2: AFTER TASK COMPLETION FOR ALL TEETH		
Q.3	How similar is this simulation of locating the canals in the provided 3D printed teeth to a real clinic scenario?	1= Not helpful/similar 2= Slightly helpful/ similar 3= Moderately helpful/similar 4= Highly helpful/ similar 5= Completely helpful/ similar
Q.4	How helpful was the imaging data provided in assisting location of the MB2 canal?	
SESSION 2: AFTER TASK COMPLETION FOR ALL TEETH		
Q5	Did recall have any impact on location of canals in Session 2?	Y/N

TABLE 4.3 Summary of questionnaire: Q.1 & 5: Y/N answer. Q.2 - 4: Five-point Likert scale provided to reflect strength of answer to question.

Additionally, each operator completed a five-part questionnaire (summarised **Table 4.3**) to assess impact of IOPA and additional CBCT imaging on identification of MB2 canals and on perceived helpfulness and confidence imparted from the allocated imaging. The questionnaire also assessed the clinical similarity of the 3D printed teeth and the role of recall on location of canals at the second session. Q.1 and Q.2 were completed after observing the imaging provided and before endodontic access cavity preparation at both session 1 and 2. Q.3 and Q.4 were populated after completion of the endodontic access cavity preparations of all three teeth at both session 1 and 2. Q.5 was answered after completion of the second session.

4.3.8.1 Session 1 protocol

Each operator was assigned to a training station in the clinical skills laboratory, DDUH. At the station there was a dedicated screen from which the simulated patient charts and imaging could be accessed and interacted with. Initially, verbal and written instructions were provided as to the specific requirements of the task. Subsequently the operators were allocated time to familiarise themselves with drilling and instrumenting of the practice 3D printed tooth. Furthermore, time was given to ensure satisfactory proficiency with regard to the viewing software and CBCT interpretation requirements specific to root canal treatment.

All operators participating in the study were allocated three mock patients for each session, and the preoperative imaging (IOPA or IOPA + CBCT) provided with each patient chart was assessed before drilling an endodontic access cavity on each M1M. After viewing the dataset, the relevant part of the questionnaire for that session was completed (Q.1 & Q.2). Thereafter, the operators were instructed to complete access cavity preparation on a tooth that had already been isolated with rubber dam. Rubber dam placement was carried out for the operator to standardise placement and to avoid excessive time being wasted providing isolation. Operators were asked to prepare the tooth in the exact same way they would clinically in terms of burs, time taken and tooth substance preservation constraints. Specifically, the operators were asked, after viewing the relevant imaging, to locate the orifice of all canals present with coronal preparation sufficient to ensure patency of each of the canals (i.e. size 10 file free in

coronal two-thirds of the root canal). To replicate the clinic as closely as possible, the participants were not informed specifically that any of the teeth had four root canals and that a MB2 canal was or was not present but instead reminded to apply normal clinical approach where it would be assumed that an MB2 canal exists in over 90% of M1M's. A range of equipment was provided to the operators. This included a highspeed air turbine handpiece, slow speed handpiece (Bien-Air Dental SA, Switzerland), with a range of diamond burs and Endo Z bur, steel cavity burs and longshank slow speed burs (Dentsply-Maillefer, Balliagues, Switzerland). Diamond coated ultrasonics were also available to locate canals, in a manner designed to reflect the operator's standard practice. It was stressed, however, that although ultrasonics could only be used intermittently, they should be used with caution on printed teeth to limit burning of the resin. Rotary nickel-titanium (NiTi) files (ProTaper Universal Gold, Dentsply-Maillefer) and K-handfiles (Flexofile, Dentsply-Maillefer), were available for coronal flare; It was emphasized, however, that this was not the point of the exercise. Individual use of magnification, i.e. loupes or operating microscope as each operator would normally use in clinics, was encouraged. On completing the task, the remainder of the questionnaire for that session was completed (Q.3 & Q.4).

4.3.8.2 Session 2 protocol

Eight weeks after session 1, to allow wash out and reduce memory recall, in an identical manner to the first session, the operator was assigned three new clinical mock-up patient charts and set up, with the manikin arch models having the same three printed left M1Ms. The teeth were pre-isolated with rubber dam as in session 1. The imaging allocation was reciprocal to session 1 (**Table 4.2**). One additional question was asked in the questionnaire (Q.5), inquiring as to the influence of recall from session 1 on location of canals in session 2.

4.3.8.3 Assessing primary and secondary outcomes

Tooth substance volume removed was recorded as per **Section 4.3.5.1**. For both sessions, procedural time for each of the three teeth was measured from the time the endodontic access cavity was started until the operator reported that they had completed location and patency of all four canals (disto-buccal, main MB [MB1], MB2,

palatal). The timer was paused and restarted for any necessary disruptions (e.g. toilet break, mechanical). If the operator reported that they could not locate the MB2 and had exhausted normal clinical efforts or they reported concern of excess dentine removal or perforation, then the procedure was completed and MB2 canal classified as not located. This was confirmed by the lead researcher using a dental operating microscope (DOM). Presence of all located canals, was confirmed with a size 10 K-handfile (Flexofile) and compared under the DOM with the identical existing accessed 3D M1M with stained canal orifices, which served as a confirmatory guide for the lead researcher. The name and number of the canal located was recorded for each accessed M1M for each operator. Any canal that was not located was explored to ensure a canal was actually present, this process was completed using a DOM, post volumetric assessment of access cavity (**Section 4.3.5.1**). Additionally, the use or absence of magnification was recorded for each operator at each session to reflect their normal practice.

4.3.9. Statistical analysis

Statistical analysis was performed using statistical software R: (Version; R 4.1.1, Foundation for Statistical Computing, Vienna, Austria, https://www.R-project.org). Descriptive statistics were initially completed for the measured variables during access cavity preparation; volume of tooth substance removed, including dimensions (bucco-palatal; depth; mesio-distal) and procedural time. This was completed for each of the three 3D-printed teeth (tooth X, Y, Z) accessed by the 18 operators at both sessions; i.e. conventional imaging alone or conventional imaging supplemented by CBCT imaging (**Appendix V**). Paired t-tests were performed to test whether there was a significant difference in the mean of the paired measurements (both sessions) for volume, time and dimension and significance was set at $p<0.05$. Shapiro-Wilk tests confirmed ($p>0.05$) that the assumption of normality was satisfied. For tooth X, Y and Z, volume removed and procedure time taken (for both sessions) overall by all operators, were displayed using bar charts and by experience (endodontist, PG, GP) group using boxplots. Fishers Exact test was completed to identify if there was a significant difference in the proportion of canals located and not located when IOPA imaging alone was provided and when CBCT was provided additionally. Linear mixed effect modelling

was employed to examine the effect of image type (conventional alone or additional CBCT) on volume removed and time taken for each tooth (X, Y, Z) while adjusting for the influence of experience level, use of magnification, tooth type and operator session. The operator, level of experience and tooth type were included as random effects. Median (Md) values extracted from the Likert scale scores recorded for Q.2 - 4 of the questionnaire relating to 'perceived helpfulness of imaging modality', 'similarity of canal location to clinical scenario' and 'confidence that the operator would locate the MB2 canal', are presented (**Table 4.10**). Additionally, a Mann-Whitney U test was completed to identify if there was a significant difference in the confidence scores and perceived helpfulness scores when provided with IOPA imaging alone compared with viewing additional CBCT imaging ($p < 0.05$).

4.4 RESULTS

4.4.1. Operator and experimental demographics

All 18 recruited operators completed both sessions, all adhering to the designated 'wash out' period of at least eight weeks. There were no drop-outs. All teeth were accessed without separation (file fracture) of any root canal instrumentation files or perforation of the teeth, resulting in all 108 teeth being suitable for analysis.

4.4.2 Endodontic access cavity procedure: Measured variables

4.4.2.1 Volume removed

The recorded mean volumes of tooth subsance removed by all operators, using IOPA and IOPA with additional CBCT imaging, are shown in **Table 4.4** and illustrated in **Figure 4.14.** The primary outcome, mean volume removed, when including all operators, was significantly greater with IOPA alone than with IOPA and additional CBCT for tooth X (p=0.011) and Y (p=0.0007). There was no significant difference in mean volume of tooth substance removed in the case of tooth Z (p=0.143). Thus, for teeth X and Y, Null Hypothesis 1 for this study (**Section 4.1.1**) was rejected, while it was accepted for tooth Z.

Tooth	Mean Volume of Tooth Substance Removed (+/- SD) (mm3)		
	IOPA only	IOPA + CBCT	p
X	96.3 (18.67)	79.9 (9.65)	.011*
Y	75.5 (13.23)	68.7 (9.21)	<.001*
Z	82.6 (12.18)	86.9 (21.95)	.143

TABLE 4.4 Mean volume of tooth substance removed during endodontic access by all operators (n=18) for tooth X, Y and Z, with IOPA imaging alone, compared with the additional availability of CBCT imaging. * = Significant reduction ($P<0$.05) in mean volume removed between IOPA and IOPA + CBCT. IOPA: Intraoral periapical radiograph, CBCT: Cone beam CT.
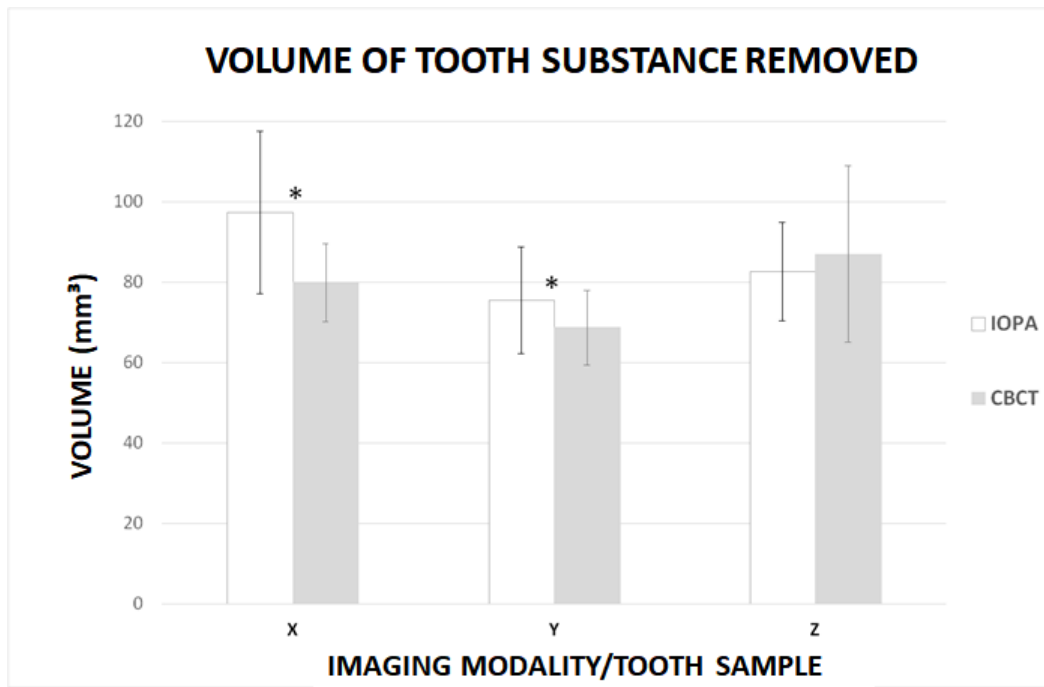
FIGURE 4.14 Mean volume of tooth substance removed (± SD) during endodontic access by all operators (n=18) for tooth X, Y and Z, with IOPA imaging alone, compared with the additional availability of CBCT imaging. * = Significant reduction ($p<0.05$) in mean volume removed between IOPA and IOPA + CBCT. IOPA: Intraoral periapical radiograph; CBCT: Cone beam CT.

Subanalysis of mean volume removed by Experience Group, using IOPA and IOPA with additional CBCT imaging, are shown in **Table 4.5** and illustrated in **Figure 4.15 a-c**. ETs removed the least tooth substance when compared with PGs and GPs, for both IOPA and IOPA with additional CBCT, with the sole exception of tooth Y but only with IOPA imaging. The ETs consistently recorded lower mean volumes removed for all three teeth (13-15%) with IOPA and additional CBCT when compared with IOPA alone, this reduction in volume removed was significant for tooth X and Y. PGs also removed significantly less tooth volume with IOPA and additional CBCT than IOPA alone for both Tooth X (↓23%) and Y (↓ 9%). In the case of tooth Z, however, a significant increase in volume of tooth removed was recorded, with IOPA and additional CBCT imaging, for PGs (↑11%) and GPs (↑16%). Thus, when the sub-analysis by Experience Group was performed, Null Hypothesis 1 was rejected for Teeth X and Y for ETs and PGs, but accepted for the GPs. For tooth Z, while for the ET group the null hypothesis was accepted, for PGs and GPs it was accepted, but in the opposite direction to that hypothesised.

| Operator | Tooth | Mean Volume Removed (+/- SD) (mm³) | | p |
		IOPA	IOPA + CBCT	
ET	X	86.1 (15.6)	72.75 (2.2)	.037*
	Y	74.9 (17.5)	64.5 (12.8)	<.001*
	Z	78.1 (12.2)	67.61 (17.4)	.148
PG	X	105.8 (19.6)	80.87 (11.9)	.003*
	Y	81.52 (5.4)	73.58 (7.4)	.002*
	Z	82.7 (14.9)	92.53 (22.6)	.044*
GP	X	97.1 (17.9)	86.13 (7.7)	.183
	Y	70.0 (13.5)	68.0 (4.3)	.749
	Z	87.2 (7.9)	100.8 (9.9)	.001*

TABLE 4.5 Mean volume of tooth substance removed (± SD) during endodontic access, by each Experience Group, for tooth X, Y and Z, with IOPA imaging alone, compared with the additional availability of CBCT imaging.

* = Significant decrease ($p<0.05$) in mean volume removed; * = Significant increase ($p<0.05$) in mean volume removed: between IOPA and IOPA+ CBCT. IOPA: Intraoral periapical radiograph, CBCT: Cone

(a) TOOTH X: VOLUME REMOVED BY EXPERIENCE GROUP WITH IOPA COMPARED WITH CBCT

(b) TOOTH Y: VOLUME REMOVED BY EXPERIENCE GROUP WITH IOPA COMPARED WITH CBCT

(c)

TOOTH Z: VOLUME REMOVED BY EXPERIENCE GROUP WITH IOPA COMPARED WITH CBCT
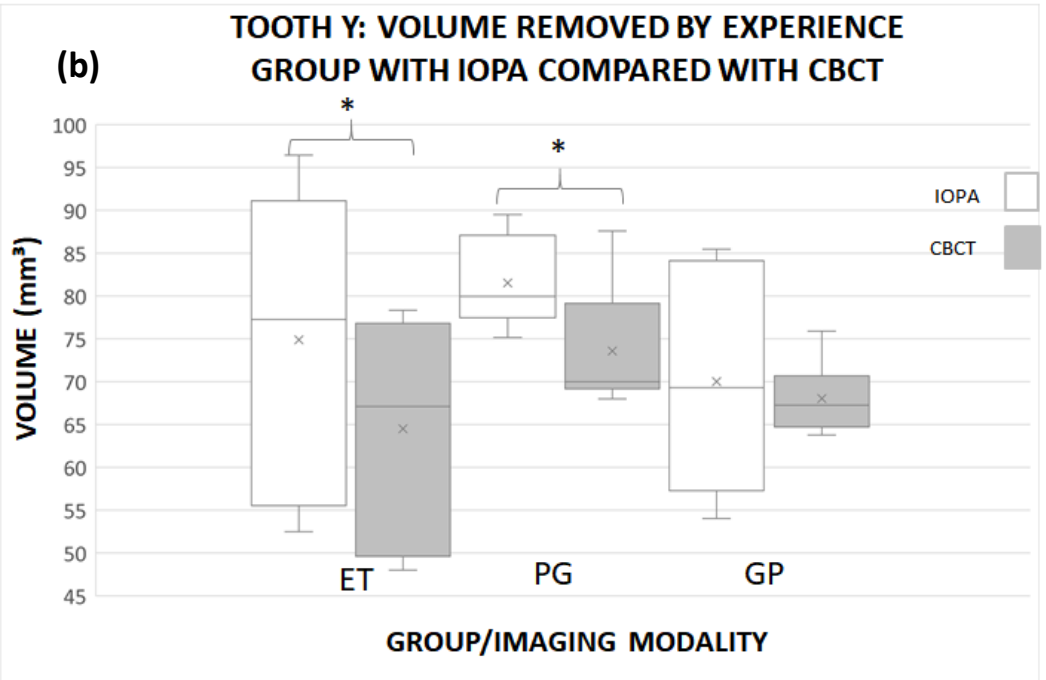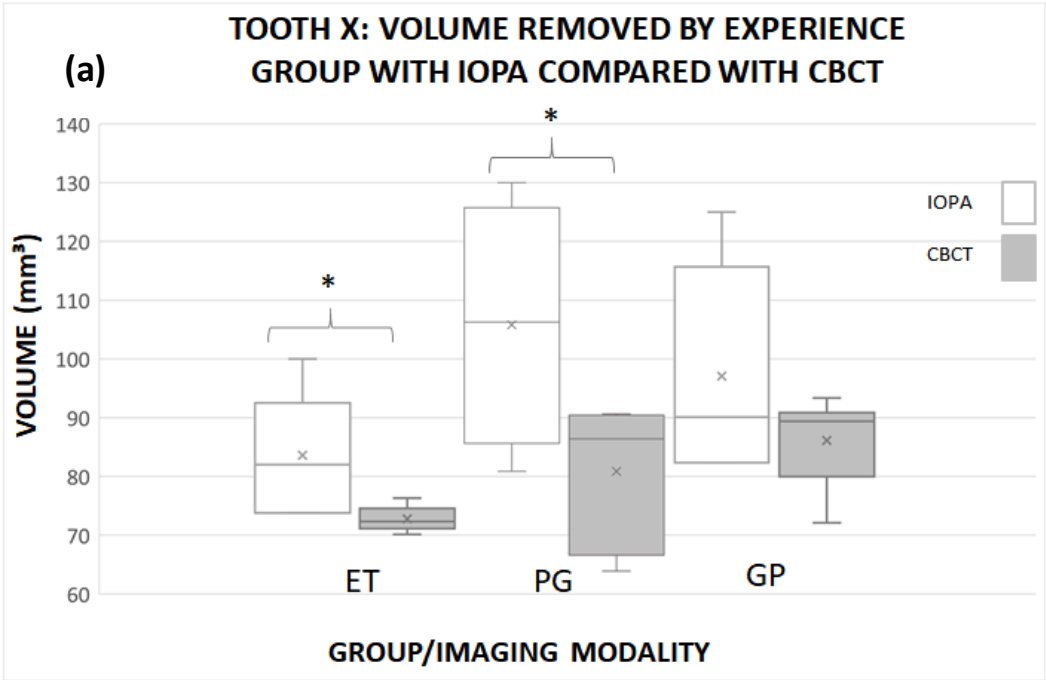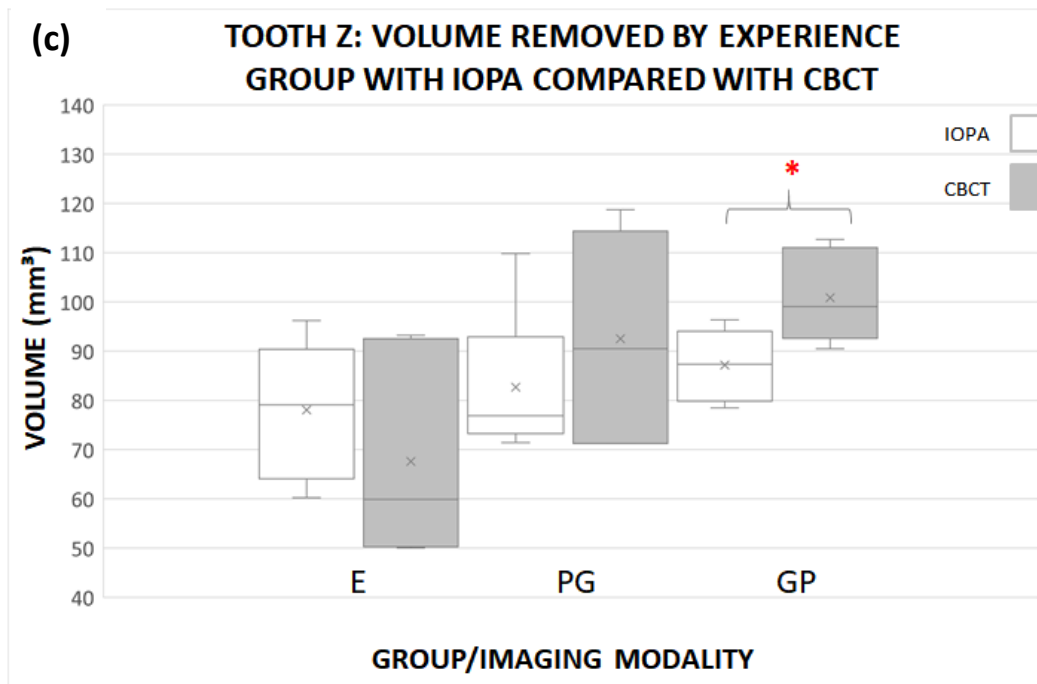
FIGURE 4.15 a) Tooth X, b) Y, c) Z: Box plots of mean volume of tooth substance removed during endodontic access cavity preparation, by each experience group, (n= 6 for each of ET, PG, GP) with IOPA imaging alone, compared with provision of CBCT imaging (± SD). * = Significant decrease (*p*<0.05) in mean volume removed; * = Significant increase (*p*<0.05) in mean volume removed: between IOPA and IOPA + CBCT. IOPA: Intraoral periapical radiograph, CBCT: Cone beam CT.

X= Indicates mean volume removed, ---- Median value

Table 4.6 displays the results of the linear mixed effects regression model, which was used to determine the factors affecting volume removed. Examination of random effects indicate that approximately 11.3% of the total variation of random effects was due to the nested effect of operator within experience group per tooth type. Approximately 5.2% of random effects was due to experience group by tooth type. The effect for tooth type alone accounts for approximately 21.9% of the total variation of random effects. Adjusting for other factors in the model: imaging modality used, experience group and magnification were all shown to have a statistically significant effect on the volume removed. The estimated mean volume removed (**Table 4.6**) with IOPA and additional CBCT was lower than IOPA alone (used as reference) by -6.1 mm³, 95% CI (-11.1, -1.2), thus **Null hypothesis 3** relating to outcome measurement: volume of tooth substance removed, was rejected for this study. The estimated mean volume removed (**Table 4.6**) for the GP group was higher than the ET group by a difference of 16.2 mm³, 95% CI (6.4, 26.0). Similarly, the estimated mean volume removed (**Table 4.6**) by PG group was higher than the ET group by 17.1 mm³, 95% CI (7.5, 26.7). Magnification was shown to have increased volume removed in comparison to the mean volume removed using no magnification by 8.0 mm³, 95% CI (0.5, 15.2). Session was not demonstrated to have a statistically significant effect on volume removed. An interaction between image type and canal identification was reported to be significant. The estimated mean volume removed when the canal was located with the use of additional CBCT imaging was lower than when the canal was not located and IOPA imaging alone was used: -23.4 mm³, 95% CI (-32.6, -14.1).

Fixed Effects		Coefficient	95% CI	p-value
Image:	IOPA	Ref		
	CBCT	-6.1	(-11.1, -1.2)	0.02*
Experience Group:	ET	Ref		
	PG	17.1	(7.5, 26.7)	0.02*
	GP	16.2	(6.4, 26.0)	0.02*
Magnification:	No	Ref		
	Yes	8.0	(0.5, 15.2)	0.04*
Session:	1	Ref		
	2	-1.2	(-6.1, 3.8)	0.63
Random Effects				
Operator: Experience Group: Tooth type variance		30.44		
Group: Tooth type variance		14.0		
Tooth type variance		59.17		
Residual variance		166.81		

TABLE 4.6 Linear mixed effects regression model: Factors effecting volume of tooth substance removed (mm³): IOPA imaging, ETs, no magnification and session 1 used as the reference (Ref), against which the other variables are compared in each category. * denotes significant $p<0.05$ level. IOPA: Intraoral periapical radiograph; CBCT: Cone beam CT

4.4.2.1.1 Endodontic access cavity dimensions

When all operators were considered together, there was no instance in which a mean access cavity dimension significantly increased when CBCT was available (**Table 4.7 a-c**). There were, however, several statistically significant reductions in mean access cavity dimensions, but with no consistent pattern. Significant reductions in mean access cavity dimensions were all less than one millimetre, ranging from 0.62 mm for bucco-palatal width (Tooth Z) to 0.78 mm for cavity depth (Tooth Y).

Looking at the results according to the experience group, more variations were seen in the impact of CBCT imaging on mean access cavity dimensions, with a distinct difference between the GPs and the other two experience groups. For both ET and PG groups, there were several significant differences in mean access cavity dimensions between conventional and additional CBCT imaging sessions for Tooth X and Y, particularly in the case of the ET group for Tooth Y (**Table 4.7b**). In contrast, the availability of CBCT had no impact on mean access cavity dimensions for ET and PG groups in the case of Tooth Z (**Table 4.7c**). No significant changes in mean access cavity dimensions were seen for the GPs except for tooth Z. This included a significant increase in depth with the addition of CBCT imaging (**Table 4.7c**).

	Mean Cavity Dimensions (+/- SD) (mm)								
a)	BP Width			Depth			MD Width		
Tooth X	IOPA	CBCT	*p*	IOPA	CBCT	*P*	IOPA	CBCT	*p*
All	6.65 (.78)	5.92 (.82)	.004 *	7.94 (.90)	7.52 (.91)	.256	5.06 (.74)	4.84 (.48)	.206
ET	6.33 (.61)	5.69 (.47)	.038 *	7.99 (.37)	7.38 (±.31)	.016 *	4.71 (1.0)	4.52 (.41)	.644
PG	6.74 (.91)	5.35 (.80)	.003 *	8.1 (.81)	6.72 (.43)	.009 *	5.22 (.72)	4.71 (.39)	.105
GP	6.99 (.79)	6.71 (.46)	.721	7.88 (.1.39)	8.47 (.83)	.513	5.26 (.38)	5.3 (.35)	.871

	Mean Cavity Dimensions (+/- SD) (mm)								
b)	BP Width			Depth			MD Width		
Tooth Y	IOPA	CBCT	*p*	IOPA	CBCT	*P*	IOPA	CBCT	*p*
All	5.93 (.46)	5.58 (.72)	.136	8.79 (.19)	8.01 (.64)	.014 *	5.45 (.71)	4.81 (.99)	.029 *
ET	5.98 (.33)	5.21 (.23)	.002 *	8.65 (.26)	7.50 (.38)	.002 *	5.45 (.58)	4.15 (.34)	.005 *
PG	5.47 (.24)	5.65 (.86)	.698	9.32 (.44)	8.01 (.53)	.001 *	5.62 (.60)	5.08 (1.39)	.274
GP	6.32 (.34)	5.93 (.84)	.386	8.41 (.1.2)	8.56 (.73)	.818	5.29 (.99)	5.20 (.78)	.880

	Mean Cavity Dimensions (+/- SD) (mm)								
c)	BP Width			Depth			MD Width		
Tooth Z	IOPA	CBCT	*p*	IOPA	CBCT	*P*	IOPA	CBCT	*p*
All	5.73 (±.78)	5.11 (±.53)	.021 *	8.39 (±.89)	9.01 (±.85)	.087	4.65 (±.54)	4.71 (±.83)	.701
ET	6.34 (±.86)	5.06 (±.48)	.055	8.28 (±.59)	8.75 (±.79)	.291	4.18 (±.35)	3.72 (±.39)	.018
PG	5.52 (±.86)	5.30 (±.86)	.645	9.02 (±1.11)	8.99 (±1.24)	.978	4.74 (±.54)	5.07 (±.51)	.410
GP	5.33 (±.73)	4.97 (±.35)	.026 *	7.88 (±.1.5)	9.28 (±.34)	.003 *	5.05 (±.45)	5.36 (±.47)	.053

TABLE 4.7 a), b), c) Tooth X, Y and Z: Mean dimensions of endodontic access cavity (mm, ± SD) for all operators and for experience groups with conventional imaging alone and with CBCT, including standard deviation and significance values. * = Significant reduction/* = Significant increase in dimension (*p*<0.05) between IOPA and IOPA + CBCT.   BP: bucco-palatal, MD: mesio-distal, IOPA: Intraoral periapical, CBCT: Cone beam computed tomography.

4.4.2.2 Procedural time

The recorded mean procedural time for all operators, using IOPA and IOPA with additional CBCT imaging, are shown in **Table 4.8** and illustrated in **Figure 4.16**. Mean procedural time was significantly greater with IOPA alone than IOPA and additional CBCT for tooth X (p=0.007) and Y (p=0.003). There was no significant difference in mean procedural time for Tooth Z between IOPA and IOPA + CBCT (p=0.92). Thus, for teeth X and Y, Null Hypothesis 2 of this study (**Section 4.1.1**) was rejected, while it was accepted for tooth Z.

Tooth	Mean Procedural TIme (minutes) (+/- SD)		
	IOPA only	IOPA + CBCT	*p*
X	24.4 (±6.7)	19.3 (±6.9)	.0007*
Y	24.2 (±8.9)	19.4 (±7.4)	.0003*
Z	24.8 (±7.5)	24.1 (±6.2)	.92

TABLE 4.8 Mean procedural time taken (minutes, ± SD) to complete endodontic access by all operators (n=18) for tooth X, Y and Z, with IOPA imaging alone, compared with the additional availability of CBCT imaging. * = Significant difference ($p<0.05$) in mean procedural time between IOPA and IOPA + CBCT. IOPA: Intraoral periapical; CBCT: Cone beam computed tomography.
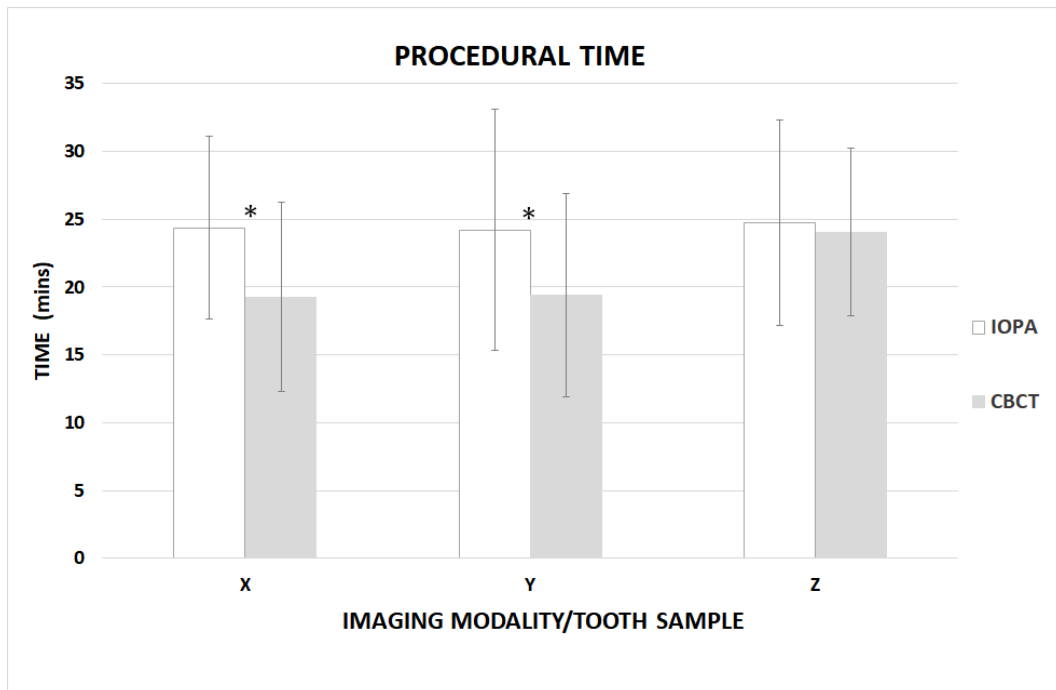
FIGURE 4.16 Mean procedural time taken (minutes, ± SD) to complete endodontic access by all operators (n=18) for tooth X, Y and Z, with IOPA imaging alone, compared with additional provision of CBCT imaging. * = Significant difference ($p<0.05$) in mean procedural times ($p<0.05$) between IOPA and IOPA + CBCT. IOPA: Intraoral periapical, CBCT: Cone beam computed tomography.

Subanalysis of mean procedural times by experience groups, using IOPA and IOPA with additional CBCT imaging, are shown in **Table 4.9** and illustrated in **Figure 4.17 a - c**. ETs and the PGs recorded significantly lower mean procedural times for Tooth X and Y but not Tooth Z. However, GPs differed from the other two experience groups, recording no significant reduction in mean procedural time for any tooth when IOPA + CBCT were available, furthermore for Tooth Z; a significantly longer procedural time was observed. The greatest reduction in mean procedural time between IOPA and IOPA and additional CBCT was recorded by PGs for all three teeth (X: ↓42.9%, Y: ↓34%, Z: ↓20.3%). Thus, when the sub-analysis by Experience Group was performed, Null Hypothesis 2 was rejected for Teeth X and Y for ETs and PGs, but accepted for the GPs. For tooth Z, the null hypothesis was accepted for ET and PG groups but was rejected for GPs, but in a contrary direction to that anticipated.

Experience Group	Tooth	Mean time (+/- SD) (minutes)		p
		IOPA	IOPA +CBCT	
ET	X	17.9 (5.6)	14.6 (5.87)	.031*
	Y	17.5 (8.4)	14.2 (5.6)	.047*
	Z	21.5 (7.2)	18.3 (3.4)	.073
PG	X	28.0 (5.8)	15.9 (2.1)	.002*
	Y	29.1 (9.9)	19.2 (8.1)	.001*
	Z	26.9 (11.0)	23.5 (4.9)	.311
GP	X	27.2 (3.5)	27.3 (3.1)	.969
	Y	25.9 (4.0)	24.9 (5.3)	.709
	Z	23.1 (1.8)	30.3 (2.1)	.004*

TABLE 4.9 Mean procedural time (minutes, ± SD) taken to complete endodontic access, by each experience group, for tooth X, Y and Z, with IOPA imaging alone, compared with the additional availability of CBCT imaging. * = Significant decrease, * = significant increase ($P<0.05$) in mean procedural time between IOPA and IOPA + CBCT. IOPA: Intraoral periapical; CBCT: Cone beam computed tomography

(a) TOOTH X: PROCEDURAL TIME OF EXPERIENCE GROUP WITH IOPA COMPARED WITH CBCT

(b) TOOTH Y: PROCEDURAL TIME OF EXPERIENCE GROUP WITH IOPA COMPARED WITH CBCT
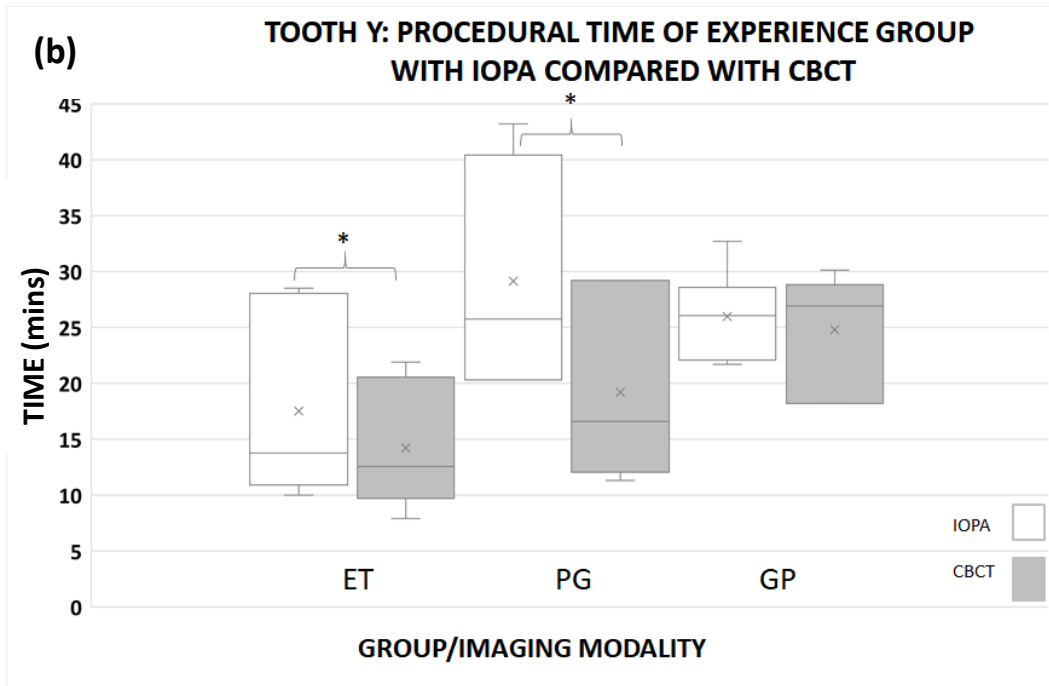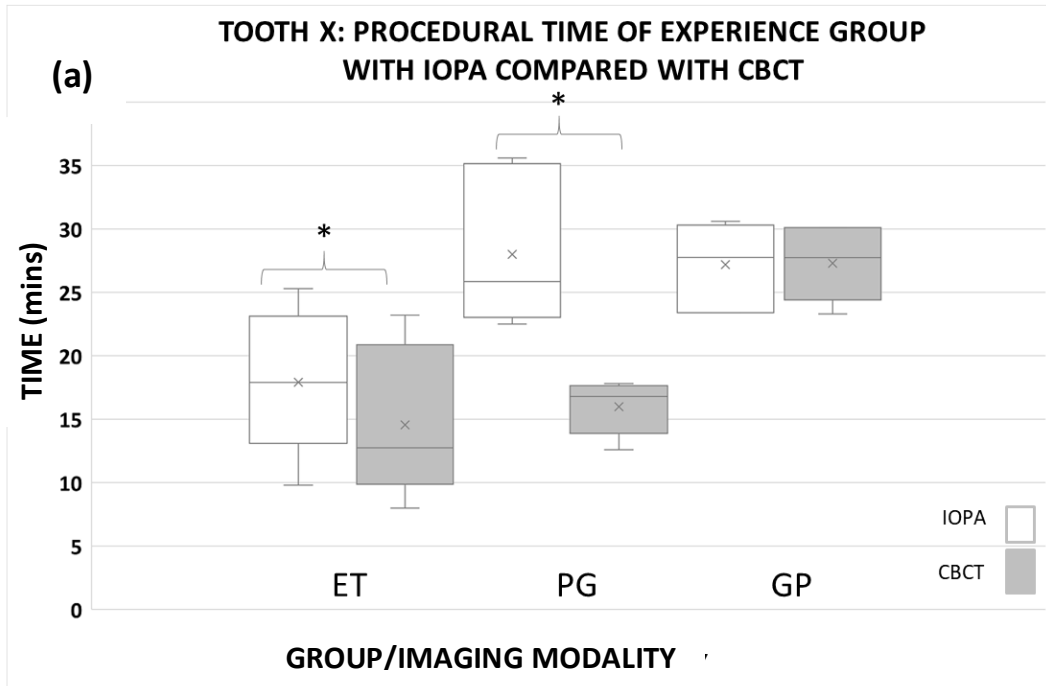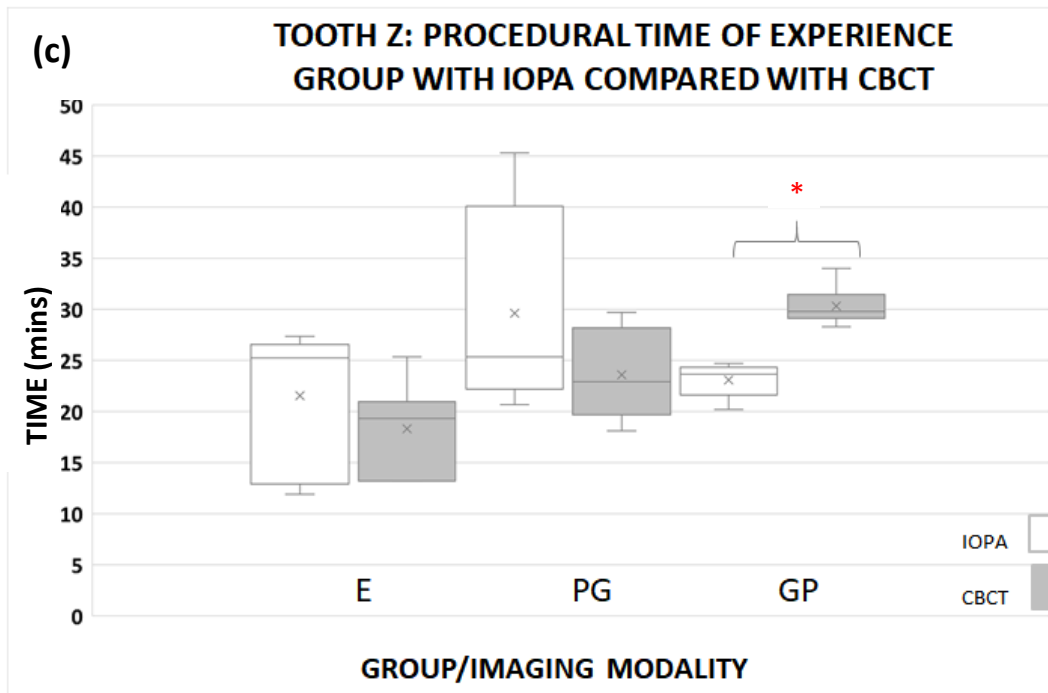
FIGURE 4.17 Tooth X **(a),** Y **(b),** Z **(c)**: Box plot of mean procedural time taken (minutes, ± SD) to complete endodontic access cavity preparation by each experience group, (n= 6: ET, PG, GP) with IOPA imaging alone, compared with provision of CBCT imaging. * = Significant reduction/* = Significant increase (*p*<0.05) in mean procedural times between IOPA and IOPA + CBCT. X= Indicates mean procedural time. ---- Median value. IOPA: Intraoral periapical, CBCT: Cone beam computed tomography

Table 4.10 displays the results of the linear mixed effects regression model that was used to determine the factors effecting procedural time. Examination of random effects indicate that approximately 7.1% of the total variation of random effects was due to the nested effect of operator per tooth type and approximately 2.1% was due to operator alone. Adjusting for other factors in the model, the imaging modality used and experience group were shown to have a statistically significant effect on the time taken (minutes). The estimated mean time taken with IOPA/CBCT was lower than IOPA: -3.6 minutes, 95% CI (-5.7, -1.4), thus **Null hypothesis 3** relating to outcome measurement: time taken to complete access cavity preparation, was rejected for this study. The estimated mean time taken for GP group was higher than for the ET group: 9.6 minutes, 95% CI (5.8, 13.4) and similarly the estimated mean time taken for the PG group was higher than for the ET group: 7.5 minutes, 95% CI (3.9, 11.1). Session and magnification were not demonstrated to have a statistically significant effect on time taken.

Fixed Effects		Coefficient	95% CI	*p*-value
Image:	**IOPA**	Ref		
	CBCT	-3.6	(-5.7, -1.4)	<0.01*
Group:	**ET**	Ref		
	PG	7.5	(3.9, 11.1)	<0.01*
	GP	9.6	(5.8, 13.4)	<0.01*
Magnification:	**No**	Ref		
	Yes	0.8	(-2.5, 4.1)	0.65
Session:	**1**	Ref		
	2	-1.2	(-3.4, 0.97)	0.28
Random Effects				
Operator: Tooth type variance		7.14		
Operator		0.84		
Residual variance		32.76		

TABLE 4.10 Linear mixed effects regression model: Factors effecting procedural time (minutes): IOPA imaging, ETs, no magnification and session 1 are used as references (ref) or standard with which the other variables are compared against in each category. *denotes significant at *p*<0.05 level of significance. IOPA: Intraoral periapical, CBCT: Cone beam computed tomography.

4.4.2.3 Proportion of canals located

All operators located the disto-buccal, main mesiobuccal canal (MB1) and palatal canal in all three teeth with both conventional imaging alone and with additional CBCT imaging. However, image modality, tooth type and experience group were discriminating factors with respect to successful location of the MB2 canal. For each of the teeth (X, Y and Z), a greater proportion of endodontic access cavity preparations resulted in successful identification of the MB2 canal when IOPA with additional CBCT were available than when IOPA imaging alone was used (**Table 4.11**). The differences were significantly different for tooth X (p=0.043) and Y (p=0.008), indicating that for these teeth null hypothesis 4 was rejected, but not for tooth Z (p=0.153). Analysis by experience groups (**Table 4.12**), indicated that for the ETs and the PGs, there was successful location of MB2 canals in 83% and 28% of endodontic access cavity preparations, respectively, using IOPA imaging alone. There were no successful MB2 canal identifications by the GPs. With additional CBCT imaging, the proportions of endodontic access cavity preparations resulting in successful identification of the MB2 canal were 100%, 83% and 28%, for ETs, PGs and GPs, respectively.

TOOTH X

IMAGING MODALITY	NOT LOCATED	LOCATED
CBCT	4 (22.2%)	14(77.8%)
IOPA	10 (55.56%)	8(44.4%)

*Fishers Exact = **0.043***

TOOTH Y

IMAGING MODALITY	NOT LOCATED	LOCATED
CBCT	3 (16.7%)	15(83.3%)
IOPA	11 (61.1%)	7(38.9%)

*Fishers Exact = **0.008***

TOOTH Z

IMAGING MODALITY	NOT LOCATED	LOCATED
CBCT	9 (50%)	9(50%)
IOPA	13 (72.2%)	5(22.8%)

Fishers Exact = 0.153

TABLE 4.11 The proportions of endodontic access cavity preparations leading to location (or non-location) of MB2 canals in the three teeth (X, Y and Z) according to the imaging available to the 18 observers. Comparison of proportions for each tooth made using Fishers Exact Test (One-sided). *= Significant difference in proportion of canals located times between IOPA and IOPA + CBCT. (P<0.05). IOPA: Intraoral periapical CBCT: Cone beam computed tomography.

GROUP/TOOTH	X		Y		Z	
N=6 (OPERATORS/CANALS)	IOPA	IOPA+CBCT	IOPA	IOPA+CBCT	IOPA	IOPA+CBCT
ET	6	6	5	6	4	6
PG	2	6	2	6	1	3
GP	0	2	0	3	0	0

TABLE 4.12 The number of endodontic access cavity preparations leading to location (or non-location) of MB2 canals in the three teeth (X, Y and Z) according to the imaging available to the three experience groups of six observers. IOPA: Intraoral periapical CBCT: Cone beam computed tomography.

4.4.3 Questionnaire data

Table 4.13 summarizes the responses given by the 18 operators to Q.1 and 2 of the questionnaire. Only a small minority of operators were able to identify MB2 canals using conventional radiographic information prior to preparing the access cavity. In contrast, when CBCT was available, all 18 operators were prospectively able to identify the MB2 canals in Teeth X and Y, with 15 operators successfully identifying the MB2 for Tooth Z.

In terms of pre-operative confidence in being able to proceed to locate the MB2 canal based on the available imaging (Q.2 of the questionnaire), an increase in median confidence score, from 'slight confidence' to 'moderate confidence' was recorded when additional CBCT imaging was available. Specifically, the Mann-Whitney U test revealed that confidence scores were significantly lower for all experience groups when provided with IOPA imaging alone [Md = 2 (X, Y, Z) , n = 18] compared with receiving additional CBCT imaging (Md = 3, n= 18), U = 9 (X), U = 20 (Y), U = 64 (Z), p = 0.001 (X, Y), p = 0.002 (Z), r = 0.84 (X), r = 0.8 (Y), r = 0.55 (Z) (Effect size r <0.3: small effect, 0.3-0.5: medium effect, >0.5: large effect).

Breaking these results down by Experience Group, the median confidence rating of ETs for all three teeth ranged from 2-3 using IOPA and was 3-4 when CBCT was available. The equivalent results for PGs were all 2 with IOPA and all 3 with CBCT, while all GPs scored median confidence ratings as 1-2 for IOPA and a range of 3-4 with additional CBCT.

	Number and proportion (%) of operators who identified canals pre-operatively (Q.1)		Median and range of confidence ratings of operators pre-operatively (Q.2)	
Tooth	**IOPA**	**IOPA + CBCT**	**IOPA**	**IOPA + CBCT**
X	4 (22.2%)	18 (100%)	2 (1-3)	3 (3-5)
Y	2 (11.1%)	18 (100%)	2 (1-3)	3 (3-5)
Z	2 (11.1%)	15 (83.3%)	2 (1-3)	3 (1-5)

TABLE 4.13 Responses of operators to Q1. & Q.2 of the questionnaire, answered pre-operatively. Q.1 asked "Can you identify an MB2 Canal from imaging provided?". Q.2 asked, "How confident are you from using the available imaging data that you could locate the MB2 canal? IOPA: Intraoral periapical radiographs, CBCT: Cone beam CT.

Table 4.14 summarises responses to Q.3, answered after access cavity preparations of all three teeth were completed for both session 1 and 2. When asked "How similar is this simulation of locating the canals in 3D printed teeth to a real clinic scenario?", the median Likert scale score was 4 ('highly similar' to the real clinical scenario), for both sessions: IOPA alone and for IOPA with CBCT imaging. Additionally, all Experience Groups recorded this median score.

Experience Group	Response regarding similarity of simulation to real clinical situation Median (and range)		
	ET	PG	GP
IOPA & IOPA + CBCT	4 (3-4)	4 (3-4)	4 (3-4)

TABLE 4.14 Responses of the operators to Q.3 of the questionnaire, when asked "How similar is this simulation of locating the canals in 3D printed teeth to a real clinic scenario?" ET: Endodontists, PG: postgraduate students, GP: general dental practitioners. IOPA: intraoral periapical radiographs, CBCT: Cone beam CT.

Additionally, verbal feedback on the clinical similarity of the 3D printed teeth to real teeth included the following responses with reported critical comments referring to:

"lack of internal staining",

"less hardness when compared to dentine"

"crumbling of undermined dentine".

Positive comments included:

"similar feedback to real teeth when instrumenting canals",

"precise replication in canal dimensions and even included pulp stones".

Table 4.15, shows that the median values recorded postoperatively for assessing helpfulness of the imaging modality in locating the MB2 canal (Q.4 of the questionnaire), which was 1 ('not helpful') with regard to IOPA imaging (ETs: 1, PGs: 1, GPs: 1) and 5 (ETs: 5, PGs: 5, GPs: 3) for IOPA with additional CBCT imaging (**Table 4.15**). Specifically the Mann-Whitney U test confirmed that with regard to helpfulness of the imaging modalities, that scores were significantly lower for all Experience Groups when provided with IOPA imaging alone (Md = 1, n = 18) compared with receiving additional CBCT imaging (Md = 5 [ET, PG], Md = 3 [GP] , n= 18), U = 0.000 (ET, PG), U = 2 (GP), p = 0.002 (ET, PG), p = 0.01 (GP), r = 0.87 (ET), r = 0.88 (PG), r = 0.48 (GP). Therefore **Null hypothesis 5** of this study was rejected for all Experience groups.

Tooth	Median (and range) of helpfulness ratings of operators post-operatively	
	IOPA	IOPA + CBCT
ET	1 (1-2)	5 (4-5)
PG	1 (1-2)	5 (4-5)
GP	1 (1-3)	3 (3-4)

TABLE 4.15 Response of operators to Q.4 of the questionnaire, answered post-operatively, which asked "How helpful was the imaging data provided in assisting location of the MB2 canal?" IOPA: Intraoral periapical radiographs, CBCT: Cone beam CT.

In response to question 5, three out of the 18 operators (16.7%) reported that recall played a role in location of canals in their second session.

4.5 DISCUSSION

The purpose of this study was to identify if supplemental CBCT imaging can potentially improve patient outcome after endodontic access cavity preparation in M1Ms, by analysing changes in tooth substance removed, procedural time taken and root canals located, specifically in relation to location of the MB2 canal, compared with the use of conventional (IOPA) and clinical methods alone, thereby justifying its increased dose and radiation detriment. Furthermore, this study investigated if operator experience level, tooth complexity, magnification and session order (CBCT first or second session) influenced these objective measurements. The subjective measurements of operator confidence and reported 'helpfulness' of additional CBCT imaging in MB2 canal location were also recorded.

A diagnostic X-ray exposure should always contribute to achieving the intended clinical outcome. The goal of justification is to avoid unnecessary radiological procedures, which would result in patients being unnecessarily exposed to ionizing radiation and its potential risks. The process of determining appropriateness of a medical procedure is an evidence-based approach to choosing the best test for a given clinical scenario, with account taken of the diagnostic efficacy of the proposed radiological procedure as well as of alternative procedures that do not use ionizing radiation (IAEA 2022). Therefore, this study was designed to demonstrate any potential evidence of CBCT imaging impacting on patient outcome, level 5 of the diagnostic efficacy evaluative framework (FRYBACK & THORNBURY 1991), in non-surgical endodontics and identify some evidence that would help to determine the appropriateness of its use.

It is important to justify the classification of this study as belonging to the level 5 of Fryback & Thornbury hierarchy (FRYBACK & THORNBURY 1991), as this might be challenged in the absence of real patients. Some might consider it as being closer to a Level 4 (Therapeutic efficacy) study. Looking back at their original paper, Fryback & Thornbury (1991) describe Level 5 (Patient outcome efficacy) studies as being concerned with "*whether there is measurable effect of the* (radiological) *image on the outcome experienced by the patient.*" The main parameters measured in this study (access cavity volume and linear dimensions, proportions of canals identified,

procedural time) are certainly outcome measures, but some flexibility in the strict definition of Level 5 efficacy studies is needed when using a 'patient model' rather than a living patient. For reasons described previously, the same patient with the same problem cannot be treated twice, with or without the novel imaging technique, while RCTs are extremely challenging to perform. Therefore, study design using well-constructed human analogues are a potentially valuable research tool that overcome some of these problems. Level 4 studies classically measure the clinician's management before the diagnostic information is obtained with the treatment performed after the diagnostic results are known, matching with the use of a 'before-after' study design. Rohlin et al. (2020) included the 'with-without' study design under the Level 4 heading, in which "paper cases" or 'clinical vignettes' containing a comprehensive set of clinical information and results of other tests are used, but this did not include any practical intervention with a measurable outcome such as in this study. Certainly, the assessments of operator confidence and reported 'helpfulness' on location of the MB2 canal related to the available imaging sit in the Level 4 category, but the main focus of the current study does not. Thus, it seems entirely justifiable to describe the current study as sitting comfortably in the Level 5 category, but while also including some aspects classifiable under the Therapeutic efficacy heading.

The end-point of any clinical treatment is evaluated using outcome measures, which are defined as objective, or subjective measurements used to evaluate the effectiveness of an intervention compared with the control (SMITH ET AL. 2015). Although this study did not include patients, modelling using 3D-printed teeth has been demonstrated to accurately reproduce tooth structure and allow effective simulation of clinical scenarios, thus enabling controlled, direct comparisons of interventions on the same teeth, which is not possible in a clinical study (TACK ET AL. 2016, LIANG ET AL. 2018, CONNERT ET AL. 2019, MAGNI ET AL. 2021). Furthermore, in studies that involve additional exposure to ionizing radiation, it would be unlikely to be ethically acceptable to justify taking a pre- and post- CBCT of every patient, (both images are required for accurate volumetric assessment), while only using the pre-operative diagnostic information available from the CBCT imaging for one arm of the study. Clearly, there are limitations to modelling studies, with printed teeth often differing in their radiolucency or

resistance to dental instruments compared with natural teeth, as well as differences between the laboratory environment and the clinical setting (REYMUS ET AL. 2020).

Is it reasonable to extrapolate this study's objective and subjective findings to the clinic and demonstrate at least surrogate or potential impact on outcomes associated with endodontic access cavities? Clinical outcome is defined as measurable changes - clinician or patient reported - in disease, health, function or quality of life that evaluate the effectiveness of an intervention or exposure (DUNCAN ET AL. 2021). Traditionally, clinical endodontic outcomes or clinical end-points were measured according to radiographic evaluation of apical disease (ESE 2006), but has now expanded to include patient-reported outcomes including pain, function, tooth survival and cost-effectiveness. In the absence of a core outcome set (COS) in endodontics (EL KARIM ET AL. 2021), recent guideline projects in endodontics have developed, by consensus, appropriate outcome measures. Long-term retention of the tooth was cited as the 'most critical' outcome measure, with pain, tenderness, swelling, need for medication', 'radiographic evidence of reduction of apical lesion' and 'tooth function (fracture, restoration longevity)', all cited as important outcomes (DUNCAN ET AL. 2021). In this study using 3D-printed teeth, the outcome measurements - access cavity volume, access cavity dimensions and number of canals located (which reflects the root canal technical quality), can be considered as surrogate measures, or 'steps on the way', that literature suggests may correlate with a real clinical outcome (LERTCHIRAKARN ET AL. 2003, SATHORN ET AL. 2005, DI FILIPPO ET AL. 2014). For example, if a root canal is not located the canal cannot be disinfected and the residual intra-radicular infection increases the likelihood of apical disease (NAIR 2006) although it is accepted that using canal location as a surrogate marker cannot fully address the impact of the effectiveness of subsequent microbial disinfection, which is a key determinant of successful endodontic outcome. Excessive dentine removal during access cavity preparation may weaken the tooth rendering it more susceptible to fracture (SATHORN ET AL. 2005). In clinical studies, these types of surrogate outcome measures are often used to present data when the equivalent clinical study would require large numbers of subjects and long-term follow up (BERGENHOLTZ & KVIST 2014).

Recent reports suggest that, of the factors influencing the survival of teeth and restorations after root canal treatment, loss of tooth structure is the most critical (AL-

NUAIMI ET AL. 2020, BHUVA ET AL. 2020). Preservation of the structural integrity is central to fracture resistance and long-term tooth survival, albeit, being one component of a multifactorial process affected by biomechanical properties of residual tooth structure (AROLA & REPROGEL 2005, NAGASIRI & CHITMONGKOLSUK 2005, REEH ET AL. 2009, EL-HELALI ET AL. 2013, AL-NUAIMI ET AL. 2017, KAFANTARI ET AL. 2019), masticatory forces (CHAN ET AL. 1998) and choice of restoration (SORENSEN & MARTINOFF 1984, AQUILINO & CAPLAN 2002, PRATT ET AL 2016). There is mounting understanding that conservation of residual tooth structure should be considered paramount prior to and during root canal treatment (SILVA ET AL. 2020), in addition to minimally invasive solutions during the subsequent restorative procedure. Specifically, it is proposed that factors related to the pre-operative anatomy of the tooth being treated, such as root canal morphology, residual root dentine thickness and canal curvature, are all factors affecting the fracture resistance of root filled teeth (LERTCHIRAKARN ET AL. 2003, SATHORN ET AL. 2005). The growing evidence base has prompted the drive towards more conservative access cavity and root canal preparations in order to preserve residual dentine (CLARK & KHADEMI 2010, KRISHAN ET AL. 2014, PLOTINO ET AL. 2017), particularly in the peri-cervical region (approximately four mm above and below the alveolar crest). Maintenance of this peri-cervical dentine (PCD), especially in molars, has been said to facilitate better distribution of occlusal loads to the radicular portion and is critical to their optimal function and long-term survival (CLARK & KHADEMI 2010) with extensive searching and troughing to locate root canals resulting in excessive dentine removal, particularly in the mesio-buccal (MB) root area. This can increase the chance of potential complications including reduced resistance to root fracture, perforation and compromised restoration (DE CHEVIGNY ET AL. 2008, GLUSKIN ET AL. 2014, AL-NUAIMI ET AL. 2017, AL-NUAIMI ET AL. 2020, BHUVA ET AL. 2021, LIN ET AL. 2022), leading to potential tooth loss (STUDEBAKER ET AL. 2018). Reduced or minimal access cavity design has gathered momentum, but has been checked by studies highlighting that although less dentine is removed, this does not significantly alter fracture resistance, with the overall restorative status of the tooth potentially have more bearing and additionally, results in reduced quality of root canal treatment (COEHLO ET AL. 2018, ROVER ET AL. 2020, SILVA ET AL. 2021). This can be summarised by suggesting that removal of sufficient tooth to complete high-quality root canal treatment remains key, but that

avoiding removing unnecessary dentine (**Figure 4.18**) in key areas such as peri-cervical area is critical (SILVA ET AL. 2021).

Axial Views
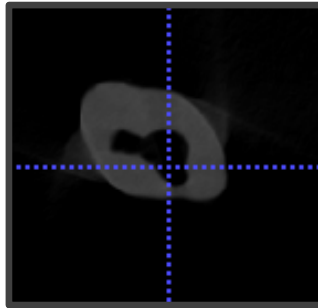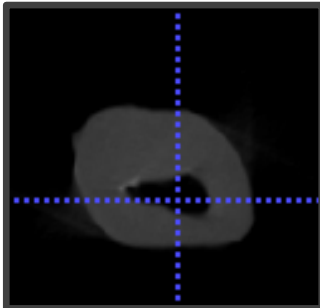
Mesio-distal
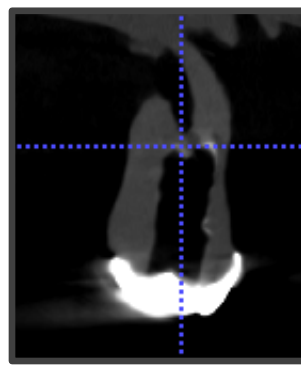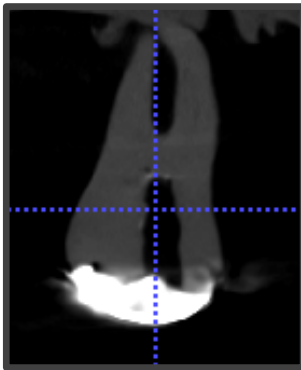
Bucco-palatal Views
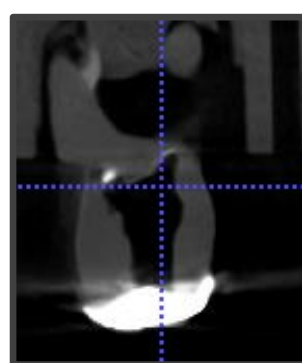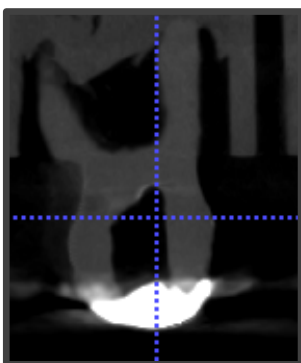
FIGURE 4.18 CBCT images of Tooth Z after access cavity preparation demonstrating the variation in dentine removal in peri-cervical dentine. Left: CBCT assisted access cavity preparation completed by ET. Right: CBCT assisted access cavity preparation completed by PG. ET: Endodontist, PG: Postgraduate

As stated, the most critical outcome measure for non-surgical root canal treatment is long-term retention of the tooth, as defined by ESE S3-level clinical practice guidelines outcome measures (DUNCAN ET AL. 2021). The aim of endodontic treatment is treatment or prevention of apical periodontitis, an aim achieved by effective chemo-mechanical debridement of the complete root canal system (ESE 2006). Therefore, identification and location of all canals is necessary to remove the microbial biofilm, which is the essential cause of apical disease (NAIR, 2006). If canals are missed, the efficacy of chemo-mechanical debridement is reduced with an increased risk of persistent disease, endodontic failure and potentially tooth loss (WOLCOTT ET AL. 2005, TSESIS & FUSS 2006, CHANG ET AL 2013, KARABUCH ET AL. 2016). If anatomically complex morphology is predicted or where conventional imaging and clinical methods alone prove insufficient, such as in the case for location of MB2s in M1Ms, CBCT imaging may be indicated (EUROPEAN COMMISSION 2012, AAE & AAOMR 2015, ESE 2016). Since the literature clearly shows that missed canals can lead to endodontic failure (WITHERSPOON ET AL. 2013, KARABUCAK ET AL. 2016) and risk of tooth loss (STUDEBAKER ET AL. 2018), this study measured MB2 canals located as a potential marker of outcome, given that all other canals in the M1M were located by all operators. With regard to CBCT imaging-assisted detection and location of the MB2 canal, the reported incidence varies (54-93.3%) according to study type (COEHLO ET AL. 2018) and the literature is considered in depth in **Section 4.5.2.**

Procedural time was recorded in this study as a component of the evaluation of a new technology (CBCT) should also be based on patient-centred outcome, individual and societal (FRYBACK & THORNBURY 1991). Practically, in a clinical simulation study, the only patient-centred outcome that could be assessed is a change in procedural time. It is known that searching for canals is a time-consuming aspect of endodontic treatment. Less time in the dental chair is always beneficial to the patient (and dentist) but as is the case for all possible benefits gained from CBCT imaging, this has to be weighed against the cost of CBCT imaging and indeed the associated increase in radiation dose (SCHWENDICKE & GÖSTEMEYER 2016, PETERSEN ET AL. 2015). Furthermore, although the procedural time was shortened with the presence of an additional CBCT scan, this may be negated overall, as the clinician will need additional viewing time to assess the CBCT scan, which is separate from the procedural time and not assessed in the current study.

This would also likely have an impact on cost-efficacy. No literature was available on CBCT imaging and procedural time in non-surgical root canal treatment.

4.5.1 Study design

4.5.1.1 Selection of teeth

Three teeth were selected for this clinical simulation study, to reflect a range of M1M mesiobuccal root canal morphologies and complexities. As root canal instrumentation was not part of the study remit, complexity and variation was reflected in two principal ways. Firstly, the bucco-palatal and apico-coronal position of the canal orifice was verified. Secondly, the approximate diameter of the MB2 orifice, at the level first identified as a separate entity on scrolling apically from the pulpal floor in the axial view using the microCT scans, was evaluated. Root canal anatomy studies indicate that the majority of MB2 canals are positioned mesial to a direct line connecting the MB1 and palatal canal, with the distance between the central MB1 and MB2 averaging around 1-2mm; however, these measurements vary slightly with the technique (scanning electron microscopy, stereomicroscopy, CBCT) used (KULID & PETER ET AL. 1990, GÖRDUYSUS ET AL. 2001, BETANCOURT ET AL. 2016). MB2 orifice diameter dimensions in the coronal aspect of M1Ms range from an average of 0.59 mm to 1.13 mm (SU ET AL. 2019). MB2 orifices that are detectable at the level of the pulp chamber floor in M1Ms can occur anywhere between 50-94% of cases (ZHANG ET AL. 2017, KIM ET AL 2020). MB2 orifices that do not appear at the level of the pulp chamber floor in M1Ms have an average vertical distance below the pulp floor of 0.76-1mm (ZHANG ET AL. 2017, KIM ET AL 2020). Comparing the three printed teeth used in the current study, Tooth X and Y were locatable at the level of the pulp chamber floor, but at different distances from the MB1 orifice. Endodontists concluded that Tooth Z, having the narrowest coronal orifice diameter and not appearing until a depth of 0.84 mm below the level of the pulp chamber floor, presented the greatest technical challenge in MB2 canal location (**Table 4.1**). Practicalities, such as the time needed for all tasks to be completed in each session, in addition to operator time limitations, dictated that three was the maximum number of teeth that could be included. Although a range of MB root morphologies were selected, it was accepted this could not represent all variations of MB2 canal origin.

4.5.1.2 3D printing process and volume assessment

MicroCT scanning, rather than CBCT, was completed on the selected teeth prior to printing due to its higher resolution imaging (voxel size 20 μm), which allows precise depiction of small morphological structures such as root canal systems. MicroCT is considered the gold standard in root canal anatomy and identification studies and evaluating fine morphological structures (DOMARCK ET AL. 2013, ACAR ET AL 2015, CHRISTIANSEN 2016, ALMEIDA ET AL. 2020). The accuracy of high-resolution 3D printing from microCT data, for a variety of applications, has been previously described in the medical and dental literature (AHN ET AL. 2018, REYMUS ET AL. 2018, ANDERSON ET AL. 2018). Medical 3D modelling techniques are particularly advanced, being used for prostheses, research and surgical simulation, as well as having educational purposes as they demonstrate advantages over traditional cadaveric and animal models (MICHAELS ET AL. 2021). Advantages of modelling include regulatory and ethical constraints, difficulty in acquisition, cost and storage of cadaveric and animal models and variation from human anatomy for the latter.

PolyJet printing, rather than other available technologies (e.g. stereolithographic [SLA] and digital light processing [DLP] printing), was used in this study due its superior accuracy (0.1-0.3 mm), precision and track record in printing fine structures such as root canal systems (ISHIDA & MIYASAKA 2016, KIM ET AL. 2016, ANDERSON ET AL. 2018). Specifically, PolyJet printing is a patented technology executed by jetting specific photopolymer materials in ultra-thin layers of 16 μm onto a build tray layer-by-layer until the model is completed. Each photopolymer layer is cured by UV light immediately after it is 'jetted', producing fully-cured models that can be handled and used immediately without the need for post-curing. A gel-like support material that is specially designed to maintain complicated geometries, is easily removed by hand and water jetting (KIM ET AL. 2016). In addition to greater accuracy, PolyJet printers have significantly higher investment costs than SLA and DLP printers (REYMUS ET AL. 2019), which unfortunately meant that the technology was not accessible in my University resulting in the teeth being sent for remote printing in another centre.

In this study, VWP was the photopolymer selected (with the supporting material: SUP705), primarily due to its compatibility with PolyJet printing and its ability to be printed in fine layers. A study evaluating and comparing tooth replicas

190

constructed with different 3D-printed resins (including VWP) concluded that all materials scored highly with regards to realism; however, a drawback for all replicas was the inability to simulate dentine hardness and to recreate internal staining that occurs *in vivo* and which demarcate the canal orifice (BITTER ET AL. 2016, REYMUS ET AL. 2020). Of all the replica materials, VWP was reported as one of the most realistic regarding gauging and negotiating the root canals, which was due to the resistance created during instrumentation by the residual soft support structure inside the root canals. In keeping with other studies, some of the operators in the current study suggested that the 'hardness' of the teeth and internal staining was not ideal (REYMUS ET AL. 2020), but reported gauging and preliminary instrumentation of the tooth as very realistic, grading the similarity to real teeth as moderate to highly similar (grade 3 and 4 on a 5-point Likert scale).

The accuracy of 3D printed teeth depends not only on the accuracy of the imaging system and the 3D printing technology, but also on the software workflow processes that follow. Moreover, an accurate segmentation process is fundamental to physically reconstruct the anatomy (i.e. labelling and extracting the geometry of a region of interest using the data from the 3D imaging modality). Manual or semi-automated segmentation algorithms are generally used for this process (KABALIUK ET AL. 2017, GALIBOURG ET AL. 2018). Semi-automated segmentation is a computer-aided approach in which the operator initially selects the threshold interval that guides the automatic 3D rendering procedure. In this study, the validated method of semi-automated segmentation was completed in ITK-SNAP, which has been shown it to be a reliable software and method of segmentation in a range of medical and dental applications (ALMUZIAN ET AL. 2018, CONNERT AT AL. 2019, LO GIUDICE ET AL. 2020, MAGNI ET AL. 2020). Nevertheless, the final rendered image is the result of the programme algorithm as well as a user-entered threshold value. All regions below a chosen pixel intensity (threshold) are identified as air, and all above in this case as tooth, which can of course be affected by the contrast of the image, image noise, individual visual perception and prior knowledge of anatomy amongst others (KABALIUK ET AL. 2017, ALMUZIAN ET AL. 2018). Segmentation of the selected teeth was completed by one individual (MM), who was experienced in tooth anatomy and segmentation processes, to avoid intra-operator variations and reduce error. Final preparations before printing, including topological

correction, decimation and smoothing, were completed using the software, Meshmixer and Blender, which are open-access online resources regularly used in medical and dental 3D printing studies (O'HARA ET AL. 2016, CONNERT ET AL. 2019).

The process of segmentation using ITK-SNAP was integral to the assessment of volume of tooth substance removed, and represents a validated and widely used method of assessing volume in a range of medical and dental settings (MARET ET AL. 2012, ADISEN ET AL. 2015, ALMUZIAN ET AL. 2018, GOMES ET AL. 2020). Volume assessment was initially completed as part of the pilot study to assess the reliability of the ITK-SNAP segmentation process. After access cavity preparation the teeth were CBCT scanned using the smallest voxel size (75 μm) and the same exposure protocol. Although Micro-CT is considered the reference-imaging tool for dental anatomical research, forensic data and measurements (GALIBOURG ET AL. 2018), it was not considered a viable option for 108 experimental teeth due to expense and time. Nonetheless, volume assessment in dental and medical research (MARET ET AL. 2012, ADISEN ET AL. 2015, ALMUZIAN ET AL. 2018, GOMES ET AL. 2020) is regularly based on reconstructions from CBCT imaging and support its reliability, recommending submillimetre isotropic voxel resolution, which has been shown to produce volumetric measurements that are the closest to microCT (MARET ET AL. 2012). Potential sources of error in assessing the volume of the access cavities included sealing of the canal orifice, with the potential of over or undersealing the canal orifices, or ill-fitting resin-based composite imprint seals covering the occlusal access. In order to prevent this, the resin-based composite was checked rigorously by scrolling through all orthogonal planes in ITK-Snap before segmentation, with identified errors corrected at that stage. Post-segmentation, extrusion or leakage of the 'segmentation bubble' beyond the cavity seal was diagnostic of an ill-fitting composite imprint, which was subsequently repositioned and the segmentation process repeated. Ultimately, the reliability and precision of the segmentation procedure was supported by the low standard deviation recorded between three repeat measurements for each tooth, ranging between ±0-0.09 mm³ for the pilot study and ± 0.2 mm for the actual study. For this reason, CBCT assessment of volume removal has largely superseded other traditional methods (ALMUZIAN ET AL. 2018).

4.5.1.3 Clinical simulation in laboratory

Clinical simulation studies using 3D printed teeth cannot replicate the clinical scenario exactly, while an *in vivo* clinical study does not allow direct comparison of the absence or presence of an intervention on the same tooth, necessary to minimise the host of confounding variables. Confounding variables are created by tooth anatomy variations, restorative status, patient differences, operator differences, variability in protocol standardisation and fluctuations of the imaging standard amongst other factors. In an attempt to overcome these, an adequately powered RCT is required, necessitating large patient numbers over a long period of time with considerable cost. From a wider perspective RCTs are rare in Endodontics with only 3.7% of all published articles (from the two major endodontic journals, International Endodontic Journal and Journal of Endodontics) being identified as RCTs (BERGENHOLTZ & KVIST 2014). Specifically, RCTs assessing patient outcome efficacy of CBCT imaging in endodontics are particularly rare, with a recent systematic review (ROSEN ET AL. 2022) identifying only one RCT and one prospective clinical trial that assessed the impact of CBCT on patient outcome (KURT ET AL. 2014, YANG ET AL. 2016). Both studies (investigating surgical and non-surgical endodontics) reported positive effects of CBCT but were identified as having a high risk of bias as per the Cochrane Handbook for Systematic Reviews of Diagnostic Test Accuracy (REITSMA ET AL. 2009). It was reported among other factors that they lacked a reference standard and the results were uninterpretable, and that the reliability of these studies were jeopardized by potential systematic errors. Generally, it was concluded that the main reason for the paucity of reliable evidence in the literature is the difficulty in conducting comparative in vivo clinical research in terms of outcome assessment was due to ethical, practical, and clinical concerns (ROSEN ET AL. 2022). The lack of RCTs assessing the impact on CBCT use in Endodontics is also seen for other areas of dentistry, with the exception of RCT studies looking at the impact of using CBCT on injury to the inferior alveolar nerve during third molar removal. Six RCTs on this topic were identified (DE TOLEDO TELLES-ARAÚJO. ET AL. 2020) and it is of interest that their meta-analysis found no difference in injuries between the CBCT group and panoramic radiography group.

This study was a clinical simulation 'with-without' study, which has been used extensively in dental imaging research (SHELLEY ET AL. 2011, CONNERT ET AL. 2019. SATO ET AL.

2020) to study the effects of an intervention that would not otherwise be practically, clinically or ethically possible was designed to recreate as closely as possible the clinical scenario at every stage. The use of an anthropomorphic phantom, which is a published method (SHELLEY ET AL. 2011, HIDALGO RIVAS ET AL. 2015) of replicating the tissues of the skull as closely as possible, was used for conventional and CBCT imaging of the teeth, at the clinically-optimised exposure protocols, to mimic the attenuation of maxillary structures in clinical imaging.   Limitations include the absence of patient movement and the impact it can have on CBCT image quality (SPIN-NETO ET AL. 2018), which could not be replicated in this study. Additionally, the absence of restoration artefact resulted in superior image quality to that generally seen in the clinic. An acrylic jig (**Figure 4.8**) was used to accurately transfer the orientation of the M1M as identified in the imaging provided, to the simulated dental arch that was securely positioned in a magnetised manikin head with an opposing arch (**Figure 4.10**). Rubber dam was already in place for the operators in order to make the procedure as efficient as possible, limit potential stress from rubber dam placement and safeguard the time needed for all three cavity preparations and questionnaire to be completed in each session.

Notably, the pilot study was carried out only by endodontists not involved in the actual study, which does not reflect the range of experience in the study proper. It is accepted that this could skew the results for sample size (http://statulator.com/SampleSize/ss2PM.html), which was based on the mean difference in volume removed in the pilot study and associated standard deviation.   It was concluded that the standard deviation was likely to be smaller between the similarly skilled ETs than would be expected with less experienced groups PGs and GPs, which would likely under-power the sample size required. However, this was counteracted by the fact that the volume differences would also have been smaller between ETs which has the effect of increasing the sample size needed and somewhat remedy the calculation.

The numbers recruited to the study, 18, exceeded the sample size of 16 matched pairs required, as indicated by the sample size calculation (**Section 4.3.6**). There were challenges and constraints to recruiting sufficient numbers of operators to each group, including the availability of practicing dentists within the DDUH in each of the selected experience groups, as well as them agreeing to 'volunteer' to carry out a two-part study

during working hours. Furthermore, for practicality and indemnity reasons, it was accepted that the groups recruited were all associated with DDUH, and therefore were a subpopulation of dentists potentially not representative of the wider population of dentists. Nevertheless, operator recruitment numbers in this study exceed other clinical simulation studies of a similar nature (SHELLEY ET AL. 2011, CONNERT ET AL. 2019. SATO ET AL. 2020).

In order to limit operator recall and to disguise the fact that the M1Ms were the same for both sessions, a 'washout' period of eight weeks between the first and second session was introduced, as well as creating two sets of IOPA and CBCT imaging for Tooth X, Y and Z, with altered abutment teeth set-up for each session. Additionally, the order of Tooth X, Y and Z were randomised within each session (https://www.randomizer.org/) and were presented in six different patient files, with differing 'mock' hospital numbers and identities, to further reduce similarity and recall from the first session. Dental clinical simulation studies with 'washout' periods have included time differences from four weeks to 12 weeks (SHELLEY ET AL. 2011, AL-SALEHI ET AL. 2016). While there is no definitive evidence on a minimum 'washout' period, it is accepted that longer is better, and a maximum of eight weeks was practical in this study due to the PGs completing their employment period in the dental hospital, after which point they would have been lost to the study. To standardise settings and remove ambient differences, both sessions were completed at exactly the same time for each operator.

4.5.2 Primary and secondary outcomes

Volume of tooth substance removed was the primary outcome measured in this study, with procedural time and the number of canals located being the secondary outcomes evaluated. Recent studies have examined the impact of CBCT imaging in guided endodontics: on volume removal, procedural time and canals located for a range of tooth types, using 3D printed teeth, extracted teeth and in the clinic (CONNERT ET AL. 2019, BUCHGREITZ ET AL. 2019, SATO ET AL. 2020). The existing literature consistently highlights that the use of a 3D printed endodontic guide generated from CBCT imaging decreases volume of tooth substance removed, reduces procedural time and increases the number of MB2 canals located, with the guide removing the impact of operator

experience. The current study did not employ a guided endodontic technique, as it is generally not applicable for molar endodontics for which there is a need for a straight-line path to the apical target point and limited accessibility in the posterior area. Other general limitations of guided endodontics include the construction time, additional expense, and possible dentinal micro-crack formation with the associated temperature increase (KRASTL ET AL. 2016, CONNERT ET AL. 2018). A further issue with location of MB2 canals is that unlike 'sclerosed' and calcified canals, the task of locating an MB2 canal is not something that would routinely require a stent and guided procedure.

One previous study (GRANADOS ET AL. 2018) examined the impact of additional CBCT imaging on conservative endodontic access cavities in 45 extracted molars, while also comparing with traditional endodontic access cavities, by measuring the ratio of the surface area of coronal access to pulp floor on the accessed upper and lower molars (3 groups; 15 per group). Although the study demonstrated a trend towards more consistent preparations and decreased procedural time with the availability of CBCT (GRANADOS ET AL. 2018), statistical significance was not recorded for either measure. The authors concluded that the limitations of the study included heterogeneity between teeth (some having variable degrees of calcified roots, these teeth being unevenly distributed between the groups) which did not allow for any meaningful comparison. Another study (CONNERT ET AL. 2014), compared dentine removal on 40 extracted molars in a clinical-simulated split-mouth design study, assessing diameter of access cavities made with conventional radiography as compared with CBCT. No significant difference was demonstrated in mean diameters between cavities prepared using conventional and CBCT imaging. This was a published abstract only (ESE conference, Lisbon, 2013). No information was provided on the tooth types or attempts to standardise the compared extracted teeth which would obviously have differed in morphology and dimensions unlike printed teeth. The minimum and maximum diameter was recorded but the depth at which the diameters were measured and the orientation of the diameter recording was not detailed.

Regarding preoperative endodontic imaging for non-surgical root canal treatment, currently intraoral periapical imaging (with the potential of an additional parallax view), remains the gold standard (ESE, 2006). It is accepted that periapical radiography can only provide two dimensional information, with its diagnostic

effectiveness limited by the superposition of anatomical structures and reports indicating that only 8% of MB2 canals in M1M teeth were identified using periapical radiography (ABUBARA ET AL. 2013). The incidence of MB2 canals in M1Ms has been reported as varying between 14% and 96.1% (KULID & PETERS 1990, BETANCOURT ET AL. 2016, ZHANG ET AL. 2017, COEHLO ET AL. 2018). Variation is dependent on the methodology used (root sectioning with direct vision of the roots, use of microscopes, microCT, CBCT scans etc.), with *ex vivo* studies reporting higher incidences of MB2 canals identified compared with clinical studies reporting MB2 canal location. An *ex vivo* study using microCT reported the incidence of MB2 to be 100%, and further reported no significant difference of the incidence of MB2 canals identified using CBCT with that of microCT (DOMARK ET AL. 2013). However, MB2 canal identification using CBCT imaging demonstrates considerable disparity, with studies quoting between 54% - 93.3%. This wide variation relates to study type (*in vivo* or *ex vivo*), population studied, voxel size, CBCT scanner (manufacturer and model) and restorative status of the tooth (BLATTNER ET AL. 2010, BAUMANN ET AL 2011, ZHANG ET AL. 2011, ABUBARA ET AL. 2013, HIEBERT ET AL. 2017, ZHANG ET AL. 2017). Furthermore, as demonstrated in **Chapter 2** of this thesis, exposure setting can affect the detection of MB2 canals. *In vivo*, MB2 location studies using clinical methods (including magnification) and conventional imaging, achieved 72-78% MB2 canal location by endodontists and trainee endodontists, with MB2 location increased by approximately 10% after the addition of CBCT imaging and vertical 'troughing' (PARKER ET AL. 2017, HIEBERT ET AL. 2017). An earlier *in vivo* study reported that with clinical experience, correct equipment and the dental operating microscope, the MB2 was located in 93% of patients (STROPKO ET AL 1999). A highly variable factor affecting the detection of MB2 canals on CBCT scans of live patients is likely to be patient movement.

The current study is novel as it specifically investigates if the additional imaging information provided by a CBCT scan (without guides), can affect the volume removed during endodontic access in 3D printed M1Ms. Whilst being aware of the limitations of a clinical simulation study using 3D printed teeth and the obstacles to directly extrapolating to the clinical situation, this model does provide a level of standardization that ensures direct comparability between operators, with the only difference to the access cavity preparation protocol being the availability of preoperative CBCT imaging

(**Table 4.16**). The results demonstrate that when adjusting for other factors, imaging modality and experience had a statistically significant effect on volume removed during endodontic access procedures on M1Ms. With availability of CBCT imaging, significantly less tooth structure was removed when all experience groups were combined, for Tooth X and Y. For Tooth Z, categorized by the endodontists in the pilot study as the most technically challenging tooth, the PGs and GPs actually removed significantly more tooth substance. For the groups with less experience, the additional diagnostic information available from the CBCT data, which indicated that the MB2 canal was present in the more challenging case (Tooth Z), appeared to result in a more destructive pursuit of the canal.

STUDY SUMMMARY:	
STRENGTHS	**WEAKNESSES**
Simulation: Reproduction of clinical situation, both for imaging and endodontic procedures, performed as accurately as possible, including the patient scenario.	**Simulation:** Unable to simulate pt. movement: CBCT imaging or pt. tolerance variation: endodontic procedures (e.g. limited opening) Microbial disinfection being a main determinant of endodontic success can only be represented in this study by measuring the surrogate marker of canal location.
Sample Size: Achieved a sample size greater than power calculation and included the greatest number of operators of any similar study in the literature.	**Sample:** Only 3 teeth types used. A greater number of teeth would have been ideal, limited by the time commitment required from participating clinicians. An alternative strategy might have been to recruit a second set of participants who worked on three different teeth.
Operators: Range of operator experience	**Operators:** Lack of experience in use of CBCT for some operators (i.e. the problem might have been in reading the scans rather than applying what the scans showed).
Novel Methodology: 3D molar teeth printed with fine anatomy using most accurate printing technology. Strict standardisation of teeth/protocol, only difference being intervention and operator. Adequate 'washout period' as session shown statistically not to impact on volume removed.	**Generalisability**: The 'reduced hardness' of 3D printed teeth, and lack of internal staining limits extrapolation of these findings. CBCT image quality varies enormously according to the manufacturer, the equipment model and the operating parameters, including X-ray exposure settings. It is likely that when CBCT images are of lower image quality, for example with larger voxel sizes, lower x-ray exposures or inferior viewing conditions, there would be an effect on surrogate outcomes measured here.
	Image quality: No patient-associated movement or artefacts from restorations

TABLE 4.16 Summary of study strengths and weaknesses. Pt Patient, CBCT: Cone beam CT.

The ETs, with or without additional CBCT imaging, removed significantly less tooth volume than all other groups with the estimated mean volume for ETs: <PG: 17.3 mm³, <GP: 16.2 mm³ (**Table 4.6**). For ETs, additional CBCT resulted in an average 13-15% reduction when all teeth were considered together, and with a significant reduction for Tooth X and Tooth Y. This significant reduction was also evident for Tooth X and Y with the PGs, which specifically for Tooth X, resulted in the highest percentage reduction in volume (26%) of any group, potentially suggesting this was the group that benefited most from the availability of CBCT imaging for cases of standard complexity. The GPs, however did not show a significant reduction in volume removal for any tooth. The results indicate that endodontic expertise is potentially necessary to translate the additional diagnostic information provided by CBCT to predictably affect volume reduction across a range of anatomical/morphological complexities. Using the mixed effects modelling, the estimated mean volume removed (**Table 4.6**) when IOPA and additional CBCT were available was lower than with IOPA alone (used as reference) by -6.1 mm³, 95% CI (-11.1, -1.2). This value is an estimated mean of the Experience Groups and is affected by the increased removal of tooth volume by the less experienced operators. However, across all teeth, the ETs removed between 10-13 mm³ (13-15%) less tooth volume, with additional CBCT imaging. The question remains as to the generalizability of the results as to whether this reduction would be repeated in a clinical situation and if this reduction in volume would have any clinical implication. If the literature supporting the importance of conservation of tooth structure in PCD to fracture resistance (CLARK & KHADEMI 2010, AL-NUAIMI ET AL. 2017, AL-NUAIMI ET AL. 2020, BHUVA ET AL. 2021) is valid, then any reduction of tooth removal in a critical area of PCD or avoidance of perforation could potentially be of clinical relevance.

Significant reduction in the dimensions of the access cavity demonstrated a similar pattern to volume reductions, being evident more for Tooth X and Y and for ETs and PGs. ETs recorded the highest number of significant reductions in dimensions in Teeth X, Y and Z. Notably, bucco-palatal and cavity depth were more regularly significantly reduced in size compared with mesio-distal width and ETs and PGs showed more frequent reductions than GPs (**Table 4.7**). Importantly, ETs recorded a statistically significant reduction in depth for the less complex teeth X and Y but recorded an

increase in depth for Tooth Z where the orifice was located below the pulpal floor, highlighting that the CBCT was useful for directing the ETs in removal of tooth substance. Similarly, to overall volume, GPs generally did not record significant reductions in access cavity dimensions, but did record a significant increase in depth for Tooth Z. A conclusion from the analysis of the dimensions of the access cavity is that increasing endodontic expertise extracts increased benefit from CBCT imaging but that no distinct dimension was particularly aided by additional CBCT.

After adjusting for other factors across all Experience Groups, magnification was shown to cause a significant increase in volume removed in comparison to the mean volume removed using no magnification, by 8.0 mm³, 95% CI (0.5, 15.2) (**Table 4.6**). Magnification was used by all ETs (4 DOM, 2 loupes), 3/6 PGs and 4/6 GPs, resulting in overall 13/18 using magnification (loupes and DOM) for both sessions and 4/18 using a DOM.

Use of magnification in endodontics, both by use of DOM and loupes, has increased greatly in recent years (BOWERS ET AL. 2010) and the associated benefits are well described (BOWERS ET AL. 2010, LOW ET AL. 2018). Quantitative benefits generally relate to MB2 canal location (BUHRLEY ET AL. 2002, NATH & SHETTY 2017) and indicate that while loupes increase MB2 canal identification, using a DOM markedly increases MB2 location, which probably reflects that only endodontists generally use DOMs. There does not appear to be any literature relating magnification to access cavity volume removal but it is reported that magnification can increase accuracy with regard to fine motor skills, particularly in the experienced user (BOWERS ET AL. 2010). The finding that magnification resulted in more tooth removal, may be contrary to what would have been expected. It could be argued that this was related to the high incidence of magnification use among the less experienced GPs and PGs (7/12), who removed significantly more tooth substance in the more challenging Tooth Z, and consequently skewed this result, however this was adjusted for in the model. The session number (first or second) did not have a statistically significant effect on volume removed or on procedural time. This finding is supportive of the study design, including the washout period of eight weeks, and the randomisation of the study teeth as it highlights that recall did not appear to influence volume removed or procedural time taken.

Furthermore, in Q.5 of the questionnaire, only three (3/18) study operators reported that recall played any role in location of canals in their second session.

After adjusting for other factors in the model, the imaging modality used and the experience group were shown to have a statistically significant effect on the time taken to complete the access cavity procedure. Procedural time results mirrored somewhat that of volume of tooth substance removed, with time taken to complete endodontic access cavity preparation significantly less both for Tooth X and Y with additional CBCT imaging for the ETs and for the PGs (**Table 4.9**). As expected, ETs demonstrated the shortest procedural time of all the Experience Groups, with or without CBCT imaging (**Table 4.10**). With additional CBCT imaging, PGs showed the greatest percentage decrease in procedural time (X: ↓42.9%, Y: ↓34%, Z: ↓20.3%), which relates to a considerably longer procedural time with IOPA imaging alone than for the ETs. When accessing the more challenging Tooth Z, no significant reductions in procedural time were recorded with additional CBCT imaging by the ETs or PGs, and conversely a significant increase in procedural time was recorded by the GPs. Overall, the procedural time and volume results infer that operators who spend less time per week carrying out molar endodontics will exhibit increased procedural time and an accompanying increase in tooth volume removed during endodontic access cavity preparations. Adjusting for other factors, the estimated mean time taken (mins) with IOPA/CBCT was lower than IOPA: -3.6 mins, 95% CI (-5.7, -1.4), this being for all Experience Groups and thus may show greater reduction for more experienced operators.

In this study, four canals were verified as being present in each 3D printed M1Ms; however, the MB2 was the only canal not located by the study participants in every tooth. This would be consistent with the literature, with MB2 location reported as ranging between 14-94% depending on study type, means of detection and level of expertise (COEHLO ET AL. 2018). Analysis of all Experience Groups, highlights that the provision of additional CBCT images increased the number of MB2 canals located in all teeth, a finding that was significant so for Tooth X and Y but not for the more challenging Tooth Z. The PGs appeared to benefit most from the visual identification of the MB2 canal on the CBCT scan. This group located 10 further MB2 canals with additional CBCT imaging. ETs, already located 83% (15/18) canals with IOPA imaging alone, and only

202

identified 3 more canals with CBCT, an increase of 17%, slightly higher than that 10% reported in other comparable *in vivo* studies (HIEBERT ET AL. 2017, PARKER ET AL. 2017). It is evident that as expertise increases the relative benefit gained from additional CBCT imaging in locating canals reduces, which agrees with previous studies in this area (STROPKO 1999). For GPs, no MB2 canals were located with IOPA (0/18) and, with additional CBCT imaging, only 5/18 MB2 canals were identified. It could be postulated that visually identifying the canal on the CBCT scan (15/18) encouraged the less experienced GPs to persist, but with the more challenging Tooth Z, which demanded more endodontic expertise, this led to more time taken and more volume removed, but still no location of the MB2 canal (0/6 for IOPA and IOPA/CBCT).

Taken together, all Experience Groups identified a very small number of MB2 canals using parallax IOPA imaging (15%), which supports the previously reported findings of 8% identification of MB2 canal using conventional imagining (ABUBARA ET AL. 2013). Equally, it was reported by all Experience Groups that IOPA imaging significantly reduced confidence in location of the MB2 canal compared with additional CBCT imaging (p= 0.001 [Teeth X, Y], p= 0.002 [Z]). Furthermore, IOPA imaging was of no practical assistance in actual location of the MB2 canal (Md score of 1: Tooth X, Y, Z) and was significantly less 'helpful' than with additional CBCT imaging [p = 0.002 (ET, PG), 0.007 (GP)]. There is no doubt that visual identification of the MB2 canal on CBCT scans by all Experience Groups (94%) engendered a significant increase in confidence of canal location across all groups. To recap, CBCT assisted MB2 identification is reported in the literature as ranging from 54% - 93.3%. Identification of MB2 canals on the CBCT scans in this study was at the higher end of this range (94%) and may be attributed to the fact that imaging was not affected by movement as it would in the clinic, that there were no coronal or endodontic restorations and the fact that the MB2 canal was verified as present in all of the teeth. The ETs and PGs reported that CBCT imaging was completely helpful (Md score of 5: ET, PG) in locating the MB2 canal. Interestingly, although a significant improvement in helpfulness of CBCT imaging over IOPA imaging alone (p= .01, r = 0.48 [moderate effect size]) was recorded, GPs rated CBCT only as moderately helpful (Md score of 3). Despite the fact that this group's MB2 location increased by 5/18 from 0/18 with IOPA imaging, in 72% of cases they could not use the imaging

information to locate the canal and this was perhaps translated in their post-operative assessment of 'helpfulness' of CBCT imaging.

It is possible that for operators with less day-to-day endodontic experience that CBCT does not have a role and can actually cause greater destruction of tooth volume particularly in more complex anatomy. Overall, the experience/knowledge level of PGs appeared to extract the greatest advantage from additional CBCT imaging, with their reported increased confidence and helpfulness of additional CBCT imaging translating into the greatest percentage increase in MB2 canal location, the greatest percentage decrease in volume removed and procedural time. Nonetheless, when the anatomy became more challenging, which is one of the indications for CBCT in endodontics (Patel et al., 2021), the additional diagnostic information provided by CBCT could not compensate for their lack of expertise relative to the ETs. The ETs did benefit from CBCT imaging, showing significant decreases in volume of tooth tissue removed (13-15%), time (15-19%) and increased number of MB2 canals located (16%); a finding particularly evident in the case of the most challenging anatomy (Tooth Z). The margins of improvement for ETs using CBCT imaging, with regards to the outcomes measured, were of a smaller magnitude than for the PGs, as experience and knowledge appeared to compensate for the absence of the extra diagnostic information when only conventional imaging was available. Endodontic expertise including knowledge and understanding of root-morphology is essential for planning and performing root canal treatment and to potentially realise the enhanced patient outcome efficacy of CBCT imaging through reduced procedural time, tooth substance removal and canal location for all complexities of morphology. Where intraoperative CBCT imaging and vertical troughing (2-2.7 mm) has been shown (PARKER ET AL. 2017), to achieve a further 10% increase in MB2 canal location, preoperative CBCT imaging would focus efforts from the beginning of treatment and most likely maximise the reduction in tooth substance removal in the PCD region.

Reduction of tooth removal from the PCD region has been shown to increase fracture resistance and potentially long-term tooth survival, however as stated earlier fracture resistance is multifactorial and among other factors, the overall restorative status of the tooth may have a more significant bearing. Additionally, as discussed, in keeping with other similar studies, the reduced 'hardness' of the teeth and lack of

internal staining in comparison to human teeth, limits extrapolation of these findings. To that end, these results highlight the need to further translate the findings into a clinical study analysing the effects of preoperative CBCT in maxillary first molar teeth. The current study provides simulated and compelling evidence of the potential advantages of the use of CBCT for the treatment of M1Ms and asks whether, for these reasons, the increased radiation dose can be justified. In order to move this question on, a prospective, adequately-powered randomised trial design would be required that addresses root canal identification, tooth fracture, tooth survival and which includes an economic evaluation.

4.6 CONCLUSIONS

Within the limitations of this clinically simulated 'with-without' study using 3D printed teeth, it can be concluded that;

- Use of additional preoperative CBCT imaging reduced tooth volume removed, procedural time and increased the number of MB2 canals located. This was evident for standard anatomies for ET's and PGs when the MB2 was at the level of the pulp chamber floor. However, the benefits were not evident for dentists who were not routinely carrying out molar root canal treatment.

- When root canal anatomy was more challenging a (an indication for CBCT in endodontics), operators with less day-to-day endodontic experience used the evidence of a MB2 canal on CBCT to warrant increased removal of tooth substance with limited benefits in terms of canals located. As a result, on the basis of this study, CBCT imaging for location of MB2 canals cannot be justified for the inexperienced operator.

- Translating these findings, a reduced volume of tooth substance removal in the PCD region could potentially impact on endodontic outcome such as fracture resistance and tooth survival and similarly, absence of apical disease through increased location of canals. Ultimately these positive results would need to be investigated in clinical longitudinal randomised studies to elucidate if CBCT can be justified or whether endodontic experience and equipment alone can achieve similar outcomes.

Chapter 5

Discussion and future research

5.1 DISCUSSION

CBCT devices have adapted in design, becoming more accessible to the primary care dental setting and are being used in a broad range of dental specialties. This expanding array of devices varies widely in technical specification and consequently in terms of image quality and dose ranges (GAÊTA-ARAUJO ET AL. 2020, KAASALAINEN ET AL 2021). Therefore, provision of optimisation protocols for all diagnostic tasks and guidance on their practical application is more crucial than ever, so as to minimise dose for the individual patient type. Optimisation has to be preceded by justification, ensuring that selection of this higher dose imaging modality will have a higher diagnostic efficacy than the lower dose existing gold standard for the specific diagnostic task, and that critically it is likely to change the subsequent treatment outcome for the patient.

Therefore, the overarching focus of this thesis was optimisation of dose and diagnostic efficacy relating to dental CBCT imaging, using endodontics as a model, a discipline perceived to necessitate high resolution imaging protocols with consequent higher doses, to guarantee diagnostic accuracy. **Chapter 1** provided an overview and introduction of the subject matter relevant to the subsequent research studies presented in the thesis. **Chapter 2** investigated optimisation of dose for CBCT imaging of root canal anatomy using an *ex vivo* model of extracted teeth and related subjective to objective image quality so as to identify a threshold dose and the corresponding objective image quality for this diagnostic task. Following on from this, **Chapter 3** examined the relationship of a range of objective IQ metrics and determinants of IQ, with the diagnostic task of root canal anatomy identification, to establish the IQ metric(s) that have a statistically significant relationship with successfully achieving this diagnostic task, so as to facilitate optimisation procedures. **Chapter 4** explored the diagnostic efficacy of dental CBCT imaging relating to endodontics, specifically, utilizing 3D printed reproductions of extracted M1Ms with the study analysing if supplemental CBCT imaging can potentially improve outcome(s) after endodontic access cavity preparation in M1Ms, compared with the use of conventional (IOPA) and clinical methods alone.

Chapter 2 investigated the potential to identify a threshold dose for imaging of root canal anatomy and forms part of a growing body of optimisation studies in a wide

range of dental disciplines attempting to identify low dose protocols (YEUNG ET AL. 2019). Low-dose protocols can be established by identifying combinations of exposure factors that lower the patient dose without an unacceptable loss of image quality for diagnostic purposes. The current work is novel in that it was the first to highlight that reducing kV and mA, and selection of standard instead of high resolution modes were still compatible with successful identification of fine root canal anatomy, which is representative of the detail required in endodontic imaging. Furthermore, it also demonstrated that increasing dose as a means of enhancing visualisation of more complex canal anatomy was ineffective. Specifically, within the limitations of an *ex vivo* study, a threshold dose for this diagnostic task was identified as less than 210mGy cm² for both CBCT systems used. This threshold dose is lower than the recently published National Diagnostic Reference Level (NDRL) for adult CBCT in the UK and Ireland (265mGy cm² - based on maxillary molar preoperative implant assessment: PHE 2019, HIQA 2021) and over 50% lower than the Finnish NDRL (550 mGy cm² - specifically for CBCT examination aimed at assessment of tooth's periapical region and root canal morphology: STUK 2016) and Swiss NDRL (639 mGy cm² - endodontic indication: DELEU ET AL. 2020).

Low dose protocols are pivotal in facilitating optimisation and from recent reviews on this subject, are generally achieved in dental CBCT imaging (DA SILVA MOURA ET AL. 2018, YEUNG ET AL. 2019) by manually reducing, tube voltage (kV), tube current (mA), exposure time (seconds), resolution, rotation arc, increasing voxel size and additionally by the selection of low dose modes (e.g. reducing tube current and exposure time with the aid of noise reduction filters) depending on the CBCT system. Notably, low dose protocols have not commonly focused on varying tube voltage, this being attributed to the fact that alteration of tube voltage has a larger impact on image quality than a change in tube current (PAUWELS ET AL 2014b, PAUWELS ET AL. 2017). The reduced focus on tube potential may perhaps also be related to the fact that there is a significant but weak correlation between kerma-area product per unit area of FOV area and tube potential, whereas patient dose is mostly dependent on FOV size and tube current - exposure time product (PAUWELS ET AL. 2017, BEGANOVIĆ ET AL. 2020, VAN ACKERMAN ET AL. 2020). Thus, in terms of protocols, a reduction of tube current - exposure time product appears more effective than a tube voltage reduction. More recent prescriptive suggestions in

paediatric imaging have focused on identifying an optimal tube voltage (noise and artefacts minimised) at a given dose then reducing tube current-exposure time product to the lowest acceptable level for that specific indication (BRASIL ET AL. 2018, PANMEKIATE ET AL. 2018).

Therefore logic dictates that reduction of effective dose can be achieved with a reduced FOV height and diameter (HORNER ET AL. 2013, BORNSTEIN ET AL. 2014) and by ensuring protocols are specific to the patient type/size/gender and the diagnostic task (PAUWELS ET AL 2017, OENNING ET AL. 2018). Additionally, the use of thyroid shields, applying specific criteria (PAUWELS ET AL. 2019, www.bir.org.uk/patientshielding) and additional copper filtration (KURAMOTO ET AL. 2021) have been demonstrated to play a role in reducing dose. Furthermore, optimisation of patient dose commences with the selection of a CBCT system with features that can best facilitate dose reduction and is applicable to the particular clinical practice. This step is more pertinent than ever with the rapidly expanding range of CBCT systems, exhibiting huge ranges in dose levels (inter - and intra -), with data on effective dose range available in only 40% of available devices (GAÊTA-ARAUJO ET AL. 2020). Establishment of a QA programme and collaboration between the physicist and clinicians, with sufficient training and expertise to uphold principles of justification and optimisation, while extracting the maximum clinical benefits from the acquired images, is essential (BROWN ET AL. 2014). Indeed, the impact of clinician CBCT training and competence were highlighted in this thesis, where it was demonstrated to have a significant impact on the diagnostic efficacy of observers in the diagnostic task of root canal identification (**Chapter 2**) and in the actual task of locating canals subsequent to CBCT interpretation (**Chapter 4**).

The principal limitation of the **Chapter 2** study, as with the majority of low dose protocols and dose reduction studies included in the current systematic reviews (DA SILVA MOURA ET AL. 2018, YEUNG ET AL. 2019), is that there has been no clinical validation of these protocols. *Ex vivo* studies, employing diverse methodologies and anthropomorphic phantoms, lack the effect of motion and often metal artefact and undoubtedly overestimate diagnostic accuracy. Whereas *in vivo* equivalent studies with their multiple combinations of variables are, for many reasons including standardisation and ethics, impossible to complete clinically. That said, studies comparing a standard

and low dose CT protocol on the same patient have been completed in a general medical setting (POLETTI ET AL. 2007, KUBO ET AL. 2016).

The emphasis on low dose protocols and optimisation strategies has been especially crucial due to the absence of automatic exposure control in the majority of CBCT systems and/or protocols (GAÊTA-ARAUJO ET AL. 2020). This finding was also highlighted by the recent EURADOS and IAEA survey (BEGANOVIĆ ET AL. 2020, SIISKONEN ET AL. 2021), which primarily identified the limited number of European countries that have established DRLs, an essential optimisation tool and requirement of the International and European Basic Safety Standards Directives. As previously discussed, these published DRLs vary considerably between countries, reflecting the existence of the exceedingly wide dose variation in dental and maxillofacial CBCT imaging. Overall, while presently several national and international organisations have published guidelines relating to appropriate use of CBCT (e.g. SEDENTEXCT, HPA, AAOMR, EADMFR, DIMITRA, ESE, EAO, AAP) and a protocol on quality control exists (DE LAS HERAS GALA. 2017), there is a deficiency of specific guidelines emanating from respective dental disciplines on the use of low-dose protocols (YEUNG ET AL. 2019), paediatric dentistry (OENNING ET AL. 2018) perhaps being the exception.

While it is apparent that there is still much to achieve in the optimisation of dental and maxillofacial CBCT imaging, ongoing technological advances in CT and, by inference in CBCT, could potentially facilitate optimisation further by taking it 'out of the hands' of the operator. Tube current modulation is one such development and is currently used in CT scanners. It modulates the tube current to compensate for the changes in average projection-based attenuation of the patient as they are being imaged, maintaining a relatively constant signal to noise ratio, thereby avoiding excessive dose while maintaining image quality (KALRA ET AL. 2004). Beam shaping filters serve to pre-filter the peripheral part of the X-ray beam which is less attenuated than the central part of the beam; it thereby functions to equalise the signal at the detector and reduces peripheral radiation exposure and dose to the patient, while improving image quality through a reduction in scatter from the peripheral anatomy (ZHANG ET AL. 2013). Artificial intelligence (AI) in CT has been shown to have the potential to reduce image noise, achieved using a convolutional-neural-network-based denoising algorithm, such that the radiation dose applied to the patient can be reduced during

data acquisition (MCCULLOUGH & LENG 2020). Additionally, AI methods to reduce metal artefacts are also anticipated. That said, caution is advised, as there are challenges to overcome, such as its lack of generalisability to other CT models. AI networks are trained using specific datasets, representing specific image characteristics particular to that scanner, and typically are not compatible with acquisition or reconstruction parameters of a different device. Furthermore, there is the quandary as to how to evaluate the performance and consistency of an algorithm that is continually learning from the processed clinical information (MCCULLOUGH & LENG 2020). Photon-counting detectors are also a promising technology in CT which enables detection of individual x-ray photons and measurement of their energy. It provides the potential to overcome the limitations of current CT detectors, by providing CT data at very high spatial resolution, without electronic noise and with inherent spectral information. Furthermore, photon-counting CT offers additional advantages, such as perfect temporal and spatial alignment to avoid motion artefacts (WILLEMINK ET AL. 2018, FLOHR ET AL. 2020).

Although, the merging of the subjective clinical evaluation of image quality with objective parameters has proved complex, it continues to be a core optimisation strategy (CHOI ET AL. 2015, PAUWELS ET AL 2015b, BRASIL ET AL. 2019). An additional key finding in **Chapter 2** was that CNR was a relevant IQ metric for the subjective task of root canal identification. Threshold CNR values were identified, above which the diagnostic task was consistently achieved. However, while canal identification improved as CNR increased for both CBCT systems, the markedly different threshold CNR values identified for the two devices unfortunately suggested that it is not possible to determine a single threshold level of objective image quality that could be universally applicable to other CBCT models.

From an optimisation perspective it is valuable to establish the relationship between IQ metrics, exposure parameters and other determining factors, with a specific diagnostic task, in order to prioritise those proven to be significant, at an optimised dose. In **Chapter 3,** binary logistic regression identified CNR as the significant predictor of successfully achieving the diagnostic task of root canal identification when adjusting for the other evaluated core IQ metrics. Albeit, it may have been expected that a spatial resolution metric would have proved to have had a significant association with

endodontic imaging. However, when specifically investigating the relationship of IQ determinants with this diagnostic task (**Table 3.2**), native pixel array (compared to 2x2 array) was demonstrated to have a statistically significant effect on successfully achieving the task. That said, it is difficult to extricate the effects of this setting from that of the accompanying increased time and basis images that forms part of this selection. Considering, other IQ determinants; higher tube voltage, tube current and rotation angle (above study baseline) significantly increased the odds of achieving the diagnostic task. This finding would not be unexpected as CNR is dictated by noise and hence dose, whereas spatial resolution metrics are dictated by other factors (e.g. voxel size, reconstruction kernel) and do not show a consistent relationship with dose. Logistic regression also confirmed that the odds of successful achievement of the diagnostic task was greater for experienced senior observers than junior observers.

This **Chapter 3** study further supports the strategy in **Chapter 2** and the potential clinically for identifying the exposure protocols that can achieve a threshold CNR level at the minimum patient dose. It is clear that there is some inter-dependence between these different IQ metrics, with noise being a principal determinant of contrast resolution and hence CNR, and also impacting to a lesser extent on spatial resolution. While IQ parameters allow objective measurements, the underlying determinants of IQ consist of a multiplicity of factors in the imaging chain (**Table 3.2**). In reality, identification or quantification of machine specifications cannot provide a complete insight or understanding into the level of image quality attained by a given CBCT model, as they are also determined by unspecified manufacturer customizations. While **Chapter 3** provided an insightful exploration of all identifiable factors that influence image quality for a particular diagnostic task, it could have been more discerning had a wider range of machines that could facilitate a clearer isolation of imaging variables that varied exclusively with machine in this study. Additionally, imaging a wider variety of M1M anatomy would allow a more insightful assessment of the impact of a broad range of tooth anatomies on successful completion of the diagnostic task.

The efficacy of CBCT as a diagnostic imaging tool in identification of root canal anatomy - representing the fine detail required in endodontic imaging as the chosen model for this thesis - should be the basis on which this imaging modality is selected and justified for this diagnostic task. In other words, there should be evidence of the

benefit of this imaging modality to the patient, which can be described in a hierarchal fashion (FRYBACK & THORNBURY 1991). The literature reports that CBCT imaging can produce 3D fine detailed images that may improve diagnostic accuracy, depending on the diagnostic task (ROSEN ET AL. 2015), but this does not necessarily translate to improved diagnostic thinking, treatment planning or indeed patient outcome. With very few exceptions, the conclusions of multiple systematic reviews investigating the diagnostic efficacy of CBCT relating to a specific clinical context or diagnostic issue, is that there is insufficient research at the higher levels of diagnostic efficacy (HORNER ET AL. 2020) and this is particularly the case regarding patient outcome efficacy for endodontic imaging (ROSEN ET AL. 2022). What evidence there is, has to be critically assessed as to its methodological quality involving a thorough analysis of risk of bias (REITSMA ET AL. 2009) and the small number of existing endodontic outcome studies, have been identified as having high levels of bias (ROSEN ET AL. 2022). The practical and ethical challenges of carrying out clinical trials to assess patient outcome efficacy to a high methodological standard has been thoroughly highlighted and discussed in **Chapter 4** of this thesis.

The **Chapter 4** study assessed the impact of CBCT imaging on quantifiable outcomes associated with endodontic access cavity preparation in M1Ms using a human analogue and highlights that a pre-operative CBCT could potentially impact on patient outcome when compared with conventional and clinical methods alone. Specifically, the findings included reduced volume of tooth substance removal, which if contained in the critical PCD region of the tooth (SILVA ET AL. 2021), could potentially impact on endodontic outcome such as fracture resistance and tooth survival. Similarly, the finding of, increased efficacy of canal location, could impact on the outcome of tooth survival through absence of apical disease as a result of more thorough chemo-mechanical debridement. Notably, it was the experienced operators that could extract the clinical diagnostic information from the pre-operative CBCT to maximise the benefits of reduced tooth substance removal, increased canal location and reduced procedural time when compared with conventional and clinical methods alone. For all operators, visualising the MB2 canal in a CBCT dataset, increased confidence in the potential to locate the canals. However, for inexperienced operators, this increased confidence, did not result in a significantly increased canal location and for complex

anatomy actually caused a more destructive pursuit of the canal resulting in increased removal of tooth substance. Therefore, based on the results of this study, the use of CBCT imaging for location of MB2 canals cannot be justified for the inexperienced operator. The study was novel as it specifically investigates if the additional imaging information provided by a CBCT scan (without guides), can affect the volume removed during endodontic access in 3D printed M1Ms.

Of course, these findings should not be misconstrued as a means of routinely advocating a pre-operative CBCT for non-surgical endodontic treatment in upper M1Ms. In reality this non clinical study with simulated optimal conditions suggests that a well-planned clinical randomised control trial is warranted and justified to investigate if the increased radiation dose associated with CBCT can be justified for this diagnostic task.

5.2 FUTURE RESEARCH

Identification of a threshold dose for root canal imaging in **Chapter 2** considered only non-endodontically treated or *de novo* teeth. The impact of root canal treatment and direct/ indirect restorations on diagnostic efficacy for a range of diagnostic tasks has been has been well reported (SCHULZE ET AL. 2011, HELVACIOGLU-YIGIT ET AL. 2016, MA RH ET AL. 2016, TALIWAR ET AL .2016, KRUSE ET AL. 2017, CAMILLO ET AL. 2020). Accepting that the MB2 canal is the most frequently missed canal during root canal treatment (KARABUCAK ET AL. 2016, MASHYAKHY ET AL. 2021), it would be clinically relevant to investigate if artefacts generated from existing root canal filling materials would deteriorate image quality sufficiently to affect MB2 canal identification and to establish if the threshold dose identified in **Chapter 2** for root canal anatomy identification was still practicable. Specifically, in an *ex vivo* set-up it would be logical to investigate if there was a significant difference in canal identification in CBCT datasets between the same de novo teeth, endodontically treated teeth and subsequently (after a washout period) when the root filling material was removed to a consistent standard, for a range of dose protocols and voxel sizes and with or without artefact reducing algorithms. It is evident that for a range of diagnostic tasks, the impact of dose protocol, imaging parameters and artefact reducing algorithms on diagnostic efficacy in the presence of root canal

214

fillings has been reported with conflicting results. Specifically, in the presence of root canal filling materials and coronal restorations, selection of lower resolution protocols and artefact reduction during image acquisition resulted in a decrease of identified image artefacts (HELVACIOGLU-YIGIT ET AL. 2016). Conversely, other studies reported that selection of artefact reduction algorithms was accompanied by increased patterns of artefacts (VASCONCELOS ET AL. 2014), in addition to a decrease in diagnostic accuracy when imaging root filled teeth for the detection of root fracture (BECHARA ET AL. 2013). Regarding selection of a smaller voxel size and high resolution modes, a decrease in artefact associated with root canal fillings/sealers was identified (BRITO-JÚNIOR ET AL. 2014), whereas it has also been reported that the selection of differing CBCT resolution modes had no influence of the diagnosis of vertical root fracture (NEVES ET AL. 2014). It seems apparent that artefact expression in relation to root canal filling materials is particular to the CBCT system (MAZZI-CHAVES ET AL. 2020). However, a number of studies have reported consistently reduced beam - hardening artefact generation with an increased tube voltage (>90 kV), when considering different CBCT systems (ESMAEILI ET AL. 2012, DRAENERT ET AL. 2014, SCHULZE ET AL. 2010, HELVACIOGLU-YIGIT ET AL. 2016). Ultimately, an increased KV, smaller voxel size and higher resolution settings will all increase patient dose so it would be worthwhile to clarify the effects of these parameters on missed root canal anatomy detection, in the presence of root canal fillings. Furthermore, if the presence of root canal filling materials had a significant impact on canal location in the endodontically treated tooth, this type of study could identify if removal of the existing root filling material should be consistently recommended before CBCT imaging of endodontically treated teeth. One practical difficulty with such studies is preventing sealer leakage into the MB2 canal *ex vivo*, a phenomenon which occurs in extracted teeth rather than clinically where the MB2 canal is filled with pulpal or necrotic material.

Ultimately, robust well-designed clinical studies are still required to confirm the findings of low dose protocol *ex vivo* studies such as in **Chapter 2**, presenting considerable challenges of testing different exposure protocols. Following on from the approach completed in the general medical field for CT optimisation studies on the same patient (POLETTI ET AL. 2007, KUBO ET AL. 2016), a theoretical study design would be to compare the manufacturer recommended high resolution protocol for endodontic

imaging with a single pre-determined optimised protocol extracted from the **Chapter 2** study results, on the same patient for specific endodontic indications. The aim would be to identify and compare the sensitivity and specificity of the high resolution and optimised settings for a particular diagnostic task(s). While encouragingly, CT optimisation studies have shown comparable sensitivity and specificity between standard and low dose protocols, such a study is nonetheless ethically dubious and furthermore would present difficulties in recruitment. An additional issue is the issue of the reliability of the high resolution CBCT acting as the reference standard, as it was identified in Chapter 2 that even the highest resolution/doses, did not reveal all root canal anatomy present for complex cases. Ultimately, all findings of such studies would be machine specific. Accepting the difficulties of clinical optimisation studies, perhaps a practical and realistic alternative could be provided by the availability of a unified index or test object that could be agreed upon by manufacturers, medical physicists and endodontists and used to classify exposure settings particular to each device for a representative endodontic patient/scenario/pathology. Specifically, this could entail a universal 3D printed model of tooth, canal anatomy, surrounding bone using a material that replicates these anatomical densities while permitting replication of these fine canal structures. Additionally, such a model could be expanded, including root fracture and resorption lesions or range of anatomical structures and pathologies.

It was concluded previously that the findings of the **Chapter 4** clinical simulation study justified the execution of an *in vivo* equivalent. Such a study is fraught with real-world clinical, practical, ethical and fiscal difficulties, requiring a large sample size, strict sample inclusion criteria and a defined follow-up period. Such a clinical outcome study would most likely benefit from a multi-centre study with regard to power and allow inclusion of a range of variables such as differing populations and operators, interpretive variances and technical differences in CBCT scanner, all of which would improve generalizability. Strict inclusion criteria involving M1M restorative status would be essential. The vast majority of M1Ms requiring *de novo* non-surgical endodontic treatment would have an extra-coronal restoration and exclusion criteria would involve teeth where the PCD had been invaded (four mm above and below the CEJ) either by restoration or indeed caries. In order to verify this any existing restoration would need to be removed, prior to the pre-operative CBCT scan. Consistent

identification of the PCD region would necessitate strict calibration for the study coordinators. Certainly, any preliminary version of this clinical study would exclude root treated upper M1Ms teeth and those with fixed prosthodontic restorations to avoid impact of artefact on diagnosis (BRULLMAN & SCHULZE 2015). It is evident even in this simple 'walk through' of the study that a planned trial would involve significant resources, planning and ethical challenges.

Based on the existing study design, a pre- and post- operative CBCT would be necessary to accurately assess volume and site of removal of tooth substance. This would be a particular ethical challenge not least of all due to the fact that the pre-operative CBCT for one arm of the study is not used for the patient's potential clinical benefit. Certainly, the possibility of denying the potential diagnostic information from CBCT imaging to patients on a randomised basis would be an additional obstacle to achieving recruitment targets and informed consent. That said, pre - and post - operative CBCT imaging is used in studies assessing orthognathic surgery (PODČERNINA ET AL. 2020), orthodontics (ALHAMMADI ET AL. 2017), and in indirect pulp capping studies (HASHEM AT AL. 2015). In addition to an assessment of surrogate outcome measures; including the volume of tooth substance removed, procedural time and number of canals located (out of total canals identified as present on CBCT), a record of any alterations in diagnostic thinking could also be recorded for the arm of the study that received the pre-operative additional CBCT imaging, subsequent to interpretation and treatment planning with periapical radiographs. Furthermore, a follow up period of at least 4 years would be necessary to record outcome measures of success; tooth retention and resistance to fracture as the traditional one year would not be sufficient to adequately monitor tooth fracture. These studies are clearly logistically difficult, but time and costings aside, the repeated calls for more high level studies highlight that, surely the impetus should be to commit to such studies rather than committing extensive secondary research time identifying the need for them.

Outcome measures from the proposed randomised controlled trial described above could be assessed alongside cost to the patient: not only monetary and time, but also radiation dosage when comparing with periapical radiography in order to achieve an assessment of CBCT imaging at level 6: societal efficacy. Studies assessing efficacy at level 6 are not common in dentomaxillofacial imaging in general and particularly so

217

for CBCT due to the difficulties in correct selection and evaluation of the correct parameters for assessing outcome and economic factors (ROHLIN ET AL. 2020). The results generated in **Chapter 4** from the outcome efficacy study using a human analogue, indicate that a reduction in procedural time was evident for molar non-surgical root canal treatment. The potential clinical implications of a reduction of procedural time include greater convenience for both the clinician and patient, but also has economic implications. Time spent on a healthcare procedure is an important determinant of the economic cost (CHRISTELL ET AL 2012, WALTER ET AL. 2012). It could be argued that three to four minutes in a procedure taking perhaps 120 minutes of chairside time would be minimal, especially considering that viewing time of the scan was not included in this measured time and, of course, does not account for time taken for CBCT scan acquisition in a practice setting. However, it is possible that the availability of CBCT information might shorten subsequent stages of the endodontic procedure or perhaps the presence of a pre-operative CBCT may impact on cost effectiveness by changing the treatment plan completely (WALTER ET AL. 2012). Therefore, it would be of considerable interest to perform a thorough economic evaluation of the effect of using CBCT imaging in non-surgical endodontics compared with the use of periapical radiography, thereby potentially providing evidence at the highest level of Fryback and Thornbury's hierarchical model (FRYBACK & THORNBURY 1991). It is evident that an RCT, although the ideal study design to assess patient outcome, is often not practicable, alternatively, a 'before-after' study design could be used to assess outcome (ROHLIN ET AL. 2020), albeit it is accepted that this is a methodologically weaker study design (GUYATT ET AL. 1986, ROHLIN ET AL. 2020). For instance, in an institution/discipline which does not yet access CBCT imaging, a trial could be performed to measure suitable defined outcome parameters before introduction of CBCT imaging and these same outcomes assessed after introduction of CBCT imaging, including aspects of economic evaluation.

In summary, this thesis makes a novel contribution to the key areas of optimisation and diagnostic efficacy relating to CBCT, providing evidence of the potential to reduce dose in endodontic imaging and the potential for CBCT imaging to impact on outcome in the field of endodontics. It is evident that developments in optimisation can be driven by technology, research, DRLs and both provision and adherence to evidence based guidelines. However, as with establishing the true

diagnostic efficacy of CBCT related to a range of diagnostic tasks, progress is hampered by heterogeneous research which is often of low methodological quality, as well as the practical and ethical difficulty of performing clinical studies which are ultimately specific only to the machines used in the respective study.

Bibliography

ABOUEI E, LEE S, FORD NL: Quantitative performance characterization of image quality and radiation dose for a CS 9300 dental cone beam computed tomography machine. J Med Imaging 2(4):044002 (2015)

ABUABARA A, BARATTO-FILHO F, AGUIAR ANELE J, LEONARDI DP, SOUSA-NETO MD; Efficacy of clinical and radiological methods to identify second mesiobuccal canals in maxillary first molars. Acta Odontol Scand 71(1): 205-259 (2013)

ACAR B, KAMBUROĞLU K, TATAR I: Comparison of micro-computerized tomography and cone-beam computerized tomography in the detection of accessory canals in primary molars. Imaging Sci Dent 45(4):205-211 (2015)

ADISEN MZ, YILMAZ S, MISIRLIOGLU M, ATIL F: Evaluation of volumetric measurements on CBCT images using stafne bone cavities as an example. Med Oral Patol Oral Cir Bucal 20(5): e580-e586 (2015)

AHMAD IA, AL-JADAA A: Three root canals in the mesiobuccal root of maxillary molars: case reports and literature review. J Endod 40(12): 2087-2094 (2014)

AHN G, LEE JS, YUN WS, SHIM JH, LEE UL: Cleft alveolus reconstruction using a three-dimensional printed bioresorbable scaffold with human bone marrow cells. Journal of Craniofacial Surgery 29(7): 1880-1883 2018

ALAMRI HM, SADRAMELI M, ALSHALHOOB MA, SADRAMELI M, ALSHEHRI MA: Applications of CBCT in dental practice: a review of the literature. Gen Dent 60: 390-400 (2012)

ALAWAJI Y, MACDONALD DS, GIANNELIS G, FORD NL: Optimization of cone beam computed tomography image quality in implant dentistry. Clin Exp Dent Res 4:268–278 (2018)

AL-EKRISH AA: Effect of exposure time on the accuracy and reliability of cone beam computed tomography in the assessment of dental implant site dimensions in dry skulls. Saudi Dent J 24: 127-134 (2012)

ALHAMMADI MS, FAYED MS, LABIB A: Three-dimensional assessment of condylar position and joint spaces after maxillary first premolar extraction in skeletal Class II malocclusion. Orthod Craniofac Res 20(2): 71-78 (2017)

ALMUQRIN AH, TAMAM N, ABDELRAZIG A, ELNOUR A, SULIEMAN A: Organ dose and radiogenic risk in dental cone-beam computed tomography examinations. Radiat Phys Chem: 176108971 (2020)

ALLISON PD: Convergence failures in logistic regression. *SAS Global Forum* 360:1-11 (2008)

ALMEIDA A, ROMEIRO K., CASSIMIRO M: Micro-CT analysis of dentinal microcracks on root canals filled with a bioceramic sealer and retreated with reciprocating instruments. Sci Rep 10: 15264 (2020)

ALMUZIAN M, GHATAM HMA, AL-MUZIAN L: Assessing the validity of ITK-SNAP software package in measuring the volume of upper airway spaces secondary to rapid maxillary expansion. J Orthod Sci 15(7) 7 (2018)

AL NAJJARA, COLOSSI D, DAUER LT, PRINS R, PATCHELL G, BARNETS I, GOREN AD, FABER RD: Comparison of adult and child radiation equivalent doses from 2 dental cone-beam computed tomography units. Am J Orthod Dentofacial Orthop 143: 784-792 (2013)

AL-NUAIMI N, PATEL S, AUSTIN RS, MANNOCCI F: A prospective study assessing the effect of coronal tooth structure loss on the outcome of root canal retreatment. Int Endod J 50: 1143–1157 (2017)

AL-NUAIMI N, CIAPRYNA S, CHIA M, PATEL S, MANNOCCI F: A prospective study on the effect of coronal tooth structure loss on the 4-year clinical survival of root canal retreated teeth, and retrospective validation of the Dental Practicality Index. Int Endod J 53: 1040–1049 (2020)

AL-OKSHI A, THEODORAKOU C, LINDH C: Dose optimization for assessment of periodontal structures in cone beam CT examinations. Dentomaxillofac Radiol 46: 20160311 (2017)

AL-OKSHI A, HORNER K, ROHLIN M: A meta-review of effective doses in dental and maxillofacial cone beam CT using the ROBIS tool. Br J Radiol 94(1123): 20210042 (2021)

ALQERBAN A, JACOBS R, FIEUWS S, NACKAERTS O, WILLEMS G, & SEDENTEXCT PROJECT CONSORTIUM: A comparison of six cone beam computed tomography systems for image quality and detection of simulated canine impaction-induced external root resorption in maxillary lateral incisors. Am J Orthod Dentofacial Orthop 140 (3): 129-139 (2011)

AL-SALEHI SK, HORNER K: Impact of cone beam computed tomography (CBCT) on diagnostic thinking in endodontics of posterior teeth: A before-after study. J Dent 53: 57-63 (2016)

AMERICAN ASSOCIATION OF ENDODONTISTS; AMERICAN ACADEMY OF ORAL AND MAXILLOFACIAL RADIOLOGY: Use of cone-beam computed tomography in endodontics Joint Position Statement of the American Association of Endodontists and the American Academy of Oral and Maxillofacial Radiology 2015 Update. Oral Surg Oral Med Oral Pathol Oral Radiol 120(4): 508-512 (2015)

AMERICAN DENTAL ASSOCIATION COUNCIL ON SCIENTIFIC AFFAIRS: The use of cone-beam computed tomography in dentistry: an advisory statement from the American Dental Association Council on Scientific Affairs. J Am Dent Assoc 143(8): 899-902 (2012)

AMERICAN THYROID ASSOCIATION (ATA): Issues Policy Statement on Minimizing Radiation Exposure from Medical, Dental Diagnostics The use of cone-beam

computed tomography in dentistry: an advisory statement from the American Dental Association Council on Scientific Affairs. J Am Dent Assoc 143: 899-902 (2012)

AMINOSHARIAE A, KULILD JC, SYED A: Cone-beam computed tomography compared with intraoral radiographic lesions in endodontic outcome studies: a systematic review. J Endod 44: 1626–1631 (2018)

ANDERSON J, WEALLEANS J, RAY J. Endodontic applications of 3D printing. International endodontic journal 51(9): 1005-1018 (2018)

ANDREASEN JO, FARIK B, MUNKSGAARD EC: Long-term calcium hydroxide as a root canal dressing may increase risk of root fracture. Dent Traumatol 18(3): 134-137 (2002)

AQUILINO SA, CAPLAN DJ: Relationship between crown placement and the survival of endodontically treated teeth. J Pros Dent 87(3): 256-263 (2002)

ARAI Y, TAMMISALO E, IWAI K, HASHIMOTO K, SHINODA K: Development of a compact computed tomographic apparatus for dental use. Dentomaxillofac Radiol 28 (4) 245-248 (1999)

ARBEITGEMEINSCHAFT DER WISSENSCHAFTLICHEN MEDIZINISCHEN FACHGESELLSCHAFTEN (AWMF): s2k-Leitlinie Dentale digitale Volumentomographie Version Nr. 9 (2013)

AROLA D, IVANCIK J, MAJD H: Microstructure and mechanical behaviour of radicular and coronal dentin. Endod Topics 20: 30–51 (2012)

AROLA D, REPROGEL RK: Effects of aging on the mechanical behaviour of human dentin. Biomaterials 26: 4051–4061 (2005)

BABA R, UEDA K, OKABE M: Using a flat-panel detector in high resolution cone beam CT for dental imaging. Dentomaxillofac Radiol 33: 285-290 (2004)

BALASUNDARUM A, SHAH P, HOEN MM, WHEATER MA, BRINGAS JS, GARTNER A, GEIST JR: Comparison of cone-beam computed tomography and periapical radiography in predicting treatment decision for periapical lesions: a clinical study. Int J Dent Article ID 920815 (2012)

BAMBA J, ARAKI K, ENDO A, OKANO T: Image quality assessment of three cone beam CT machines using the SEDENTEXCT CT phantom. Dentomaxillofac Radiol 42: 20120445 (2013)

BARRET HH, MYERS KJ, HOESCHEN C, KUPINSKI MA, LITTLE MP: Task-based measures of image quality and their relation to radiation dose and patient risk. Phys Med Biol 60: R1–R75 (2015)

BAUMAN R, SCARFE W, CLARK S, MORELLI J, SCHEETZ J, FARMAN A: Ex vivo detection of mesiobuccal canals in maxillary molars using CBCT at four different isotropic voxel dimensions. Int Endod J 44: 752-758 (2011)

BECHARA BB, MOORE WS, MCMAHAN CA, NOUJEIM M: Metal artefact reduction with cone beam CT: an in vitro study. Dentomaxillofac Radiol 41: 248–253 (2012a)

BECHARA BB, MOORE WS, MCMAHAN CA, NOUJEIM M. Evaluation of a cone beam CT artefact reduction algorithm. Dentomaxillofac Radiol 41(5): 422–428 (2012b)

BECHARA B, MCMAHAN CA, MOORE WS, NOUJEIM M, GEHA H, TEIXEIRA FB: Contrast-to-noise ratio difference in small field of view cone beam computed tomography machines. J Oral Science 54 (3): 227-232 (2012c)

BECHARA G, MCMAHN A, NASSEH I, GEHA H, HAYEK E, KHAWAM G, M, NOUJEIM M: Number of basis images effect on detection of root fractures in endodontically treated teeth using a cone beam computed tomography machine: an in vitro study. Oral Surg Oral Med Oral Pathol Oral Radiol 115: 676-681 (2013)

BECHARA G, MCMAHAN CA, MOORE WS, NOUJEIM M, TEIXEIRA FB, GEHA H: Cone beam CT scans with and without artefact reduction in root fracture detection of endodontically treated teeth. Dentomaxillofac Radiol 42: 20120245 (2013)

BEGANOVIĆ A, CIRAJ-BJELAC O, DYAKOV I, GERSHAN V, KRALIK I, MILATOVIĆ A, ŠALÁT D, STEPANYAN K, VLADIMIROV A, VASSILEVA J: IAEA survey of dental cone beam computed tomography practice and related patient exposure in nine Central and Eastern European countries. Dentomaxillofac Radiol 49: 20190157 (2020)

BERG BI, GERTSCH A, ZEILHOFER HF, SCHWENZER-ZIMMERER K, BERG S, HASSFELD S, JURGENS P: Cone beam computed tomography and radiation dosage: application frequency and knowledge of dentists in Switzerland. Swiss Dent J 124(4): 419-433 (2014)

BERGENHOLTZ G, KVIST T: Evidence-based endodontics. Endod Topics 31(1): 3-18 (2014)

BETANCOURT P, NAVARRO P, MUÑOZ G, FUENTES R: Prevalence and location of the secondary mesiobuccal canal in 1,100 maxillary molars using cone beam computed tomography. BMC Med Imaging 16(1): 66 (2016)

BHUVA B, GIOVARRUSCIO M, RAHIM N, BITTER K, MANNOCCI F. The restoration of root filled teeth: a review of the clinical literature. Int Endod J 54(4): 509-535 (2021)

BITTER K, GRUNER D, WOLF O, SCHWENDICKE F: Artificial versus natural teeth for preclinical endodontic training: a randomized controlled trial. Journal of Endodontics 42: 1212–1217 (2016)

BJERKLIN K, ERICSON S: How a computerized tomography examination changed the treatment plans of 80 children with retained and ectopically positioned maxillary canines. Angle Orthod 76(1): 43-51 (2006)

BLATTNER TC, GEORGE N, LEE CC, KUMAR V, YELTON CD. Efficacy of cone-beam computed tomography as a modality to accurately identify the presence of second mesiobuccal canals in maxillary first and second molars: a pilot study. J Endod 36(5): 867–870 (2010)

BORISOVA R, INGILIZOVA C AND VASSILEVA J: Patient dosimetry in pediatric diagnostic radiology Radiat Prot Dosim 129: 155–159 (2008)

BORNSTEIN MM, SCARFE WC, VAUGHN VM, JACOBS R: Cone Beam Computed Tomography in Implant Dentistry: A Systematic Review Focusing on Guidelines, Indications, and Radiation Dose Risks. Oral Maxillofac Implants 29 (SUPPL): 55–77 (2014)

BOWERS DJ, GLICKMAN GN, SOLOMON ES, HE J. Magnification's effect on endodontic fine motor skills. J Endod 36(7): 1135-1138 (2010)

BRADY E, MANNOCCI F, BROWN J, WILSON R, PATEL S: A comparison of cone beam computed tomography and periapical radiography for the detection of vertical root fractures in non endodontically treated teeth. Int Endod J 47: 735–746 (2014)

BRAGATTO FP, IWAKI FILHO L, KASUYA AV, CHICARELLI M, QUEIROZ AF, TAKESHITA WM, IWAKI LC: Accuracy in the diagnosis of vertical root fractures, external root resorptions, and root perforations using cone-beam computed tomography with different voxel sizes of acquisition. J Conserv Dent 19(6): 573–577 (2016)

BRASIL DM, PAUWELS R, COUCKE W, HAITER-NETO F, JACOBS R: Image quality optimization of narrow detector dental computed tomography for paediatric patients. Dentomaxillofac Radiol 48(5): 20190032 (2019)

BRAUN X, RITTER L, JERVØE-STORM PM, FRENTZEN M: Diagnostic accuracy of CBCT for periodontal lesions. Clin Oral Investig 18: 1229-1236 (2014)

BRISEÑO-MARROQUÍN B, PAQUÉ F, MAIER K, WILLERHAUSEN B, WOLF TG: Root Canal Morphology and Configuration of 179 Maxillary First Molars by Means of Micro-Computed Tomography: An Ex Vivo Study. J Endod 41(12): 2008-2013 (2015)

BRITISH INSTITUTE OF RADIOLOGY: Guidance on using shielding on patients for diagnostic radiology applications. A joint report of the British Institute of Radiology (BIR), Institute of Physics and Engineering in Medicine (IPEM), Public Health England (PHE), Royal College of Radiologists (RCR), Society and College of Radiographers (SCoR) and the Society for Radiological Protection (SRP). (2020)

BRITO-JÚNIOR M, SANTOS LAN, FARIA-E-SILA A, PEREIRA RD, SOUSA-NETO MD: Ex vivo evaluation of artifacts mimicking fracture lines on cone-beam computed tomography produced by different root canal sealers Int Endod J 47(1): 26-31 (2014)

BROWN AA, SCARFE WC, SCHEETZ JP, SILVEIRA AM, FARMAN AG: Linear accuracy of cone beam CT derived 3D images. Angle Orthod 79: 150-157 (2009)

BROWN J, JACOBS R, LEVREING JAGHAGEN E, LINDH C, BAKSI G, SCHULZE D, SCHULZE R: Basic training requirements for the use of dental CBCT by dentists: a position paper prepared by the European Academy of DentoMaxilloFacial Radiology. Dentomaxillofac Radiol 43: 20130291 (2014)

BRÜLLMANN & D'HOEDT: The modulation transfer function and signal-to-noise ratio of different digital filters: a technical approach. Dentomaxillofac Radiol 40: 222-229 (2011)

BRÜLLMANN D & SCHULZE RK: Spatial resolution in CBCT machines for dental/maxillofacial applications-what do we know today? Dentomaxillofac Radiol 44(1): 20140204 (2015)

BUCHGREITZ J, BUCHGREITZ M, BJØRNDAL L: Guided root canal preparation using cone beam computed tomography and optical surface scans – an observational study of pulp space obliteration and drill path depth in 50 patients. Int Endod J 52(5): 559-568 (2019)

BUHRLEY LJ, BARROWS MJ, BEGOLE EA, WENCKUS CS: Effect of magnification on locating the MB2 canal in maxillary molars. J Endod 28: 324-327 (2002)

BUSHBERG JT, SEIBERT JA, LEIDHOLDT JR E: The Essential Physics of Medical Imaging. 4th ed. Lippincott Williams & Wilkins (LWW) 2020.

BYRANT JA, DRAGE NA, RICHMOND S: Study of the scan uniformity from an i-CAT cone beam computed tomography dental imaging system. Dentomaxillofac Radiol 37(7): 365-424 (2008)

CAMILO CC, BRITO-JÚNIOR M, FARIA-E-SILVA AL, QUINTINO AC, DE PAULA AF, CRUZ-FILHO AM, SOUSA-NETO MD: Case Report Artefacts in Cone Beam CT Mimicking an Extrapalatal Canal of Root-Filled Maxillary Molar Hindawi Publishing Corporation. Case Reports in Dentistry ID 797286 (2020)

CASSOLA VF, MILIAN FM, KRAMER R, DE OLIVEIRA LIRA CSA, KHOURY HJ: Standing adult human phantoms based on the 10th, 50th nd 90th mass and height percentiles of male and female Caucasian populations. Phys Md Biol 56: 3749-3772 (2011)

CHAN CP, TSENG SC, LIN CP, HUANG CC, TSAI TP, CHEN CC: Vertical root fracture in non-endontically treated teeth—A clinical report of 64 cases in chinese patients. J Endod 24(10): 678-681 (1998)

CHANG E, LAM E, SHAH P, AZARPAZHOOH A: Cone-beam computed tomography for detecting vertical root fractures in endodontically treated teeth: a systematic review. J Endod 42: 177–185 (2016)

CHANG SW, LEE J-K, LEE Y: In-depth morphological study of mesiobuccal root canal systems in maxillary first molars: review. Restor Dent Endod 38(1): 2-10 (2013)

CHOI E, FORD NL: Measuring absorbed dose for i-Cat CBCT examinations in child, adolescent and adult phantoms. Dentomaxillofac Radiol 44: 20150018 (2015)

CHOI JW, LEE SS, CHOI SC, H MS, H KH, YI WJ, KANG SR, HAN DH, KIM EK: Relationship between physical factors and subjective image quality of cone-beam computed tomography images according to diagnostic task. Oral Surg Oral Med Oral Pathol Oral Radiol 119(3): 357-365 (2015)

CHOI JW: Factors affecting modulation transfer function measurements in cone-beam computed tomographic images. Imaging Sci Dent 49: 131-137 (2019)

CHRISTELL H, BIRCH S, HEDESIU M, HORNER K, IVANAUSKAITÉ D, NACKAERTS O, ROHLIN M, LINDH C; SEDENTEXCT CONSORTIUM: Variation in costs of cone beam CT examinations among healthcare systems. Dentomaxillofac Radiol 41: 571–577 (2012)

CHRISTELL H, BIRCH S, BONDEMARK L, HORNER K, LINDH C; SEDENTEXCT CONSORTIUM. The impact of Cone Beam CT on financial costs and orthodontists' treatment decisions in the management of maxillary canines with eruption disturbance. Eur J Orthod 40(1): 65-73 (2018)

CHRISTIANSEN BA: Effect of micro-computed tomography voxel size and segmentation method on trabecular bone microstructure measures in mice. Bone Rep 5: 136-140 (2016)

CLARK D, KHADEMI j: Modern molar endodontic access and directed dentin conservation. Dent Clin North Am 54(2): 249-73 (2010)

CLÉ-OVEJERO A, SÁNCHEZ-TORRES A, CAMPS-FONT O, GAY-ESCODA C, FIGUEIREDO R, VALMASEDA-CASTELLÓN E: Does 3-dimensional imaging of the third molar reduce the risk of experiencing inferior alveolar nerve injury owing to extraction?: A meta-analysis. J Am Dent Assoc 148: 575–583 (2017)

COELHO MS, LACERDA MFLS, SILVA MHC, RIOS MA: Locating the second mesiobuccal canal in maxillary molars: challenges and solutions. Clin Cosmet Investig Dent 10: 195-202 (2018)

CONNERT T, REIN D, ELAYOUTI A, GODT A: Does CBCT help to reduce the amount of dentine removal during access cavity preparation? Int Endod J 47: 53 R13 Abstract (2014)

CONNERT T, ZEHNDER MS, WEIGER R: Microguided endodontics: accuracy of a miniaturized technique for apically extended access cavity preparation in anterior teeth. J Endod 43: 787–790 (2018)

CONNERT T, KRUG R, EGGMANN F, EMSERMANN I, ELAYOUTI A, WEIGER R, KÜHL S, KRASTL G: Guided Endodontics versus Conventional Access Cavity Preparation: A Comparative Study on Substance Loss Using 3-dimensional-printed Teeth. J Endod 45(3): 327-331 (2019)

COOK V, TIMOCK A, CROWE J, WANG M, COVELL D: Accuracy of alveolar bone measurements from cone beam computed tomography acquired using varying settings. Orthod Craniofacial Res 18: 127–136(2015)

CORBELLA S, DEL FABBRO M, TAMSE A, ROSEN E, TSESIS I, TASCHIERI S: Cone beam computed tomography for the diagnosis of vertical root fractures: a systematic review of the literature and meta-analysis. Oral Surg Oral Med Oral Pathol Oral Radiol 118: 593–602 (2014)

COSTA EDD, QUEIROZ PM, SANTAELLA GM, CAPELOZZA ALA, AMBROSANO GMB, FREITAS DQ. Influence of scan mode (partial/full rotations) and FOV size in the formation of artefacts in cone beam CT. Dentomaxillofac Radiol 48(4): 20180340 (2019)

CVEK M: Prognosis of luxated non-vital maxillary incisors treated with calcium hydroxide and filled with gutta-percha. A retrospective clinical study. Endod Dent Traumatol 8(2): 45-55 (1992)

DA SILVA MOURA W, CHIQUETO K, PITHON GM, NEVES LS, CASTRO R, HENRIQUES JFC: Factors influencing the effective dose associated with CBCT: a systematic review. Clin Oral Investig 23: 1319–1330 (2021)

DAVIES J, JOHNSON B, DRAGE NA: Effective doses from cone beam CT investigation of the jaws. Dentomaxillofac Radiol 41(1): 30–36 (2012)

DRAENERT F, COPPENRATH F, HERZOG P: Beam hardening artefacts occur in dental implant scans with the Newtom cone beam ct but not with the dental 4-row multidetector CT Dentomaxillofac Radiol 36: 198-203 (2007)

DE CHEVIGNY C, DAO TT, BASRANI BR, MARQUIS V, FARZANEH M, ABITBOL S, FRIEDMAN S Treatment outcome in endodontics: the Toronto study-phases 3 and 4: orthograde retreatment. 34(2): 131-137 (2008)

DE KINKELDER R, KALKMAN J, FABER DJ, SCHRAA O, KOK PH, VERBRAAK FD, VAN LEEUWEN TG: Heartbeat-induced axial motion artifacts in optical coherence tomography measurements of the retina. Invest Ophthalmol Vis Sci 52: 3908–3913 (2011)

DE LAS HERAS GALA H, TORRESIN A, DASU A, RAMPADO O, DELIS H, HERNÁNDEZ GIRÓN I, THEODORAKOU C, ANDERSSON J, HOLROYD J, NILSSON M, EDYVEAN S, GERSHAN V, HADID-BEURRIER L, HOOG C, DELPON G, SANCHO KOLSTER I, PETERLIN P, GARAYOA ROCA J, CAPRILE P, ZERVIDES C: Quality control in cone-beam computed tomography (CBCT) EFOMP-ESTRO-IAEA protocol (summary report). Physica Medica 3: 67–72 (2017)

DE MAN B, BASU S. Distance-driven projection and backprojection in three dimensions. Phys Med Biol 49: 2463–2475 (2004)

DE PAULA-SILVA FW, WU MK, LEONARDO MR, BEZERRA LA, WESSELINK PR: Accuracy of Periapical Radiography and Cone-Beam Computed Tomography Scans in Diagnosing Apical Periodontitis Using Histopathological Findings as a Gold Standard. J Endod 35: 1009-1012 (2009)

DE TOLEDO TELLES-ARAÚJO G, PERALTA-MAMANI M, CAMINHA RDG, DE FATIMA MORAES-DA-SILVA A, RUBIRA CMF, HONÓRIO HM, RUBIRA-BULLEN IRF: CBCT does not reduce neurosensory disturbances after third molar removal compared to panoramic radiography: a systematic review and meta-analysis. Clin Oral Investig 24(3): 1137-1149 (2020)

DE VOS W, CASSELMAN J, SWEENEN GR: Cone beam computerized tomography (CBCT) imaging of the oral and maxillofacial region: a systematic review of the literature. Dentomaxilofac Radiol 38: 609-625 (2009)

DI FILIPPO G, SIDHU S, CHONG B: Apical periodontitis and the technical quality of root canal treatment in an adult sub-population in London. Br Dent J 216: E22 (2014).

DÖLEKOĞLU S, FIŞEKÇIOĞLU E, IGÜY MI, IGÜ Y: The usage of digital radiography and cone beam computed tomography among Turkish dentists. DentomaxillofacRadiol 40: 379–384 (2011)

DOMARK JD, HATTON JF, BENISON RP, HILDEBOLT CF: An ex vivo comparison of digital radiography and cone-beam and micro computed tomography in the detection of the number of canals in the mesiobuccal roots of maxillary molars. J Endod 39(7): 901–905 (2013)

DONALDSON K, O'CONNOR S, HEATH N: Dental cone beam CT image quality possibly reduced by patient movement. *Dentomaxillofac Radiol* 42: 91866873 (2013)

DRAGE N, CARMICHAEL F, BROWN J: Radiation protection: protection of patients undergoing cone beam computed tomography examinations. Dent Update 37(8): 547-548 (2010)

DRAGO C, CARPENTIERI J: Treatment of maxillary jaws with dental implants: guidelines for treatment. J Prosthodont 20: 336-347 (2011)

DULA K, BENIC GI, BORNSTEIN M, DAGASSAN- BERNDT D, FILIPPI A, HICKLIN S, KISSLINGJEGER F, LUEBBERS H-T, SCULEAN A, SEQUEIRA- BYRON P, WALTER C, ZEHNDER M: SADMFR Guidelines for the Use of Cone-Beam Computed Tomography/ Digital Volume Tomography Endodontics, Periodontology, Reconstructive Dentistry, Pediatric Dentistry. A consensus workshop organized by the Swiss Association of Dentomaxillofacial Radiology. S Dent J 125: 945–953 (2015)

DUNCAN HF, NAGENDRABABU V, EL-KARIM I, DUMMER PMH: Outcome measures to assess the effectiveness of endodontic treatment for pulpitis and apical periodontitis for use in the development of European Society of Endodontology S3-level clinical practice guidelines: A consensus-based development. Int Endod J 54(12): 2184-2194 (2021)

DURACK C, PATEL S, DAVIES J, WILSON R, MANNOCCI F: Diagnostic accuracy of small volume cone beam computed tomography and intraoral periapical radiography for the detection of simulated external inflammatory root resorption. Int Endod J 44 (2): 136-147 (2011)

EE J, FAYD MI, JOHNSON BR: Comparison of endodontic diagnosis and treatment planning decisions using cone-beam volumetric tomography versus periapical radiography. J Endod 40(7): 910-916 (2014)

EL-HELALI R, DOWLING AH, MCGINLEY EL, DUNCAN HF, FLEMING AH: Influence of resin-based composite restoration technique and endodontic access on cuspal deflection and cervical microleakage scores. J Dent 41(3): 216-222 (2013)

EL KARIM IA, DUNCAN HF, CUSHLEY S, NAGENDRABABU V, KIRKEVANG LL, KRUSE C, CHONG BS, SHAH PK, LAPPIN M, MCLISTER C, LUNDY FT, CLARKE M. A protocol for the Development of Core Outcome Sets for Endodontic Treatment modalities (COSET): an international consensus process. Int Endod J 22(1): 812 (2021)

EL SAHILI N, DAVID-TCHOUDA S, THORET S, NASSEH I, BERBERI A, FORTIN T: Effect of milliamperage reduction on pre-surgical implant planning using cone beam computed tomography by surgeons of varying experience. J Maxillofac Oral Surg 17: 520–530 (2018)

ENGEL KJ, SPIES L, VOGTMEIER G, LUHTA R: Impact of CT detector pixel-to-pixel crosstalk on image quality. Physics of Medical Imaging 61422F (2006)

ESMAEILI F, JOHARI M, HADDADI P, VATANKHAH M: Beam hardening artifacts: comparison between two cone beam computed tomography scanners. J. Dent Res Dent Clin Dent Prospects 6(2): 49-53 (2012)

ESPOSITO S, CARDAROPOLI M, COTTI E: A suggested technique for the application of the cone beam computed tomography periapical index. Dentomaxillofac Radiol 40: 506-512 (2011)

EUROPEAN COMMISSION: Radiation Protection 1136. European Guidelines on Radiation Protection in Dental Radiology. Luxembourg: Office for official Publications of the European Communities (2004)

EUROPEAN COMMISSION: Radiation protection 172: Evidence based guidelines on cone beam CT for dental and maxillofacial radiology. Luxembourg: Office for Official publications of the European Communities (2012)

EUROPEAN SOCIETY OF ENDODONTOLOGY: Quality guidelines for endodontic treatment: consensus report of the European Society of Endodontology. Int Endod J 39(12): 921-930 (2006)

EUROPEAN SOCIETY OF ENDODONTOLOGY (ESE): PATEL S, BROWN J, SEMPER M, ABELLA F, MANNOCCI F: ESE position statement: Use of cone beam computed tomography in Endodontics: developed by. Int Endod J 52(12): 1675-1678 (2019)

EZELDEEN M, STRATIS A, COUCKE W, CODARI M, POLITIS, JACOBS R: As Low Dose as Sufficient Quality: Optimization of Cone-beam Computed Tomographic Scanning Protocol for Tooth Autotransplantation Planning and Follow-up in Children. J Endod 43: 210-217 (2017)

FACULTY OF GENERAL DENTAL PRACTICE (UK). In: HORNER K, EATON KA, eds. Selection criteria for dental radiography. 3rd edn (updated). London, UK: Faculty of General Dental Practice (UK) Royal College of Surgeons of Surgeons of England (2018)

FLOHR T, PETERSILKA M, HENNING A, ULZHEIMER S, FERDA J, SCHMIDT B: Photon-counting CT review. Phys Med 79: 126-136 (2020)

FRYBACK DG, THORNBURY JR: The efficacy of diagnostic imaging. Med Decis Making 11(2): 88-94 (1991)

GAÊTA-ARAUJO H, ALZOUBI T, VASCONCELOS KDF, ORHAN K, PAUWELS R, CASSELMAN JW, JACOBS R. Cone beam computed tomography in dentomaxillofacial radiology: a two decade overview. Dentomaxillofac Radiol 49: 20200145 (2020)

GALIBOURG A, DUMONCEL J, TELMON N, CALVET A, MICHETTI J, MARET D: Assessment of automatic segmentation of teeth using a watershed-based method. Dentomaxillofac Radiol 47(1): 20170220 (2020)

GHAEMINIA H, MEIJER GJ, SOEHARDI A, BORSTLAP WA, MULDER J, BERGE SJ: Position of the impacted third molar in relation to the mandibular canal. Diagnostic accuracy of cone beam computed tomography compared with panoramic radiography. Int J Oral Maxillofac Surg 38: 964-971 (2009)

GHAEMINIA H, MEIJER GJ, SOEHARDI A, BORSTLAP WA, MULDER J, VLIJMEN OJC: The use of cone beam CT for the removal of wisdom teeth changes the surgical approach compared with panoramic radiography: a pilot study. Int J Oral Maxillofac Surg 40: 834–839 (2011)

GHAEMINIA H, GERLACH NL, HOPPENREIIS TH JM, KICKEN M, DINGS JP, BORSTLAP WA, DE HAAN T, BERGÉ SJ, MEIJER GJ, MAAL TJ: Clinical relevance of cone beam computed tomography in mandibular third molar removal: A multicentre, randomised, controlled trial. J Craniomaxillofac Surg 43(10): 2158–2167 (2015)

GLUSKIN AH, PETERS CI, PETERS OA: Minimally invasive endodontics: challenging prevailing paradigms BDJ 216(6): 347 (2014)

GOLDMAN LW: Principles of CT: radiation dose and image quality. Journal Nucl Med Tech 35(4): 213–225 (2007)

GOMES AF, BRASIL DM, SILVA AIV: Accuracy of ITK-SNAP software for 3D analysis of a non-regular topography structure. *Oral Radiol* 36: 183–189 (2020)

GÖRDUYSUS MO, GÖRDUYSUS M, FRIEDMAN S. Operating microscope improves negotiation of second mesiobuccal canals in maxillary molars. J Endod 27: 683–686 (2001)

GOULSTON R, DAVIES J, HORNERK, MURPHY F: Dose optimization by altering the operating potential and tube current exposure time product in dental cone beam CT: a systematic review. Dentomaxilofac Radiol 45: 20150254 (2016)

GRANADOS JM, RIFAEY H, SAFAVI K, TADINADA A, CHAN IP: Conservative Endodontic Access – Cone Beam Computed Tomography (CBCT)-Guided Preparation and its Impact on Endodontic Referrals. Master's Theses. 1105. https://opencommons.uconn.edu/gs_theses/1105

GUERRERO ME, BOTETANO R, BELTRAN J, HORNER K, JACOBS R: Can preoperative imaging help to predict postoperative outcome after wisdom tooth removal? A randomized controlled trial using panoramic radiography versus cone beam CT. Clin Oral Invest 18 (1): 335-342 (2014a)

GUERRERO ME, NOIEGA J, CASTRO C, JACOBS R: Does cone-beam CT alter treatment plans? Comparison of preoperative implant planning using panoramic versus cone-beam CT images. Imaging Sci Dent 44: 121-128 (2014b)

GUO J, VAHIDNIA A, SEDGHIZADEH P, ENCISO R: Evaluation of Root and Canal Morphology of Maxillary Permanent First Molars in a North American Population by Cone-beam Computed Tomography. J Endod 40(5): 635-639 (2014)

GUO XL, LI G, ZHENG JQ, MA RH, LIU FC, YUAN FS: Accuracy of detecting vertical root fractures in non-root filled teeth using cone beam computed tomography: effect of voxel size and fracture width. Int Endod J 52: 887–898 (2019)

GUYATT GH, TUGWELL PX, FEENY DH, DRUMMOND MF, HAYNES RB: The role of before-after studies of therapeutic impact in the evaluation of diagnostic technologies. Journal Chronic Dis 39(4): 295-304 (1986)

HALL EJ, BRENNER DJ: Cancer risks from diagnostic radiology. Br J Radiol 81: 362-378 (2008)

HANEY E, GANSKY SA, LEE JS, JOHNSON E, MAKI K, MILLER AJ, HUANG JC: Comparative analysis of traditional radiographs and cone-beam computed tomography volumetric images in the diagnosis and treatment planning of maxillary impacted canines. Am J Orthod Dentofacial Orthop 137 (5): 590-597 (2010)

HARRIS D, HORNER K, GRÖNDAHL K, JACOBS R, HELMROT E, BENIC GI, BORNSTEIN MM, DAWOOD A, QUIRYNEN M. E.A.O. guidelines for the use of diagnostic imaging in implant dentistry 2011. A consensus workshop organized by the European Association for Osseointegration at the Medical University of Warsaw. Clin Oral Implants Res 23(11): 1243-1253 (2012)

HASHEM D, BROWN JE, PATEL S, MANNOCCI F, DONALDSON AN, WATSON T, BANERJEE A: An In Vitro Comparison of the Accuracy of Measurements Obtained from High- and Low-resolution Cone-beam Computed Tomography Scans. J Endod 39: 394-397 (2013)

HATCHER DC: Operational principles for cone-beam computed tomography. J Am Dent Assoc 141 Suppl 3: 3S-6S (2010)

HEALTH PROTECTION AGENCY: Guidance on the safe use of dental cone beam CT (Computed Tomography) Equipment. HPA-CRCE-010. Chilton: Health Protection Agency (2010)

HELLÉN-HALME K, LITH A: Effect of ambient light level at the monitor surface on digital radiographic evaluation of approximal carious lesions: an in vitro study. Dentomaxillofac Radiol 41(3): 192-196 (2012)

HELVACIOGLU-YIGIT D, DEMIRTURK KOCASARAC H, BECHARA B, NOUJEIM M: Evaluation and Reduction of Artifacts Generated by 4 Different Root-end Filling Materials by Using Multiple Cone-beam Computed Tomography Imaging Settings. J Endod 42(2): 307-14 (2016)

HIDALGO RIVAS JA, DAVIES J, HORNER K, THEODORAKOU C: Effectiveness of thyroid gland shielding in dental CBCT using a paediatric anthropomorphic phantom. Dentomaxillofac Radiol 44(3): 20140285 (2015)

HIDALGO RIVAS JA, HORNER K, THIRUVENKATACHARI B, DAVIES J, THEODORAKUOU C: Development of a low-dose protocol for cone beam CT examination of the anterior maxilla in children. Br J Radiol 88: 20150559 (2015)

HIEBERT B M, ABRAMOVITCH K, RICE D, TORABINEJAD M: Prevalence of Second Mesiobuccal Canals in Maxillary First Molars Detected Using Cone-beam Computed Tomography, Direct Occlusal Access, and Coronal Plane Grinding. Int Endod J 43(10): 1711-1715 (2017)

HILES P, GILLIGAN P, DAMILAKIS J, BRIERS E, CANDELA-JUAN C, FAJ D, FOLEY S, FRIJA G, GRANATA C, DE LAS HERAS GALA H, PAUWELS R, SANS MERCE M, SIMANTIRAKIS G, VANO E: European consensus on patient contact shielding. Phys Med 96: 198-203 (2022)

HEALTH INFORMATION AND QUALITY AUTHORITY, HIQA: Guidance on the establishment, use and review of diagnostic reference levels for medical exposure to ionising radiation. https://www.hiqa.ie/reports-and-publications/guide/guidance-establishment-use-and-review-diagnostic-reference-levels (2021)

HIRSCH E, WOLF U, HEINICKE F, SILVA MA: Dosimetry of the cone beam computed tomography Veraviewepocs 3D compared with the 3D Accuitomo in different fields of view. Dentomaxillofac Radiol 37(5): 268-273 (2008)

HOL C, HELLÉN-HALME K, TORGERSEN G, NILSSON M, MØYSTAD A: How do dentists use CBCT in dental clinics? A Norwegian nationwide survey, Acta Odontologica Scandinavica 73(3): 195-201 (2015)

HOLROYD JR, WALKER A: Recommendations for the design of X-ray facilities and quality assurance of dental cone Beam CT (computed tomography) system: Health Protection Agency HPA-RPD-065 (2010)

HORNER K, ISLAM M, FLYGARE L, TSIKLAKIS K, WHITES E: Basic principles for use of dental cone beam CT: consensus guidelines of the European Academy of Dental and Maxillofacial Radiology. Dentomaxillofac Radiol 38: 187-195 (2009)

HORNER K, JACOBS R, SCHULZE R: Dental CBCT equipment and performance issues. Radiat Prot Dosimetry 153(2): 212-218 (2013)

HORNER K, O'MALLEY L, TAYLOR, GLENNY A M: Guidelines for clinical use of CBCT: a review. Dentomaxillofac Radiol 44(1): 20140225 (2015)

HORNER K, BARRY S, DAVE M, DIXON C, LITTLEWOOD A, PANG CL, SENGUPTA A, SRINIVASAN V. DIAGNOSTIC EFFICACY OF CONE BEAM COMPUTED TOMOGRAPHY IN PAEDIATRIC DENTISTRY: A SYSTEMATIC REVIEW: Eur Arch Paediatr Dent 21(4): 407-426 (2020)

IKRAM GH, PATEL S, MANOCI F: Micro-computed tomography of tooth tissue volume changes following endodontic procedures and post space preparation. Int J Endod 42(12): 1071-1076 (2009)

INTERNATIONAL ATOMIC ENERGY AGENCY (IAEA): Radiation Protection in Dental Radiology, Safety Reports Series No. 108, IAEA, Vienna. STI/PUB/1972 ¦ 978-92-0-138421-8 (2022)

IRCP Publication 60. Recommendations of the International Commission on Radiological Protection. Annals of the IRCP: 21 (1990)

IRCP Publication 103. The 2007 Recommendations of the International Commission on Radiological Protection. Annals of the IRCP: 37 (2007)

ISHIDA Y, MIYASAKA T: Dimensional accuracy of dentalcasting patterns created by 3D printers. Dent Mater J 35(2): 250-256 (2016)

ISIDOR S, FAABORG-ANDERSEN M, HINTZE H, KIRKEVANG L, FRYDENBERG M, HAITER-NETO F, WENZEL A: Effect of monitor display on detection of approximal caries lesions in digital radiographs. Dentomaxillofac Radiol 38(8): 537-541 (2009)

KAFANTARI N, GULABIVALA K, GEORGIOU G, KNOWLES J, NG YL: Effect of Heated Sodium Hypochlorite on the Viscoelastic Properties of Dentin Evaluated Using Dynamic Mechanical Analysis. J Endod 45(9): 1155-1160 (2019)

JACOBS R, QUIRYNEN M, BORNSTEIN MM: Neurovascular disturbances after implant surgery. Periodontol 2000 66(1): 188-202 (2014)

JORDAN RE, ABRAMS L, KRAUS BS: Kraus dental anatomy and occlusion. 2nd Ed. St. Louis Mosby year book. (1992)

KAASALAINEN T, EKHOLM M, SIISKONEN T, KORTESNIEMI M: Dental cone beam CT: An updated review. Physica Medica 88: 193-217 (2021)

KABALIUK N, NEJATI A, LOCH C, SCHWASS D, CATER J, JERMY M: Strategies for Segmenting the Upper Airway in Cone-Beam Computed Tomography (CBCT) Data. Open J Med Imaging 7: 196-219 (2017)

KAFANTARI N, GULABIVALA K, GEORGIOU G, KNOWLES J, NG YL: Effect of Heated Sodium Hypochlorite on the Viscoelastic Properties of Dentin Evaluated Using Dynamic Mechanical Analysis. J Endod 45(9): 1155-1160 (2019)

KALENDER WA, BUCHENAU S, DEAK P, KELLERMEIER M, LANGNER O, VAN STRATEN M, VOLLMAR S, WILHARM S: Technical approaches to the optimization of CT. Phys Med 24(2): 71-79 (2008)

KALRA MK, MAHER MM, TOTH TL, SCHMIDT B, WESTERMAN BL, MORGAN HT, SAINI S. Techniques and applications of automatic tube current modulation for CT: Radiology 233(3): 649-657 (2004)

KALLIO-PULKKINEN S, HUUMONEN S, HAAPEA M, LIUKKONEN E, SIPOLA A, TERVONEN O, NIEMINEN MT: Effect of display type, DICOM calibration and room illuminance in bitewing radiographs. Dentomaxillofac Radiol 45(1): 20150129 (2015)

KAMBOROĞLU K, KURSUN S: A comparison of the diagnostic accuracy of CBCT images of different voxel resolutions used to detect simulated small internal resorption cavities. Int Endod J 43: 798-807 (2010)

KAMBUROGLU K, KOLSUZ E, MURAT S, EREN H, YÜKSEL S, PAKSOY C: Assessment of buccal marginal alveolar peri-implant and periodontal defects using a cone beam CT system with and without the application of metal artefact reduction mode. Dentomaxillofac Radiol 42: 20130176 (2013)

KARABUCAK B, BUNES A, CHEHOUD C, KOHLI R, SETZER F: Prevalence of apical periodontitis in endodontic premolars and molars with untreated canal: a cone-beam computed tomography study. J Endod 42: 538–541 (2016)

KATEBZADEH N, DALTON BC, TROPE M: Strengthening immature teeth during and after apexification. J Endod 24(4): 256-259 (1998)

KAYUGAWA A, OHKUBO M, WADA S. Accurate determination of ct point-spread-function with high precision. J Appl Clin Med Phys 14(4): 216-226 (2013)

KEHRWALD R, SAMPAIO DE CASTRO H, SALMERON S, MATHEUS RA, MACHADO G, SANTAELLA GM, QUEIROZ PM: Influence of Voxel Size on CBCT Images for Dental Implants Planning. Eur J Dent 16: 381-385 (2022)

KILJUNEN T, KAASAKAINEN T, SUOMALAINEN T, SUOMSLSINEN A, KORTESNIEMI M: Dental cone beam CT: A Review. Physica Medica 31(8): 844-860 (2015)

KIM I, PATEL M, HIRT S, KANTOR M: Clinical research and diagnostic efficacy studies in the oral and maxillofacial radiology literature: 1996–2005. Dentomaxillofac Radiol 40(5): 274-281 (2011)

KIM DS, RASHSURENO, KIM EK: Conversion coefficients for the estimation of effective dose in cone-beam CT. Imaging Sci Dent 44: 21-29 (2014)

KIM GB, LEE S, KIM H: Three-Dimensional Printing: Basic Principles and Applications in Medicine and Radiology. Korean J Radiol 17(2): 182-197 (2016)

KIM DH, CHA B, JIANG J, CHEN IP: Prevalence and Morphology of MB2 Canals in Maxillary Molars by Cone Beam Computed Tomography (CBCT) and Rate of Treatment in Endodontic Practice with Pre-operative CBCT Images. MRD 5(3): 000614 (2020)

KLINTSTRÖM E, SMEDBY O, KLINTSTRÖM B, BRISMAR TB, MORENO R: Trabecular bone histomorphometric measurements and contrast-to-noise ratio in CBCT. Dentomaxillofac Radiol 43: 20140196 (2014)

KNOTTNERUS JA, VAN WEEL C, MURIS JW: Evaluation of diagnostic procedures [published correction appears in BMJ 324(7335): 477-480 (2002)

KOIVISTOJ, KILJUNEN T, TAPIOVAARA M, WOLFF J, KORTESNIEMI M: Assessment of radiation exposure in dental cone-beam computerized tomography with the use of metal-oxide semiconductor field-effect transistor (MOSFET) dosimeters and Monte Carlo simulations. Oral Surg Oral Med Oral Pathol Oral Radiol 114: 393-400 (2012)

KRASTL G, ZEHNDER MS, CONNERT T: Guided Endodontics: a novel treatment
approach for teeth with pulp canal calcification and apical pathology. Dent Traumatol 32: 240–246 (2016)

KRUPINSKI EA, WILLIAMS MB, ANDRIOLE K, STRAUSS KJ, APPLEGATE K, WYATT M, BJORK S, SEIBERT JA: Digital radiography image quality: image processing and display. J Am Coll Radiol 4(6): 389-400 (2007)

KRUSE C, SPIN-NETO R, WENZEL A, KIRKEVANG LL: Cone beam computed tomography and periapical lesions: a systematic review analysing studies on diagnostic efficacy by a hierarchical model. Int Endod J 48(9): 815–828 (2015)

KRUSE C, SPIN-NETO R, REIBEL J, WENZEL A, KIRKEVANG LL: Diagnostic validity of periapical radiography and CBCT for assessing periapical lesions that persist after endodontic surgery. Dentomaxillofac Radiol 46: 20170210 (2017)

KRUSE C, SPIN-NETO R, WENZEL A, VAETH M, KIRKEVANG LL: Impact of cone beam computed tomography on periapical assessment and treatment planning five to eleven years after surgical endodontic retreatment. Int Endod J 51(7): 729-737 (2018)

KRUSE C, SPIN-NETO, R, EVAR KRAFT DC, VAETH M, KIRKEVANG LL: Diagnostic accuracy of cone beam computed tomography used for assessment of apical periodontitis: an ex vivo histopathological study on human cadavers. Int Endod J 52(4): 439-450 (2019)

KUBO T, OHNO Y, TAKENAKA D, NISHINO M, GAUTAM S, SUGIMURA K, KAUCZOR HU, HATABU H, ILEAD STUDY GROUP: Standard-dose vs. low-dose CT protocols in the evaluation of localized lung lesions: Capability for lesion characterization-iLEAD study. Eur J Radiol Open 24(3) 67-73 (2016)

KULILD J, PETERS D: Incidence and configuration of canal systems in the mesiobuccal root of maxillary first and second molars. J Endod 16: 311-317 (1990)

KURAMOTO T, TAKARABE S, SHIOTSUKI K, SHIBAYAMA Y, HAMASAKI H, AKAMINE H, OKAMURA K, CHIKUI T, KATO T, YOSHIURA K: X-ray dose reduction using additional copper filtration for dental cone beam CT. Phys Med 81: 302-307 (2021)

KURT SN, ÜSTÜN Y, ERDOGAN Ö, EVLICE B, YOLDAS O, ÖZTUNC H: Outcomes of periradicular surgery of maxillary first molars using a vestibular approach: A prospective, clinical study with one year follow up. J Oral Maxillofac Surg 72(6): 1049-1061 (2014)

KUSNOTO B, KAUR P, SALEM A, ZHANG Z, GALANG-BOQUIREN MT, VIANA G, EVANS CA, MANASSE R, MONAHAN R, BEGOLE E: Implementation of ultra-low-dose CBCT for routine 2D orthodontic diagnostic radiographs: Cephalometric landmark identification and image quality assessment. Semin Orthod 21: 233–247 (2015)

KWONG JC, PALOMO JM, LANDERS MA, FIGUEROA A, HANS MG: Image quality produced by different cone-beam computed tomography settings. Am J Orthod Dentofacial Orthop, 133 (2), 317-327 (2008)

KYRIACOU Y, KOLDITZ D, LANGNER O, KRAUSE J, KALENDER W: Digital Volume Tomography (DVT) and Multislice Spiral CT (MSCT): An Objective Examination of Dose and Image Quality. Fortschr Röntgenstr 183: 144–153 (2011)

LANG H, KORKMAZ Y, SCHNEIDER K, RAAB W H: Impact of endodontic treatments on the rigidity of the root. J Dent Res 85: 364–368 (2006)

LARSSON JP, PERSLIDEN J, SANDBORG M, CARLSSON GA: Transmission ionization chambers for measurements of air collision kerma integrated over beam area. Factors limiting the accuracy of calibration. Phys Med Biol 41: 2831-2398 (1996)

LEE SJ, LEE EH, PARK SH, CHO KM, KIM JW: A cone-beam computed tomography study of the prevalence and location of the second mesiobuccal root canal in maxillary molars. Restor Dent Endod 45(4): e46 (2020)

LERTCHIRAKARN V, PALAMARA JE, MESSER HH: Patterns of vertical root fracture: factors affecting stress distribution in the root canal. J Endod 29: 523– 528 (2003)

LENNON S, PATEL S, FOSCHI F, WILSON R, DAVIES J, MANNOCCI F: Diagnostic accuracy of limited-volume cone-beam computed tomography in the detection of periapical bone loss: 360° scans versus 180° scans. Int Endod J 44(12): 11181127 (2011)

LI X, SAMEI E, SEGARS WP, STURGEON GM, COLSHER JG, TONCHEYA G, YOSHIZUMI TT, FRUSH DP: Patient-specific radiation dose and cancer risk estimation in CT: part 11. application to patients. Med Phys 38(1): 408-419 (2011)

LIANG X, LIAO W, CAI H, JIANG S, CHEN S: 3D-Printed Artificial Teeth: Accuracy and Application in Root Canal Therapy. J Biomed Nanotechnol 14(8): 1477-1485 (2018)

LIEDKE GS, DA SILVEIRA HE, DA SILVEIRA HL, DUTRA V, DE FIGUEIREDO JA: Influence of voxel size in the diagnostic ability of cone beam tomography to evaluate simulated external root resorption. J Endod 35(2): 233-235 (2009

LIN F, ORDINOLA-ZAPATA R, FOK ASL, LEE R. Influence of minimally invasive endodontic access cavities and bonding status of resin composites on the mechanical property of endodontically-treated teeth: A finite element study. Dent Mater 38(2): 242-250 (2022)

LOFTHAG-HANSEN S, THILANDER-MANG A, EKESTUBBE A, HELMROT E, GRONDAHL K: Calculating effective dose on a cone beam computed tomography device: 3D Accuitomo and 3D Accuitomo FPD. Dentomaxillofac Radiol 37(2): 72-79 (2008)

LOFTHAG-HANSEN S: Cone beam computed tomography radiation dose and image quality assessments. Swed Dent J Suppl 209: 4 –55 (2010)

LOFTHAG-HANSEN S, THILANDER-KING A, GRÖNDAHL K: Evaluation of subjective image quality in relation to diagnostic task for cone beam computed tomography with different fields of view. Eur J Radiol 80: 483-488 (2011)

LO GIUDICE A , RONSIVALLE V, GRIPPAUDO C, LUCCHESE A, , MURAGLIE S, LAGRAVÈRE MO, ISOLA G: One Step before 3D Printing—Evaluation of Imaging Software Accuracy for 3-Dimensional Analysis of the Mandible: A Comparative Study Using a Surface-to-Surface Matching Technique. Materials 13(12): 2798 (2020)

LOUBELE M, MAES F, JACOBS R, VAN STEENBERGHE D, WHITE SC, SUETENS P: Comparative study of image quality for MSCT and CBCT scanners for dentomaxillofacial radiology applications. Radiat Prot Dosimetry 129(1-3): 222–226 (2008)

LOUBELE M, BOGAERTS R, VAN DIJCK E, PAUWELS R, VANHEUSDEN S, SUETENS P, MARCHAL G, SANDERINK G, JACOBS R: Comparison between effective radiation dose of CBCT and MSCT scanners for dentomaxillofacial applications. Eur J Radiol 71: 461-468 (2009)

LOW JF, DOM TNM, BAHARIN SA: Magnification in endodontics: A review of its application and acceptance among dental practitioners. Eur J Dent 12(4): 610-616 (2018)

LUCKOW M, DEYHLE H, BECKMANN F, DAGASSAN-BERNDT, MÜLLER B: Tilting the jaw to improve the image quality or to reduce the dose in cone-beam computed tomography. Eur J Radiol 80(3): e389-e393 (2011)

LUDLOW JB, DAVIES-LUDLOW LE, BROOKS SL, HOWERTON WB: Dosimetry of 3 CBCT idevices for oral and maxillofacial radiology: CB Mercurary, NewTom 3 G and i-Cat. Dentomaxillofac Radiol 35: 219-226 (2006)

LUDLOW JB, DAVIES-LUDLOW LE, WHITE SC: Patient risk related to common dental radiographic examinations: the impact of 2007 International Commission on Radiological Protection recommendations regarding dose calculation. J Am Dent Assoc 139: 1237-1243 (2008)

LUDLOW JB, IVANOVIC M: Comparative dosimetry of dental CBCT devices and 64-slice CT for oral and maxillofacial radiology. Oral Surg Oral Med Oral Pathol Oral Radiol Endod 106(1): 106-114 (2008)

LUDLOW JB: Dose and risk in dental diagnostic imaging with emphasis on dosimetry of CBCT. Korean J Oral Maxillofac Radiol 39: 175-184 (2009)

LUDLOW JB: A manufacturer's role in reducing the dose of cone beam computed tomography examinations: effect of beam filtration. Dentomaxillofac Radiol 40: 115-122 (2011)

LUDLOW JB, WALKER C: Assessment of phantom dosimetry and image quality of i-CAT FLX cone-beam computed tomography. Am J Orthod Dentofacial Orthop_144(6): 802-817 (2013)

LUDLOW JB, TIMOTHY R, WALKER C, HUNTER R, BENAVIDES E, SAMUELSON B, SCHESKE J: Effective dose of dental CBCT—a meta-analysis of published data and additional data for nine CBCT units. Dentomaxillofac Radiol 44: 20140197 (2015)

MA RH, GE ZP, LI G: Detection accuracy of root fractures in cone-beam computed tomography images: a systematic review and meta-analysis. Int Endod J 49: 646–54 (2016)

MAGNI E, JÄGGI M, EGGMANN F, WEIGER R, CONNERT T: Apical pressures generated by several canal irrigation methods: A laboratory study in a maxillary central incisor with an open apex. Int Endod J 54(10): 1937-1947 (2021)

MAH E, RITENOUR ER, YAO H. A review of dental cone-beam CT dose conversion coefficients. Dentomaxillofac Radiol 50(3):20200225 (2021)

MALOUL A, FIALKOV J, WHYNE C: The impact of voxel size-based inaccuracies on the mechanical behavior of thin bone structures. Ann Biomed Eng 39: 1092-1100 (2011)

MÅNSSON LG. METHODS FOR THE EVALUATION OF IMAGE QUALITY: A REVIEW. Radiat Prot Dosimetry 90(1-2): 89-99 (2000)

MARCU M, HEDESIU M, SALMON B, PAUWELS R, STRATIS A, OENNING ACC, COHEN ME, JACOBS R, BACIUT M, ROMAN R, DINU C, ROTARU H, BARBUR I; DIMITRA RESEARCH GROUP : Estimation of the radiation dose for pediatric CBCT indications: a prospective study on ProMax3D. Int J Paediatr Dent 28(3): 300–9 (2018)

MARET D, TELMON, PETERS OA, LEPAGE B, TREIL J, INGLÈSE JM, PEYRE A, KAHN JL, SIXOU M: Effect of voxel size on the accuracy of 3D reconstructions with cone beam CT. Dentomaxillofac Radiol 41(8): 649–655 (2012)

MARINE PM, STABIN MG, FERNALD MJ, BRILL AB: Changes in radiation dose with variations in human anatomy: larger and smaller normal-stature adults. J Nucl Med 51: 806–811 (2010)

MARSHALL G, SYKES AE: Systematic reviews: a guide for radiographers and other healthcare professionals. Radiography 17: 158-164 (2011)

MARTIN CJ, SHARP PF, SUTTON DG. Measurement of image quality in diagnostic radiology. Appl Radiat Isot 50: 21–38 (1999)

MARTINS JNR, MARQUES D, SILVA EJNL, CARAMÊS J, VERSIANI MA: Prevalence Studies on Root Canal Anatomy Using Cone-beam Computed Tomographic Imaging: A Systematic Review. J Endod 45: 372-386 (2019)

MASHYAKHY M, HADI FA, ALHAZMI HA, ALFAIFI RA, ALABSI FS, BAJAWI H, ALKAHTANY M, ABUMELHA A: Prevalence of Missed Canals and Their Association with Apical Periodontitis in Posterior Endodontically Treated Teeth: A CBCT Study. Int J Dent 28: 9962429 (2021)

MATTHEWS JD, FORSYTHE AV, BRADY Z, BUTLER MW, GOERGEN SK, BYRNES GB, GILES GG, WALLACE AB, ANDERSON PR, GUIVER TA, MCGALE P, CAIN TM, DOWTY JG, BICKERSTAFFE AC, DARBY SC: Cancer risks in 680,000 people exposed to computed tomography scans in childhood or adolescence: data linkage study of 11 million Australians. BMJ 346: f2360 (2013)

MATZEN LH, CHRISTENSEN J, HINTZE H, SCHOU S, WENZEL A: Diagnostic accuracy of panoramic radiography, stereo-scanography and cone beam CT for assessment of mandibular third molars before surgery. Acta Odontol Scan 71: 1391-1398 (2013)

MATZEN LH, WENZEL A: Efficacy of CBCT for assessment of impacted mandibular third molars: a review – based on a hierarchical model of evidence. Dentomaxillofac Radiol 44: 20140189 (2015)

MATZEN LH, BERKHOUT E. Cone beam CT imaging of the mandibular third molar: a position paper prepared by the European Academy of DentoMaxilloFacial Radiology (EADMFR). Dentomaxillofac Radiol 48(5): 20190039 (2019)

MAZZI-CHAVES JF, DE FARIA VASCONCELOS K, PAUWELS R, JACOBS R, SOUSA-NETO MD. CONE-BEAM COMPUTED TOMOGRAPHIC-BASED ASSESSMENT OF FILLED C-SHAPED CANALS: Artifact Expression of Cone-beam Computed Tomography as Opposed to Micro-computed Tomography and Nano-computed Tomography. J Endod 46(11): 1702-1711 (2020)

MCCOLLOUGH CH, LENG S: Use of artificial intelligence in computed tomography dose optimisation. Ann ICRP 49(suppl): 113–25 (2020)

MCGUIGAN MB, THEODORAKOU C, DUNCAN HF, DAVIES J, SENGUPTA A, HORNER K: An investigation into dose optimisation for imaging root canal anatomy using cone beam CT. Dentomaxillofac Radiol 49(7): 20200072 (2020)

MCILGORM DL, LAWINSKI C, NG S, MCNULTY JP: Quality of commercial-off-the-shelf'(COTS) monitors displaying dental radiographs. BDJ 215(11): E22-E22 (2013)

MEADS CA, DAVENPORT CF: Quality assessment of diagnostic before-after studies: development of methodology in the context of a systematic review. BMC Med Res Methodol 19(9): 3 (2009)

MELO SL, BORTOLUZZI EA, ABREU M, CORREA L, CORREA M: Diagnostic ability of a cone-beam computed tomography scan to assess longitudinal root fractures in prosthetically treated teeth. J Endod 36(11): 1879-1882 (2010)

MICHAELS R, WITSBERGER CA, POWELL AR: 3D printing in surgical simulation: emphasized importance in the COVID-19 pandemic era. J 3D Print Med 10: 2217/3dp-2121-0009 (2021)

MILEMAN PA, VAN DEN HOUT WB: Evidence-based diagnosis and clinical decision making. Dentomaxillofac Radiol 38: 1-10 (2009)

MIRACLE AC, MUKHERJI SK: Conebeam CT of the head and neck, part 1: physical principles. AJNR Am J Neuroradiol 30(6): 1088-1095 (2009)

MOLEN AD: Considerations in the use of cone-beam computed tomography for buccal bone measurements. Am J Orthod Dentofacial Orthop. 137(4): S130-S135 (2010)

MORI S, ENDO M, NISHIZAWA K, TSUNOO T, AOYAMA T, FUJIWARA H, MURASE K: Enlarged longitudinal dose profiles in cone-beam CT and the need for modified dosimetry. Med Phys 32: 1061-1069 (2005)

MORANT JJ, SALVADÓ M, HERNÁNDES-GIRÓN I, CASANOVAS R, ORTRGA R, CALZADO A: Dosimetry of a cone beam CT device for oral and maxillofacial radiology using Monte Carlo techniques and ICRP adult reference computational phantoms. Dentomaxillofac Radiol 42(3): 92555893 (2013)

MOTA DE ALMEIDA FJ, KNUTSSIN K, FLYGARE L: The effect of cone beam CT (CBCT) on therapeutic decision-making in endodontics. Dentomaxillofac Radiol. 43(4): 20130137 (2014)

MOTA DE ALMEIDA FJ, KNUTSSIN K, FLYGARE L: The impact of cone beam computed tomography on the choice of endodontic diagnosis. Int Endod 48: 564–572 (2015)

MOYNIHAN R, DOUST J, HENEY D: Preventing overdiagnosis: how to stop harming the healthy. BMJ 344: e3502 (2012)

MOZZO ET AL. A new volumetric CT machine for dental imaging based on the cone-beam technique preliminary results. Eur Radiol 8: 1558-1564 (1998)

NAGASIRI R, CHITMONGKOLSUK S: Long-term survival of endodontically treated molars without crown coverage: a retrospective cohort study. J Prosthet Dent 93(2): 164-70 (2005)

NAIR PN: On the causes of persistent apical periodontitis: a review. Int Endod J 39(4): 249-281 (2006)

NAKAHARA S, TACHIBANA M, WATANABE Y: One-year analysis of Elekta CBCT image quality using NPS and MTF. J. Appl. Clin. Med. Phys 17(3): 211-222 (2016)

NAKAYA Y, KAWATA Y, NIKI N, UMETATNI K, OHMATSU H, MORIYAMA N: A method for determining the modulation transfer function from thick microwire profiles measured with x-ray microcomputed tomography. Med Phys 39(7): 43474364 (2012)

NATH KS, SHETTY K: Comparative evaluation of second mesiobuccal canal detection in maxillary first molars using magnification and illumination. Saudi Endod Journal 7(3): 166-169 (2017)

NATIONAL COUNCIL ON RADIATION PROTECTION AND MEASUREMENTS (2005) NCRP Report No. 145.Radiation Protection in Dentistry (2005)

NATIONAL RESEARCH COUNCIL OF THE NATIONAL ACADEMIES 2006 Health Risks from Exposure to Low Levels of Ionizing Radiation: BEIR V11 (Washington DC: The National Academies Press)

NEMTOI A, CZINK C, HABA D, GAHLEITNER A: Cone beam CT: a current overview of devices. Dentomaxillofac Radiol 42: 20120443 (2013)

NEVES FS, VASCONCELOS TV, VAZ SL, FREITAS DQ, HAITER-NETO F: Evaluation of reconstructed images with different voxel sizes of acquisition in the diagnosis of simulated external root resorption using cone beam computed tomography. Int Endod J 45: 234-239 (2012)

NEVES FS, FREITAS DQ, CAMPOS PS, EKESTUBBE A, LOFTHAG-HANSEN S: Evaluation of cone-beam computed tomography in the diagnosis of vertical root fractures: the influence of imaging modes and root canal materials. J Endod 40: 1530-1536 (2014)

NIEBLER S, SCHOMER E, TJADEN H, SCHWANECKE U, SCHULZE R: Projection-based improvement of 3D reconstructions from motion-impaired dental cone beam CT data. Med Phys 46(10): 4470-4480 (2019)

NIKOLIC-JAKOBA N, SPIN-NETO R, WENZEL A: Cone-Beam Computed Tomography for Detection of Intrabony and Furcation Defects: A Systematic Review Based on a Hierarchical Model for Diagnostic Efficacy. J Periodontal 87(6): 630-644 (2016)

NOFFKE CE, FARMAN AG, NEL S, NZIMA N: Guidelines for the safe use of dental and maxillofacial CBCT: a review with recommendations for South Africa. SADJ 66(6) :262-266 (2011).

OBUCHOWSKI NA: How many observers are needed in clinical studies of medical imaging? Am J Roentgenol 182(4): 867-869 (2004)

OENNING AC, JACOBS R, PAUWELS R, STRATIS A, HEDESIU M, SALMON B; DIMITRA Research Group, http://www.dimitra.be. Cone-beam CT in paediatric dentistry: DIMITRA project position statement. Pediatr Radiol 48(3): 308-316 (2018)

OENNING C, PAUWELS R, STRATIS A, DE FARIA VASCONCELOS C, TIJSKENS E, DE GRAUWE A, JACOBS R, SALMON B, & DIMITRA RESEARCH GROUP: Halve the dose while maintaining image quality in paediatric Cone Beam CT. Sci Rep: 9(1): 5521 (2019) Erratum in: Sci Rep 10(1): 2474 (2020)

O'HARA RP, CHAND A, VIDIYALA S, ARECHAVALA SM, MITSOURAS D, RUDIN S, IONITA CN: Advanced 3D Mesh Manipulation in Stereolithographic Files and Post-Print Processing for the Manufacturing of Patient-Specific Vascular Flow Phantoms. Proc SPIE Int Soc Opt Eng 27: 9789:978909 (2016)

ORGILL J, ANAMALI S, VIJAYAN S, ALLAREDDY V: The role of monitors in the visualization and assessment of the inferior alveolar canal, Oral Surg Oral Med Oral Pathol Oral Radiol 128(4): 173-174 (2019)

ÖZER SY. Detection of vertical root fractures by using cone beam computed tomography with variable voxel sizes in an in vitro model. J Endod 37: 75-79 (2011)

PANMEKIATE S, RUNGWITTAYATHON P, SUPTAWEEPONBOON W, TANGTRAITHAM N, PAUWELS R: Optimization of exposure parameters in dental cone beam computed tomography using a 3-step approach. Oral Surg Oral Med Oral Pathol Oral Radiol 126(6): 545-552 (2018)

PAPADAKIS AE, PERISINAKIS K, DAMILAKIS J: Automatic exposure control in pediatric and adult multidetector CT examinations: a phantom study on dose reduction and image quality. Med Phys 35(10): 4567-4576 (2008)

PARASHAR V, WHAITES E, MONSOUR P, CHAUDHRY J, GEIST JR: Cone beam computed tomography in dental education: a survey of US, UK, and Australian dental schools. Dent Educ 76 (11): 1443-1447 (2012)

PARKER J, MOL A, RIVERA EM, TAWIL P: CBCT uses in clinical endodontics: the effect of CBCT on the ability to locate MB2 canals in maxillary molars. Int Endod J 50(12): 1109-1115 (2017)

PARSA A, IBRAHIM N, HASSAN B, MOTRONI A, VAN DER STELT P, WISMEIJER D: Influence of cone beam CT scanning paramters on grey value measurements at an implant site. Dentomaxillofac Radiol 42:79884780 (2013)

PATEL S, WILSON R, DAWOOD A, MANNOCCI F: The detection of periapical pathosis using periapical radiography and cone beam computed tomography - part 1: pre-operative status. Int Endod J 45(8): 702-710 (2012)

PATEL K, MANNOCCI F, PATEL S: The Assessment and Management of External Cervical Resorption with Periapical Radiographs and Cone-beam Computed Tomography: A Clinical Study. J Endod 42(10): 1345-1440 (2016)

PATEL S, PATEL R, FOSCHI F, MANNOCCI F: The impact of different diagnostic imaging modalities on the evaluation of root canal anatomy and endodontic residents' stress levels: a clinical study. J Endod 45: 406-413 (2019)

PAUWELS R, STAMATAKIS H, MANOUSARIDIS G, WALKER A, MICHIELSEN K, BOSMANS H, BOGAERTS R, JACOBS R, HORNER K, TSIKLAKIS K; SEDENTEXCT PROJECT CONSORTIUM: Development and applicability of a quality control phantom for dental cone beam CT. J Appl Clin Med Phys 12: 245-260 (2011)

PAUWELS R, BEINSBERGER J, COLLAERT B, THEODORAKU C, ROGERS J, WALKER A, COCKMARTIN L, BOSMANS H, JACOBS R, BOGAERTS R, HORNER K, THE SEDENTEXCT PROJECT CONSORTIUM: Effective dose range for dental cone beam computed tomography scanners. Eur J Radiol 81: 267-271 (2012a)

PAUWELS R: Optimization of cone beam computed tomography for dentomaxillofacial applications. Doctoral thesis in Biomedical Sciences Leuven (2012b)

PAUWELS R, THEODORAKOU C, WALKER A, BOSMANS H, JACOBS R, HORNER K, BOGAERTS R, SEDENTEXCT PROJECT CONSORTIUM: Dose distribution for dental cone beam CT and its implications for defining a dose index. Dentomaxillofac Radiol 41: 583-593 (2012c)

PAUWELS R, BEINSBERGER J, STAMATAKIS H, TSIKLAKIS K, WALKER A, BOSMANS H, BOGAERTS R, JACOBS R, HORNER K; SEDENTEXCT PROJECT CONSORTIUM: Comparison of spatial and contrast resolution for cone-beam computed tomography scanners. Oral Surg Oral Med Oral Pathol Oral Radiol 114: 127-135 (2012d)

PAUWELS R, STAMATAKIS H, BOSMANS H, BOGAERTS R, JACOBS R, HORNER K, TSIKLAKIS K, SEDENTEXCT PROJECT CONSORTIUM: Quantification of metal artefacts on cone beam computed tomography images. Clin Oral Implants Res A100: 91-94 (2013)

PAUWELS R, COCKMARTIN L, IVANAUSKAITE D, URBONIENE A, GAVAL S, DONTA C, TSIKLAKIS K, JACOBS R, BOSMANS H, BOGAERTS R, HORNER K AND THE SEDENTEXCT PROJECT CONSORTIUM: Estimating cancer risk from dental cone-beam CT exposure based on skin dosimetry. Phys Med Biol 59: 3877-3891 (2014a)

PAUWELS R, SILKOSESSAK O, JACOBS R, BOGAERTS R, BOSMANS H, PANMEKIATE S: A pragmatic approach to determine the optimal kVp in cone-beam CT: balancing contrast-to-noise ratio and radiation dose. Dentomaxillofac Radiol 43(5): 20140059 (2014b)

PAUWELS R, ARAKI K, SIEWERDSEN JH, THONGVIGITMANEE SS: Technical aspects of dental CBCT: state of the art. Dentomaxillofac Radiol 44(1): 20140224 (2015a)

PAUWELS RP, SEYNAEVE L, GUIMARAES HERIQUES JC, DE OLIVEIRA-SANTOS C, SOUZA PC, WESTPHALEN FH, RUBIRA-BULLEN IRF, RIBEIRO-ROTTA RF, ROCKENBACH MIB, HAITER-NETO F, PITTAYAPAY P, BOSMANS H, BOGAERTS R, JACOBS R: Optimization of dental cone-beam CT exposures through mAs reduction. Dentomaxillofac Radiol 44(9): 20150108 (2015b)

PAUWELS R, JACOBS R, BOGAERTS J, BOSMANS H, PANMEKIATE S: Reduction of scatter-induced image noise in cone beam computed tomography: effect of field of view size and position. Oral Surg Oral Med Oral Pathol Oral Radiol 121(2): 188-195 (2016)

PAUWELS R., JACOBS R., BOGAERT R, BOSMANS H, PANMEKIATE: Determination of size-specific exposure settings in dental cone-beam CT. Eur Radiol 27: 279–285 (2017).

PAUWELS R, HORNER K, VASSILEVA J, REHANI MM. Thyroid shielding in cone beam computed tomography: recommendations towards appropriate use. Dentomaxillofac Radiol 48(7): 20190014 (2019)

PEARCE MS, SALOTTI JA, LITTLE MP, MCHUGH K, LEE C, KIM KP, HOWE NL, RONCKERS CM, RAJARAMAN P, CRAFT AW, PARKER L, DE GONZÁLEZ AB: Radiation exposure from CT scans in childhood and subsequent risk of leukaemia and brain tumours: a retrospective cohort study. Lancet 380: 499-505 (2012)

PETERSEN L, CHRISTENSEN J, OLSEN K, WENZEL A: Image and surgery-related costs comparing cone beam CT and panoramic imaging before removal of impacted mandibular third molars. Dentomaxillofac Radiol 43(6): 20140001 (2014)

PETERSEN LB, MATZEN LH, OLSEN K, VAETH M, WENZEL A: Economic implications of routine CBCT examination before surgical intervention of the lower third molar in the Danish population. Dentomaxillofac Radiol 44(6):20140406 (2015)

PETERSEN LB, VAETH M, WENZEL A: Neurosensoric disturbances after surgical removal of the mandibular third Molar based on rather panoramic imaging or cone beam CT scanning: A randomized controlled trial (RCT). Dentomaxillofac Radiol 45(2): 20150224 (2016)

PETERSSON A, AXELSSON S, DAVIDSON T, FRISK F, HAKEBERG M, KVIST T, NORLUND A, MEJA`RE I, PORTENIER I, SANDBERG H, TRANÆUS S, BERGENHOLTZ G: Radiological diagnosis of periapical bone tissue lesions in endodontics: a systematic review. Int Endod J 45: 783–801 (2012)

PITTAYAPAT P, LIMCHAICHANA-BOLSTAD N, WILLEMS G, JACOBS R: Three-dimensional cephalometric analysis in orthodontics: a systematic review. Orthod Craniofac Res 17(2): 69–91 (2014)

PODČERNINA J, URTĀNE I, PIRTTINIEMI P, ŠALMS Ģ, RADZIŅŠ O, ALEKSEJŪNIENĖ J. Evaluation of Condylar Positional, Structural, and Volumetric Status in Class III Orthognathic Surgery Patients. Medicina (Kaunas) 56(12): 672 (2020)

POLETTI PA, PLATON A, RUTSCHMANN OT, SCHMIDLIN F, IISELIN FS, BECKER CD: Low-Dose Versus Standard-Dose CT Protocol in Patients with Clinically Suspected Renal Colic. Am J Roentgenol 188(4): 927-933 (2007)

POPE O, SATHORN C, PARASHOS P: Comparative Investigation of Cone-beam Computed Tomography and Periapical Radiography in the Diagnosis of a Healthy Periapex. J Endod 40(3): 360-365 (2014)

PRATT I, AMINOSHARIAE A, MONTAGNESE TA, WILLIAMS KA, KHALIGHINEJAD N, MICKEL A Eight-Year Retrospective Study of the Critical Time Lapse between Root Canal Completion and Crown Placement: Its Influence on the Survival of Endodontically Treated Teeth. J Endod 42(11): 1598-1603

PRESTON DL, RON E, TOKUOKA S, FUNAMOTO S, NISHI N, SODA M, MABUCIHI K, KODAMA K: Solid cancer incidence in atomic bomb survivors 1958-1998. Radiat Res 168: 1-64 (2007)

Public Health England PHE-CRCE: dose to patients from dental radiographic X-ray imaging procedures in the UK -2017 review: (2019)

QIAO J, WANG S, DUAN J, ZHANG Y, QIU Y, SUN C, LIU D: The accuracy of cone beam computed tomography in assessing maxillary molar furcation involvement. J Clin Periodontol 41: 269-274 (2014)

QU XM, LI G, LUDLOW JB, ZHANG ZY, MA XC: Effective radiation dose of ProMax 3D cone-beam computerized tomography scanner with different protocols. Oral Surg Oral Med Oral Pathol Oral Radiol Endod 110(6): 770-776 (2010)

QU X, LI G, ZHANG Z, MA X: Thyroid shields for radiation dose reduction during cone beam computed tomography scanning for different oral and maxillofacial regions. Eur J Radiol 81: 376-380 (2012)

QUEIROZ PM, DDS, GROPPO FC, OLIVEIRA ML, HAITER-NETO F, QUEIROZ FREITAS D: Evaluation of the efficacy of a metal artifact reduction algorithm in different cone beam computed tomography scanning parameters. Oral Surg Oral Med Oral Pathol Oral Radiol Endod 123: 729-776 (2017)

REEH ES, MESSER HH, DOUGLAS WH: Reduction in tooth stiffness as a result of endodontic and restorative procedures. J Endod 15(11): 512–516 (2009)

REITSMA H, RUTJES A, WHITING P, VLASSOV V, LEEFLANG M, DEEKS J: Assessing Methodological Quality Key Points. Cochrane Handbook for Systematic Reviews of Diagnostic Test Accuracy; Cochrane: London, UK (2009)

REYMUS M, FOTIADOU C, KESSLER A, HECK K, HICKEL R, DIEGRITZ C: 3D printed replicas for endodontic education. Int J Endod 52(1): 123-30 (2019)

REYMUS M, STAWARCZYK A, WINKLER J, KESS S, KRASTL G, KRUG R: A critical evaluation of the material properties and clinical suitability of in-house printed and commercial tooth replicas for endodontic training. Int Endod J 53(10): 1446-1454 (2020)

ROBB RA: Dynamic spatial reconstructor: an X-ray video fluoroscopic CT scanner for dynamic volume imaging of moving organs. IEEE Trans Med Imaging 1(1): 22-33 (1982)

ROBERTS JA, DRAGE NA, DAVIES J, THOMAS DW: Effective dose from cone beam CT examinations in dentistry. Br J Radiol 82: 35-40 (2009)

RODRÍGUEZ G, ABELLA F, DURÁN-SINDREU F, PATEL S, ROIG M: Influence of cone beam tomography in clinical decision making among specialists. J Endod 43(2): 194-199 (2017)

RENTON T, DAWOOD A, SHAH A, SEARSON L, YILMAZ Z: Post-implant neuropathy of the trigeminal nerve. A case series. Br Dent 212(11): E17 (2012)

ROEDER F, WACHTLIN D, SCHULTZE R: Necessity of 3D visualization for the removal of lower wisdom teeth: required sample size to prove non-inferiority of panoramic radiography compared to CBCT. Clin Oral Investig 16: 699-706 (2012)

ROHLIN M, HORNER K, LINDH C, WENZEL A: Through the quality kaleidoscope: reflections on research in dentomaxillofacial imaging. Dentomaxillofac Radiol 49(6): 20190484 (2020)

ROOD JP, SHEBAB BA: The radiological prediction of inferior alveolar nerve injury during third molar surgery. Br J Oral Maxillofac Surg 28(1): 20-25 (1990)

ROSEN E, TASCHIERI S, DEL FABBRO M, BEITLITUM I, TSESIS I: The Diagnostic Efficacy of Cone-beam Computed Tomography in Endodontics: A Systematic Review and Analysis by a Hierarchical Model of Efficacy. J Endod 41(7): 1008-1014 (2015)

ROSEN E, GOLDBERGER T, BEITLITUM I, LITTNER D, TSESIS I: Diagnosis Efficacy of Cone-Beam Computed Tomography in Endodontics—A Systematic Review of High-Level-Evidence Studies. Appl Sci 12(3): 938 (2022)

ROVER G, DE LIMA CO, BELLADONNA FG, GARCIA LFR, BORTOLUZZI EA, SILVA EJNL, TEIXEIRA CS: Influence of minimally invasive endodontic access cavities on root canal shaping and filling ability, pulp chamber cleaning and fracture resistance of extracted human mandibular incisors. Int Endod J 53(11): 1530-1539 (2020)

SALINEIRO FCS, KOBAYASHI-VELASCO S, BRAGA MM, CAVALCANTI MGP: Radiographic diagnosis of root fractures: a systematic review, meta-analyses and sources of heterogeneity. Dentomaxillofac Radiol 46: 20170400 (2017)

SANMARTÍ-GARCIA G, VALMASEDA-CASTELLÓN E, GAY-ESCODA C. Does computed tomography prevent inferior alveolar nerve injuries caused by lower third molar removal? J Oral Maxillofac Surg 70(1): 5–11 (2012)

SATHORN C, PALAMARA JE, PALAMARA D, MESSER HH: Effect of root canal size and external root surface morphology on fracture susceptibility and pattern: a finite element analysis. Journal of Endodontics 31(4): 288-292 (2005

SATO M: Efficacy of 3D-Printed Guide vs Conventional method for Conservative Endodontic Access Preparation in Extracted Upper Molars. Master's Theses, UOC 2020

SCARFE WC, FARMAN AG: What is cone beam and how does it work? Dent Clin Am 52(4): 707-730 (2008)

SCHULZE D, HEILAND M, THURMAN H, ADAM G: Radiation exposure during midfacial imaging using 4 and 16-slice computed tomography: cone beam computed tomography systems and conventional tomography. Dentomaxilofac Radiol 33(2): 83-86 (2004)

SCHULZE RK, BERNDT D, D'HOEDT B: On cone-beam computed tomography artifacts induced by titanium implants. Clin Oral Implants Res 21(1): 100-107 (2010)

SCHULZE R, HEIL U, GROSS D, BRUELLMANN DD, DRANISCHNIKOW E, SCHWANECKE U, SCHOEMER E: Artefacts in CBCT; a review. Dentomaxilofac Radiol 40(5): 265-273 (2011)

SCHULZE RKW & DOERING CI: Simple computation of the approximated modulation transfer function (MTF) using spreadsheet-software: method and evaluation in five maxillofacial CBCT-devices. Dentomaxilofac Radiol 48(4): 20180350 (2019)

SCHWENDICKE F, GÖSTEMEYER G: Cost-effectiveness of Single- Versus Multistep Root Canal Treatment. J Endod 42(10): 1446-1452 (2016)

SERT S, BAYIRLI GS: Evaluation of the Root Canal Configurations of the Mandibular and Maxillary Permanent Teeth by Gender in the Turkish Population
J Endod 30(6): 391-398 (2004)

SHELLEY AM, BRUNTON P, HORNER K: Subjective Image Quality Assessment of Cross Sectional Imaging Methods for the Symphyseal Region of the Mandible Prior to Dental Implant Placement. J Dent 39 (11): 764-770 (2011)

SHELLEY AM, FERRERO A, BRUNTON P, GOODWIN M, HORNER K: The impact of CBCT imaging when placing dental implants in the anterior edentulous mandible: a before–after study. Dentomaxillofac Radiol 44(4): 20140316 (2015)

SIEGEL MJ, SCHMIDT B, BRADLEY D, SUES C, HILDEBOLT C: Radiation dose and image quality in pediatric CT: Effect of technical factors and phantom size and shape. Radiol 233(2): 515-522 (2004)

SIISKONEN T, GALLAGHER A, CIRAJ BJELAC O, NOVAK L, SANS MERCE M, FARAH J, DABIN J, MALCHAIR F, KNEŽEVIC Z, KORTESNIEMI M: A European perspective on Dental Cone Beam Computed Tomography (CBCT) systems with a focus on optimisation utilizing DRLs (Diagnostic Reference Levels). J Radiol Prot 41(2): 33461178 (2021)

SILVA JNL, OLIVEIRA VB, SILVA AA, BELLADONNA FG, PRADO M, ANTUNES HS, DE-DEUS G: Effect of access cavity design on gaps and void formation in resin composite restorations following root canal treatment on extracted teeth. Int J Endod 53(11): 1540-1548 (2020)

SILVA EJNL, LIMA CO, BARBOSA AFA, AUGUSTO CM, SOUZA EM, LOPES RT, DE-DEUS G, VERSIANI MA: Preserving dentine in minimally invasive access cavities does not strength fracture resistance of restored mandibular molars. Int Endod J 54(6): 966-974 (2021)

SMITH SW: Digital Signal Processing: A Practical Guide for Engineers and Scientists. 4th ed. Elsevier (2003)

SMITH PG, MORROW RH, ROSS DA: Field Trials of Health Interventions: A Toolbox. 3rd ed Oxford (UK): Chapter 12, Outcome measures and case definition (2015)

SÖNMEZ G, KOÇ C, KAMBUROĞLU K: Accuracy of linear and volumetric measurements of artificial ERR cavities by using CBCT images obtained at 4 different voxel sizes and measured by using 4 different software: an ex vivo research. Dentomaxillofac Radiol 47(08): 20170325 (2018)

SORENSEN JA, MARTINOFF JT: Intracoronal reinforcement and coronal coverage: a study of endodontically treated teeth. J Prosthet Dent 51(6): 780-784 (1984)

SPIN-NETO R, GOTFREDSEN E, WENZEL A: Impact of voxel size variation on CBCT-based diagnostic outcomes in dentistry: a systematic review. J Digit Imaging 26(4): 813-820 (2013a)

SPIN-NETO R, MUDRAK J, MATZEN LH, CHRISTENSEN J, GOTFREDSEN E, WENZEL A: Cone beam CT image artefacts related to head motion simulated by a robot skull: visual characteristics and impact on image quality. Dentomaxillofac Radiol 42(2): 32310645 (2013b)

SPIN-NETO R, MATZEN LH, SCHROPP L, GOTFREDSEN E, WENZEL A: Factors affecting patient movement and re-exposure in cone beam computed tomography examination. Oral Surg Oral Med Oral Pathol Oral Radiol 119(5): 572-578 (2015)

SPIN-NETO R, WENZEL A: Patient movement and motion artefacts in cone beam computed tomography of the dentomaxillofacial region: a systematic literature review. Oral Surg Oral Med Oral Pathol Oral Radiol Endod 121(4): 425-433 (2016)

SPIN-NETO R, MATZEN LH, SCHROPP L, GOTFREDSEN E, WENZEL A: Movement characteristics in young patients and the impact on image quality: Dentomaxillofac Radiol 45(4): 20150426 (2016)

SPIN-NETO R, COSTA C, SALGADO DM, ZAMBRANA NR, GOTFREDSEN E, WENZEL A: Patient movement characteristics and the impact on CBCT image quality and interpretability. Dentomaxillofac Radiol 47(1): 20170216 (2018)

STRÅLSÄKERHETSCENTRALEN, STUK: Reference levels for patient radiation exposure in cone-beam computed tomography examinations of adults' head region. STUK, Decision 12/3020/ (2016)

STRATIS A, ZHANG G, LOPEZ-RENDON X, JACOBS R, BOGAERTS R, BOSMANS H: Customisation of a Monte Carlo dosimetry tool for dental cone-beam CT systems. Radiat Prot Dosimetry 169(1-4): 378-85 (2016)

STROPKO JJ: Canal morphology of maxillary molars: Clinical observations of canal configurations. JEndod 25(6): 446-450 (1999)

STUDEBAKER B, HOLLENDER L, MANCL L, JOHNSON JD, PARANJPE A: The Incidence of Second Mesiobuccal Canals Located in Maxillary Molars with the Aid of Cone-beam Computed Tomography. J Endod 44(4): 565–570 (2018)

SU CC, HUANG RY, WU YC, CHENG WC, CHIANG HS, CHUNG MP, TSAI YW, CHUNG CH, SHIEH YS: Detection and location of second mesiobuccal canal in permanent maxillary teeth: a cone-beam computed tomography analysis in a Taiwanese population. Arch Oral Biol 98: 108-114 (2019)

SUOMALAINEN A, KILJUNEN T, KASER Y, PELTOLA J, KORTESNIEMI M: Dosimetry and image quality of four dental cone beam computed tomography scanners compared with multislice computed tomography scanners. Dentomaxilofac Radiol 38(6): 367-378 (2009)

SUR J, SEKI K, KOIZUMI H, NAKAJIMA K, OKANO T: Effects of tube current on cone-beam computerized tomography image quality for presurgical implant planning *in vitro.* Oral Surg Oral Med Oral Pathol Oral Radiol 110: e29-e33 (2010)

TACK P, VICTOR J, GEMMEL P, AND ANNEMANS L: 3D-printing techniques in a medical setting: a systematic literature review BioMed Eng OnLine 15(1):115 (2016)

TADINADA A, MARCZAK A, YADAV S: Diagnostic efficacy of a modified low-dose acquisition protocol for the preoperative evaluation of mini-implant sites. Imaging Sci Dent 47: 141-147 (2017)

TALWAR S, UTNEJA S, NAWAL RR, KAUSHIK A, SRIVASTAVA D, OBEROY SS: Role of cone-beam computed tomography in diagnosis of vertical root fractures: a systematic review and meta-analysis. J Endod 42(1): 12–24 (2016)

TANG W, WU Y, SMALES R J. Identifying and reducing risks for potential fractures in endodontically treated teeth. J Endod 36(4): 609–617 (2010)

TAPIOVAARA M: Review of relationships between physical measurements and user evaluation of image quality. Radiat Prot Dosimetry 129(1-3): 244-248 (2008)

THEODORAKU C, WALKER A, HORNER K, PAUWELS R, BOGAERTS R, JACOBS R & SEDENTEXCT PROJECT CONSORTIUM: Estimation of paediatric organ and effective doses from dental cone beam CT using anthropomorphic phantoms. Br J Radiol 85(1010): 153-160 (2012)

TORABINEJAD M, RICE DD, MAKTABI O, OYOYO U, ABRAMOVITCH K: Prevalence and size of periapical radiolucencies using cone-beam computed tomography in teeth wit hout apparent intraoral radiographic lesions: a new periapical index with a clinical recommendation. J Endod 44(3): 389-394 (2018)

TRAN TTN, JIN DSC, SHIH KL, HSU ML, CHEN JC: An Image Quality Comparison Study Between Homemade and Commercial Dental Cone-Beam CT Systems. J. Med. Biol. Eng. 41: 870–880 (2021)

TSESIS I, FUSS Z: Diagnosis and treatment of root perforations. End Top 13: 95-107 (2006)

TSISKLAKIS K, DONTA C, GAVALA S, KARAYIANNI K, KAMENOPOULOU V, HOURDAKIS CJ: Dose reduction in maxillofacial imaging using low dose Cone Beam CT. Eur J Radiol 56(3): 413-417 (2005)

TYNDALL DA, PRICE JB, TETRADIS S, GANZ SD, HILDEBOLT C, SCARFE WC: American Academy of Oral and Maxillofacial Radiology. Position statement of the American Academy of Oral and Maxillofacial Radiology on selection criteria for the use of radiology in dental implantology with emphasis on cone beam computed tomography. Oral Surg Oral Med Oral Pathol Oral Radiol 113(6): 817–826 (2012)

TUBIANA M, FEINENDEGEN LE, YANG C, KAMINSKI JM: The linear no-threshold relationship is inconsistent with radiation biologic and experimental data. Radiol 251(1): 13-22 (2009)

URABA S, EBIHARA A, KOMATSU K, OHBAYASHI N, OKIJI T: Ability of cone-beam computed tomography to detect periapical lesions that were not detected by periapical radiography: a retrospective assessment according to tooth group. J Endod 42(8): 1186-1190 (2016)

VAN ACKER JWG., PAUWELS NS, CAUWELS RGEC, RAJASEKHARAN S: Outcomes of different radioprotective precautions in children undergoing dental radiography: a systematic review. Eur Arch Paediatr Dent 21(4): 463–508 (2020)

VAN GOMPEL G, SLAMBROUCK K, DEFRISE M, BATENBURG KJ, DE MEY J, SIJBERS J: Iterative correction of beam hardening artifacts in CT. Med Phys 38 Suppl 1: S36 (2011)

VASCONCELOS KF, NICOLIELO LF, NASCIMENTO MC, HAITER-NETO F, BÓSCOLO FN, VAN DESSEL J, EZELDEEN M, LAMBRICHTS I, JACOBS R: Artefact expression associated with several cone-beam computed tomographic machines when imaging root filled teet. Int Endod J 48(10): 994-1000 (2014)

VASCONCELOS KF, CODARI M, QUEIROZ PM, NICOLIELO LFP, FREITAS DQ, SFORZA C, JACOBS R, HAITER-NETO F: The performance of metal artifact reduction algorithms in cone beam computed tomography images considering the effects of materials, metal positions, and fields of view. Oral Surg Oral Med Oral Pathol Oral Radiol 127(1): 71-76 (2019)

VENSKUTONIS T, PLOTINO G, JUODZBALYS G, MICKEVIČIENE L: The Importance of Cone-beam Computed Tomography in the Management of Endodontic Problems: A Review of the Literature. J Endod 40(12): 1895-1901 (2014)

VERTUCCI FJ: Root Canal Anatomy of the Human Permanent Teeth. Oral Surg Oral Med Oral Pathol 58(5): 589-599 (1984)

WALTER C, WEIGER R, DIETRICH T, LANG NP, ZITZMANN NU: Does three-dimensional imaging offer a financial benefit for treating maxillary molars with furcation involvement? A pilot clinical case series Clin Oral Implants Res. 23(3): 351-358 (2012)

WALTRICK KB, NUNES DE ABREU MJ, CORRÊA M, ZASTROW MD, DUTRA VD: Accuracy of linear measurements and visibility of the mandibular canal of cone-beam computed tomography images with different voxel sizes: an in vitro study. J Periodontal 84(1): 68-77 (2013)

WANDERLEY VA, NEVES FS, NASCIMENTO MCC, QUEIROZ DE MELO MONTEIRO G, SIQUEIRA LOBO N, FARIAS ARAUJO L: Detection of incomplete root fractures in endodontically treated teeth using different high-resolution cone-beam computed tomography imaging protocols. J Endod 43(10): 1720–1724 (2017)

WANG G, VANNIER MW, CHENG PC: Iterative X-ray cone-beam tomography for metal artifact reduction and local region reconstruction. Microsc Microanal 5(1): 58-65 (1999)

WANG MF, XIE X, LI G, ZHANG Z: Relationship between CNR and visibility of anatomical structures of cone-beam computed tomography images under different exposure parameters. Dentomaxillofac Radiol 49(5): 20190336 (2020)

WATANABE H, HONDA E, KURABAYASHI T: Modulation transfer function evaluation of cone beam computed tomography for dental use with the oversampling method. Dentomaxillofac Radiol 39(1): 28-32 (2010)

WATANABE H, HONDA E, TETSUMURA A, KURABAYASHI T: A comparative study for spatial resolution and subjective image characteristics of a multi-slice CT and a cone-beam CT for dental use. Eur J Radiol 77(3): 397-402 (2011)

WHITE SC & PHAROAH MJ: Oral Radiology. Principles and Interpretation, St. Louis, Mosby (2013)

WHITE SC, SCARFE WC, SCHULZE RKW, LURIE AG, DOUGLASS JM, FARMAN AG, LAW CS, LEVIN MD, SAUER RA, VALACHOVIC RW, ZELLER GG, GOSKE MJ: The Image Gently in Dentistry campaign: promotion of responsible use of maxillofacial radiology in dentistry for children. Oral Surg Oral Med Oral Pathol Oral Radiol 118(3): 257-261 (2014)

WILLEMINK MJ, PERSSON M, POURMORTEZA A, PELC NJ, FLEISCHMANN D. PHOTON-COUNTING CT: Technical Principles and Clinical Prospects. Radiology 289(2): 293-312 (2018)

WOELBER JP, FLEINER J, RAU J, RATKA-KRÜGER P, HANNIG C: Accuracy and usefulness of CBCT in periodontology: a systematic review of the literature. Int J Periodontics Restor Dent 38(2): 289–97 (2018)

WOLCOTT J, ISHLEY D, KENNEDY W, JOHNSON S, MINNICH S, MEYERS J: A 5 yr clinical investigation of second mesiobuccal canals in endodontically treated and retreated maxillary molars. J Endod 31(4): 262-64 (2005)

WOLF TG, FISCHER F, SCHULZE RKF: Correlation of objective image quality and working length measurements in different CBCT machines: An ex vivo study. Sci Rep 10(1): 1-7 (2020)

YADAV S, PALO L, MAHDIAN M, UPADHYAY M, TADINADA A: Diagnostic accuracy of 2 cone-beam computed tomograohy protocols for detecting arthritic changes in temporomandibular joints. Am J Orthod Dentofacial Orthop 147(3): 339-344 (2015)

YALDA FA: Aspects of Dental and Maxillofacial Cone Beam Computed Tomography (CBCT). PhD thesis, University of Manchester, 2019.

YALDA AF, THEODORAKOU C, CLARKSON RJ, DAVIES J, FEINBERG L, SENGUPTA A, HORNER K: Determination of a cone-beam CT low-dose protocol for root fracture diagnosis in non-endodontically treated anterior maxillary teeth. Dentomaxillofac Radiol 51(2): 20210138 (2022)

YANG, Y.M.; GUO, B.; GUO, L.Y.; YANG, Y.; HONG, X.; PAN, H.Y.; ZOU, W.L.; HU, T: CBCT-Aided Microscopic and Ultrasonic Treatment for Upper or Middle Thirds Calcified Root Canals. Biomed Res Int 4793146 (2016)

YEUNG, AWK, JACOBS R, BORNSTEIN MM: Novel low-dose protocols using cone beam computed tomography in dental medicine: a review focusing on indications, limitations, and future possibilities. Clin Oral Invest 23(6): 2573–2581 (2019)

YI J, SUN Y, LI Y, LI C, LI X, ZHAO Z: Cone-beam computed tomography versus periapical radiograph for diagnosing external root resorption: A systematic review and meta-analysis. Angle Orthod 87(2): 328–337 (2017)

YU L, LIUX, LENG S, KOFLER JM, RAMIREZ-GIRALDO JC, QU M, CHRISTNER J, FLETCHER JG, MCCOLLOUGH CH: Radiation dose reduction in computed tomography: techniques and future perspective. Imaging Med 1(1): 65-8 (2009)

ZHANG K, LI M, DAI J, WANG S: Image quality of cone beam CT on respiratory motion. Nucl Sci Tech 22: 111–17 (2011)

ZHANG G, MARSHALL N, BOGAERTS R, JACOBS R, BOSMANS H: Monte Carlo modelling for dose assessment in cone beam CT for oral and maxillofacial applications. Med Phys 40(7): 072103 (2013)

ZHANG Y, XU H, WANG D, GU Y, WANG J, TU S, QIU X, ZHANG F, LUO Y, XU S, BAI J, SIMONE G, ZHANG G: Assessment of the Second Mesiobuccal Root Canal in Maxillary First Molars: A Cone-beam Computed Tomographic Study. J Endod 43(12): 1990-1996 (2017)

ZIJDERVELD SA, VAN DEN BERGH JP, SCHULTEN EA, TEN BRUGGENKATE CM. Anatomical and surgical findings and complications in 100 consecutive maxillary sinus floor elevation procedures. J Oral Maxillofac Surg 66(7): 1426-1438 (2008)

Appendices

Appendix I: Raw data (**Chapter 2)** noting percentage of MB2 canal identified by junior hospital dentists and senior staff.

	DAP	Molar in UL6 Position				Molar in UL7 Position				UL8 Molar in UL8 Position			
		JHDs		Senior staff		JHDs		Senior Staff		JHDs		Senior Staff	
		%	SD	%	SD	%	SD	%	SD	%	SD	%	SD
PX	90.3	82.8	13.9	90	5	81.6	9.6	91	9.4	35.8	6.1	41.7	1.5
PX	135.3	92	8.3	95.7	1.2	88.8	11.5	97	1.7	42.3	8.2	44.4	2.4
PX	139.4	93.4	13.2	98.3	1.9	89.4	13.2	95.3	4.5	40.6	6.1	50.6	2.2
PX	195	94	8.7	96.4	6.5	92.6	11.2	97.7	0.6	45.2	10.1	53.3	6.5
PX	244.6	97.4	3.7	99.3	1.2	93.3	4.3	95.7	1.2	49.2	6.8	61	3.6
PX	209.3	99	1.7	99.6	0.9	95	5.9	97	1.7	58.6	18.1	61.7	2.9
PX	294	99.4	1.3	100	0	97.6	2.8	98	0	60	18.9	65.6	8.5
PX	373.3	100	0	100	0	97.8	1.8	98.7	1.2	61.3	15.8	67.6	14.5
AC	90.5	92.6	6.7	97.3	5.9	86.6	8.7	90.2	2.9	33.9	12.2	58	4.5
AC	118	91.3	5.6	94.3	2.3	83.8	7.8	87.3	3.5	36.3	13.3	46.6	5.3
AC	120.9	93.3	4.4	94.9	2.9	86.6	4.87	91.5	1.5	44.6	8.8	46.3	1.5
AC	143.8	93.3	5.4	94.9	5.7	85.6	7.9	90.7	1.2	43.6	6.8	60.5	2.8
AC	147.1	96.3	6.1	93	1	85.7	5.9	91.1	3.2	43.6	11.1	57.8	4.4
AC	154.6	92	4.4	94.9	3.5	90.3	10.3	93	4.5	44.6	10.6	59.5	1.5
AC	163.2	96	4.8	96.9	3.1	81	9.4	86.5	3.6	49.4	14.7	55.8	9.7
AC	174.9	94	4.4	96.8	3.2	87.6	9.1	89.6	8.7	45.3	8.7	58.4	4.2
AC	181.7	98	2	98.6	1.1	86.6	7.6	95.4	1.1	53.6	18.2	59	14.3
AC	187.5	97.3	3.3	98.1	0.5	96.4	3.4	97.8	2.5	58.1	9.8	62.3	8.8
AC	203.2	96	1	98	1.1	93.6	4.4	97.8	0.8	54.3	12.6	60.2	5.1
AC	207.9	96.6	4.5	97.7	0.8	96.6	1.5	97.4	1.4	53.3	17.8	59	9.6
AC	233.9	96.3	3.5	98.7	1.1	94.6	6.6	96	1.7	53.8	8.6	58.9	5.3
AC	240.7	96.6	2.2	97.9	0.5	93	3.5	94.8	3	55.1	7.4	59.4	5.7
AC	251.2	98.1	2.8	98.7	1.2	93	4.5	95.2	2.7	58	23.6	63.7	25.3
AC	257.6	96	1	100	0	94.6	1.8	97.4	1.6	62.1	10.6	63	6.9
AC	294	96	3.5	100	0	94.3	6.3	96.8	2.5	59.3	17.9	63.5	7.2
AC	304.6	93.3	11.5	97.4	5.8	96.4	4.3	96.4	2.9	50.3	4.5	57.2	3.7
AC	306.7	96.6	7.6	97.6	2.1	97	1.7	98.8	1.1	56.6	12.2	64.6	5.7
AC	316.8	93.6	5.5	98.6	3.1	96.6	3.13	98	0	56.3	12.1	61.6	6.42
AC	324.4	97.7	2.2	98.3	2.1	96.7	2.2	98.3	0.6	58.6	14.4	73	12.3
AC	405.1	100	0	100	0	98.3	1.5	98.7	1.1	63.3	12.7	69	7.8
AC	409.5	100	0	100	0	97.8	2.88	98.8	1.1	61.6	12.1	68.9	18.3
AC	410.5	100	0	100	0	96	2.6	88.2	1.7	59.7	12.7	73	13.8
AC	427.3	99.3	0.9	100	0	98	0	96.4	3.1	57.6	8.9	75.7	12.7
AC	517.5	100	0	100	0	98	0	97.6	2.4	65	14.3	72	15.9
AC	520.2	100	0	100	0	98.6	1.5	98.9	1.1	68.6	19.5	76	12.5
AC	568.9	100	0	100	0	99	1.7	99.1	0.8	68.5	22.3	74.3	12.4
AC	714.4	100	0	100	0	98.6	1.5	99.8	0.9	66.0	4.8	80.6	10.4

JHD: Junior hospital dentist, PX: ProMax Scanner, AC: Accuitomo Scanner, SD: Standard deviation

Appendix II: Trialling and assessment of volumetric measurement in ITK-SNAP
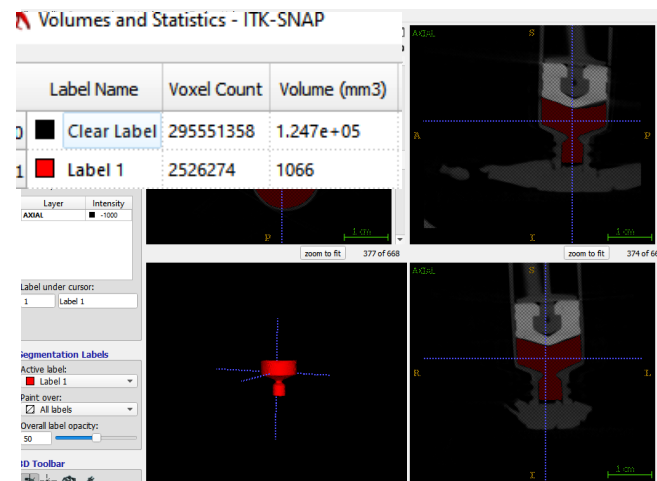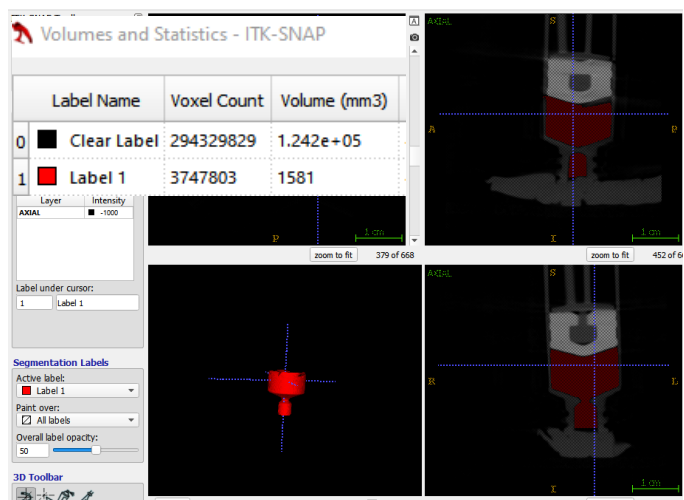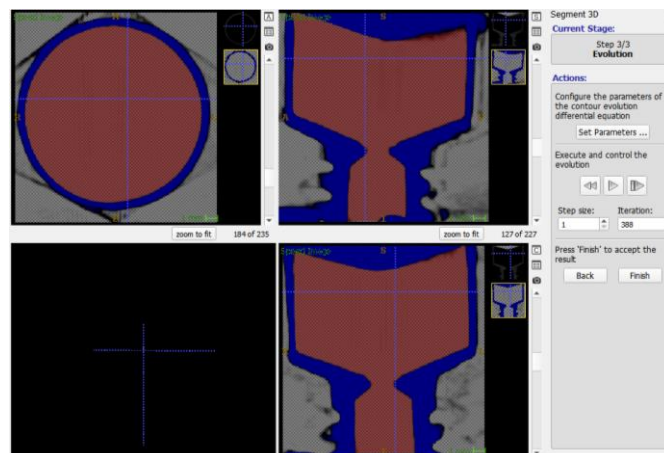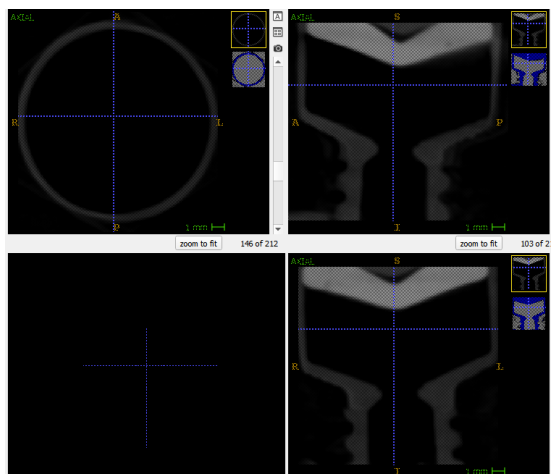
Appendix III: Volumetric assessment of pilot study endodontic access cavities

IOPA	VOLUME (MM³)					
1	88.45	83.66	95.46	88.67	82.44	103.87
2	88.46	83.65	95.46	88.66	82.46	103.72
3	88.44	83.69	95.46	88.63	82.44	103.75
AVERAGE	88.45	83.67	95.46	88.65	82.45	103.78
SD ±	0.01	0.02	0	0.02	0.01	0.08

CBCT/IOPA	VOLUME (MM³)					
1	76.02	70.34	95.33	78.46	76.46	99.56
2	76.19	70.33	95.34	78.48	76.34	99.55
3	76.1	70.34	95.36	78.46	76.36	99.58
AVERAGE	76.10	70.34	95.34	78.47	76.39	99.56
SD±	0.09	0.01	0.02	0.01	0.06	0.02

Appendix IV: Power calculation from pilot study data (**Chapter 4**)

	VOLUME (mm³)	
	IOPA	**CBCT/IOPA**
Operator 1	88.45	76.10
	83.67	70.34
	95.46	95.34
Operator 2	88.65	78.47
	82.45	76.39
	103.75	99.56
Mean	90.41	82.7
SD	7.99	11.81

Mean Difference between IOPA and CBCT/IOPA: 7.7 mm³
Approximate SD: ± 9.9

Appendix V: Raw data showing volume, time and access cavity dimesnions for each operator and tooth (**Chapter 4**)

<u>Tooth X</u>

GROUP	Operator ID	Session	Image	Tooth Type	MAG	CANALS	Volume removed mm³	Time taken (mins)	MB WIDTH (mm)	DEPTH (mm)	MD WIDTH (mm)
ET	ET1	2	IOPA	X	M	1	73.79	14.2	6.85	8.01	4.98
ET	ET2	2	IOPA	X	M	1	78.45	16.3	6.14	7.49	4.2
ET	ET3	2	IOPA	X	M	1	85.56	22.4	6.12	8.4	5.15
ET	ET4	1	IOPA	X	M	1	73.79	9.8	5.38	7.95	4.23
ET	ET5	1	IOPA	X	M	1	90	19.5	6.36	7.43	3.38
ET	ET6	1	IOPA	X	M	1	115	25.3	7.11	8.1	6.3
AVERAGE							86.09	17.92	6.33	7.89	4.71
SD±							15.57	5.64	0.61	0.37	1.01

GROUP	Operator ID	Session	Image	Tooth Type	MAG	CANALS	Volume removed mm³	Time taken (mins)	MB WIDTH (mm)	DEPTH (mm)	MD WIDTH (mm)
PG	PG1	2	IOPA	X	M	0	110.34	26.3	7.21	7.46	5.15
PG	PG2	2	IOPA	X	NM	0	87.21	22.5	5.78	8.45	4.78
PG	PG3	2	IOPA	X	NM	1	124.29	35.6	7.67	8.98	5.98
PG	PG4	1	IOPA	X	NM	0	102.2	25.4	6.81	7.42	5.83
PG	PG5	1	IOPA	X	M	1	130	35	7.5	9.01	5.55
PG	PG6	1	IOPA	X	NM	0	80.87	23.2	5.47	7.28	4.05
AVERAGE							105.81	28	6.74	8.1	5.22
SD±							19.64	5.83	0.92	0.81	0.72

GROUP	Operator ID	Session	Image	Tooth Type	MAG	CANALS	Volume removed mm³	Time taken (mins)	MB WIDTH (mm)	DEPTH (mm)	MD WIDTH (mm)
GP	GP1	2	IOPA	X	M	0	125	30.2	7.4	9.56	5.45
GP	GP2	2	IOPA	X	NM	0	82.36	23.4	5.78	6.45	5.21
GP	GP3	2	IOPA	X	NM	0	84.36	25.3	6.15	6.19	4.78
GP	GP4	1	IOPA	X	NM	0	82.36	23.4	7.24	8.52	5.34
GP	GP5	1	IOPA	X	M	0	95.87	30.2	7.9	8.99	5.67
GP	GP6	1	IOPA	X	NM	0	112.56	30.6	6.9	7.37	5.13
AVERAGE							97.085	27.18	6.89	7.85	5.26
SD±							17.97	3.52	0.79	1.39	0.30

GROUP	Operator ID	Session	Image	Tooth Type	MAG	CANALS	Volume removed mm³	Time taken (mins)	MB WIDTH (mm)	DEPTH (mm)	MD WIDTH (mm)
ET	ET1	1	CBCT	X	M	1	71.45	12.1	5.4	7.36	4.32
ET	ET2	1	CBCT	X	M	1	72.39	13.4	5.45	7.1	4.01
ET	ET3	1	CBCT	X	M	1	70.14	20.1	5.32	7.39	4.98
ET	ET4	2	CBCT	X	M	1	72.26	8	5.4	7.45	5.01
ET	ET5	2	CBCT	X	M	1	76.3	10.5	6.32	7.48	4.2
ET	ET6	2	CBCT	X	M	1	74.01	23.2	6.29	7.55	4.57
AVERAGE							72.75	14.55	5.69	7.39	4.51
SD±							2.15	5.87	0.47	0.16	0.41

GROUP	Operator ID	Session	Image	Tooth Type	MAG	CANALS	Volume removed mm³	Time taken (mins)	MB WIDTH (mm)	DEPTH (mm)	MD WIDTH (mm)
PG	PG1	1	CBCT	X	M	1	90.67	17.8	4.56	6.92	4.98
PG	PG2	1	CBCT	X	NM	1	63.89	14.3	4.89	6.78	4.36
PG	PG3	2	CBCT	X	NM	1	85.21	16.4	6.31	6.34	4.51
PG	PG4	2	CBCT	X	NM	1	87.57	17.2	5.78	6.92	5.09
PG	PG5	2	CBCT	X	M	1	90.35	17.6	6.08	7.27	4.8
PG	PG6	2	CBCT	X	NM	1	67.52	12.6	4.48	6.09	4.49
AVERAGE							80.87	15.98	5.35	6.72	4.71
SD±							11.96	2.09	0.80	0.43	0.29

GROUP	Operator ID	Session	Image	Tooth Type	MAG	CANALS	Volume removed mm³	Time taken (mins)	MB WIDTH (mm)	DEPTH (mm)	MD WIDTH (mm)
GP	GP1	1	CBCT	X	M	1	89.45	24.78	6.01	7.89	5.12
GP	GP2	1	CBCT	X	NM	0	90.01	30.1	7.01	9.67	5.98
GP	GP3	1	CBCT	X	NM	0	93.35	29.87	7.23	8.99	5.19
GP	GP4	2	CBCT	X	NM	0	72.09	30.1	6.67	7.7	5.23
GP	GP5	2	CBCT	X	M	0	82.6	25.6	6.34	7.67	4.98
GP	GP6	2	CBCT	X	NM	1	89.29	23.3	7	8.89	5.3
AVERAGE							86.13	27.29	6.71	8.47	5.30
SD±							7.72	3.08	0.46	0.83	0.35

Tooth Y

GROUP	Operator ID	Session	Image	Tooth Type	MAG	CANALS	Volume removed mm³	Time taken (mins)	MB WIDTH (mm)	DEPTH (mm)	MD WIDTH (mm)
ET	ET1	2	IOPA	Y	M	0	89.34	27.9	6.17	8.26	5.23
ET	ET2	2	IOPA	Y	M	1	75.78	11.2	5.56	8.73	6.14
ET	ET3	2	IOPA	Y	M	1	56.56	14.2	5.78	8.98	4.95
ET	ET4	1	IOPA	Y	M	1	78.77	10	5.77	8.51	6.23
ET	ET5	1	IOPA	Y	M	1	52.49	13.3	6.45	8.85	4.95
ET	ET6	1	IOPA	Y	M	1	96.45	28.5	6.17	8.6	5.18
AVERAGE							74.89	17.52	5.98	8.66	5.45
SD±							17.48	8.41	0.33	0.26	0.58

GROUP	Operator ID	Session	Image	Tooth Type	MAG	CANALS	Volume removed mm³	Time taken (mins)	MB WIDTH (mm)	DEPTH (mm)	MD WIDTH (mm)
PG	PG1	2	IOPA	Y	M	0	80.56	26.2	5.43	9.71	5.6
PG	PG2	2	IOPA	Y	NM	0	78.23	39.5	5.7	9.3	6.48
PG	PG3	2	IOPA	Y	NM	1	86.3	20.3	5.79	9.98	5.59
PG	PG4	1	IOPA	Y	NM	0	75.17	43.2	5.1	9.01	6.03
PG	PG5	1	IOPA	Y	M	1	89.5	20.3	5.48	8.93	4.72
PG	PG6	1	IOPA	Y	NM	0	79.37	25.3	5.36	8.98	5.3
AVERAGE							81.52	29.13	5.48	9.32	5.62
SD±							5.35	9.85	0.25	0.44	0.60

GROUP	Operator ID	Session	Image	Tooth Type	MAG	CANALS	Volume removed mm³	Time taken (mins)	MB WIDTH (mm)	DEPTH (mm)	MD WIDTH (mm)
GP	GP1	2	IOPA	Y	M	0	83.67	32.7	6.62	9.24	5.67
GP	GP2	2	IOPA	Y	NM	0	54.02	21.7	6.27	6.78	4.35
GP	GP3	2	IOPA	Y	NM	0	85.47	27.2	6.37	9.12	6.37
GP	GP4	1	IOPA	Y	NM	0	58.36	22.2	6.45	7.45	4.35
GP	GP5	1	IOPA	Y	M	0	62.75	25.7	5.67	7.89	4.56
GP	GP6	1	IOPA	Y	NM	0	75.87	26.4	6.54	9.95	6.45
AVERAGE							70.02	25.98	6.32	8.405	5.29
SD±							13.45	3.99	0.34	1.22	0.99

GROUP	Operator ID	Session	Image	Tooth Type	MAG	CANALS	Volume removed mm³	Time taken (mins)	MB WIDTH (mm)	DEPTH (mm)	MD WIDTH (mm)
ET	ET1	1	CBCT	Y	M	1	78.34	20.1	5.32	7.55	4.13
ET	ET2	1	CBCT	Y	M	1	66.47	10.3	5.21	7.37	4.17
ET	ET3	1	CBCT	Y	M	1	50.14	12.7	5.02	7.24	4.3
ET	ET4	2	CBCT	Y	M	1	67.75	7.9	5.29	7.05	3.98
ET	ET5	2	CBCT	Y	M	1	48	12.4	5.55	7.65	4.3
ET	ET6	2	CBCT	Y	M	1	76.3	21.9	4.88	8.15	3.99
AVERAGE							64.5	14.22	5.21	7.50	4.15
SD±							12.84	5.56	0.24	0.38	0.14

GROUP	Operator ID	Session	Image	Tooth Type	MAG	CANALS	Volume removed mm³	Time taken (mins)	MB WIDTH (mm)	DEPTH (mm)	MD WIDTH (mm)
PG	PG1	1	CBCT	Y	M	1	70.23	17.1	5.01	8.03	4.01
PG	PG2	1	CBCT	Y	NM	1	69.56	29.2	5.45	7.98	6.46
PG	PG3	2	CBCT	Y	NM	1	76.35	12.3	5.58	8.12	4.33
PG	PG4	2	CBCT	Y	NM	1	68	29.2	7.35	7.98	7.2
PG	PG5	2	CBCT	Y	M	1	87.58	11.3	5.4	7.95	4.6
PG	PG6	2	CBCT	Y	NM	1	69.75	16.1	5.1	8.35	3.9
AVERAGE							73.58	19.2	5.65	8.07	5.08
SD±							7.44	8.05	0.86	0.15	1.39

GROUP	Operator ID	Session	Image	Tooth Type	MAG	CANALS	Volume removed mm³	Time taken (mins)	MB WIDTH (mm)	DEPTH (mm)	MD WIDTH (mm)
GP	GP1	1	CBCT	Y	M	1	68.95	26.45	5.78	7.88	5.2
GP	GP2	1	CBCT	Y	NM	0	63.78	28.4	7.21	8.23	6.12
GP	GP3	1	CBCT	Y	NM	1	65.02	18.2	5.12	7.98	4.98
GP	GP4	2	CBCT	Y	NM	0	67.75	27.4	5.34	8.9	3.98
GP	GP5	2	CBCT	Y	M	0	75.89	30.12	6.65	9.85	5.98
GP	GP6	2	CBCT	Y	NM	1	66.76	18.2	5.32	8.55	4.95
AVERAGE							68.03	24.9	5.90	8.57	5.20
SD±							4.28	5.25	0.84	0.73	0.78

Tooth Z

GROUP	Operator ID	Session	Image	Tooth Type	MAG	CANALS	Volume removed mm³	Time taken (mins)	MB WIDTH (mm)	DEPTH (mm)	MD WIDTH (mm)
ET	ET1	2	IOPA	Z	M	0	88.45	24.2	6.23	8.27	4.54
ET	ET2	2	IOPA	Z	M	1	65.34	13.24	5.65	7.89	4.38
ET	ET3	2	IOPA	Z	M	1	73.25	26.3	6.57	8.85	3.98
ET	ET4	1	IOPA	Z	M	0	60.24	11.9	5.23	7.33	4.13
ET	ET5	1	IOPA	Z	M	1	84.91	26.3	7.65	8.85	3.91
ET	ET6	1	IOPA	Z	M	1	96.2	27.35	6.75	8.5	4.13
AVERAGE							78.06	21.54	6.35	8.28	4.18
SD±							12.16	7.20	0.93	0.65	0.27

GROUP	Operator ID	Session	Image	Tooth Type	MAG	CANALS	Volume removed mm³	Time taken (mins)	MB WIDTH (mm)	DEPTH (mm)	MD WIDTH (mm)
PG	PG1	2	IOPA	Z	M	1	87.25	38.35	5.65	9.98	4.99
PG	PG2	2	IOPA	Z	NM	0	78.65	20.67	5.99	8.01	5.45
PG	PG3	2	IOPA	Z	NM	0	73.87	23.5	5.89	7.78	4.34
PG	PG4	1	IOPA	Z	M	0	75.15	22.7	4.35	8.84	4.41
PG	PG5	1	IOPA	Z	M	0	109.83	45.3	5.55	10.57	4.89
PG	PG6	1	IOPA	Z	NM	0	71.42	27.2	5.7	8.91	4.35
AVERAGE							82.69	29.62	5.52	9.02	4.73
SD±							14.85	11.02	0.65	1.21	0.45

GROUP	Operator ID	Session	Image	Tooth Type	MAG	CANALS	Volume removed mm³	Time taken (mins)	MB WIDTH (mm)	DEPTH (mm)	MD WIDTH (mm)
GP	GP1	2	IOPA	Z	M	0	85.36	23.8	4.56	7.31	5.74
GP	GP2	2	IOPA	Z	NM	0	78.47	22.1	5.28	7.13	5.35
GP	GP3	2	IOPA	Z	NM	0	93.29	24.7	5.89	8.03	4.55
GP	GP4	1	IOPA	Z	NM	0	80.3	20.2	5.56	7.95	4.9
GP	GP5	1	IOPA	Z	M	0	96.34	23.5	5.8	8.95	4.36
GP	GP6	1	IOPA	Z	NM	0	89.34	24.2	4.89	7.88	5.35
AVERAGE							87.18	23.08	5.33	7.87	5.04
SD±							7.85	1.75	0.53	0.71	0.56

GROUP	Operator ID	Session	Image	Tooth Type	MAG	CANALS	Volume removed mm³	Time taken (mins)	MB WIDTH (mm)	DEPTH (mm)	MD WIDTH (mm)
ET	ET1	1	CBCT	Z	M	1	92.28	19.13	5.24	9.29	4.12
ET	ET2	1	CBCT	Z	M	1	62.45	13.2	5.35	8.99	3.57
ET	ET3	1	CBCT	Z	M	1	50.02	19.5	4.48	8.25	3.25
ET	ET4	2	CBCT	Z	M	1	57.34	13.2	5.54	8.1	3.6
ET	ET5	2	CBCT	Z	M	1	50.35	19.5	4.43	7.94	3.54
ET	ET6	2	CBCT	Z	M	1	93.22	25.34	5.31	9.96	4.23
AVERAGE							67.61	18.31	5.05	8.75	3.71
SD±							17.44	3.38	0.51	0.591	0.31

GROUP	Operator ID	Session	Image	Tooth Type	MAG	CANALS	Volume removed mm³	Time taken (mins)	MB WIDTH (mm)	DEPTH (mm)	MD WIDTH (mm)
PG	PG1	1	CBCT	Z	M	1	71.26	23.34	4.76	8.18	4.58
PG	PG2	1	CBCT	Z	NM	0	112.93	27.67	5.3	10.03	4.73
PG	PG3	1	CBCT	Z	NM	0	99.87	29.7	5.79	9.98	5.36
PG	PG4	2	CBCT	Z	M	1	118.73	20.2	6.23	10.24	5.54
PG	PG5	2	CBCT	Z	M	1	71.26	18.1	4.42	8.18	4.58
PG	PG6	2	CBCT	Z	NM	0	81.13	22.5	5.32	7.33	5.63
AVERAGE							92.53	23.5	5.30	8.99	5.07
SD±							22.55	4.88	0.73	1.04	0.45

GROUP	Operator ID	Session	Image	Tooth Type	MAG	CANALS	Volume removed mm³	Time taken (mins)	MB WIDTH (mm)	DEPTH (mm)	MD WIDTH (mm)
GP	GP1	1	CBCT	Z	M	0	99.37	29.7	4.35	8.99	5.46
GP	GP2	1	CBCT	Z	NM	0	93.29	30.6	5.14	9.15	5.75
GP	GP3	1	CBCT	Z	NM	0	110.47	29.9	4.98	9.29	4.87
GP	GP4	2	CBCT	Z	NM	0	90.5	34	5.34	9.95	5.34
GP	GP5	2	CBCT	Z	M	0	112.67	28.3	5.5	9.35	4.95
GP	GP6	2	CBCT	Z	NM	0	98.75	29.4	4.5	8.95	5.75
AVERAGE							100.84	30.31	4.96	9.28	5.35
SD±							9.97	2.12	0.44	0.36	0.36

Appendix VI Non-thesis learning activities, publication, presentations and positions of responsibility

Non-thesis learning activities completed:

- **Postgraduate certificate (PG Cert) in Dental Cone Beam CT Radiological Interpretation (Kings College London):** Part-time distance learning qualification over 1 year. Physics, anatomy and interpretation delivered by lecture, self-study, face to face, summative and formative assessment. (60 Credits = 30 ECTS Credits) (January-September 2018)
- **DDUH Postgraduate research seminars (2 day events)**: 2017, 2018, 2019, 2021, 2022
- **British Society of Maxillofacial Dental Radiology (BSMFDR):** Annual Scientific Meeting (2017, 2018, 2019, 2021)
- **International Congress of Dento-Maxillo-Facial Radiology:** 22nd International Congress of Dento-Maxillo-Facial Radiology and the 70th Annual Session of the American Academy of Oral and Maxillofacial Radiology, Philadelphia USA (August 2019)
- **International Association of Dental Research (IADR):** Irish Division Annual Scientific Meeting, Cork, Ireland, October 2019

Publications and Presentations

- **International peer reviewed publications from this doctorate:**

- MCGUIGAN MB, DUNCAN HF, HORNER K: An analysis of effective dose optimisation and its impact on image quality and diagnostic efficacy relating to dental cone beam computed tomography (CBCT). Swiss Dent J 128(4): 297-316 (2018).
  PMID: 29589667
- MCGUIGAN MB, THEODORAKOU C, DUNCAN HF, DAVIES J, SENGUPTA A, HORNER K: An investigation into dose optimisation for imaging root canal anatomy using cone beam CT. Dentomaxillofac Radiol 49(7): 20200072 (2020).
  PMID: 32464075

- **Oral research presentations from this doctorate:**

- MCGUIGAN MB (2018) Dose optimization, image quality and operator decision-making relating to dental cone beam computed tomography (CBCT). DDUH Research Seminar Series: May 2018
- MCGUIGAN MB (2018) Dose optimization and diagnostic efficacy relating to dental cone beam computed tomography (CBCT). Postgrdauate Hatton prize

competition. Irish Division of the IADR Annual Scientific Meeting, Cork, Ireland October 2019.

- **MCGUIGAN MB** (2019) Establishment of a threshold dose for root canal anatomy imaging using cone beam: 22nd International Congress of Dento Maxillo-Facial and the 70th Annual Session of the American Academy of Oral and Maxillofacial Radiology, Philadelphia USA: August 2019

- **Invited external oral presentations related to this doctorate:**
- **MCGUIGAN MB** (2022) Does the enhanced diagnostic accuracy of CBCT translate into a positive impact on patient outcome: Irish Endodontic Society Annual Scientific Meeting, Dublin, Ireland: May 2021
- **MCGUIGAN MB** (2022) HIQA Compliance for Installations Providing Medical Exposures to Ionising radiation: Irish Endodontic Society annual scientific meeting: Dublin, Ireland: May 2021

- **Invited internal oral presentations related to this doctorate:**
- **MCGUIGAN MB** (2020) HIQA and EPA Compliance in DDUH: Staff training week, DDUH Dublin Ireland: December 2020
- **MCGUIGAN MB** (2021) Clinicains role in optimisation in DDUH: Staff Training week, DDUH, Dublin, Ireland, April 2021
- **MCGUIGAN MB** (2022) Video: Compliance in DDUH: Referral through to reporting. Training week, DDUH Dublin Ireland: September 2022

Positions of responsibility related to radiology and this doctorate:
- Clinical Teacher in Radiology, DDUH (3rd, 4th year undergraduate Dental Science, 2017-present).
- Member Irish Dental Council subcommittee on 'Radiation Protection and Education' (2020-present).
- HIQA inspection working group, DDUH (2020-present)
- Radiation Protection Liaison Practitioner, DDUH (2020-present)

Appendix VII Publications

An analysis of effective dose optimization and its impact on image quality and diagnostic efficacy relating to dental cone beam computed tomography (CBCT)

Article in Swiss Dental Journal · March 2018

3 authors, including:

Margarete McGuigan
Trinity College Dublin
5 PUBLICATIONS   **234** CITATIONS

SEE PROFILE

Henry Fergus Duncan
Trinity College Dublin
113 PUBLICATIONS   **1,958** CITATIONS

SEE PROFILE

Some of the authors of this publication are also working on these related projects:

Vital pulp therapy View project

PRILE guidelines View project

Margarete B McGuigan[1]
Henry F Duncan[2]
Keith Horner[3]

[1] Division of Oral and Maxillo-
facial Surgery, Medicine,
Pathology & Radiology, Dublin
Dental University Hospital,
Trinity College Dublin, Lincoln
Place, Dublin 2, Ireland
[2] Division of Restorative
Dentistry & Periodontology,
Dublin Dental University
Hospital, Trinity College
Dublin, Lincoln Place,
Dublin 2, Ireland
[3] School of Dentistry, University
of Manchester, UK

CORRESPONDENCE
M B McGuigan
Dublin Dental University
Hospital
Trinity College Dublin
University of Dublin
Lincoln Place
Dublin 2
Ireland
Tel. +353 (1) 6127356
Fax +353 (1) 6127297
E-mail: Margarete.McGuigan@
dental.tcd.ie

An analysis of effective dose optimization and its impact on image quality and diagnostic efficacy relating to dental cone beam computed tomography (CBCT)

SUMMARY

The potential of high resolution, three-dimensional (3D) images which overcome limitations such as superimposition and anatomical noise of two-dimensional (2D) conventional imaging, has made cone beam computed tomography (CBCT) an increasingly popular imaging modality in many dental applications. It is in light of the increasingly prevalent use of CBCT, particularly in a primary dental care setting, that the goal of this review is to investigate what evidence-based guidance is available to the clinician to justify and reduce radiation risk of this higher dose imaging modality while maintaining diagnostically acceptable images. To this end, the literature on radiation dose and related patient risk was comprehensively investigated, before an analysis of the ways in which dose can be optimized and the implications that optimization has on image quality was discussed. Finally, although it is accepted that CBCT has the potential to improve diagnosis, it is uncertain if its use has positive ramifications on issues of diagnostic efficacy, including clinical decision-making and patient outcome. In order to investigate these issues, the levels of evidence of the existing studies and their validity were assessed. On review of the available literature, it is evident that there is limited practical advice available to dentists regarding dose optimization and any existing protocols may not be readily transferable to every CBCT machine, the manufacturers' role is not often conducive to dose limitation and that the bulk of evidence is at lower levels of evidence. Furthermore, there is minimal supporting evidence to suggest an impact of CBCT on diagnostic thinking and consequent choice of treatment and no evidence of a positive effect of CBCT on patient outcome.

Introduction

Since its introduction in the 19th century, dentomaxillofacial radiology (DMFR) has relied on two-dimensional (2D) imaging, with more recent advancements in radiographic film and digital radiography offering lower doses and faster image production. Conventional 2D radiographs, however, are limited by superimposition, distortion, magnification and misrepresentation of structures (Scarfe & Farman 2008) with planar 2D interpretation of the three-dimensional (3D) maxillofacial anatomy creating a superimposed image, which prevents optimal visualization due to overlaying structures (Kiljunen et al. 2015). The introduction in medicine of computed tomography, later followed by cone beam computed tomography (CBCT) (Robb 1982), heralded the clinical progression from 2D to 3D images generated by computer-enabled reconstruction of the acquired data.

Dental CBCT was introduced commercially in Europe in 1999 (Mozzo et al. 1998; Arai et al. 1999) and has since its inception become an increasingly popular imaging modality with a recent report indicating that there are at least 47 different devices (from 20 companies) commercially available in Europe (Nemtoi et al. 2013). Rapid advances in detector technology and computer software systems able to handle large volumes of data has propelled the evolution from initial basic prototypes into faster, more sophisticated imaging tools targeted at specific clinical applications (e.g. small volume scanners used in endodontics: Accuitomo 3D; J. Morita Corporation, Kyoto, Japan). CBCT certainly offers a significant benefit over conventional CT imaging by allowing high resolution 3D visualization of the maxillofacial skeleton with adjustable field of views (FOV) sizes and concomitant reduction in patient dose (Schulze et al. 2004). This 3D visualization offers a wide range of potential applications within dentistry, primarily aimed at examination of the hard tissues as well as the various sinuses and air cavities of the maxillofacial region (De Vos et al. 2008); however, CBCT appears to be of limited value for soft tissue evaluation due to limited low-contrast resolution (Scarfe & Farman 2008). Common dental applications include implant planning, maxillofacial surgery, endodontics and orthodontics (Alamri et al. 2012); but use must be tempered by the understanding that the effective dose of CBCT is significantly higher than traditional intraoral periapical radiography (IOPA) and panoramic radiography (Roberts et al. 2009). CBCT is also limited by a relatively large degree of noise and artefacts on imaging of high density tissues and metal objects due to scatter, beam hardening and photon starvation (Schulze et al. 2011). Given the explosion of higher-dose CBCT imaging in dentistry there is certainly an evolving need for robust, evidence-based directives and guidelines on selection criteria and specific dose optimization protocols in key procedures (Horner et al. 2013, 2015). The widespread and increasing use of CBCT in dental practice (Berg et al. 2014; Dölekoğlu et al. 2011; Hol et al. 2015) has raised other concerns, with a shift in reporting responsibilities from radiologists to dentists who may not be appropriately trained to interpret all the structures visible on the CBCT scan (Parashar et al. 2012). As a result, the European Academy of DMFR (EADMFR) has highlighted the lack of dental undergraduate (and perhaps postgraduate) training in this novel evolving technology and has recommended appropriate training in justification, acquisition and interpretation of CBCT imaging (Brown et al. 2014).

CBCT offers clear advantages in 3D visualization and diagnostic accuracy (Patel et al. 2009; Matzen et al. 2013), which are reflected in guidelines advocating its use in specific clinical applications (European Commission 2012; ESE 2014). Notably, questions remain as to what quantifiable impact 3D imaging has in modifying diagnosis, treatment planning and outcome when compared with conventional radiography. As health care professionals, we must consider if the benefit of CBCT imaging outweighs the associated radiation risks for each individual patient.

Consequently, the aim of this review is to understand radiation risk which involves quantification of dose and an appreciation of dosimetry techniques and their limitations. Reduction of this risk through processes of justification and optimization will be addressed. Specifically, the parameters that can influence CBCT dose will be explored in conjunction with measures and protocols to aid the operator in achieving dose optimization while investigating what impact this has on image quality for a range of diagnostic tasks. Finally, the impact of CBCT on decision-making and treatment outcome will be accessed and gaps in our knowledge highlighted.

Materials and Methods

A comprehensive MEDLINE search up to May 2017 was conducted using various medical subject headings (MeSH) in combination with "and" or "or". The major MeSH terms searched were "Radiography, Dental", "Tomography, X-Ray", "Diagnostic Imaging" and "Radiographic Image Enhancement" in combination with a series of related subheadings. In addition, the following terms were added "optimization" and "CBCT". Bibliographies of all relevant papers and previous review articles were hand-searched. Any relevant work published in the English language and presenting pertinent information related to this review was considered for inclusion. Titles were generally excluded if they were conference reports or if aspects of CBCT were discussed that were not the subject of the current review.

Review

Optimization in CBCT involves quantification of the radiation dose and risk for patients, while assessing the impact on image quality for specific diagnostic tasks. In order to fully consider CBCT optimization, this review will analyse the literature on dose and risk as well as the impact of optimization on image quality and diagnostic efficacy of CBCT.

Radiation Damage and Protection

Each radiological exposure involves interaction of body tissues with ionizing radiation and therefore carries the potential of permanent alteration in cellular DNA with the ultimate risk of latent tumour formation and hereditable effects. This chance happening is described as a stochastic effect, where the magnitude of risk is believed to be proportional to the radiation dose; notably there is no threshold dose below which these effects will not occur (IRCP 2007). Furthermore, risk is sex and age dependent, being greatest for children (10-year-old 3× higher risk than 30-year-old) and up to 40% more for females than males (IRCP 1990; European Commission 2012).

Practitioners should be aware of the potential effects of ionizing radiation and understand the increased doses attributable to CBCT imaging, this reinforcing the importance of strict adherence to the IRCP principles of justification and optimization (IRCP 2007). Indeed, the preliminary process of justification can be the most effective means of dose reduction particularly for young children and adolescents. Guidance documents and position statements provide a framework for selection criteria to ensure CBCT scans are prescribed appropriately, ensuring a net poten-

tial benefit to the patient. Therefore, in general, guidelines do not advocate CBCT as a routine imaging tool but only when an alternative reduced-dose imaging technique is diagnostically insufficient (Horner et al. 2009; European Commission 2012; FGDP [UK] 2013; ESE 2014; SADMFR 2015 [Dula et al. 2015]); however, routine use of CBCT has been recommended by some (Drago & Carpentieri 2011; Noffke et al. 2011) but not all groups in implant dentistry. Valid guideline documents should be extracted from the evidence base rather than relying solely on expert opinion and general consensus; however, a recent review (Horner et al. 2015) identified only two evidence-based guidance documents at the time of publication (European Commission 2012; AWMF 2013). This review (Horner et al. 2015) highlights the need for more rigorous and consistent reporting of guidelines, free of potential bias, facilitated by the use of the AGREE 11 (Appraisal of Guidelines for Research & Evaluation 11) instrument. That said, it is recognized that evidence-based guidelines can only reflect the validity of the research that exists. The inherent difficulties of achieving studies at higher hierarchical levels of diagnostic efficacy are discussed subsequently.

Optimization is defined as maintaining doses at levels which are "as low as reasonably achievable" (ALARA), while ensuring that images are still of diagnostic quality (IRCP 2007). Broad guideline documents serve to direct the practitioner in achieving this goal of minimizing patient exposure while achieving the diagnostic information required. Optimization involves a range of factors, from maintenance and selection of equipment most suited to clinical/imaging needs of patient base, selection of the appropriate exposure parameters (Tab. I), limitation of the exposed volume to use of shielding devices and establishing a dose reference level (DRL) (European Commission 2012; HPA 2010). The inherent difficulty of creating a standardized optimization protocol in CBCT imaging relates to the range of clinical protocols and diversity of available CBCT systems. The clinician's expectation of high resolution and "visually pleasing" CBCT images, perhaps without due consideration of dose implications, has prompted the adoption of a modification of the ALARA principle. The concept of "as low as diagnostically acceptable" (ALADA) acknowledges the link between dose and image quality and encourages the minimum exposure possible for the specific diagnostic task (White et al. 2014). The ALADA principle evolved from the drive to increase radiation protection in paediatric populations associated with the increased awareness of their sensitivity to diagnostic radiation (Theodorakou et al. 2012; Pauwels et al. 2014a; White et al. 2014; Hidalgo Rivas et al. 2015; Hall & Brenner 2008).

What Do We Understand by Patient Dose?

Patient dose monitoring is an essential part of quality assurance (QA) to ensure doses are kept as low as reasonably achievable and allow comparison to DRLs (European Commission 2004). DRLS do not indicate the desired dose level for a specific diagnostic task but instead define a reference dose or threshold above which operators should investigate the potential for dose reduction measures (Yu et al. 2009). Dosimetry is also essential to study the radiation-induced risk of different types of diagnostic imaging examinations enabling comparison of imaging modalities/devices which can influence directives on justification and dose reduction strategies.

Absorbed dose (D_T) describes the amount of energy absorbed from the radiation beam per unit mass at a site of interest. The SI unit for this is the gray (Gy) representing one joule per kilogramme but the milligray (mGy) is more appropriate in the context of diagnostic imaging (White & Pharoah 2013). Although useful for quality control purposes (IRCP 2007), radiation absorbed dose gives no indication of stochastic risk. A complicating factor when considering "dose" of radiation is that different types of radiation have different biological effectiveness, in terms of their potential to cause damage. Particulate radiation (high-energy protons, neutrons, alpha particles) cause greater damage than X-rays. Thus, an absorbed dose of 1 mGy from X-rays would give less damage to tissues than 1 mGy from high-energy proton radiation. The differing radiobiological effectiveness of different types of radiation is taken into account by attributing a radiation weighting factor (W_R) to the absorbed dose, resulting in the concept of equivalent dose (H_T), which can be calculated as: $D_T \times W_R$. Fortunately, the W_R of X-rays is 1, but the SI unit of equivalent dose is changed from the gray to the sievert (Sv).

Effective dose (E) (recommended by The International Commission on Radiological Protection [IRCP]) is a more relevant index when considering patient dose. It enables a measure of radiation risk from different exposures of ionizing radiation to various body tissues/organs which exhibit a range of radiosensitivities. Specifically, it is calculated as a product of the equivalent doses to the irradiated tissues and the tissue weighting factor (W_T) (which reflects the degree of sensitivity of each of the tissues to radiation and relative contribution to overall risk). These weighted doses are then summed to deliver the effective dose, which is typically expressed in millisieverts (mSv) or microsieverts (µSv). $E = \Sigma W_T \times H_T$. Importantly, effective dose allows an approximate comparison of radiation-induced risk among different types of examinations. Thus, it becomes possi-

Tab. I	The effects of exposure and image quality parameters on dose and image quality				
	Exposure and image parameters				
	↑ kV	↑ mAs	↓ FOV	↓ Voxel size	↑ No of projections
Dose	↑	↑	↓	↑ is device dependent	↑
Spatial resolution	X	X	X	↑	↑
Contrast	↓	X	↑	X	X
Noise	↓	↓	↓	↑	↓
Artefacts	↓ Beam hardening	X	↑ Truncation artefact	X	X

ble to compare the radiation-associated risk of, for example, an intraoral radiograph with a chest radiograph or a CT scan of the abdomen.

The most recent tissue weighting factors are provided by the IRCP (IRCP 2007) which revised the existing figures from 1990 (IRCP 1990). Particularly relevant to dental imaging, new tissue weighting factors for salivary glands, oral mucosa, lymph nodes and brain have been included (EUROPEAN COMMISSION 2012). This updating of tissue weighting factors results in a 10% increase in the weighting ascribed to tissues located in the maxillofacial region. Being a relatively recent imaging modality, most CBCT dosimetry research studies have used the updated tissue weighting factors but along with the variation in CBCT device parameters it is worth considering these issues when comparing dose estimations from different studies.

How is Dose Quantified?

In order to compare radiation risk between different types of examination, effective dose is considered the most appropriate metric. Since effective dose cannot be measured directly in vivo, it is only possible to quantify it in laboratory studies or by computer modelling. Traditionally, ascertaining the dosimetry necessary for the calculation of effective dose involved the use of anthropomorphic phantoms constructed from materials that have comparable X-ray attenuation characteristics to human tissue. Multiple thermoluminescent dosimeters (TLDs) are distributed throughout the phantom (position dependent on tissues to be evaluated) to allow for accurate measurement of absorbed dose. Notably, no standards have been set as to the number or locations of the TLDs, often leading to low reproducibility of this technique (LUDLOW ET AL. 2006, 2015; PAUWELS ET AL. 2012A). This fact, compounded by the use of a range of phantoms have resulted in studies that are not readily comparable and highlights the need for a standardized method of dose measurements to enable comparison between studies (PAUWELS ET AL. 2012A).

Computed dose simulations using virtual phantoms have been developed. These virtual phantoms potentially negate the need for the laborious task of repeated dosimetry on standard adult or paediatric phantoms, which do not allow for consideration of population variation in size (KOIVISTO ET AL. 2012; MORANT ET AL. 2012). This technique allows simulation of the interaction of radiation with matter and provides a quick way of modelling the multitude of potential variations within imaging systems and patients. It has been widely used in radiotherapy dosimetry but has also been used in a small number of dental CBCT studies (STRATIS ET AL. 2016; EZELDEEN ET AL. 2017). Appraisal of the use of virtual phantoms with Monte Carlo simulation of exposure as a dependable replacement for anthropomorphic phantoms suggests that further development of virtual phantoms is necessary (ZHANG ET AL. 2013).

Neither laboratory studies using phantoms nor complex computer modelling has direct use in clinical situations. For measuring dose in clinical facilities, particularly for dose audits, alternative measures are needed from which effective dose can be estimated. In the context of dental CBCT, examples of these include dose area product (DAP), also known as kerma area product (KAP). This is a simple, less laborious technique for indirectly estimating effective dose. DAP is defined as the air collision kerma integrated over the beam area. It can be measured using a DAP meter (calibrated ionization chamber that measures dose and beam size at a fixed point). Additionally, DAP

can be available via machine output data (determined computationally, based on the X-ray tube output and field size settings), however, these data can be unreliable and calibration is required (AL-OKSHI ET AL. 2017). Measured DAP values can then be converted to effective dose using conversion factors (KIM ET AL. 2014). There are conflicting opinions as to the accuracy of this dose index in the calculation of effective dose. DAP has been recommended for establishing achievable doses and, possibly, diagnostic reference levels and is described as relating "reasonably well" with effective dose (HOLROYD & WALKER 2010; EUROPEAN COMMISSION 2012). However, the central point of the scan is not always in the centre of the clinical area of interest and patient dose measurements could be either underestimated or overestimated. It has been demonstrated that within a small field of view (FOV), although effective doses exhibited a threefold change over three separate locations, DAP remained unchanged (LUDLOW 2009). Additionally, an average of 35% absolute error in calculation of the effective dose resulted when using DAP, even when using conversion factors specific for FOV size, arch location and patient type (KIM ET AL. 2014). Furthermore, it was concluded that since imaging factors (FOV size and positioning) govern the actual distribution of dose throughout the patient, generally it would not be possible to link DAP values to patient effective doses (PAUWELS ET AL. 2012A). Accepting its limitations (LARSSON ET AL. 1996; LUDLOW & IVANOVIC 2008) and being aware that its precision as a measure of risk is questionable (LUDLOW ET AL. 2015), it was reported that DAP could be used to assess dose reduction strategies and compare the results from different CBCT units (LOFTHAG-HANSEN 2010; GOULSTON ET AL. 2016).

Interestingly, use of dose height product (DHP) in place of area resulted in statistically improved accuracy in the estimation of effective dose, with a reduction in absolute error to 19% from 35% evidenced with DAP (LUDLOW ET AL. 2015). Ludlow theorized that DHP may correlate more with effective dose than DAP due to the nature of the vertical distribution of radiosensitive organs. Therefore, an increase in height of the FOV results in new and potentially radiosensitive tissues being brought into the area of direct exposure, while an increase in beam width merely results in an increased dose to tissues that are already being exposed. It was concluded that the use of DHP as a means of estimating effective dose merits further investigation (LUDLOW ET AL. 2015). CT dose index volume (CDTI) is the international assessment metric used to measure the radiation output of CT scanners. Studies have revealed that CDTI measurement methodology does not accommodate the cone shaped beam of CBCT and the larger FOVs (MORI ET AL. 2005).

It has been established that owing to its unique exposure geometry (eliciting a dose distribution which can be asymmetrical and exhibits a strong dose gradient outside the primary beam), CBCT requires a specific dose index that copes with differences in FOV, diameter, positioning and varying degrees of rotation arc (PAUWELS ET AL. 2012C). Alternative dose indices have been explored by the SEDENTEXCT team but further work is necessary to establish if such indices are appropriate for establishing DRLs (EUROPEAN COMMISSION 2012).

What Are the Reported CBCT Doses and How Does CBCT Compare to Conventional Radiography?

The effective dose ranges quoted for CBCT reflect the range of devices and imaging protocols (collimation of the cone beam, exposure factors, image quality parameters), in addition to the

location of the radiation field with respect to the radiosensitive organs, which leads to a considerable difference in absorbed dose for all organs in the head and neck region (Pauwels et al. 2012a; Theodorakou et al. 2012; Bornstein et al. 2014; Pauwels et al. 2014a; Ludlow et al. 2015). As a result of this diversity between devices, it is not possible in the field of CBCT to establish a single average effective dose when making comparisons to conventional 2D radiography and multi-slice CT (MSCT) (Pauwels et al. 2012a). Effective dose for CBCT has been quoted in tens to several hundred μSv, demonstrating a twenty-fold range (Pauwels et al. 2012a; European Commission 2012; Pauwels et al. 2014a; Ludlow et al. 2015). If effective dose calculations are categorised by FOV size (see optimization section), dose ranges have been demonstrated using a broad selection of devices such as: small FOV: 19–44 μSv, medium FOV: 28–265 μSv and large FOV: 68–368 μSv (Pauwels et al. 2012). These figures clearly demonstrate the impact of FOV size of which FOV height is believed to be the key determinant of effective dose (Pauwels et al. 2014a). An intraoral periapical radiograph (IOPA) effective dose is quoted as less than 1.5 μSv when all parameters are fully optimized (Ludlow et al. 2008). Reported effective dose ranges for panoramic radiography are 2.7–24.3 μSv and less than 6 μSv for cephalometric radiography (European Commission 2012), this confirming the fact that radiation dose and risk is considerably greater for CBCT than conventional radiography. It is generally accepted that effective doses for CBCT are well below those for common MSCT protocols, with a range of dose being reported as 280–1,410 μSv (European Commission 2012). However, CBCT images with a large FOV and high exposure factors can have comparable dose ranges with low-dose MSCT protocols (Loubele et al. 2009; Suomalainen et al. 2009; Kyriacaou et al. 2011).

The effective dose from a dental CBCT exposure is mainly defined by the absorbed dose of the remainder organs (38%), salivary glands (25%), thyroid gland (19%) and red bone marrow (14%). If the effective dose of a small FOV upper anterior scan (19 μSv) is compared with a lower molar scan (40 μSv), the observed difference in effective dose can be attributed to the increased absorbed dose, particularly of the salivary glands and thyroid gland associated with a mandibular scan (Pauwels et al. 2012a). This variation clearly demonstrates the impact of FOV position relative to the radiosensitive organs on patient dose.

When appropriate child settings are selected, effective doses for children and adolescents (measured in paediatric and adolescent phantoms) have been reported as similar to effective doses measured in adult phantoms; the lowest effective doses reported resulted from small FOV and "small-patient" settings (Theodorakou et al. 2012). In the paediatric phantom, equal contributions to effective dose come from the remainder organs, salivary and thyroid glands. Other studies have reported that, where imaging protocols remained constant (adult setting), the highest absorbed dose was measured in all locations in the small-child phantom and the lowest in the adult phantom which attenuated more radiation due to its increased diameter (Al Najjar et al. 2013; Choi & Ford 2015). An increasing number of paediatric CBCT scans are being performed with indications including impacted teeth, orthodontics and dentomaxillofacial development, highlighting the need for appropriate justification and dedicated paediatric protocols optimized for the imaging task (Choi & Ford 2015; Hidalgo Rivas et al. 2015).

Risk Considerations Related to CBCT

Effective dose was developed for use in radiation protection to provide a measure of overall risk of stochastic effects from diagnostic radiation exposure. However, with regards to CBCT imaging, it is generally measured in a standard phantom, estimating risk for an average-sized adult reference patient. This does not reflect the risk of the individual patient who varies in size and mass with a concomitant variation in dose (Marine et al. 2010; Cassola et al. 2011). This has implications particularly for children, being physically smaller, with more tissue (e.g. brain and thyroid now closer to dental area) in the primary beam and subject to scatter radiation; therefore, absorbed dose to the head and neck regions will be higher if appropriate "child settings" are **not** used (Borisiva et al. 2008; Theodoraku et al. 2012; Al Najjar et al. 2013). Furthermore, this increased risk is compounded by age (owing to their larger proportion of dividing cells and a longer remaining lifespan to express stochastic effects) and gender sensitivity (female risk > male risk) to potential stochastic effects from radiation (IRCP 1990). It was concluded that, since effective dose is not individual-specific, it is not a suitable quantity for individual patient risk estimation but is considered a useful indicator of relative risk when comparing a range of examination protocols or differing imaging modalities (Ludlow et al. 2015). Interestingly, a method to estimate patient-specific dose and cancer risk from CT examinations has been developed by combining a validated Monte Carlo programme with patient-specific anatomical models (Li et al. 2011).

There is continuing debate about the level of risk associated with diagnostic imaging and the validity of the linear-no-threshold model (LNT) of extrapolating cancer risk from higher doses to lower levels of exposure (IRCP 2007; Tubiana et al. 2009). The uncertainty lies with the inherent limitations associated with the studies available for risk analysis of low doses (Pauwels et al. 2014a). Such data includes the life-span study of atomic bomb survivors, which serves as a model for determining cancer risk for low doses (Preston et al. 2007). Additionally, epidemiological studies on the cancer risk of CT scan exposures to the maxillofacial region suggest that increased risks associated with doses applicable to CT are not hypothetical and are independent of extrapolations and modelling. These studies have demonstrated a significant increase in brain cancer and leukaemia among the scanned subjects, the increased incidence being associated with increasing dose and young age at the time of exposure (Pearce et al. 2012; Matthews et al. 2013). These studies support the LNT hypothesis of a proportional increase in cancer risk and heritable defects concomitant with any exposure of radiation above zero. Of note, other dose risk models exist which are diverse from the LNT hypothesis (e.g. radiation hormesis and supralinear models) while others adhere to the principles of the LNT hypotheses while involving a dose and dose-rate effectiveness factor (DDREF) to compensate for the potentially lower biological effectiveness of low doses. However, current literature appears to support the LNT hypothesis (IRCP 2007; Barret et al. 2015).

When considering risk specifically associated with CBCT, it has been estimated that the lifetime attributable risk (LAR) for cancer induction is between 2.7 and 9.8 per million examinations (Pauwels et al. 2014a). Children exhibit the highest cancer risk in this spectrum due to their increased radiosensitivity, which highlights the importance of an understanding of this increased risk by operators and referrers and implementation

of a more rigorous application of the ALARA principle (Horner et al. 2009). These LAR figures were calculated by applying established correlation factors (Pauwels 2012a, 2012b) to measured skin doses on patients receiving CBCT scans to estimate patient organ dose. Individual effective dose was then calculated using tissue weighting factors (IRCP 2007). Finally, lifetime attributable cancer risk was calculated from gender- and age-specific risk factors reported in the Biological Effects of Ionizing Radiation (BEIR) V11 report (National Research Council of the National Academies 2006).

Technical and Imaging Parameters that Influence Dose Optimization

The technical principles and details of CBCT design have been reviewed in detail (Scarfe & Farman 2008; Nemtoi et al. 2013; Kiljunen et al. 2015; Pauwels et al. 2015a). The aim of the current review is to analyse the manner in which technical specifications, optimum selection of exposure and image quality parameters can minimize radiation and risk to the patient, while maintaining image quality and diagnostic accuracy. This aim adheres to the principle of optimization stipulated by the IRCP (IRCP 2007).

CBCT imaging is accomplished using a rotating gantry (similar to a panoramic system) to which an X-ray source and opposing detector are fixed in a C-shaped arm arrangement (Pauwels et al. 2015a). Scanning can be performed in a standing (most common but susceptible to patient movement), sitting or supine position (space-demanding) according to device design or patient requirements. Each unit has a device specific stabilization method to minimise patient motion which can degrade image quality (Spin-Neto et al. 2016; Donaldson et al. 2015). The fundamental principle of X-ray production is similar for two- and three-dimensional imaging modalities, the X-ray tubes differing mainly in the size of the exit window (i.e. collimation), the range of exposure factors and the amount of beam filtration (Pauwels et al. 2015a). Dental CBCT utilizes a cone- or pyramid-shaped X-ray beam, which is directed at the required FOV, the X-ray source and detector rotating around a rotation fulcrum fixed within the centre of the region of interest. Rotation times vary most commonly between 10 and 40 seconds during which the X-ray exposures (at certain degree intervals) result in several hundred 2D projections (raw data) being acquired by the detector. These images have been described as similar to lateral and posterior-anterior cephalometric images, each slightly offset from the other (Scarfe & Farman 2008). Only one rotation sequence is required to acquire sufficient data for image reconstruction as the beam incorporates the entire FOV. This differs from medical CT which uses a fan shaped beam in a helical movement and acquires only individual slices of the FOV at a time.

Exposure Settings

The dose associated with each CBCT scan is affected by exposure parameters; tube operating potential ("voltage"), measured in kilovolt (kV), and tube current exposure time product, measured in milliampere (mA). These parameters are initially determined by the manufacturer, perhaps with an emphasis on delivering images of high quality rather than dose optimization. Some CBCT models have preset exposure settings for differing clinical applications (e.g. endodontic mode) and for patients of different sizes thus enabling a degree of dose and image optimization. Other devices enable the operator to select the kV, mA

and exposure time within a specified range allowing the user the possibility of reducing dose for a smaller patient/child or for a particular diagnostic task. This necessitates operator knowledge and experience and demands evidence-based guidance regarding the impact of exposure parameters on image quality for specific diagnostic tasks. Collaboration of the clinician with a medical physicist and engineer can facilitate further optimization. The use of automatic exposure control (AEC – used in CT imaging) has been introduced in CBCT imaging. The aim of AEC is to automatically modify the tube current to accommodate attenuation differences due to patient size, shape and anatomy, for example when the mA values are varied depending on the density distribution of a scout image (Kalender et al. 1999). In CT, AEC has been found to lead to a significant dose reduction and could negate the need to manually adapt the kV and mA according to patient size (Papadakis et al. 2008).

Current Exposure Time Product (mA)

For the CBCT devices available, tube current ranges from 1 to 32 mA (Kiljunen et al. 2015). Both the tube current and exposure time (seconds) determines the quantity of X-ray photons produced which reach the detector. When other exposure factors are kept constant, a linear relationship exists between current exposure time product (mA) and patient dose i.e. increasing mA values cause a proportional increase in dose. With regards to image quality, an increased mA value decreases image noise by increasing signal at the detector but since the beam penetration remains the same, contrast is unaffected.

Tube Voltage

Typical tube voltages in existing CBCT scanners vary most commonly between 60 and 90 kV (full range 40–120 kV) (Kiljunen et al. 2015). As tube voltage increases, the mean energy/penetrating power but also the quantity of the photons in an X-ray beam increases and, overall, radiation dose is increased (other factors being constant). However, unlike current exposure time product the relationship between tube voltage and dose is not linear. Higher kV values increase the detector signal due to the increased photon count and a decreased absorption ratio. In respect to image quality, at a higher kV value the difference in X-ray attenuation between tissues of differing density is decreased, which can result in a decreased image contrast (Tab. II). Conversely, a lower kV value can lead to increased image contrast with regards to the hard tissue of the maxillofacial region (Drage et al. 2010). However, this dynamic of increased contrast at lower beam energies is not fully translatable to CBCT due to the complementary information of projectional data from many angles (Pauwels et al. 2014b). Nevertheless, there is the potential to decrease the voltage and thus dose while maintaining image contrast, which is especially pertinent for smaller patients/children where less penetrating X-rays (80 kV or less) are required (Yu et al. 2009). A reduced kV value is associated with increased noise; however, the compensating effect of better contrast maintains the contrast-to-noise ratio (CNR) (Karmazyn et al. 2013). With the greater attenuation associated with larger patients and accompanying increase in noise, a greater tube voltage has been recommended (Seigel et al. 2004).

Certainly, optimization by kV and mA reduction below the manufacturer's recommendations has been investigated with maintenance of image quality (objective and subjective), facilitating diagnostic accuracy and significant dose reductions

Tab. II Image quality characteristics

Image quality characteristic	Definition	Determining factors	Characterized by:
Spatial resolution	Ability to discriminate small structures in an image. Especially relevant where depiction of fine detail is critical for diagnosis. Spatial resolution is approx. one order of magnitude lower than that of PR (periapical radiography).	Nominal detector pixel size, fill factor, detector motion blur, grey-level resolution, reconstruction technique applied, patient movement, scatter, imaging parameters (see Tab. I)	Traditionally, assessed visually in line-pairs per millimeter ($lp\,mm^{-1}$). Considering movement and scatter effects, a realistic spatial resolution of $\geq 1\,lp\,mm^{-1}$ has been suggested (HORNER ET AL. 2015) Automated assessment: modulation transfer function (MTF) – the ability of the system to transfer a signal of a given spatial frequency. It is a metric for the objective measurement of spatial resolution in X-ray-based tomographic modalities
Contrast	Ability to distinguish tissues or materials of differing densities. Contrast resolution of CBCT is limited by scattered radiation and FPD-related artefacts (saturation, dark current and bad pixels). CBCT soft tissue contrast is lower than MDCT.	Dynamic range of detector, bit depth of reconstructed images, exposure factors (see Tab. I)	Contrast to noise ratio (CNR) – combines contrast and noise and is a metric of imaging performance with respect to large structures of varying attenuation.
Noise	Scattered radiation that is recorded by pixels on the detector contributes to image degradation. Scatter α total mass of tissue contained within the primary X-ray beam, increasing with object thickness and field size. Additional sources: **Quantum noise:** statistical variations in the homogeneity of the incident X-ray beam. **Electronic noise:** caused by the conversion and transmission of the detector signal.	Exhibits an interdependent relationship with spatial resolution i.e. factors that improve one (e.g. voxel size) degrades the other.	CNR: can be enhanced by changing some parameters during scanning procedure such as the FOV, mA, kV and projection number. However, high-density materials such as metals can cause beam hardening and streak artefact which leads to a decrease in the CNR.
Artefacts	**Inherent artefacts:** – Scatter – Partial volume averaging – Cone-beam effect **Procedure-related artefacts:** – Undersampling **Scanner related artefacts:** – Circular artefact **Introduced artefacts:** – Cupping and extinction artefact – Patient motion artefact	– Capture of scattered photons. – Selected voxel size is larger than size of object being imaged. – Divergence of the X-ray beam means that structues at the top or bottom of the image field or only exposed when X-ray source is on the opposite side of the patient. – Too few basis projections or incomplete scanning trajectory. – Imperfections in scanner detection or poor calibration. – Both of these artefacts are a result of beam hardening (absorption of lower-energy photons in preference to higher-energy photons as the beam passes through a given material and is more pronounced for denser materials i.e. metal) – Patient motion causes misregistration of data, the smaller the voxel size the more marked the effect of patient movement.	– Increased noise, streak artefacts. – "Step appearance" in image or homogeneity of pixel intensity. – Streaking artifacts and greater peripheral noise. – Misregistration of data by reconstruction software (aliasing) resulting in increased image noise and appearance of fine striations radiating from the edge of image moiré pattern. – Circular or ring streaks. – Distortion of metallic structures due to differential absorption. – Streaks and dark bands between two dense objects. – Double contours in the reconstructed image.

FPD – flat panel detector; MDCT – multi-detector computed tomography

Tab. III Studies demonstrating exposure factor reductions that maintained images of diagnostic quality in a range of diagnostic tasks

Study	Diagnostic task	Exposure factors altered	Reference standard	Dosimetry	Recommendation of low–dose protocol	Principle conclusions
KWONG ET AL. 2008	Diagnostic quality of images assessed via questionnaire	– kV – mA	No standard	Not recorded	Not described	– Images at reduced kV and mA generally maintained DA – High observer variation in quantifying image quality
BROWN ET AL. 2009	Orthodontic linear accuracy (LA) study	Exposure time	Dry human skull measurements	Not recorded	Not described	Reduced exposure time (projections) did not reduce DA
SUR ET AL. 2010	Implant planning, identification of relevant anatomic landmarks	– mA – Exposure time by using 180˚ and 360˚ rotations	Reference exposure 80 kVp, 8 mA, 360˚ rotation	Not recorded	Not described	Reducing rotation at 4 mA provided acceptable image quality, image quality at 2 mA provided acceptable image quality only with 360˚ scans.
DURACK ET AL. 2011	Detection of simulated external inflammatory resorption (EIR)	Exposure time by using 180˚ and 360˚ rotations	Reference exposure 90 kVp/3 mA/17.5 s, 360˚ rotation	Not recorded	Not described	Reducing rotation from 360˚ to 180˚ with small FOV reduced exposure time but not DA
LENNON ET AL. 2011	Detection of simulated periapical bone loss	Exposure time by using 180˚ and 360˚ rotations	No standard	Not recorded	Not described	– Reducing rotation from 360˚ to 180˚ reduced exposure time but not DA – Wide range of interobserver variation
AL–EKRISH 2012	Implant planning/dimensional accuracy	Exposure time (three different times)	Dry human skull measurements	Not recorded	Not described	Reliability and dimensional accuracy remain the same with the chosen reductions in exposure time.
HASHEM ET AL. 2013	LA of simulated external inflammatory resorption	Exposure time by using 180˚ and 360˚ rotations	Dry porcine hemimandible measurements	Not recorded	Not described	Reducing rotation from 360˚ to 180˚ produced equally accurate measurements.
WALTRICK ET AL. 2013	Implant planning/LA and visibility of mandibular canal	Exposure time by using 3 different resolution settings	Dry human skull measurements	Not recorded	Not described	All protocols produced an image adequate for measurements and mandibular canal visualization.

MBC – marginal bone crest; CEJ – cementoenamel junction; ED – effective dose; TAT – tooth autotransplantation

Fig. 1 The effect of exposure factors (kV, mA) and choice of exposure parameter (voxel size) on image quality is demonstrated by exposing the 16 region of a dry skull using a ProMax 3D Classic (Planmeca Oy, Finland) CBCT scanner. From exposure A to C, kV, mA values are reduced and voxel size is increased by selecting smaller–patient settings and moving from high–resolution to ultra–low–dose (ULD) settings. Although the image sharpness is reduced, it remains diagnostically acceptable with the identification of the MB2 still possible (exposure C.), illustrating the principle of optimization.

Tab. III Studies demonstrating exposure factor reductions that maintained images of diagnostic quality in a range of diagnostic tasks
<div align="right">continued</div>

Study	Diagnostic task	Exposure factors altered	Reference standard	Dosimetry	Recommendation of low– dose protocol	Principle conclusions
Yadav et al. 2015	Detecting arthritic change in the TMJ	Exposure time with 180˚ and 360˚ rotations	Dry human skulls with simulated soft tissue and artificial joint lesions	Not recorded	Not described	Images were equally diagnostic at 180˚ and 360˚ rotations (other exposure factors remained identical).
Hidalgo Rivas et al. 2015	Evaluation of impacted maxillary canines and possible adjacent resorption in paediatric skull phantom. Objective measure of image quality	– kV – mA	Reference image data sets using highest and lowest exposures possible with device being used	DAP metre	80 kV, 3 mA	Implementation of a low-dose protocol (particular to the single device used in study) could achieve up to a 50% dose reduction while maintaining image quality sufficient for evaluation of impacted maxillary canines. Optimum CNR was achieved at a lower tube voltage than maximum.
Al-Okshi et al. 2017	Assessment of periodontal space at apical third of root, MBC and CEJ. Objective measure of image quality	– kV – mA – Trajectory arc – 180˚, 360˚	No standard	DAP metre	80 kV/5 mA/ 360˚ or 17.5 s	CNR and visualization of periodontal structures were not compromised at this lower-dose protocol. 180˚ rotation degraded image quality.
EzEldeen et al. 2017	Planning and tooth replica fabrication (TAT) and follow-up on three different CBCT devices	kV, mA and time Altered via selecting a range of predefined protocols (18) on three CBCT machines (FOV alteration necessary pre-/postop)	Reference CBCT scanning protocol validated for accurate tooth and bone segmentation	Monte Carlo dose simulations for three paediatric models	Predefined low-dose protocols specific to device	Use of device-specific predefined low-dose protocols can achieve considerable ED reductions while maintaining image quality for TAT.

MBC – marginal bone crest; CEJ – cementoenamel junction; ED – effective dose; TAT – tooth autotransplantation

(Tab. III, Fig. 1). Unfortunately, the effect of changing one or both of the exposure factors is not straightforward. An objective image quality study recommended that a low-dose protocol should constitute reduction of the tube current exposure time product (depending on the clinical application), while keeping the tube voltage constant at 90 kV (highest kV value in device studied) as this achieved the highest CNR at low-dose levels (Pauwels et al. 2015b). The inference of Pauwel's study (2015b) being that the increase in noise for a given mA reduction would be less than that seen with a kV reduction. However, another study (same CBCT scanner used), assessing image quality relating to the anterior maxilla in a paediatric skull phantom, found that dose reductions (50% less than manufacturer's recommendations) could be achieved with a reduction in X-ray tube voltage (80 kV) and indeed for a range of combinations of kV and mA (Hidalgo Rivas et al. 2015). Optimizing kV and mA settings is difficult and involves appropriate balancing, where sufficient image quality is achieved dependent on imaging task at the lowest dose possible and the need for more studies in this area has been highlighted (European Commission 2012).

Field of View
The dimensions of the field of view (FOV) are dependent largely on the size and shape of the detector, the beam projection geometry and the ability to collimate the beam (Scarfe et al. 2008). The FOV is either cylindrical or spherical and collimation of the primary X-ray beam using adjustable lead shields limits exposure to the anatomical area of interest, thus avoiding unnecessary exposure. CBCT devices can be categorized according to the dimensions of the FOV. Some devices offer a single fixed FOV, with the majority offering a few pre-set options of FOV, particular to a specific indication. Other devices allow freely adjustable FOVs within certain limitations with another option being the stitching together of adjacent 3D volumes to achieve a larger FOV. The drawback of stitching being that the over–

lapped area is imaged twice, doubling the exposure to such areas. FOVs (described as diameter [D] × height [H] in cm^2) can range from small (<10 cm in field height, e.g. D × H: 4 × 4 cm^2, suitable for imaging a localized dentoalveolar area [1–3 teeth] and 8 cm × 8 cm^2, suitable for imaging the dentate areas of the maxilla and mandible) to medium (10–15 cm in field height). Large FOVs (>15 cm in field height) are required for full cranio-facial imaging (up to dimensions of 26 × 26 cm^2).

Reducing the FOV size (specifically in field height) is the most straightforward method of reducing patient radiation dose and is a key factor in CBCT optimization (Davies et al. 2012; Pauwels et al. 2012a; Theodorakou et al. 2012; Bornstein et al. 2014; Pauwels et al. 2014a; Ludlow et al. 2015). Neverthe-less, with the diversity of devices and scan options, an approx-imate ten-fold variation in dose for an equivalent FOV was re-ported between the units studied (Bornstein et al. 2014). FOV size and collimation in addition to diagnostic image quality are key determinants in the diagnostic application of a CBCT de-vice (Hirsch et al. 2008; Loubele et al. 2009). In relation to im-age quality, an increase in FOV results in a relatively greater amount of scatter reaching the detector and thus is accompa-nied by a relative increase in noise/artefacts and a reduction in contrast.

Larger FOVs have implications for the thyroid gland, espe-cially for children. This radiosensitive organ has a significant contribution to effective dose (17–20% in adults, 30–37% in children) (IRCP 2007) and can be exposed to scatter (contribu-tion of internal scatter is uncertain) and possibly to the pri-mary beam in dental CBCT. Use of thyroid shields has demon-strated a thyroid dose reduction in children (17–42%) and adults (20–49%) (Tsiklakis et al. 2005; Qu et al. 2012; Hidalgo-Rivas et al. 2015). Thyroid shielding is not mandatory in the EU as it was concluded that the thyroid gland is not normally in the primary beam during dental CBCT scans (HPA 2010; Euro-pean Commission 2012). However, it is advised that a decision should be made locally with the aid of a medical physics expert concerning large FOV scans, if it is likely the thyroid lies in or close to the primary beam. Notably, in the USA, dentists are advised to use thyroid shielding routinely for all dental radi-ography and for CBCT as long as this does not interfere with the examination (www.thyroid.org, www.imagegently.org). However, if the thyroid shield lies within the X-ray beam, even if outside the displayed FOV, it will attenuate the beam and produce artefacts on CBCT scans. Furthermore, if an AEC is used, at least in theory, a thyroid shield may reduce the dose to the receptor sufficiently to increase automatically the expo-sure.

Filtration
Filtration serves to limit patient exposure to lower energy pho-tons, which will contribute to skin dose but not to image for-mation. Therefore, highly filtered X-ray beams have an in-creased mean energy, reduced entrance exposure and suffer less from beam hardening, but can be associated with loss of contrast (Lofthag-Hansen et al. 2008; Roberts et al. 2009; Lud-low 2011). CBCT scanners typically utilize aluminium filtration (2.5–12 mm) with some devices using additional copper filtra-tion. Dose reductions associated with additional copper filtra-tion in selected CBCT devices have been reported (Ludlow & Ivanovic 2008; Qu et al. 2010; Ludlow 2011; Koivisto et al. 2012). In reality, clinicians using CBCT have no easy means of changing filtration, which would require the input of a medi-cal physics expert and an equipment engineer. Even then, this would be challenging without cooperation from equipment manufacturers.

Detector
The X-ray detector samples the attenuated beam in its trajecto-ry. The incoming X-ray photons are converted by X-ray detec-tors to an electrical signal. The majority of modern CBCT scan-ners utilize indirect flat panel detectors (FPD) consisting of a pixel array of hydrogenated amorphous silicon thin-film tran-sistors (TFT) or complementary metal oxide semiconductors (CMOS). In both cases a layer of scintillator material (gadolin-ium oxysulfide or caesium oxide) converts X-ray photons to light photons. Subsequently, the light is detected on the photo-diodes and read from the entire detector array to compile a raw-data digital image (Kiljunen et al. 2015). FPDs offer higher spatial and contrast resolution, greater dynamic range and re-duced peripheral distortion compared with the earlier gen-eration image intensifiers and charged coupled devices (CCD) technology, which have gradually been superseded (Baba et al. 2004; Nemtoi et al. 2013; Pauwels et al. 2015a). Involvement of a medical physics expert at installation is deemed essential to op-timize the detectors parameters with regards to dose and image quality (European Commission 2012).

Image Quality Parameters: Exposure Frequency, Rotation Arc, Number of Projections, Voxel Size
Exposure Frequency: Continuous v Pulsed Exposure
Certain CBCT units utilize continued X-ray exposure; i.e. expo-sure time equals scan time. However, constant exposure during signal integration contributes to patient dose but not to image formation as most detectors are unable to record X-ray expo-sure during the acquisition process. To avoid this unnecessary exposure, many CBCT units have a pulsed/intermittent X-ray emission to coincide with detector activation, ensuring that there is no exposure being made between projections. Pulsed-emission systems not only result in a reduced dose but also may exhibit improved spatial resolution owing to a reduced-motion effect (Pauwels et al. 2015a).

Rotation Arc
The rotation angle generally varies between 180° and 360° (CBCT device dependent), the majority of scanners having a single fixed rotation angle with some devices enabling selection of a variable rotation arc according to scan protocol (Horner et al. 2013; Nemtoi et al. 2013). A shorter scan arc results in a re-duced scan time and hence dose (lower total mA value) with a 180° arc resulting in an approximately 50% dose reduction compared to a 360° arc. Images produced by partial rotation have been associated with increased reconstruction artefacts (Scarfe & Farman 2008; Bechara et al. 2013). Additionally, while it would be expected that this reduced mA value would be accompanied by increased noise and reduced image quality, studies demonstrate that for particular diagnostic tasks image quality and diagnostic accuracy can be maintained (Lofthag-Hansen et al. 2011; Durack et al. 2011; Lennon et al. 2012). This finding implies that manufacturers' recommendations for ex-posure factors are too high for these tasks.

Number of Projections
The number of acquired projection images ("basis images") during the scan arc movement is determined by the rotation

time, frame rate (number of projection images per second), the completeness of the trajectory arc and the speed of the rotational movement (Scarfe & Farman 2008). A greater amount of projection data generally necessitates a longer scan time, with greater potential for patient movement and consequently a higher patient dose. However, enhanced image quality accompanies increased projection data; providing more information to reconstruct the image, allowing for greater spatial and contrast resolution and an increased signal-to-noise ratio and decreased metallic artefacts (Pauwels et al. 2013). Moreover, minimizing the "raw" images (at a level compatible with sufficient image quality) can result in reduced patient dose (via ↓ mA). It has been demonstrated that an increased number of projections does not influence linear accuracy (Brown et al. 2009). Notably, it is reported that increasing exposure does not improve the appearance of metal artefacts sufficiently to justify the increased radiation exposure (Pauwels et al. 2013). Additionally, there are metal artefact reduction techniques that can be employed during reconstruction (Van Gompel et al. 2011). Other artefact reducing techniques involve the iterative reconstruction process or using more sophisticated projection and back-projection techniques (Wang et al. 1999; De Man et al. 2004). All these methods, however, require extensive computational power and further work is necessary before they are available in commercial CBCT units (Schulze et al. 2011).

Voxel Size
Voxels (the individual volume elements) produced in formatting the volumetric data set, dictates the spatial resolution of a CBCT image (Scarfe & Farman 2008). Voxel size can be selected on most dental CBCT systems according to the particular diagnostic task. Overall, voxel sizes of CBCT equipment range from 0.075 to 0.6 mm, although individual machines will not normally provide the full range. The smaller the voxel size, the higher the spatial resolution (Fig. 1) and therefore smaller voxel sizes are selected when a high level of detail is required e.g. for endodontic purposes (Liedke et al. 2009; Kamboroğlu & Kursun 2010; Melo et al. 2010; Maret et al. 2012). However, voxel dimensions primarily depend on the pixel size on the area detector and smaller pixels capture fewer X-ray photons which result in more image noise. This may require a compensatory increase in radiation dose to achieve a sufficient signal-to-noise ratio to achieve this improved diagnostic image quality (via ↑ mA or basic images). Some devices allow the operator to control exposure factors used with different resolutions, while others automatically dictate exposure factors accompanying particular voxel sizes in order to keep noise relatively constant. Notably, a study reported that the patient dose was doubled on selection of the high resolution from standard on a particular CBCT unit (Ludlow & Walker 2013). In the pursuit of dose optimization, the lowest resolution (larger voxel size) option should be selected where the nature of the diagnostic task permits (European Commission 2012). Indeed, the effect of voxel size on diagnostic outcome has not yet been systematically demonstrated (Spin-Neto et al. 2013). From the small numbers of studies systematically reviewed, a trend of increased diagnostic accuracy relating to higher voxel resolutions was evidenced, however, it is not yet possible to suggest general protocols for the different diagnostic tasks and further studies are needed to establish accurate guidelines.

It is apparent from the aforementioned that the image quality (ability of CBCT images to display the required anatomical fea-

tures and/or pathologies) and consequent dose of CBCT imaging is influenced by a number of variables (Tab. I). Such variables include: the individual device (e.g. detector, filtration, FOV capabilities etc.), the exposure parameters (kV, mA) and image quality parameters (voxel size/resolution, basis images [dependent on rotation arc, exposure frequency]). Selection of the optimal combination of scanning parameters to reduce dose can prove a challenge to the operator with very little in the way of practical guidance. While general recommendations on dose optimization exist (HPA 2010; European Commission 2012; American Dental Association Council on Scientific Affairs 2012), a recent review highlighted the need for more specific guidance on how optimization can be achieved in practice (Goulston et al. 2016). Nevertheless, it is accepted that establishment of diagnostic task-specific protocols may prove difficult due to wide range of CBCT devices and capabilities. The development of low-dose protocols in a range of diagnostic applications has gone some way in beginning to achieve optimization (Hidalgo Rivas et al. 2015; Al-Okshi et al. 2017) as could device-specific low-dose preset options (EzEldeen et al. 2017).

Image Quality
In keeping with the ALADA principle, the image quality attained should be sufficient to achieve the specific diagnostic task, but at the minimum exposure possible. The operator must be aware that the acceptable level of image quality and the radiation dose may vary according to the particular diagnostic task and, indeed, the anatomical region investigated/position of the pathology (Lofthag-Hansen et al. 2011; Neves et al. 2012). Image quality is described in terms of spatial resolution, contrast, noise and presence of artefacts (Tab. II) but on a simple level can be assessed relative to achieving the diagnostic task e.g. visualization of a periapical radiolucency, identification of the second mesiobuccal canal (MB2). A number of parameters impact on image quality: tube current, tube voltage, FOV, voxel size, number of projections and type of detector (Maret et al. 2012; Spin-Neto et al. 2013; Pauwels et al. 2015a). As previously established, there is a great array of CBCT devices available commercially, exhibiting a range of technical specifications, doses and image quality capabilities (Hatcher 2010; Nemtoi 2013). In order to achieve optimization of these devices, it is essential to use a standardized approach to assessing image quality (Pauwels et al. 2011). Image quality can be assessed using subjective and objective methods.

Subjective Evaluation
This is considered as the benchmark when assessing image quality in relation to achieving a specific diagnostic task. It involves the standardized presentation of images (anthropomorphic phantoms, human skulls or jaws) to a specified number of observers who are provided with a scale to grade their ability to identify the presence of anatomical structures and/or grade the sufficiency of the image quality for a particular task e.g. root resorption, implant planning and periapical diagnosis (Alqerban et al. 2011; Durack et al. 2011; Esposito et al. 2011; Lofthag-Hansen et al. 2011; Shelley et al. 2011). This technique is limited by its inherent subjectivity (inter-observer, intra-observer, case-sample variability, and the use of non-standardised skull and jaw models, which limits comparison) (Tapiovaara 2006; Lofthag-Hansen et al. 2011). Furthermore, findings are often limited to the CBCT device investigated due to the large diversity in image quality between scanners (Pauwels et al. 2012d).

Objective Evaluation

This involves quantitative measurement (on physical test objects) of physical factors such as: spatial resolution, contrast resolution, image density/pixel intensity, image noise, artefacts, on the basis that they equate to clinical image quality, using test phantoms (Watanabe et al. 2011). Identifying the need for a standardized phantom appropriate for dental CBCT, the SEDENTEXCT project developed a quality control phantom (SEDENTEXCT IQ phantom) which enables reproducible measurement of these technical image quality parameters on any CBCT device and thus is utilized for assessing device performance and quality control (Pauwels et al. 2011; Bamba et al. 2013; Ludlow & Walker 2013). While objective evaluation is essential for quality assurance (QA) of CBCT devices and these physical indices are germane, there is no direct means by which to relate them to clinical diagnostic accuracy (Martin et al. 1999; Månsson 2000; Watanabe et al. 2011). Studies have shown a significant association of physical factors (modulation transfer function [MTF] and/or contrast-to-noise ratio [CNR]) with subjective image quality and related this to the ability to achieve a specific diagnostic task (Choi et al. 2015; Hidalgo Rivas et al. 2015; Al-Okshi et al. 2017). Choi and co-workers (2015) demonstrated that a better physical image quality (higher MTF and CNR value) was required to achieve the clinical task of periapical diagnosis compared with implant planning in the mandible, the findings corresponding in part to a study on subjective image quality in relation to diagnostic task (Lofthag-Hansen et al. 2011). However, both of these studies' findings were not related to dose measurements.

Is There Evidence That ALADA Is Practicable in a Range of Dental Diagnostic Tasks?

Reduced exposure protocols can be achieved while maintaining adequate image quality and thus diagnostic accuracy for a range of clinical tasks (European Commission 2012; Goulston et al. 2015). These results relate to the diagnostic task investigated using specified CBCT scanner(s) and that technical specifications limit translation to all CBCT scanners. As previously discussed it has been established that size and position of FOV relative to the radiosensitive organs and the scanned individual have a substantial impact on dose optimization (Davies et al. 2012; Pauwels et al. 2012a; Theodorakou et al. 2012; Pauwels et al. 2013). Nonetheless, several *in vitro* studies specifically demonstrate that a reduction in exposure factors (kV, mA, exposure time – also altered through rotation time or voxel size/resolution) can be consistent with sufficient image quality to enable diagnosis in a range of clinical applications (Tab. III). Furthermore, two of these studies included dose measurements, recommending low-dose protocols for their respective diagnostic tasks (Hidalgo Rivas et al. 2015; Al-Okshi et al. 2017). One low dose protocol established a 50% dose reduction from the manufacturer's recommended protocol (Hidalgo Rivas et al. 2015), which highlights the difficulty for practitioners in optimizing exposures. Other studies demonstrated the limitations of lower exposures relating to specific sites or pathology location (Lofthag-Hansen et al. 2011; Neves et al. 2012), reporting that although 180° rotations produced diagnostic images for maxillary implant planning, this was not the case for mandibular implant planning or periapical diagnosis (Lofthag-Hansen et al. 2011). In the same way, Neves et al. (2012) suggested a reduced-dose scanning protocol produced images of diagnostic quality for detection of external root resorption (ERR) with the caveat that the position of root resorption may affect the ability to diagnose at lower exposures.

Generally, studies have reported that image quality is consistently degraded with reduced exposure factors (Suomalainen et al. 2009; Luckow et al. 2011; Parsa et al. 2013). The most commonly investigated diagnostic task with regard to optimization of exposure factors was that of implant planning, perhaps reflecting the almost ubiquitous use of CBCT in this dental application. Oddly, considering that children have a significantly increased radiation risk, there is a limited literature regarding optimization of exposure factors in orthodontic diagnostic tasks, while in the available studies it has been highlighted that orthodontic scanning in a child phantom resulted in on average an effective dose 36% greater than in the adult phantom (Ludlow & Walker. 2013). One orthodontic study found that reduced exposure time was consistent with maintenance of diagnostic accuracy (Brown et al. 2009).

In conclusion, it is evident that radiation doses, significantly reduced from the manufacturer's recommendations can be achieved (via reduced kV, mA or time), while maintaining acceptable image quality and applied for certain diagnostic tasks and particular devices (Tab. III). Nonetheless, it has been emphasized that radical reductions in dose are futile if image quality degrades to the point of being non-diagnostic, thereby necessitating a repeat scan (Ludlow & Walker. 2013). Evidentially more research is needed, perhaps in collaboration with industry, to further assist practitioners in this important area.

How Valid Is the Research on Dose Optimization and Image Quality?

The majority of studies relating optimization to image quality are *in vitro* and thus of low hierarchal evidence-based standing (Marshall & Sykes 2011). Variations in CBCT device setting and properties make it impossible to reliably compare dose estimations from different studies. A systematic review of the literature on CBCT imaging in the oral and maxillofacial region highlighted inconsistent reporting on device settings and properties concluding, that a specific list of CBCT device parameters (e.g. exposure time, FOV, detector type, rotation arc etc.) should be documented to enable comparison (De Vos et al. 2009). Unfortunately, this policy has not been universally adopted, but is reiterated in a more recent literature on optimization (European Commission 2012; Goulston et al. 2016). These reviews highlight among other issues, the need for international compliance on a standardized method of accurately measuring patient dose using a standard commercially available phantom and the use of consistent reference standards were diagnostic accuracy is measured.

Diagnostic Efficacy of CBCT
Does CBCT Have a Greater Diagnostic Efficacy than Conventional Techniques?

The final section of this review analyses the evidence comparing the diagnostic efficacy of CBCT and conventional techniques for specific clinical tasks. If it is accepted that the diagnostic accuracy of CBCT is superior to conventional techniques, albeit at a higher dose to the patient, can this enhanced accuracy deliver a net benefit to the patient as evidenced by an impact on diagnosis, clinical decision-making and treatment outcome?

Tab. IV	Hierarchal model of classification of diagnostic accuracy (Fryback & Thornbury 1991)	
Level of diagnostic efficacy	**Definition and parameters measured**
1. Technical Efficacy	Evaluates technical quality of imaging modality: i.e. noise, contrast, resolution, presence of artefacts and includes dose and dimensional accuracy.
2. Diagnostic Accuracy (DA) Efficacy	Evaluates accuracy of imaging modality in establishing a correct diagnosis when compared with the reference or "gold standard" technique: sensitivity, specificity, predictive values, ROC curves.
3. Diagnostic Thinking Efficacy	Evaluates the ability of the imaging modality to improve diagnostic decisions. Evidenced in before-and-after studies where an alternative diagnostic conclusion is made with new imaging modality when compared with diagnosis made using the existing conventional imaging modality.
4. Therapeutic Efficacy	Evaluates the impact that the imaging modality has on the choice of treatment. Evidenced in clinical studies (before-and-after) by observing the changes in treatment strategies where the new imaging modality scan is or is not supplied.
5. Patient Outcome Efficacy	Evaluates the impact of the imaging modality on patient outcome. Has this new diagnostic technique lead to an improved treatment strategy with a concomitant improved outcome for the patient, e.g. reduction in postoperative complications? This is assessed via randomized controlled trials (RCT) comparing patient outcome using new technique compared with existing "gold standard".
6. Societal Efficacy	Assesses the cost-benefit ratio of the imaging modality to society as a whole.

Critical appraisal of the literature on CBCT imaging efficacy is best facilitated by a hierarchal classification model, which categorizes six ascending levels of diagnostic efficacy (Fryback & Thornbury 1991). The levels start with the simple goal of procuring the most accurate image and ascends to the complex target of improving patient outcome and societal impact with the aim of effecting evidence-based changes in patient care and health policy (Tab. IV). The lower tiers (levels 1 and 2) focus on image quality (National Council on Radiation Protection and Measurements 2005; Krupinski et al. 2007) and diagnostic accuracy of CBCT (Ghaeminia et al. 2009; Matzen et al. 2013; Patel et al. 2016). Such technical and diagnostic efficacy studies constitute the bulk of evidence in the literature and are less time consuming and expensive than study designs required at higher levels of efficacy, however, even these research domains are considered incomplete (European Commission 2012; Kim et al. 2011; Rosen et al. 2015; Petersson et al. 2012). While these principally lab-based studies are essential in establishing accuracy and report that CBCT exhibits higher sensitivity and specificity than intra-oral radiography for several diagnostic tasks (Petersson et al. 2012), albeit often in the absence of a relevant reference method, they do not provide any evidence of impact on patient care. Critically, accuracy studies should use a non-radiographic reference standard, which is an exact reflection of the true situation (Mileman & van den Hout 2009) and could include histology (De Paula-Silva et al. 2009) or intrasurgical visualization (Qiao et al. 2014; Ghaeminia et al. 2009). *Ex vivo* simulation studies on dry skulls (Durack et al. 2009; Braun et al. 2014) utilize direct visualization/measurement as a reference, however, it is questionable whether artificially created lesions represent either the true topography or borders of resorption or periodontal lesions (Petersson et al. 2012). Furthermore, considering the effect of patient movement on image quality, these studies are even further removed from the *in vivo* reality (Nikolic-Jakoba et al. 2016).

Levels 3 and 4 evaluate whether an imaging modality can give rise to a change in diagnostic thinking or patient management and therefore begin to consider impact on patient's health. Before-and-after studies are frequently used to investigate the impact of diagnostic and therapeutic choices at levels 3 and 4 (Guyatt et al. 1986; Fryback & Thornbury 1991; Meads & Davenport 2009). The number of studies published at this level are much reduced compared to technical and diagnostic efficacy studies and the need for more research in these higher levels has been repeatedly highlighted (European Commission 2012; Bornstein et al. 2014; Rosen et al. 2015; Nikolic-Jakoba et al. 2016). Level 3 evidence suggests that CBCT does have an impact on diagnostic thinking efficacy in more complex and challenging cases with regards to implant placement and endodontics but cannot be justified for routine use (Shelley et al. 2015; Ee J et al. 2014; Mota de Almeida et al. 2015; Al-Salehi & Horner 2016). Additionally, in an orthodontic study on impacted canines, CBCT did increase confidence in diagnosis, especially for more critical information such as the labiopalatal position of the canine cusp tip (Haney et al. 2010). Albeit, it was accepted that most impacted teeth can be accurately diagnosed/localized with conventional radiographs, nonetheless, there are undoubtedly cases which benefit from CBCT imaging (Bjerklin & Ericson 2006).

Therapeutic efficacy studies (level 4) revealed a range of CBCT impact on therapeutic decisions, perhaps influenced by study design (e.g. case selection method, teeth numbers, observer numbers/experience) and/or diagnostic task investigated. An endodontic study (24 teeth) revealed there was no significant difference in lesion size recorded or treatment strategy for periapical lesions in non-complex cases between periapical radiography (PR) and CBCT imaging (Balasundarum et al. 2012). Although the numbers of subjects enrolled in the study are small, it does highlight that if CBCT does not actually alter the treatment plan, then the increased diagnostic accuracy of CBCT in recognizing apical periodontitis is of no real benefit (De Paula-Silva et al. 2009; Patel et al. 2009; Venskutonis et al. 2014). It could be argued that the increased sensitivity of CBCT does diagnose AP lesions of smaller dimensions that would otherwise go undiagnosed and untreated by PR, this constituting an

increased therapeutic efficacy; however, this is not clear as the possibility of reduced specificity of CBCT in diagnosing AP has been reported *in vivo* (Pope et al. 2014). Pope's (2014) study reports on error in interpretation of the healthy periapex on CBCT scans and the inherent flaw of applying PR interpretation of health and disease to CBCT, thereby risking overdiagnosis (Moynihan et al. 2012).

Other endodontic studies have demonstrated a significant impact of CBCT imaging on treatment planning choices in complex cases (Ee et al. 2014; Mota de Almeida et al. 2014; Patel et al. 2016; Rodríguez et al. 2017; Venskutonis et al. 2014) with the general consensus being that the increased diagnostic information from a CBCT scan compared with conventional radiography had a substantial impact on treatment planning of high-difficulty cases (e.g. resorption, surgical cases). An orthodontic study showed that CBCT imaging evoked a change in treatment plan from conventional imaging but only in a minority of cases (27%), concluding that the additional diagnostic information did not translate to a significant change in treatment plan (Haney et al. 2010). Implant studies reported a significant change in treatment plan with CBCT imaging for more challenging cases (narrower implants selected in the anterior mandible with CBCT) and high-risk anatomical regions (posterior jaw-longer implants selected using panoramic images) (Shelley et al. 2015; Guerrero et al. 2014b); however, when all cases were considered a significant change in treatment plan between the two imaging modalities was not demonstrated. In general, these studies reflect the majority of current guidelines/position statements across the dental disciplines, which highlight that use of CBCT is not recommended routinely, but is only advisable in more complex cases where conventional radiography does not elucidate the diagnostic information required (AAE and AAOMR 2011; EAO 2012 [Harris et al. 2012]; European Commission 2012; FGDP [UK] 2013; ESE 2014). Notable exceptions to this conservative approach to CBCT prescription do exist (Drago & Carpentieri 2011; Noffke et al. 2011; AAOMR 2012 [Tyndall et al. 2012]), with routine use of cross-sectional imaging in dental implant planning and treatment advocated, based on a reduced risk of neurosensory and neurovascular injury (Zijderveld et al. 2008; Renton et al. 2012; Roeder et al. 2102; Jacobs et al. 2013). This routine CBCT use has been questioned by other groups who elicited opposing conclusions from the literature, highlighting the lack of evidence-based guidance in most national and international guidelines on implant dentistry and described their recommendations as largely expert opinion and consensus driven (Bornstein et al. 2014; Horner et al. 2015).

Ultimately, if clinicians are exposing patients to diagnostic ionizing radiation which is of significantly higher dose than that of the existing diagnostic imaging modality of choice, the new imaging modality should demonstrate a positive impact on patient outcome (level 5 – Patient outcome efficacy), preferably in a cost-effective manner (level 6 – Societal efficacy). Randomized controlled trials (RCTs) are the optimal study design to assess these levels of accuracy (Fryback & Thornbury 1991). Generally, RCTs are expensive and time consuming, often resulting in low subject numbers and underpowered studies (Roeder et al. 2012). Furthermore, they can be ethically difficult or impossible to perform with regards to diagnostic imaging modalities (Mileman & van den Hout 2009) and it has been argued that due to their longitudinal nature and the fast pace of CBCT technology development, their results can be redundant

even before publication (Kim et al. 2011). Perhaps not surprisingly there are very few studies published which assess patient outcome efficacy (Level 5). Three studies investigating surgical extraction of impacted mandibular third molars (Guerrero et al. 2014a; Ghaeminia et al. 2015; Petersen et al. 2016) failed to demonstrate any beneficial impact of CBCT over panoramic imaging on patient related outcomes (i.e. neurosensory disturbances and other postoperative complications). Although, it should be recognized that the studies were small, with an inadequate sample size for a comparative prospective study (Roeder et al. 2012). A recent systematic review (Matzen & Wenzel 2015) concluded that for most cases, periapical or panoramic imaging may be sufficient for removal of mandibular third molars; however, CBCT may be indicated where conventional imaging reveals one or more signs of close contact between the tooth and the mandibular canal (Rood & Shebab 1990), but only if it is believed that CBCT imaging will subsequently elicit a change in treatment plan or patient outcome. This conclusion is open to subjective interpretation and probably encourages a pattern of CBCT prescription for impacted mandibular third molars that correlates with the clinician's experience. A further RCT, comparing the impact of panoramic and CBCT imaging on periradicular surgery, elicited a significant difference in operator-related outcome (operating time), but this did not appear to have any positive ramifications on patient outcome (Kurt et al. 2014).

Societal efficacy studies (level 6) aim to prove that implementation of this diagnostic imaging modality is an efficient use of societal resources and can provide medical benefits to society. There is a paucity of RCTs investigating societal efficacy. One prospective RCT reported on the absolute and relative costs of a CBCT scan compared with that of a panoramic examination undertaken for third molar surgery, identifying a 3–4 times greater cost associated with CBCT than panoramic imaging but there was no significant difference in resources consumed between the imaging groups, either surgically or postsurgery (Petersen et al. 2014). The same group also published an epidemiological study in Denmark (Petersen et al. 2015), which highlighted the higher economic implications of potential routine use of CBCT in extraction of mandibular third molar teeth. Importantly, this study actually considers the radiation risk implications associated with this potential policy change (calculation of cancer incidence – 0.46 per year) which is necessary when contemplating societal efficacy. Other level 6 studies are descriptive; a cost analysis study noted that a demonstrated cost-effectiveness of CBCT imaging in one healthcare system cannot necessarily be translated to another (Christell et al. 2012). A periodontal case series reported that CBCT-based treatment decisions for maxillary molars with furcation defects can lead to time and cost benefits when compared with conventional radiography in a Swiss dental health setting (Walter et al. 2012). Based on the cost analyses performed, it was concluded that CBCT as an additional diagnostic measure is only justified when more invasive therapies are planned and, considering the potential increased radiation risk associated with additional imaging, cases should be judged on an individual basis. Again, this conclusion is open to subjective interpretation.

In conclusion there is a lack of studies exhibiting the impact of CBCT at higher levels of efficacy (European Commission 2012; Matzen & Wenzel 2015; Rosen 2015; Nikolic-Jakoba et al. 2016), with one recent review concluding that the effectiveness of

CBCT in a range of dental disciplines has barely been evaluated (MATZEN & WENZEL 2015). Unfortunately, regardless how compelling the results of the technical and diagnostic accuracy efficacy studies, this literature is not indicative of any translational benefit of CBCT to patient's treatment and outcome or indeed to society.

Conclusions

– Conventional radiography is limited by the inability to describe the 3D anatomy of teeth and their related structure. It has therefore been recommended that CBCT be used in select cases in which conventional radiography cannot supply satisfactory diagnostic information.

– CBCT is a more sensitive diagnostic tool than conventional radiography but delivers a significantly greater patient dose. Therefore, unless the benefit to the patient can be justified there is a risk of overexposure. Furthermore, there is concern that with increased diagnostic sensitivity there is a loss of specificity which may result in over-representation of disease, which highlights a need for establishing an "atlas of normal" particular to CBCT, in order to correctly diagnose pathology.

– The clinician in practice prescribes, exposes, analyses and reports on the CBCT image. Therefore, appropriate training in justification, acquisition and interpretation is paramount.

– There is a lack of evidence that CBCT imaging has a significant impact on decision-making and treatment outcome. Therefore, at present, the clinician remains unsupported in their justification of CBCT imaging.

– With an awareness of the potential stochastic radiation risks of CBCT, being particularly pertinent to the young, judicious case selection is essential to ensure that the benefits–risk ratio remains in favour of the individual patient. Guidelines constructed from the best available evidence serve to aid the clinician's justification. Unfortunately, these available guidelines are of varying quality with the majority being based on expert opinion. It is important that a more critical systematic approach is adopted in the formulation of new guidelines.

– It is accepted in CBCT that FOV height and relation of the FOV to the radiosensitive organs are the main determinants of effective dose. Additionally, optimization of exposure and imaging parameter factors, can achieve significant dose reductions, while maintaining image quality for a range of diagnostic tasks, but this is not necessarily translatable to all devices. Further development of low dose protocols in key diagnostic areas would greatly aid the clinician.

– Despite the lack of evidence on the efficacy of CBCT, its use is expanding rapidly in dental practice. It is a lucrative, industry-driven business, sold on the basis of improved, attractive and high-quality imaging. Critical evaluation of manufacturer's advice and default protocols necessitates appropriate undergraduate and postgraduate training and knowledge of the evidence base regarding CBCT imaging.

– The current literature on CBCT imaging reveals the need for consistent and standardized testing and reporting to allow effective comparisons of dose calculations and optimization techniques on image quality. Diagnostic accuracy studies do not always reflect the clinical situation and inconsistent reference standards make ready comparison between results impossible. Notably, higher hierarchal level studies are rare, with only four RCTs assessing clinical outcome efficacy. Nevertheless, for the purpose of establishing robust guidelines for appropriate use of CBCT, research in the future should be directed at higher level clinical studies.

Zusammenfassung
Einleitung
Die Möglichkeit, hochauflösende dreidimensionale (3D) Röntgenbilder zu erstellen, hat die digitale Volumentomografie (DVT) in der zahnärztlichen Praxis immer populärer gemacht. Einige inhärente Probleme der konventionellen zweidimensionalen (2D) Radiografie wie beispielsweise Überlagerungen oder andere anatomisch bedingte Einschränkungen in der Interpretierbarkeit («anatomical noise») können dabei überwunden werden. In Anbetracht der stetig steigenden Nutzung der DVT, gerade auch bei zahnärztlichen Erstbehandlungen, haben es sich die Autoren dieser Übersichtsarbeit zum Ziel gemacht, herauszufinden, welche evidenzbasierte Information dem Kliniker zur Verfügung steht, um das mit der DVT einhergehende erhöhte Bestrahlungsrisiko zu rechtfertigen, und dieses allenfalls zu reduzieren, um noch immer eine diagnostisch akzeptable Bildqualität zu erhalten.

Material und Methoden
Die Literatur über Strahlendosis und das damit einhergehende Patientenrisiko wurde eingehend untersucht. Anschliessend wurde geschaut, wie sich die Strahlendosis optimieren lässt und wie sich eine solche Optimierung auf die Bildqualität auswirkt. Obwohl es als anerkannt gilt, dass DVT die Diagnostik in vielen Gebieten der Zahnmedizin verbessern kann, ist nicht unbedingt klar, inwieweit dadurch Behandlungsentscheide und Behandlungserfolge tatsächlich verbessert werden können. Um diese Punkte genauer anzuschauen, wurden die Evidenz und die Validität der zum Thema vorhandenen Studien geprüft.

Resultate
Die DVT-basierte 3D-Visualisierung des maxillofazialen Skeletts kann im Vergleich zur konventionellen (2D) Radiografie mehr diagnostische Informationen liefern. Die DVT ist dabei allerdings mit einer erhöhten Strahlenbelastung verbunden, was die Wichtigkeit einer strikten Befolgung von Indikationsstellung, Rechtfertigung und Bildoptimierung unterstreicht. Bei der Durchsicht der zum Thema vorhandenen Literatur wurde klar, dass die Optimierung bzw. Reduktion der Strahlendosis für eine gegebene diagnostische Fragestellung eine genügende Bildqualität liefern kann. Es ist allerdings so, dass die meisten dieser Studien ein niedriges Evidenzniveau aufweisen und dass ein standardisiertes Vorgehen weitestgehend fehlt. Zur Optimierung der Strahlendosis gibt es wenig praktische Hilfe für Zahnärzte, und existierende Protokolle lassen sich nicht auf jedes Gerät übertragen. Hinzu kommt, dass die Bedienungsanleitungen der Geräte normalerweise keine Aussagen zur Dosisreduktion machen. Es gibt wenig Daten, die eine Verbesserung der Diagnostik und des entsprechenden Behandlungsentscheids dank DVT aufgezeigt haben. Weiterhin gibt keine Evidenz für einen Effekt der DVT auf den Behandlungserfolg.

Diskussion
Die bestehende Literatur unterstreicht die Notwendigkeit, spezifische Richtlinien zur Dosisoptimierung bei gegebenen diagnostischen Fragestellungen zu erarbeiten. Zudem müssen klinische Studien durchgeführt werden, um den Einfluss der DVT auf höhere Ebenen der diagnostischen Wirksamkeit zu untersuchen.

Résumé

Introduction

La tomographie volumique numérique (TVN) (ou Cone Beam CT, CBCT) est de plus en plus populaire en pratique médico-dentaire, car elle permet d'obtenir des images radiographiques tridimensionnelles (3D) en haute résolution. Certaines difficultés inhérentes à la radiographie conventionnelle bidimensionnelle (2D), telles que les superpositions ou autres limitations d'interprétation liées au «bruit anatomiques», peuvent être surmontées de cette manière. En raison de l'utilisation croissante de la TVN, notamment lors du traitement médico-dentaire initial, les auteurs de ce travail de revue ont cherché à identifier les informations factuelles obtenues ainsi par le clinicien et justifiant le risque inhérent à l'augmentation de l'exposition aux rayons X associée à cette méthode; en outre, les auteurs se sont demandés comment réduire au mieux ce risque tout en préservant une qualité d'image acceptable du point de vue du diagnostic.

Matériel et méthodes

La littérature sur la dose de rayonnement et le risque associé pour la santé du patient a été étudiée de façon approfondie. Puis les auteurs ont cherché à savoir comment optimiser la dose de rayonnement, et dans quelle mesure une telle optimisation affecte la qualité d'image. Même s'il est généralement admis que la TVN permet d'améliorer le diagnostic dans de nombreux domaines de la médecine dentaire, on ne sait pas très clairement dans quelle mesure cette technique d'imagerie permet réellement d'améliorer les décisions thérapeutiques, et donc les résultats des traitements. Afin d'examiner de plus près ces différents aspects, le degré d'évidence et la validité des études existantes sur ce sujet ont été évalués.

Résultats

Par rapport à la radiographie conventionnelle (2D), la visualisation 3D du squelette maxillo-facial par TVN peut fournir davantage d'informations diagnostiques. Cependant, la TVN est associée à une exposition accrue aux radiations, d'où l'importance du respect strict des indications de cet examen, de ses justifications et de l'optimisation de l'image. L'étude de la littérature existante sur ce sujet a montré clairement que l'optimisation, respectivement la réduction de la dose de rayonnement en fonction d'une question diagnostique donnée peut être compatible avec une qualité d'image suffisante. Cependant, la plupart de ces études ont un faible niveau de preuve et les procédures suivies ne sont généralement pas standardisées. Dans ces études, les médecins-dentistes trouvent peu d'indications pratiques pour optimiser la dose de rayonnement, et les protocoles existants ne peuvent pas être transposés à tous les appareils. En outre, les guides d'utilisation des appareils ne donnent généralement pas d'indications sur la réduction de la dose. Les données qui ont montré une amélioration du diagnostic et de la décision thérapeutique correspondante grâce à la TVN sont peu nombreuses. De plus, il n'existe à ce jour aucune évidence d'un effet positif de la TVN sur les résultats thérapeutiques.

Discussion

La littérature existante souligne la nécessité de développer des directives spécifiques pour l'optimisation de la dose en fonction des différentes questions diagnostiques qui peuvent se poser. En outre, des études cliniques doivent être réalisées pour évaluer l'influence de la TVN quant à la possibilité d'obtenir des niveaux plus élevés d'efficacité diagnostique.

References

Alamri H M, Sadrameli M, Alshalhoob M A, Sadrameli M, Alshehri M A: Applications of CBCT in dental practice: a review of the literature. Gen Dent 60: 390–400 (2012)

Al-Ekrish A A: Effect of exposure time on the accuracy and reliability of cone beam computed tomography in the assessment of dental implant site dimensions in dry skulls. Saudi Dent J 24: 127–134 (2012)

Al Najjara, Colossi D, Dauer L T, Prins R, Patchell G, Barnets I, Goren A D, Faber R D: Comparison of adult and child radiation equivalent doses from 2 dental cone-beam computed tomography units. Am J Orthod Dentofacial Orthop 143: 784–792 (2013)

Al-Okshi A, Theodorakou C, Lindh C: Dose optimization for assessment of periodontal structures in cone beam CT examinations. Dentomaxillofac Radiol 46: 20160311 (2017)

Alqerban A, Jacobs R, Fieuws S, Nackaerts O, Willems G, SEDENTEXCT Project Consortium: A comparison of six cone beam computed tomography systems for image quality and detection of simulated canine impaction-induced external root resorption in maxillary lateral incisors. Am J Orthod Dentofacial Orthop 140: 129–139 (2011)

Al-Salehi S K, Horner K: Impact of cone beam computed tomography (CBCT) on diagnostic thinking in endodontics of posterior teeth: A before-after study. J Dent 53: 57–63 (2016)

American Association of Endodontists, American Academy of Oral and Maxillofacial Radiology: Use of cone-beam computed tomography in endodontics Joint Position Statement of the American Association of Endodontists and the American Academy of Oral and Maxillofacial Radiology. Oral Surg Oral Med Oral Pathol Oral Radiol Endod 111: 234–237 (2011)

American Thyroid Association (ATA): Issues policy statement on minimizing radiation exposure from medical, dental diagnostics The use of cone-beam computed tomography in dentistry: an advisory statement from the American Dental Association Council on Scientific Affairs. J Am Dent Assoc 143: 899–902 (2012)

Arai Y, Tammisalo E, Iwai K, H Ashimoto K, Shinoda K: Development of a compact computed tomographic apparatus for dental use. Dentomaxillofac Radiol 28: 245–248 (1999)

Arbeitgemeinschaft der Wissenschaftlichen Medizinischen Fachgesellschaften (AWMF): s2k-Leitlinie Dentale digitale Volumentomographie Version Nr. 9 (2013)

Baba R, Ueda K, Okabe M: Using a flat-panel detector in high resolution cone beam CT for dental imaging. Dentomaxillofac Radiol 33: 285–290 (2004)

Balasundarum A, Shah P, Hoen M M, Wheater M A, Bringas J S, Gartner A, Geist J R: Comparison of cone-beam computed tomography and periapical radiography in predicting treatment decision for periapical lesions: a clinical study. Int J Dent Article ID 920815 (2012)

Bamba J, Araki K, Endo A, Okano T: Image quality assessment of three cone beam CT machines using the SEDENTEXCT CT phantom. Dentomaxillofac Radiol 42: 20120445 (2013)

Barret H H, Myers K J, Hoeschen C, Kupinski M A, Little M P: Task-based measures of image quality and their relation to radiation dose and patient risk. Phys Med Biol 60: R1–R75 (2015)

Bechara G, Mcmahn A, Nasseh I, Geha H, Hayek E, Khawam G, M, Noujeim M: Number of basis images effect on detection of root fractures in endodontically treated teeth using a cone beam computed tomography machine: an in vitro study. Oral Surg Oral Med Oral Pathol Oral Radiol 115: 676–681 (2013)

Berg B I, Gertsch A, Zeilhofer H F, Schwenzer-Zimmerer K, Berg S, Hassfeld S, Jurgens P: Cone beam computed tomography and radiation dosage: application frequency and knowledge of dentists in Switzerland. Swiss Dent J 124: 419–433 (2014)

Bjerklin K, Ericson S: How a computerized tomography examination changed the treatment plans of 80 children with retained and ectopically positioned maxillary canines. Angle Orthod 76: 43–51 (2006)

Borisova R, Ingilizova C, Vassileva J: Patient dosimetry in pediatric diagnostic radiology. Radiat Prot Dosim 129: 155–159 (2008)

Bornstein M M, Scarfe W C, Vaughn V M, Jacobs R: Cone Beam Computed Tomography in Implant Dentistry: A Systematic Review Focusing on Guidelines, Indications, and Radiation Dose Risks. Oral Maxillofac Implants 29 (SUPPL): 55–77 (2014)

Braun X, Ritter L, Jervøe-Storm P M, Frentzen M: Diagnostic accuracy of CBCT for periodontal lesions. Clin Oral Investig 18: 1229–1236 (2014)

Brown A A, Scarfe W C, Scheetz J P, Silveira A M, Farman A G: Linear accuracy of cone beam CT derived 3D images. Angle Orthod 79: 150–157 (2009)

Brown J, Jacobs R, Levreing Jaghagen E, Lindh C, Baksi G, Schulze D, Schulze R: Basic training requirements for the use of dental CBCT by dentists: a position paper prepared by the European Academy of DentoMaxilloFacial Radiology. Dentomaxillofac Radiol 43: 20130291 (2014)

Cassola V F, Milian F M, Kramer R, De Oliveira Lira C S A, Khoury H J: Standing adult human phantoms based on the 10th, 50th nd 90th mass and height percentiles of male and female Caucasian populations. Phys Md Biol 56: 3749–3772 (2011)

Choi E, Ford N L: Measuring absorbed dose for i-Cat CBCT examinations in child, adolescent and adult phantoms. Dentomaxillofac Radiol 44: 20150018 (2015)

Choi J W, Lee S S, Choi S C, Heo M S, Huh K H, Yi W J, Kang S R, Han D H, Kim E K: Relationship between physical factors and subjective image quality of cone-beam computed tomography images according to diagnostic task. Oral Surg Oral Med Oral Pathol Oral Radiol 119: 357–365 (2015)

Christell H, Birch S, Hedesiu M, Horner K, Ivanauskaité D, Nackaerts O, Rohlin M, Lindh C, SEDENT-EXCT Consortium: Variation in costs of cone beam CT examinations among healthcare systems. Dentomaxillofac Radiol 41: 571–577 (2012)

Davies J, Johnson B, Drage N A: Effective doses from cone beam CT investigation of the jaws. Dentomaxillofac Radiol 41: 30–36 (2012)

De Man B, Basu S: Distance-driven projection and backprojection in three dimensions. Phys Med Biol 49: 2463–2475 (2004)

De Paula-Silva F W, Wu M K, Leonardo M R, Bezerra L A, Wesselink P R: Accuracy of Periapical Radiography and Cone-Beam Computed Tomography Scans in Diagnosing Apical Periodontitis Using Histopathological Findings as a Gold Standard. J Endod 35: 1009–1012 (2009)

De Vos W, Casselman J, Sweenen G R: Cone beam computerized tomography (CBCT) imaging of the oral and maxillofacial region: a systematic review of the literature. Dentomaxilofac Radiol 38: 609–625 (2009)

Dölekoğlu S, Fişekçioğlu E, Igüy M I, Igü Y: The usage of digital radiography and cone beam computed tomography among Turkish dentists. DentomaxillofacRadiol 40: 379–384 (2011)

Donaldson K, O'Connor S, Heath N: Dental cone beam CT image quality possibly reduced by patient movement. Dentomaxillofac Radiol 42: 91866873 (2013)

Drage N, Carmichael F, Brown J: Radiation protection: protection of patients undergoing cone beam computed tomography examinations. Dent Update 37: 542–544, 547–548 (2010)

Drago C, Carpentieri J: Treatment of maxillary jaws with dental implants: guidelines for treatment. J Prosthodont 20: 336–347 (2011)

Dula K, Benic G I, Bornstein M, Dagassan-Berndt D, Filippi A, Hicklin S, Kisslingjeger F, Luebbers H-T, Sculean A, Sequeira-Byron P, Walter C, Zehnder M: SADMFR Guidelines for the use of cone-beam computed tomography/digital volume tomography endodontics, periodontology, reconstructive dentistry, pediatric dentistry. A consensus workshop organized by the Swiss association of dentomaxillofacial radiology. S Dent J 125: 945–953 (2015)

Durack C, Patel S, Davies J, Wilson R, Mannocci F: Diagnostic accuracy of small volume cone beam computed tomography and intraoral periapical radiography for the detection of simulated external inflammatory root resorption. Int Endod J 44: 136–147 (2011)

Ee J, Fayd M I, Johnson B R: Comparison of endodontic diagnosis and treatment planning decisions using cone-beam volumetric tomography versus periapical radiography. J Endod 40: 910–916 (2014)

Esposito S, Cardaropoli M, Cotti E: A suggested technique for the application of the cone beam computed tomography periapical index. Dentomaxillofac Radiol 40: 506–512 (2011)

European Commission: Radiation Protection 1136. European Guidelines on Radiation Protection in Dental Radiology. Luxembourg: Office for official Publications of the European Communities. (2004)

European Commission: Radiation protection 172: Evidence based guidelines on cone beam CT for dental and maxillofacial radiology. Luxembourg: Office for Official publications of the European Communities. (2012)

European Society of Endodontology, Patel S, Durack C, Abella F, Roig M, Shemesh H, Lambrechts P, Lemberg K: European Society of Endodontology position statement: the use of CBCT in endodontics. Int Endod J 47: 502–504 (2014)

EzEldeen M, Stratis A, Coucke W, Codari M, Politis, Jacobs R: As Low Dose as Sufficient Quality: Optimization of Cone-beam Computed Tomographic Scanning Protocol for Tooth Autotransplantation Planning and Follow-up in Children. J Endod 43: 210–217 (2017)

Horner K, Eaton K A: Selection criteria for dental radiography. Faculty of General Dental Practice 3rd edn. London, UK (2013)

Fryback D G, Thornbury J R: The efficacy of diagnostic imaging. Med Decis Making 11(2): 88–94 (1991)

Ghaeminia H, Meijer G J, Soehardi A, Borstlap W A, Mulder J, Berge S J: Position of the impacted third molar in relation to the mandibular canal. Diagnostic accuracy of cone beam computed tomography compared with panoramic radiography. Int J Oral Maxillofac Surg 38: 964–971 (2009)

Ghaeminia H, Gerlach N L, Hoppenreijs Th J M, Kicken M, Dings J P, Borstlap W A, de Haan T, Bergé S J, Meijer G J, Maal T J: Clinical relevance of cone beam computed tomography in mandibular third molar removal: A multicentre, randomised, controlled trial. J Craniomaxillofac Surg 43: 2158–2167 (2015)

Goulston R, Davies J, Hornerk, Murphy F: Dose optimization by altering the operating potential and tube current exposure time product in dental cone beam CT: a systematic review. Dentomaxilofac Radiol 45: 20150254 (2016)

Guerrero M E, Botetano R, Beltran J, Horner K, Jacobs R: Can preoperative imaging help to predict postoperative outcome after wisdom tooth removal? A randomized controlled trial using panoramic radiography versus cone beam CT. Clin Oral Invest 18: 335–342 (2014a)

Guerrero M E, Noiega J, Castro C, Jacobs R: Does cone-beam CT alter treatment plans? Comparison of preoperative implant planning using panoramic versus cone-beam CT images. Imaging Science in Dentistry 44: 121–128 (2014b)

Guyatt G H, Tugwell P X, Feeny D H, Drummond M F, Haynes R B: The role of before-after studies of therapeutic impact in the evaluation of diagnostic technologies. Journal Chronic Dis 39: 295–304 (1986)

Hall E J, Brenner D J: Cancer risks from diagnostic radiology. Br J Radiol 81: 362–378 (2008)

Haney E, Gansky S A, Lee J S, Johnson E, Maki K, Miller A J, Huang J C: Comparative analysis of traditional radiographs and cone-beam computed tomography volumetric images in the diagnosis and treatment planning of maxillary impacted canines. Am J Orthod Dentofacial Orthop 137: 590–597 (2010)

Harris D, Horner K, Gröndahl K, Jacobs R, Helmrot E, Benic G I, Bornstein M M, Dawood A, Quirynen M: E.A.O. guidelines for the use of diagnostic imaging in implant dentistry 2011. A consensus workshop organized by the European Association for Osseointegration at the Medical University of Warsaw. Clin Oral Implants Res 23: 1243–1253 (2011)

Hashem D, Brown J E, Patel S, Mannocci F, Donaldson A N, Watson T, Banerjee A: An In Vitro Comparison of the Accuracy of Measurements Obtained from High- and Low-resolution Conebeam Computed Tomography Scans. J Endod 39: 394–397 (2013)

Hatcher D C: Operational principles for cone-beam computed tomography. J Am Dent Assoc 141 Suppl 3: 3S–6S (2010)

Health Protection Agency: Guidance on the safe use of dental cone beam CT (Computed Tomography) Equipment. HPA-CRCE-010. Chilton: Health Protection Agency (2010)

Hidalgo Rivas J A, Davies J, Horner K, Theodorakou C: Effectiveness of thyroid gland shielding in dental CBCT using a paediatric anthropomorphic phantom. Dentomaxillofac Radiol 44 (3): 20140285 (2015)

Hidalgo Rivas J A, Horner K, Thiruvenkatachari B, Davies J, Theodorakuou C: Development of a low-dose protocol for cone beam CT examination of the anterior maxilla in children. Br J Radiol 88: 20150559 (2015)

Hirsch E, Wolf U, Heinicke F, Silva M A: Dosimetry of the cone beam computed tomography Veraviewepocs 3D compared with the 3D Accuitomo in different fields of view. Dentomaxillofac Radiol 37: 268–273 (2008)

Hol C, Hellén-Halme K, Torgersen G, Nilsson M, Møystad A: How do dentists use CBCT in dental clinics? A Norwegian nationwide survey, Acta Odontologica Scandinavica 73: 195–201 (2015)

Holroyd J R, Walker A: Recommendations for the design of X-ray facilities and quality assurance of dental cone Beam CT (computed tomography) system: Health Protection Agency HPA-RPD-065 (2010)

Horner K, Islam M, Flygare L, Tsiklakis K, Whites E: Basic principles for use of dental cone beam CT: consensus guidelines of the European Academy of Dental and Maxillofacial Radiology. Dentomaxillofac Radiol 38: 187–195 (2009)

Horner K, Jacobs R, Schulze R: Dental CBCT equipment and performance issues. Radiat Prot Dosimetry 153: 212–218 (2013)

Horner K, O'Malley L, Taylor K, Glenny A M: Guidelines for clinical use of CBCT: a review. Dentomaxillofac Radiol 44: 20140225 (2015)

IRCP: Publication 60. Recommendations of the International Commission on Radiological Protection. Ann IRCP: 21 (1990)

IRCP: Publication 103. The 2007 Recommendations of the International Commission on Radiological Protection. Ann IRCP: 37 (2007)

Jacobs R, Quirynen M, Bornstein M M: Neurovascular disturbances after implant surgery. Periodontol 2000 66: 188–202 (2013)

Kalender W A, Buchenau S, Deak P, Kellermeier M, Langner O, Van Straten M, Vollmar S, Wilharm S: Technical approaches to the optimization of CT. Phys Med 24: 71–79 (2008)

Kamboroğlu K, Kursun S: A comparison of the diagnostic accuracy of CBCT images of different voxel resolutions used to detect simulated small internal resorption cavities. Int Endod J 43: 798–807 (2010)

Karmazyn B, Liang Y, Klahr P, Jennings S G: Effect of Tube Voltage on CT Noise Levels in Different Phantom Sizes. Am J Roentgenol 200: 1001–1005 (2013)

Kiljunen T, Kaasalainen T, Suomalainen A, Kortesniemi M: Dental cone beam CT: A Review. Phys Med 31: 844–860 (2015)

Kim I, Patel M, Hirt S, Kantor M: Clinical research and diagnostic efficacy studies in the oral and maxillofacial radiology literature: 1996–2005. Dentomaxillofac Radiol 40: 274–281 (2011)

Kim D S, Rashsureno, Kim E K: Conversion coefficients for the estimation of effective dose in cone-beam CT. Imaging Sci Dent 44: 21–29 (2014)

Koivistoj, Kiljunen T, Tapiovaara M, Wolff J, Kortesniemi M: Assessment of radiation exposure in dental cone-beam computerized tomography with the use of metal-oxide semiconductor field-effect transistor (MOSFET) dosimeters and Monte Carlo simulations. Oral Surg Oral Med Oral Pathol Oral Radiol 114: 393–400 (2012)

Krupinski E A, Williams M B, Andriole K, Strauss K J, Applegate K, Wyatt M, Bjork S, Seibert J A: Digital radiography image quality: image processing and display. J Am Coll Radiol 4: 389–400 (2007)

Kurt S N, Üstün Y, Erdogan Ö, Evlice B, Yoldas O, Öztunc H: Outcomes of periradicular surgery of maxillary first molars using a vestibular approach: A prospective, clinical study with one year follow up. J Oral Maxillofac Surg 72: 1049–1061 (2014)

Kwong J C, Palomo J M, Landers M A, Figueroa A, Hans M G: Image quality produced by different cone-beam computed tomography settings. Am J Orthod Dentofacial Orthop 133: 317–327 (2008)

Kyriacou Y, Kolditz D, Langner O, Krause J, Kalender W: Digital Volume Tomography (DVT) and Multislice Spiral CT (MSCT): An Objective Examination of Dose and Image Quality. Fortschr Röntgenstr 183: 144–153 (2011)

Larsson J P, Persliden J, Sandborg M, Carlsson G A: Transmission ionization chambers for measurements of air collision kerma integrated over beam area. Factors limiting the accuracy of calibration. Phys Med Biol 41: 2831–2398 (1996)

Lennon S, Patel S, Foschi F, Wilson R, Davies J, Mannocci F: Diagnostic Accuracy Of Limited-Volume cone-beam computed tomography in the detection of periapical bone loss: 360˚ scans versus 180˚ scans. Int Endod J 44: 11181127 (2011)

Li X, Samei E, Segars W P, Sturgeon G M, Colsher J G, Toncheva G, Yoshizumi T T, Frush D P: Patient-specific radiation dose and cancer risk estimation in CT: part 11. application to patients. Med Phys 38: 408–419 (2011)

Liedke G S, da Silveira H E, da Silveira H L, Dutra V, De Figueiredo J A: Influence of voxel size in the diagnostic ability of cone beam tomography to evaluate simulated external root resorption. J Endod 35: 233–235 (2009)

Lofthag-Hansen S, Thilander-Mang A, Ekestubbe A, Helmrot E, Grondahl K: Calculating effective dose on a cone beam computed tomography device: 3D Accuitomo and 3D Accuitomo FPD. Dentomaxillofac Radiol 37: (2008)

Lofthag-Hansen S: Cone beam computed tomography radiation dose and image quality assessments. Swed Dent J Suppl 209: 4–55 (2010)

Lofthag-Hansen S, Thilander-King A, Gröndahl K: Evaluation of subjective image quality in relation to diagnostic task for cone beam computed tomography with different fields of view. Eur J Radiol 80: 483–488 (2011)

Loubele M, Bogaerts R, Van Dijck E, Pauwels R, Vanheusden S, Suetens P, Marchal G, Sanderink G, Jacobs R: Comparison between effective radiation dose of CBCT and MSCT scanners for dentomaxillofacial applications. Eur J Radiol 71: 461–468 (2009)

Luckow M, Deyhle H, Beckmann F, Dagassan-Berndt D, Müller B: Tilting the jaw to improve the image quality or to reduce the dose in cone-beam computed tomography. Eur J Radiol 80: e389–e393 (2011)

Ludlow J B, Davies-Ludlow L E, Brooks S L, Howerton W B: Dosimetry of 3 CBCT idevices for oral and maxillofacial radiology: CB Mercuray, NewTom 3 G and i-Cat. Dentomaxillofac Radiol 35: 219–226 (2006)

Ludlow J B, Davies-Ludlow L E, White S C: Patient risk related to common dental radiographic examinations: the impact of 2007 International Commission on Radiological Protection recommendations regarding dose calculation. J Am Dent Assoc 139: 1237–1243 (2008)

Ludlow J B, Ivanovic M: Comparative dosimetry of dental CBCT devices and 64-slice CT for oral and maxillofacial radiology. Oral Surg Oral Med Oral Pathol Oral Radiol Endod 106: 106–114 (2008)

Ludlow J B: Dose and risk in dental diagnostic imaging with emphasis on dosimetry of CBCT. Korean J Oral Maxillofac Radiol 39: 175–184 (2009)

Ludlow J B: A manufacturer's role in reducing the dose of cone beam computed tomography examinations: effect of beam filtration. Dentomaxillofac Radiol 40: 115–122 (2011)

Ludlow J B, Walker C: Assessment of phantom dosimetry and image quality of i-CAT FLX cone-beam computed tomography. Am J Orthod Dentofacial Orthop 144: 802–817 (2013)

Ludlow J B, Timothy R, Walker C, Hunter R, Benavides E, Samuelson B, Scheske J: Effective dose of dental CBCT – a meta-analysis of published data and additional data for nine CBCT units. Dentomaxillofac Radiol 44: 20140197 (2015)

Månsson L G: Methods for the evaluation of image quality: a review. Radiat Prot Dosimetry 90: 89–99 (2000)

Maret D, Telmon N, Peters O A, Lepage B, Treil J, Inglèse J M, Peyre A, Kahn J L, Sixou M: Effect of voxel size on the accuracy of 3D reconstructions with cone beam CT. Dentomaxillofac Radiol 41: 649–655 (2012)

Marine P M, Stabin M G, Fernald M J, Brill A B: Changes in radiation dose with variations in human anatomy: larger and smaller normal-stature adults. J Nucl Med 51: 806–811 (2010)

Marshall G, Sykes A E: Systematic reviews: a guide for radiographers and other healthcare professionals. Radiography 17: 158–164 (2011)

Martin C J, Sharp P F, Sutton D G: Measurement of image quality in diagnostic radiology. Appl Radiat Isot 50: 21–38 (1999)

Mathews J D, Forsythe A V, Brady Z, Butler M W, Goergen S K, Byrnes G B, Giles G G, Wallace A B, Anderson P R, Guiver T A, McGale P, Cain T M, Dowty J G, Bickerstaffe A C, Darby S C: Cancer risks in 680,000 people exposed to computed tomography scans in childhood or adolescence: data linkage study of 11 million Australians. BMJ 346: f2360 (2013)

Matzen L H, Christensen J, Hintze H, Schou S, Wenzel A: Diagnostic accuracy of panoramic radiography, stereo-scanography and cone beam CT for assessment of mandibular third molars before surgery. Acta Odontol Scan 71: 1391–1398 (2013)

Matzen L H, Wenzel A: Efficacy of CBCT for assessment of impacted mandibular third molars: a review – based on a hierarchical model of evidence. Dentomaxillofac Radiol 44: 20140189 (2015)

Meads C A, Davenport C F: Quality assessment of diagnostic before-after studies: development of methodology in the context of a systematic review. BMC Med Res Methodol 9: 3 (2009)

Melo S L, Bortoluzzi E A, Abreu M, Correa L, Correa M: Diagnostic ability of a cone-beam computed tomography scan to assess longitudinal root fractures in prosthetically treated teeth. J Endod 36: 1879–1882 (2010)

Mileman P A, van den Hout W B: Evidence-based diagnosis and clinical decision making. Dentomaxillofac Radiol 38: 1–10 (2009)

Morant J J, Salvado M, Hernandes-Giron I, Casanovas R, Ortrga R, Calzado A: Dosimetry and image quality of iCat FLX cone-beam computed tomography. Am J Orthod Dentofacial Orthop 144: 802–817 (2013)

Mori S, Endo M, Nishizawa K, Tsunoo T, Aoyama T, Fujiwara H, Murase K: Enlarged longitudinal dose profiles in cone-beam CT and the need for modified dosimetry. Med Phys 32: 1061–1069 (2005)

Mota de Almeida F J, Knutssin K, Flygare L: The effect of cone beam CT (CBCT) on therapeutic decision-making in endodontics. Dentomaxillofac Radiol 43: 20130137 (2014)

Mota de Almeida F J, Knutssin K, Flygare L: The impact of cone beam computed tomography on the choice of endodontic diagnosis. Int Endod 48: 564–572 (2015)

Moynihan R, Doust J, Heney D: Preventing overdiagnosis: how to stop harming the healthy. BMJ 344: e3502 (2012)

Mozzo E, Procacci C, Tacconi A, Martini P T, Andreis I A: A new volumetric CT machine for dental imaging based on the cone-beam technique preliminary results. Eur Radiol 8: 1558–1564 (1998)

National Council on Radiation Protection and Measurements: NCRP Report No.145. Radiation Protection in Dentistry www.ncrppublications.org/Reports/145 (2005)

National Research Council of the National Academies: Health Risks from Exposure to Low Levels of Ionizing Radiation: BEIR V11 (Washington DC: The National Academies Press) https://doi.org/10.17226/11340 (2006)

Nemtoi A, Czink C, Haba D, Gahleitner A: Cone beam CT: a current overview of devices. Dentomaxillofac Radiol 42: 20120443 (2013)

Neves F S, Vasconcelos T V, Vaz S L, Freitas D Q, Haiter-Neto F: Evaluation of reconstructed images with different voxel sizes of acquisition in the diagnosis of simulated external root resorption using cone beam computed tomography. Int Endod J 45: 234–239 (2012)

Nikolic-Jakoba N, Spin-Neto R, Wenzel A: Cone-Beam Computed Tomography for Detection of Intrabony and Furcation Defects: A Systematic Review Based on a Hierarchical Model for Diagnostic Efficacy. J Periodontal 87: 630–44 (2016)

Noffke C E, Farman A G, Nel S, Nzima N: Guidelines for the safe use of dental and maxillofacial CBCT: a review with recommendations for South Africa. SADJ 66: 264–266 (2011)

Papadakis A E, Perisinakis K, Damilakis J: Automatic exposure control in pediatric and adult multidetector CT examinations: a phantom study on dose reduction and image quality. Med Phys 35(10): 4567–4576 (2008)

Parashar V, Whaites E, Monsour P, Chaudhry J, Geist J R: Cone beam computed tomography in dental education: a surve y of US, UK, and Australian dental schools. Dent Educ 76: 1443–1447 (2012)

Parsa A, Ibrahim N, Hassan B, Motroni A, van der Stelt P, Wismeijer D: Influence of cone beam CT scanning paramters on grey value measurements at an implant site. Dentomaxillofac Radiol 42:79884780 (2013)

Patel S, Dawood A, Mannocci F, Wilson R, Pitt Ford T: Detection of periapical bone defects in human jaws using cone beam computed tomography and intraoral radiography. Int Endod J 42: 507–515 (2009)

Patel K, Mannocci F, Patel S: The Assessment and Management of External Cervical Resorption with Periapical Radiographs and Cone-beam Computed Tomography: A Clinical Study. J Endod 42: 1345–1440 (2016)

Pauwels R, Stamatakis H, Manousaridis G, Walker A, Michielsen K, Bosmans H, Bogaerts R, Jacobs R, Horner K, Tsiklakis K, SEDENTEXCT Project Consortium: Development and applicability of a quality control phantom for dental cone beam CT. J Appl Clin Med Phys 12: 245–260 (2011)

Pauwels R, Beinsberger J, Collaert B, Theodoraku C, Rogers J, Walker A, Cockmartin L, Bosmans H, Jacobs R, Bogaerts R, Horner K, SEDENTEXCT Project Consortium: Effective dose range for dental cone beam computed tomography scanners. Eur J Radiol 81: 267–271 (2012a)

Pauwels R: Optimization of cone beam computed tomography for dentomaxillofacial applications. Dissertation of University of Leuven (2012b)

Pauwels R, Theodorakou C, Walker A, Bosmans H, Jacobs R, Horner K, Bogaerts R, SEDENTEXCT Project Consortium: Dose distribution for dental cone beam CT and its implications for defining a dose index. Dentomaxillofac Radiol 41: 583–593 (2012c)

Pauwels R, Beinsberger J, Stamatakis H, Tsiklakis K, Walker A, Bosmans H, Bogaerts R, Jacobs R, Horner K; SEDENTEXCT Project Consortium: Comparison of spatial and contrast resolution for cone-beam computed tomography scanners. Oral Surg Oral Med Oral Pathol Oral Radiol 114: 127–135 (2012d)

Pauwels R, Stamatakis H, Bosmans H, Bogaerts R, Jacobs R, Horner K, Tsiklakis K, SEDENTEXCT Project Consortium: Quantification of metal artefacts on cone beam computed tomography images. Clin Oral Implants Res A100: 91–94 (2013)

Pauwels R, Cockmartin L, Ivanauskaite D, Urboniene A, Gaval S, Donta C, Tsiklakis K, Jacobs R, Bosmans H, Bogaerts R, Horner K, SEDENTEXCT Project Consortium: Estimating cancer risk from dental cone-beam CT exposure based on skin dosimetry. Phys Med Biol 59: 3877–3891 (2014a)

Pauwels R, Silkosessak O, Jacobs R, Bogaerts R, Bosmans H, Panmekiate S: A pragmatic approach to determine the optimal kVp in cone-beam CT: balancing contrast-to-noise ratio and radiation dose. Dentomaxillofac Radiol 20140059 (2014b)

Pauwels R, Araki K, Siewerdsen J H, Thongvigitmanee S S: Technical aspects of dental CBCT: state of the art. Dentomaxillofac Radiol 44: 20140224 (2015a)

Pauwels R, Seynaeve L, Henriques J C, de Oliveira-Santos C, Souza P C, Westphalen F H, Rubira-Bullen I R, Ribeiro-Rotta R F, Rockenbach M I, Haiter-Neto F, Pittayapat P, Bosmans H, Bogaerts R, Jacobs R: Optimization of dental cone-beam CT exposures through mAs reduction. Dentomaxillofac Radiol 44: 20150108 (2015b)

Pearce M S, Salotti J A, Little M P, McHugh K, Lee C, Kim K P, Howe N L, Ronckers C M, Rajaraman P, Craft A W, Parker L, de González A B: Radiation exposure from CT scans in childhood and subsequent risk of leukaemia and brain tumours: a retrospective cohort study. Lancet 380: 499–505 (2012)

Petersen L, Christensen J, Olsen K, Wenzel A: Image and surgery-related costs comparing cone beam CT and panoramic imaging before removal of impacted mandibular third molars. Dentomaxillofac Radiol 43: 20140001 (2014)

Petersen L B, Matzen L H, Olsen K, Vaeth M, Wenzel A: Economic implications of routine CBCT examination before surgical intervention of the lower third molar in the Danish population. Dentomaxillofac Radiol 44: 20140406 (2015)

Petersen L B, Vaeth M, Wenzel A: Neurosensoric disturbances after surgical removal of the mandibular third molar based on rather panoramic imaging or cone beam CT scanning: A randomized controlled trial (RCT). Dentomaxillofac Radiol 45: 20150224 (2016)

Petersson A, Axelsson S, Davidson T, Frisk F, Hakeberg M, Kvist T, Norlund A, Mejàre I, Portenier I, Sandberg H, Tranæus S, Bergenholtz G: Radiological diagnosis of periapical bone tissue lesions in endodontics: a systematic review. Int Endod J 45: 783–801 (2012)

Pope O, Sathorn C, Parashos P: Comparative Investigation of Cone-beam Computed Tomography and Periapical Radiography in the Diagnosis of a Healthy Periapex. J Endod 40: 360–365 (2014)

Preston D L, Ron E, Tokuoka S, Funamoto S, Nishi N, Soda M, Mabuchi K, Kodama K: Solid cancer incidence in atomic bomb survivors 1958–1998. Radiat Res 168: 1–64 (2007)

Qiao J, Wang S, Duan J, Zhang Y, Qiu Y, Sun C, Liu D: The accuracy of cone beam computed tomography in assessing maxillary molar furcation involvement. J Clin Periodontol 41: 269–274 (2014)

Qu X M, Li G, Ludlow J B, Zhang Z Y, Ma X C: Effective radiation dose of ProMax 3D cone-beam computerized tomography scanner with different protocols. Oral Surg Oral Med Oral Pathol Oral Radiol Endod 110: 770–776 (2010)

Qu X, Li G, Zhang Z, Ma X: Thyroid shields for radiation dose reduction during cone beam computed tomography scanning for different oral and maxillofacial regions. Eur J Radiol 81: 376–380 (2012)

Robb R A: Dynamic spatial reconstructor: an X-ray video fluoroscopic CT scanner for dynamic volume imaging of moving organs. IEEE Trans Med Imaging 1: 22–33 (1982)

Roberts J A, Drage N A, Davies J, Thomas D W: Effective dose from cone beam CT examinations in dentistry. Br J Radiol 82: 35–40 (2009)

Rodríguez G, Abella F, Durán-Sindreu F, Patel S, Roig M: Influence of cone beam tomography in clinical decision making among specialists. J Endod 43: 194–199 (2017)

Renton T, Dawood A, Shah A, Searson L, Yilmaz Z: Post-implant neuropathy of the trigeminal nerve. A case series. Br Dent 212: e17 (2012)

Roeder F, Wachtlin D, Schultze R: Necessity of 3D visualization for the removal of lower wisdom teeth: required sample size to prove non-inferiority of panoramic radiography compared to CBCT. Clin Oral Investig 16: 699–706 (2012)

Rood J P, Shebab B A: The radiological prediction of inferior alveolar nerve injury during third molar surgery. Br J Oral Maxillofac Surg 28(1): 20–25 (1990)

Rosen E, Taschieri S, Del Fabbro M, Beitlitum I, Tsesis I: The Diagnostic Efficacy of Cone-beam Computed Tomography in Endodontics: A Systematic Review and Analysis by a Hierarchical Model of Efficacy. J Endod 41: 1008–1014 (2015)

Scarfe W C, Farman A G: What is cone beam and how does it work? Dent Clin Am 52: 707–730 (2008)

Schulze D, Heiland M, Thurman H, Adam G: Radiation exposure during midfacial imaging using 4 and 16-slice computed tomography: cone beam computed tomography systems and conventional tomography. Dentomaxillofac Radiol 33: 83–86 (2004)

Schulze R, Heil U, Gross D, Bruellmann D D, Dranischnikow E, Schwanecke U, Schoemer E: Artefacts in CBCT; a review. Dentomaxillofac Radiol 40: 265–273 (2011)

Shelley A M, Brunton P, Horner K: Subjective Image Quality Assessment of Cross Sectional Imaging Methods for the Symphyseal Region of the Mandible Prior to Dental Implant Placement. J Dent 39: 764–770 (2011)

Shelley A M, Ferrero A, Brunton P, Goodwin M, Horner K: The impact of CBCT imaging when placing dental implants in the anterior edentulous mandible: a before–after study. Dentomaxillofac Radiol 44: 20140316 (2015)

Siegel M J, Schmidt B, Bradley D, Sues C, Hildebolt C: Radiation dose and image quality in pediatric CT: Effect of technical factors and phantom size and shape. Radiology 233: 515–522 (2004)

Spin-Neto R, Gotfredsen E, Wenzel A: Impact of voxel size variation on CBCT-based diagnostic outcomes in dentistry: a systematic review. J Digit Imaging 26: 813–820 (2013)

Spin-Neto R, Matzen L H, Schropp L, Gotfredsen E, Wenzel A: Movement characteristics in young patients and the impact on image quality: Dentomaxillofac Radiol 45: 20150426 (2016)

Stratis A, Zhang G, Lopez-Rendon X, Jacobs R, Bogaerts R, Bosmans H: Customisation of a Monte Carlo dosimetry tool for dental cone-beam CT systems. Radiat Prot Dosimetry 169: 378–85 (2016)

Suomalainen A, Kiljunen T, Kaser Y, Peltola J, Kortesniemi M: Dosimetry and image quality of four dental cone beam computed tomography scanners compared with multislice computed tomography scanners. Dentomaxilofac Radiol 38: 367–378 (2009)

Sur J, Seki K, Koizumi H, Nakajima K, Okano T: Effects of tube current on cone-beam computerized tomography image quality for presurgical implant planning in vitro. Oral Surg Oral Med Oral Pathol Oral Radiol 110: e29–33 (2010)

Tapiovaara M: Review of relationships between physical measurements and user evaluation of image quality. Radiat Prot Dosimetry 129: 244–248 (2008)

Theodoraku C, Walker A, Horner K, Pauwels R, Bogaerts R, Jacobs R, SEDENTEXCT Project Consortium: Estimation of paediatric organ and effective doses from dental cone beam CT using anthropomorphic phantoms. Br J Radiol 85: 153–160 (2012)

Tsisklakis K, Donta C, Gavala S, Karayianni K, Kamenopoulou V, Hourdakis C J: Dose reduction in maxillofacial imaging using low dose Cone Beam CT. Eur J Radiol 56: 413–417 (2005)

Tyndall D A, Price J B, Tetradis S, Ganz S D, Hildebolt C, Scarfe W C: American Academy of Oral and Maxillofacial Radiology. Position statement of the American Academy of Oral and Maxillofacial Radiology on selection criteria for the use of radiology in dental implantology with emphasis on cone beam computed tomography. Oral Surg Oral Med Oral Pathol Oral Radiol 113: 817–826 (2012)

Tubiana M, Feinendegen L E, Yang C, Kaminski J M: The linear no-threshold relationship is inconsistent with radiation biologic and experimental data. Radiology 251: 13–22 (2009)

Van Gompel G, Van Slambrouck K, Defrise M, Batenburg K J, de Mey J, Sijbers J, Nuyts J: Iterative correction of beam hardening artifacts in CT. Med Phys 38: S36 (2011)

Venskutonis T, Plotino G, Juodzbalys G, Mickevičiene L: The importance of cone-beam computed tomography in the management of endodontic problems: A review of the literature. J Endod 40: 1895–1901 (2014)

Walter C, Weiger R, Dietrich T, Lang N P, Zitzmann N U: Does three-dimensional imaging offer a financial benefit for treating maxillary molars with furcation involvement? A pilot clinical case series. Clin Oral Implants Res 23: 351–358 (2012)

Waltrick K B, Nunes de Abreu M J, Corrêa M, Zastrow M D, Dutra V D: Accuracy of linear measurements and visibility of the mandibular canal of cone-beam computed tomography images with different voxel sizes: an in vitro study. J Periodontal 84: 68–77 (2013)

WANG G, VANNIER M W, CHENG P C: Iterative X-ray cone-beam tomography for metal artefact reduction and local region reconstruction. Microsc Microanal 5: 58–65 (1999)

WATANABE H, HONDA E, TETSUMURA A, KURABAYASHI T: A comparative study for spatial resolution and subjective image characteristics of a multi-slice CT and a cone-beam CT for dental use. Eur J Radiol 77: 397–402 (2011)

WHITE S C, SCARFE W C, SCHULZE R K W, LURIE A G, DOUGLASS J M, FARMAN A G, LAW C S, LEVIN M D, SAUER R A, VALACHOVIC R W, ZELLER G G, GOSKE M J: The Image Gently in Dentistry campaign: promotion of responsible use of maxillofacial radiology in dentistry for children. Oral Surg Oral Med Oral Pathol Oral Radiol 118: 257–261 (2014)

WHITE S C, PHAROAH M J: Oral Radiology. Principles and Interpretation, 7th Edition, St. Louis, Mosby (2013)

YADAV S, PALO L, MAHDIAN M, UPADHYAY M, TADINADA A: Diagnostic accuracy of 2 cone-beam computed tomograohy protocols for detecting arthritic changes in temporomandibular joints. Am J Orthod Dentofacial Orthop 147: 339–344 (2015)

YU L, LIUX, LENG S, KOFLER J M, RAMIREZ-GIRALDO J C, QU M, CHRISTNER J, FLETCHER J G, MCCOLLOUGH C H: Radiation dose reduction in computed tomography: techniques and future perspective. Imaging Med 1: 65–68 (2009)

ZHANG G, MARSHALL N, BOGAERTS R, JACOBS R, BOSMANS H: Monte Carlo modelling for dose assessment in cone beam CT for oral and maxillofacial applications. Med Phys 40: 072103 (2013)

ZIJDERVELD S A, VAN DEN BERGH J P, SCHULTEN E A, TEN BRUGGENKATE C M: Anatomical and surgical findings and complications in 100 consecutive maxillary sinus floor elevation procedures. J Oral Maxillofac Surg 66: 1426–1438 (2008)

RESEARCH ARTICLE

An investigation into dose optimisation for imaging root canal anatomy using cone beam CT

[1]Margarete B McGuigan, [2]Christie Theodorakou, [1]Henry F Duncan, [3]Jonathan Davies, [4]Anita Sengupta and [1,4]Keith Horner

[1]Dublin Dental University Hospital, Trinity College Dublin, Dublin, Ireland; [2]Christie Medical Physics and Engineering, The Christie NHS Foundation Trust, Manchester, UK; [3]Guy's Hospital, Guy's and St Thomas' NHS Foundation Trust, London, UK; [4]Division of Dentistry, School of Medical Sciences, The University of Manchester, Manchester, UK

Objectives: To identify a dose as low as diagnostically acceptable and a threshold level of image quality for cone beam CT (CBCT) imaging root canals, using maxillary first molar (M1M) second mesiobuccal (MB2) canals of varying complexity for two CBCT scanners.

Methods: Dose–area product (DAP) and contrast-to-noise ratio (CNR) were measured for two scanners at a range of exposure parameters. Subjective-image-quality assessment at the same exposures was performed for three M1Ms of varying MB2 complexity, positioned in an anthropomorphic phantom. Nine raters (three endodontists, three dental radiologists and three junior staff) assessed canal visibility, using a 5-point confidence scale rating.

Results: Identification of simple-moderate MB2 canal complexity was achieved at a range of protocols, with DAP values of ≥209.3 and ≥203.2 mGy cm² and CNRs of 3 and 7.6 for Promax®3D and Accuitomo-F170® respectively. For complex canal anatomy, target subjective image quality was not achieved, even at the highest DAP values for both scanners. Junior staff classified significantly more images as undiagnostic compared with senior staff ($p = 0.043$).

Conclusions: In this first study to address optimisation of CBCT imaging of root canal anatomy, a similar threshold dose for both scanners was identified for M1Ms with simple-moderate MB2 canal complexity. Increasing dose to enhance visualisation of more complex canal anatomy was ineffective. Selection of standard protocols (while avoiding lower kV/mA protocols) instead of high-resolution scans was a practical means of reducing patient dose. CNR is not a transferable measure of image quality.

Dentomaxillofacial Radiology (2020) **49**, 20200072. doi: [10.1259/dmfr.20200072](https://doi.org/10.1259/dmfr.20200072)

Introduction

The use of cone beam CT (CBCT) in dentistry is not routinely indicated, but can be justified when conventional radiography is insufficient for the specific diagnostic task.[1–5] Nevertheless, CBCT use is becoming increasingly prevalent in primary care, where there is potentially less supervision and a range of training and experience among its users.[6] CBCT can provide acceptable image quality over a wide range of exposures; therefore, a risk exists of over exposing the patients, without any diagnostically useful gain in image quality.[7]

An awareness of the need to "tailor" dose according to the specific diagnostic indication, while also considering patient type, has prompted the evolution from the dose optimisation strategy ALADA (As low as diagnostically acceptable) toward ALADAIP (As Low as Diagnostically Acceptable being Indication-oriented

and Patient-specific).[8] Selection criteria guidelines and general dose optimisation guidance serve to aid the practitioner in the appropriateness of CBCT exposure.[3,9] The pertinence of employing low dose protocols has recently been highlighted,[10] with protocols achieving significant dose reductions suggested in the dental disciplines of paediatric dentistry,[11] orthodontics,[12] tooth autotransplantation (TAT),[13] periodontology[14] and implant dentistry.[15] In the process of optimisation, both the acceptable clinical level of the image quality and the radiation dose may differ according to diagnostic tasks.[16] Although such studies have provided evidence to assist in optimisation efforts for particular scanner models used, there is no evidence that the objective image quality measurements can be transferred to a different manufacturer's CBCT equipment or even to different models from the same manufacturer. Thus, there is a need to identify if a threshold level of objective image quality exists for a specific diagnostic task that might be readily transferable to a different scanner, avoiding the time-consuming assessments used in this kind of research study.

Within endodontics, limited volume, high-resolution CBCT is indicated where the diagnostic yield from conventional radiography is inadequate, such as in cases of complex/atypical anatomy, resorption, perforation and complicated endodontic surgery.[1,3,5] Complex and atypical anatomy is of particular relevance as evaluation of tooth complexity is subjective and because the success of treatment depends on location, negotiation and chemomechanical debridement of the entire root canal system prior to filling.[17,18] Recognised differences in maxillary first molar root canal morphology exist due to the anatomic variations of the second mesiobuccal (MB2) canal,[19,20] within which there is an inherent range of complexity.[21,22] Of all dental applications of CBCT, endodontics is the one for which a high level of image quality is invariably recommended.[3] Imaging the MB2 root canal anatomy of upper first molars represents a good clinical test of image quality needs of an endodontist. High-resolution settings are often selected in such situations, although it is essential to recognise that this is only achieved by changing exposure parameters in ways that increase patient dose, so optimisation of exposures is especially relevant to endodontic practice.

Clinically, image quality is ultimately subjective, being based on whether the diagnostic task can be achieved in the opinion of the reporting clinician. Because of inter- and intraclinician variability in assessment of radiological images, it is important to relate such subjective assessments to objective measurements of image quality, in this case CNR, with the purpose of identifying if minimally acceptable values exist for specific diagnostic tasks that could potentially aid in the process of dose optimisation.[23] Validated methods of assessing objective and subjective image quality using a SedentexCT phantom and anthropomorphic phantoms respectively have been used in the pursuit of optimizing

doses for specific diagnostic tasks[12,14,15] but not for identification of root canal anatomy/imaging for endodontic purposes. As high-resolution protocols are currently recommended for CBCT imaging to assess root canal anatomy,[3] in addition to studying the impact of altering tube voltage and tube current-exposure time product, this study planned to investigate the effect of available scanning protocols including high resolution and 180° scans on achieving this clinical task.

Therefore, the overall aim of this study was to identify a threshold level of dose for CBCT which is ALADA for adequate imaging of MB2 root canal anatomy of maxillary first molars and, additionally, to quantify the objective image quality at this threshold dose. By performing this for two scanner types, some insight into the transferability of the results would be obtained. Additional objectives included investigating the impact of anatomy complexity on establishing this threshold dose and examining the impact of operator experience on diagnostic efficacy.

Methods and materials

Sample selection and preparation
The use of extracted teeth for this study was approved by St James Hospital/Tallaght University Hospital Dublin (2019–02). Maxillary left permanent first molars were selected from a bank of extracted teeth. After extraction, the teeth were washed with water and the adherent tissue removed gently by scraping before being immersed in a 2% sodium hypochlorite solution (Milton solution, Proctor & Gamble Ireland, Dublin, Ireland) for 24 h, prior to storage in a sterile saline solution until ready to use. Included teeth were limited to maxillary permanent first molars (as identified by coronal and root anatomic–morphological appearance and dimension) of normal external anatomy, a mesiodistal crown diameter of 10 mm ± 0.2,[24] three mature distinct roots with closed apices, absence of root fracture, caries or resorption, a complete pulpal floor and no evidence of previous root canal treatment. 12 left maxillary molars which visually adhered to the inclusion criteria, were imaged using the ProMax® 3D Classic CBCT scanner (Planmeca, Helsinki, Finland) to confirm the inclusion characteristics and root canal morphology. From the 12 scanned teeth, 3 representative left maxillary molars of varying MB complexity were provisionally selected for microCT analysis.

MicroCT analysis
In order to analyse comprehensively the MB root canal system complexity, the three left maxillary molars were subjected to detailed analysis using microCT (μCT 40 SCANCO Medical AG, Brüttisellen, Switzerland). MicroCT analysis was completed at 70 kVp, 114 mA, 8 W with a spatial resolution of 20 μm. For each tooth, a microCT three-dimensional (3D) model of the root canal
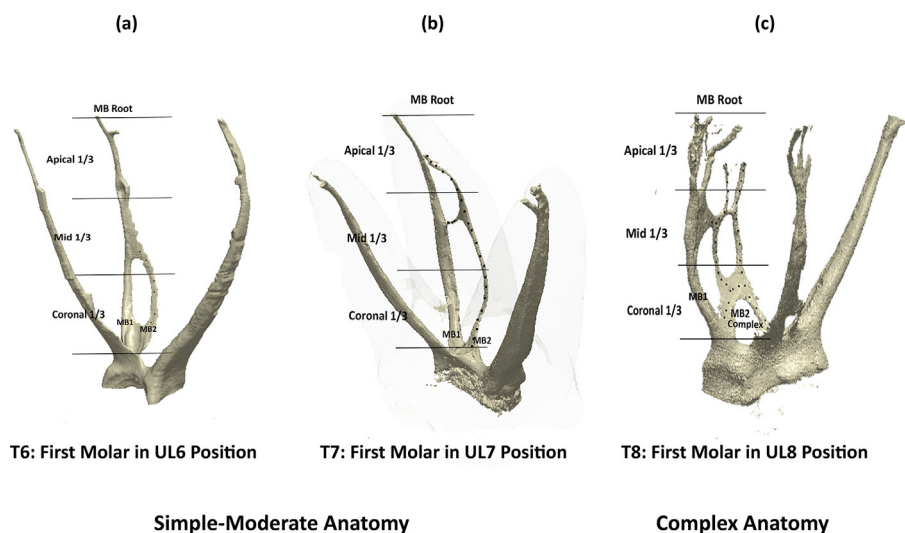
Figure 1 MicroCT 3D models of the root canal systems of the three maxillary molars: (a) T6 (b) T7 (simple-moderate anatomy) and (c) T8 (complex anatomy) constructed with 3D IPO image processing language (v. 5.15, Scanco Medical, Brüttisellen, IPSwitzerland). 3D, three-dimensional.

system was constructed with 3D IPO image processing language (v. 5.15, Scanco Medical, Brüttisellen, Switzerland). The reconstructed microCT 3D models of the root canal systems and two-dimensional (2D) slices (*n* = 502 per tooth) were viewed independently by two endodontists (defined as an individual who has completed a 3-year full time training programme in endodontics) who by consensus, confirmed the teeth as maxillary first molars. In order to facilitate comparison between the three teeth, the diameter of the main trunk of the MB2 canal was measured. The maximum width of the MB2 canal in the coronal third was; T6 - 760 μm; T7 - 710 μm; T8 - 735 μm and the minimum diameter, which was either in the middle or apical third of the root was; T6 - 200 μm; T7 - 145 μm; T8 - 163 μm. Subsequently, the canal number, configuration and complexity of the MB2 canals of each of the three maxillary molars were determined and classified accordingly. Specifically, the root canal systems of three representative maxillary first molars were classified into simple, moderate and complex morphology as seen in Figure 1a–c. The "root canal system" was defined as arising from an orifice(s) in the pulp floor, continuing through the canal(s) to the apically positioned foramen (or foramina).[25] The maxillary molar positioned in the skull in the first molar position was named T6, (Figure 1a). The MB2 root canal system of T6 originated from one orifice in the pulpal floor, before the MB1 and MB2 canal splits 1–2 mm apical to the pulp floor in the coronal third of the root. The MB2 canal rejoined the MB1 canal in the coronal aspect of the mid-third of the root before terminating in one foramen. This is a common anatomical variation that is relatively easy to manage and was therefore classified to be of simple complexity. The maxillary first molar in the second molar position in the skull was named T7 (Figure 1b). The MB2 root canal system

of T7 originated from two orifices in the floor of the pulp chamber and terminated just short of the MB1 in the apical third of the root. T7 exhibited an added anatomical feature of an anastomosis between the MB1 and MB2 in the mid-root area and, as a result T7, was considered to be of simple to moderate complexity. The maxillary first molar occupying the third molar position in the skull was called T8 (Figure 1c). The MB root canal system of T8 exhibited three separate MB canals (MB2 and MB3 [within the MB2 complex]), with multiple connections between the MB2, MB3 canals and MB1 canal in the middle third of the root. Consequently, T8 was classified as having complex anatomy, being categorised as high difficulty with respect to diagnosis and treatment.[26]

CBCT scanners and selected exposure parameters
Two scanners were selected to perform CBCT imaging: Accuitomo F170® (J. Morita, Kyoto, Japan) and ProMax® 3D Classic. The smallest available voxel size and field-of-view (FOV) option applicable to each scanner were selected according to the manufacturers' guidelines for endodontic imaging. For the Accuitomo F170®; the FOV was 4 cm (diameter: D) x 4 cm (height: H) and 80 μm voxel size, the FOV for the ProMax® 3D was 5 cm (D) x 5 cm (H) with a 100 μm voxel size. There were 33 different scanning protocols for the Accuitomo F170®: X-ray tube operating potentials of 70, 80, 90 kV and X-ray tube current selections of 3, 5, 7 and 9 mA. These combinations were completed using a full rotation 360° at normal (17.5 s) and high resolution (30 s) settings (excluding at 9 mA, for which high resolution settings are not possible) and then again at half rotation: 180° (9 s). For the ProMax® 3D scanner the same X-ray tube voltages 70, 80, 90 kV were used, with X-ray tube

currents of 3.2, 5, 7.1 and 9 mA, which were the closest possible corresponding options to the Accuitomo F170® that could be selected. This resulted in 12 exposure combinations for the ProMax® 3D. Rotations of 180° and high resolution options altering time alone were not features of the ProMax® 3D scanner. These combinations represent a wide range of exposures, including those employed in clinical practice and recommended in manufacturer protocols for endodontic imaging.

Dose measurements
Dose measurements were performed on each CBCT scanner for the chosen exposure settings. Dose–area product (DAP) values (mGy cm²) were obtained using a calibrated DAP meter sensor with an active area of 7 cm (VacuDap; VacuTech Messtechnik GmbH, Dresden, Germany) positioned at the centre of the X-ray tube window; this completely intercepted the radiation field (4 × 4 cm: Accuitomo® F170 and 5 × 5 cm: ProMax® 3D) for all combinations of kV and mAs. For the Accuitomo F170®, this resulted in 33 DAP values (as exposures at 9 mA were not possible at high resolution setting) and 12 DAP values for the ProMax® 3D. To assess consistency of the units, the DAP values were repeated and recorded four times for 80 kV, 5 mA at normal and high resolution where applicable and the coefficient of variation calculated.

Image quality: objective measurement
To assess objective image quality, contrast resolution was measured using the SedentexCT IQ phantom (Leeds Test Objects, Boroughbridge, UK): 162 mm (H) x 160 mm (D) along with the corresponding polytetrafluoroethylene (PTFE) insert, consisting of five rods of PTFE of differing diameters (1, 2, 3, 4 and 5 mm) embedded in polymethylmethacrylate (PMMA). The PTFE insert was selected as being representative of dental hard tissue.[12,14]

The insert was positioned in the upper left molar region in the phantom (as per position of experimental teeth in skull) and the remaining phantom columns in the SedentexCT IQ were filled with PMMA inserts. The dedicated dental CBCT phantom was mounted on a rigid tripod and positioned as per standard patient set-up. In total, all inserts were scanned individually at all exposure protocols for Accuitomo F170® (x33) and ProMax® 3D (x12).

Calculating CNR
The resulting 45 data sets from the PTFE insert scans were individually exported as DICOM files into Image J software v. 145 s (National Institute of Health, Bethseda, MD). Axial images were analysed at a 16-bit scale. On these images, a circular region of interest (12 mm²) was drawn on the 5 mm diameter rod of the PTFE insert and another in the background PMMA thereby enabling pixel value calculation of each material. Beginning at the centre of the 5 mm rod and moving upwards (to avoid possible interference in pixel values created by the air gap between the test insert and the blank PMMA) measurements were performed on five consecutive axial images. For each scanning protocol, the mean and standard deviation of the pixel values from the five slices were recorded for the PTFE rod and background material and CNR calculated using the formula:

$$CNR = \frac{(MPV_{insert} - MPV_{background})}{\sqrt{(standard\ deviation_{insert} + standard\ deviation_{background})/2}}$$

Image quality: subjective measurement
The three selected left maxillary molars were mounted in a dried adult skull (obtained from the Anatomy Department of Trinity College Dublin) from which the existing molars had been carefully extracted by sectioning the roots to avoid damage to surrounding bone. Mounting of the three teeth selected for the study involved careful osteoplasty of the alveolar bone using a stainless steel rosehead bur in a slow-speed handpiece to acquire a best possible fit, prioritising an optimal position of the buccal roots. The three study teeth were maintained in place with a radiolucent modelling wax. The skull and implanted teeth were positioned in a head-shaped polystyrene container, specifically designed to house the skull along with upper cervical spine vertebrae (C1-C4) and immersed in water to simulate soft tissue density. This anthropomorphic phantom was the same as that used in previous studies,[12,27] designed to replicate the clinical scenario as closely as possible, with the skull and cervical vertebrae being soaked in water for 48 h before imaging to ensure water had displaced air from all trabecular spaces.

The container design facilitated fixation to a tripod stand and allowed positioning as for a patient set-up with initial scout images confirming centering of the FOV on the upper left molar region. The phantom was then exposed to all 33 scanning protocols as described for the Accuitomo F170® scanner, this being completed in one session ensuring imaging consistency. This same protocol was repeated for all 12 scanning combinations described for the Promax® 3D scanner.

Image evaluation
Including both scanners, there were 45 CBCT data sets available for observation. An additional nine datasets (20%) were randomly selected and duplicated within the study sample to assess intraobserver variability, the observer being blinded to the duplicates. The resulting 54 data sets were randomised (via a downloaded internet programme https://app.studyrandomizer.com/); volume acquisition parameters anonymised and each allocated a number 1–54.

Images were viewed with the viewing software provided by the manufacturer; Accuitomo datasets using i-Dixel One Volume Viewer software (Morita, Japan) and the ProMax data sets viewed using Planmeca Romexis software (Helsinki, Finland). Evaluation of all
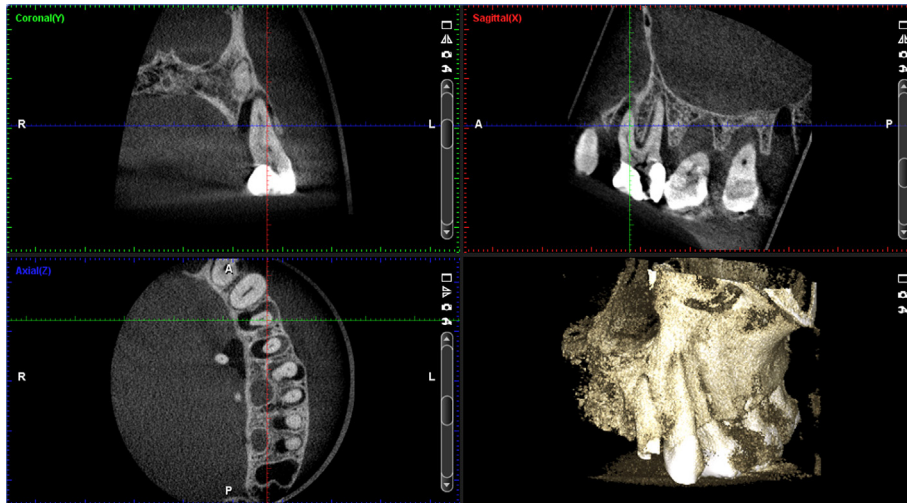
Figure 2 ProMax® 3D dataset (viewed with Romexis software) of the three implanted maxillary molars which were evaluated in all three orthogonal planes to identify the presence and extent of the MB2 canal at the exposure parameters of that image set (80 kV, 5 mA). 3D, three-dimensional. MB2, second mesiobuccal.

the images was facilitated using a new Acer V176LBMD 17" HD Ready Monitor (Acer UK, London), with lumininance of 250 cd/m², dynamic contrast ratio of 100,000,000:1 and resolution of 1280 × 1024 pixels. The technical specifications of the monitor are within the range indicated by the Health Protection Agency as required for diagnostic purposes of dental CBCT images (Health Protection Agency, 2010). Evaluation of the monitor using a test pattern [Society of Motion Picture and Television Engineers test pattern (SMPTE)] was carried out to determine that each distinct greyscale levels and all of the bars on each of the resolution test patterns could be individually resolved.

Subjective evaluation of image quality was performed by nine observers, consisting of six senior hospital dentists (three dental and maxillofacial radiologists and three endodontists) and three junior hospital dentists (dentist with ≤2 years post qualification). The observers were informed that the purpose of the study was to evaluate the effect of differing acquisition parameters on identification of MB2 canal anatomy in maxillary first molars. All observers had exposure to CBCT image interpretation and software. Nonetheless, due to their differing skill sets, range of CBCT interpretation experience and familiarity with the two viewing software systems utilised in the study, a standardised interactive tutorial was given by one of the researchers (MM) prior to the observation and reinforced with a printed document. Viewing conditions for all observers were consistent. Ambient room lighting was recorded using an illuminance meter and ensured that this was less than 50 lux. Observers were able to adjust contrast and brightness as required and to rotate and tilt the volumetric data using the three orthogonal reconstructions, a screenshot from one of the data sets can be seen in Figure 2. No time restriction was placed on the period of observation.

Each observer completed a 7-part questionnaire, which they answered using a 5-point rating scale of agreement for each of the 3 maxillary first molars for all 54 scans, circling the number which corresponded to their answer (Table 1). Questions (Qs) 1–4 related to the presence of the MB2 canal at the pulp floor, in the coronal third, middle third and apical third of the

Table 1 Summary form of questionnaire, with a rating scale to reflect the confidence the observers had in their response

Can you identify a **separate** second mesiobuccal canal (MB2) in the root anatomy for each maxillary first molar:	**0 = No - Complete Confidence**
	1 = No - Partial Confidence
Q1- At level of pulp floor?	**2 = Unsure**
	3 = Yes - Partial Confidence
Q2- Within coronal third?	**4 = Yes - Complete Confidence**
Q3- Within mid-third?	
Q4- Within apical-third?	
Q5- If identified, is the MB2 canal continuously visible from its perceived origins coronally to its termination?	
Q6- Are you confident that this volume is diagnostically acceptable?	
Q7- For each volume 1–54, can you trace over the microCT depiction of the MB2 canal anatomy that you can **definitively identify** from the image set for the first molar teeth in positions UL6, UL7, UL8 with the provided red pen.	

MB2, second mesiobuccal.

tooth, but did not address continuity of the canal, which was considered in Q5. Q6 related to the confidence the observer had in the acceptability of the image quality of the scan. While Q5 dealt with canal continuity using a confidence scale, a final required task (Q7) involved a quantitative assessment of canal visibility. This involved tracing the extent of the MB2 canal that they could definitively identify for each of the three teeth, using the microCT images of the molar anatomy as a template. These tracings of the anatomy were then measured using a calibrated acetate overlay and the percentage of the MB2 anatomy identified (recorded as a percentage of the total length identified on microCT) and assigned to each of the three maxillary molars per volume. To assess repeatability of this measurement technique, five randomly chosen data sets were selected to repeat the measurements.

The observers had been familiarised with the questionnaire as part of the instruction tutorial. The questionnaire was piloted by 2 endodontists and 2 junior hospital dentists who evaluated 10 randomly chosen data sets and their feedback on the instructions and questionnaire was used to refine the final documents.

Data analysis
Diagnostic acceptability (Q6) responses for each of the 45 data sets (excluding repeats) were examined and if the percentage of observers recording a scan as diagnostically acceptable (*i.e.* agreed or strongly agreed options) fell below 67% (*i.e.* 6 out of 9 observers), it was considered a negative result and was excluded from further analysis.

Assessment of pilot study results identified target levels for specific subjective imaging tasks: identification of the percentage of MB2 root canal identifiable and secondly for both confidence in the presence of the canal at the different levels of the root (Qs 1–4, Table 1) and identification of canal continuity (Q5, Table 1).

On analysis of percentage of MB2 root canal anatomy identified by each observer for each of the three maxillary first molars at every diagnostic exposure protocol in the pilot study, a target subjective image task was provisionally set as identifying 95% of the MB2 canal anatomy. This task included identification of the canal at the level of the pulp chamber floor and the coronal third of the MB root, which by consensus was deemed most relevant from an endodontist's perspective.

Employing the confidence scale ratings from questionnaires for diagnostic exposure protocols from the pilot study, the median of the observers' confidence scale rating (CSR) responses for the identification of the MB2 canal for Q's 1–4 at the level of the pulpal floor and in the coronal, middle and apical thirds of the root were identified for each of T6, T7 and T8. Similarly, the median CSR responses related to Q5: identification of a continuous MB2 canal from perceived origin to termination, were established. Using these data, a second target subjective image task of achieving median CSRs

of 3.5 was set from the pilot study. This corresponded to 95% MB2 canal anatomy identification, achieving close to complete confidence in identifying the MB2 canal in all thirds of the root canal and identifying the MB2 canal continuously from origin to its termination.

These combined subjective image tasks were used to indicate the CNR values necessary to achieve the diagnostic task of root canal identification and from which the corresponding threshold exposure factors and DAP values could be identified.

Statistical analysis
Statistical analysis was performed using IBM SPSS Statistics (v. 24.0; IBM Corporation, NY). Intra and interobserver agreement for subjective image quality assessment was calculated using Cohen's κ test (*K*) using the scale for strength of agreement described by Altman; $K < 0.20$: poor, $K = 0.21–0.40$: fair, $K = 0.41–0.60$: moderate, $K = 0.61–0.80$: good, $K = 0.81–1.00$: very good.[28] Intraobserver agreement was calculated for each of the observers by considering their responses for Q's 1–5 (identification of root canal anatomy) in the questionnaire and also separately for Q6 (diagnostic acceptability of the data sets). To facilitate the analysis, the responses to the six questions were dichotomised, with values 4 and 5 considered as a positive result while 1, 2 and 3 were considered as negative result.[12,29] Interobserver agreement was evaluated for Q's 1–6 separately. The proportion of acceptable/unacceptable images identified by the junior hospital dentists and senior hospital dentists (endodontists and radiologists) was calculated. Contingency tables and a χ^2 test was used to determine statistical significance of the difference in proportions of these two groups with statistical significance set at $p<0.05$.

Results

Dose measurements
DAP values for the ProMax® 3D Classic (Table 2a) and Accuitomo F170® (Table 2b), demonstrate expected variations according to exposure settings. DAP value reproducibility for the ProMax® 3D scanner, based on four measurements at 80 kV and 5 mA resulted in a standard deviation (SD) of ±0.96 mGy cm². For the Accuitomo F170®, reproducibility at 80kV and 5 mA

Table 2a For ProMax® 3D:

DAP values				
Tube current		**Tube voltage (kV)**		
mA	**mAs**	**70**	**80**	**90**
3.2	38.4	49.5	90.3	135.3
5	60	77.1	139.4	209.3
7.1	85.2	107.6	195	294
9	108	134.4	244.6	373.3

DAP, Dose–area product.

Table 2b Accuitomo F170®: DAP values and associated exposure protocols of datasets that observer assessment identified as being:

				DAP values								
Tube current				Tube voltage (kV)								
mA		mAs		70			80			90		
	180°	S	HR	180°	S	HR	180°	S	HR	180°	S	HR
3	27	52.5	92.4	54.3	106.4	187.5	72.3	143.8	251.2	90.5	181.7	316.8
5	45	87.5	154	88.5	174.9	306.7	118.0	233.9	409.5	147.1	294	517.5
7	63	122.5	215.6	120.9	240.7	426.3	163.2	324.4	568.9	203.2	405.1	714.4
9	81	157.5	277.2	154.6	304.6	N/A	207.9	410.5	N/A	257.6	520.2	N/A

Undiagnostic: ■
Diagnostic: ▨
Diagnostic and achieving 'combined target subjective image tasks': ▢
DAP, dose–area product.

for both standard and high resolution settings had a resulting SD ±1.07 and ±1.39 mGy cm² respectively.

Image quality: Objective measurement
Figure 3a and b relate CNR values to DAP values for the ProMax® 3D and Accuitomo F170® respectively. This approximates to a second-order polynomial relationship. Figure 3b demonstrates that high resolution settings achieve comparatively lower CNR values than the standard and 180° scans for the Accuitomo F170®
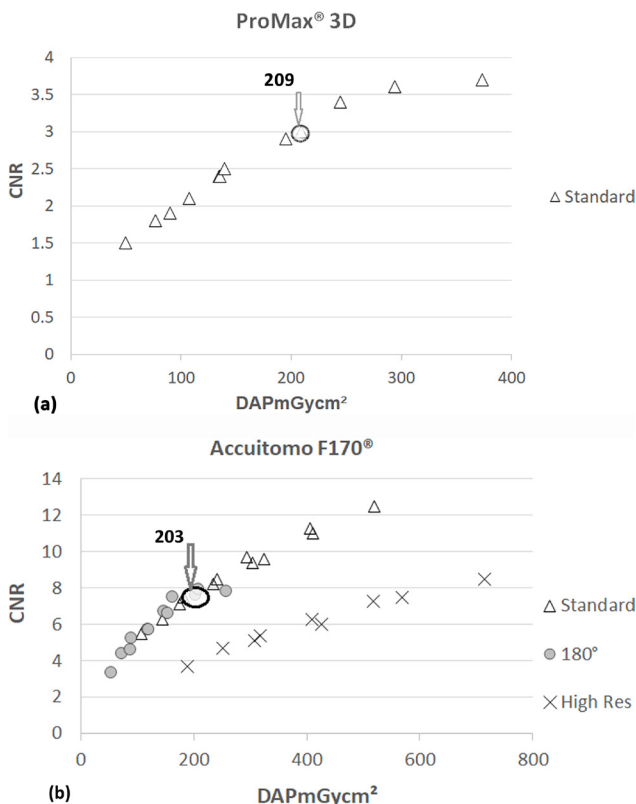

Figure 3 CNR values plotted against DAP values for (a) ProMax® 3D and (b) Accuitomo F170®. Additionally, the DAP values corresponding to the CNR value necessary to achieve the combined subjective image tasks for root canal identification are highlighted. CNR, contrast-to-noise ratio; DAP, dose–area product.

at equivalent DAP. CNR values are notably lower for the Promax® 3D compared with the Accuitomo F170® at equivalent kV and mA protocols (Figure 3a and b).

Image quality: subjective measurement
κ values for intraobserver agreement are detailed in Table 3. Junior hospital dentists demonstrated fair–moderate strength of agreement ($\kappa = 0.31$–0.56), while senior hospital dentists (radiologists and endodontists) exhibited good–very good strength of agreement ($\kappa = 0.65$–1) for questions relating to identification of root canal anatomy and continuity of the canal (Q1–5) as well as the diagnostic acceptability of the data sets (Q6). Interobserver agreement for questions relating to root canal anatomy identification (Q2–5) and diagnostic acceptability (Q6) ranged from moderate to good ($\kappa = 0.45$–0.58). Levels of agreement were only fair for Q1: identification of the MB2 canal at the level of the pulp chamber floor ($\kappa = 0.27$).

The proportion of data sets judged as being of acceptable/unacceptable image quality (Q6) by the radiologist and endodontists were similar, being 84%/16% and 81%/19% respectively, but differed from the judgments of junior hospital dentists; 67%/33%. Using the χ^2 test, a significant difference was identified ($p = 0.043$) with junior staff classifying significantly more images as undiagnostic compared with senior staff.

Tables 2a and 2b shows the results of the subjective image quality assessments for ProMax® 3D and Accuitomo F170® respectively at each exposure protocol and corresponding DAP value. Four scans taken using the ProMax® 3D and four using Accuitomo F170® were categorised as undiagnostic and excluded from further analysis.

On analysing the percentage of MB2 root canal anatomy identified by each observer for the 37 diagnostic data sets, for simple-moderately complex anatomy, senior staff consistently identified a marginally increased percentage (0–7.2%) of MB2 root canal anatomy than junior staff; the difference was not evident at the highest DAP values for both scanners (Supplementary Table 1). This trend between junior and senior staff was repeated for complex anatomy, but with

Table 3 Intraobserver agreement of the nine observers (END = Endodontist, RAD = Radiologist, JHD = Junior hospital dentist) for Q's 1–5 (root canal anatomy identification and continuity) and Q6 (diagnostic acceptability), measured using κ.

Observer code	END1	END2	END3	RAD1	RAD2	RAD3	JHD1	JHD2	JHD3
κ Values: Q's 1–5	0.65	0.69	0.71	0.67	0.73	0.69	0.50	0.51	0.56
κ Values: Q6	0.73	1	0.76	1	1	0.76	0.31	0.55	0.53

END, Endodontist; JHD, Junior hospital dentis; RAD, Radiologist.

margin of difference increasing (1.9–18.1%); however, for complex anatomy, increasing the DAP values did not reduce the differences between junior and senior staff in the percentage of canal identified. Agreement within both groups was greatly reduced for complex anatomy, as reflected by their greatly increased standard deviation values.

Repeatability assessment of the recording of the percentage of canal identified using the 5 repeat volumes (15 teeth) demonstrated that while 10 teeth showed no

difference from the original recording, 5 teeth exhibited a small variation ranging from 1 to 1.7%.

CNR values necessary to achieve diagnostic task of root canal identification
Figure 4a and b highlights that the percentage of MB2 canal anatomy identified increased along with CNR values. The target subjective image task of identifying ≥95% of the MB2 canal anatomy corresponded to a CNR of 3 for simple to moderate anatomy (T6, T7) for the ProMax® 3D and a markedly different CNR of 7.6 for the Accuitomo F170® scanner. The target subjective image task was not achieved at any DAP value for complex anatomy (T8).

The second subjective task of achieving median CSR's ≥ 3.5 for Q's 1–4 and Q5 were related to CNR for both scanners and are depicted in Figure 5a–d. With the ProMax® 3D scanner; for simple-moderate anatomy, achieving median CSR responses of ≥3.5 occurred at a CNR of 3 for both identifying the MB2 canal in all thirds of root canal anatomy (Q's 1–4) and for identifying it as continuous from perceived origin to termination (Q5) and at 3.6 and 3.7 respectively for complex anatomy (Figure 5a and b). For the Accuitomo F170® scanner, median CSR responses of ≥3.5 for both tasks Q1-4 and Q5 for simple-moderate anatomy corresponded to a CNR value of 7.5 and 7.3 respectively and at 8.5 and 11.3 values for complex anatomy (Figure 5c and d).
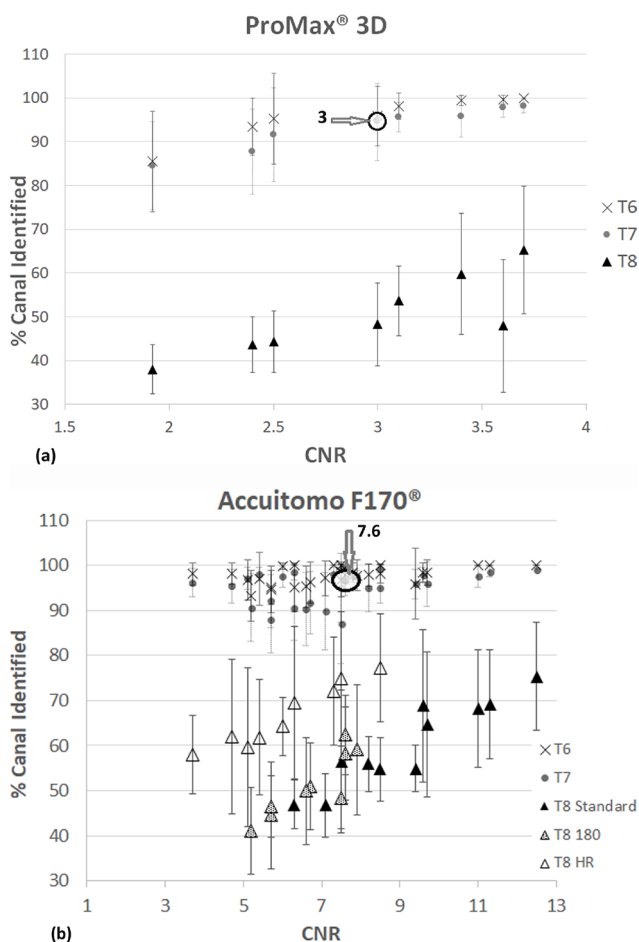
Identifying DAP and exposure protocols that correspond to threshold CNR values
As shown in Figure 3a and b, the DAP values necessary to achieve the combined subjective image tasks for simple-moderate MB root canal complexity (T6, T7), were 209.3 and 203.2 mGy cm² for Promax® 3D and Accuitomo F170® scanners respectively. For complex anatomy (T8), this subjective image task was not achieved, even at the highest DAP values for both scanners.

For maxillary first molars exhibiting simple-moderate root canal complexity, Table 2a, b summarise the exposure protocols and resultant DAP values that were considered undiagnostic, diagnostic and those which were at or above the "threshold dose" to achieve the combined "target subjective image quality tasks." For the ProMax® 3D the threshold dose (≥209.3 mGy cm²), included 90 kV protocols of 5 mA and above and one 80 kV/ 9 mA protocol (Table 2a). For the Accuitomo F170®, the threshold dose (≥203.2 mGy cm²) was achieved for

Figure 4 Mean percentage of MB2 canal anatomy identified by all observers related to CNR values, calculated for each exposure protocol judged as diagnostically acceptable for (a) ProMax® 3D and (b) Accuitomo F170®. Regarding simple-moderate anatomy, a CNR of ≥3 and ≥7.6 were necessary to achieve the subjective task (*i.e.* identifying ≥95% MB2 canal anatomy) for the ProMax® 3D and Accuitomo F170® respectively. CNR, contrast-to-noise ratio; MB2, second mesiobuccal.
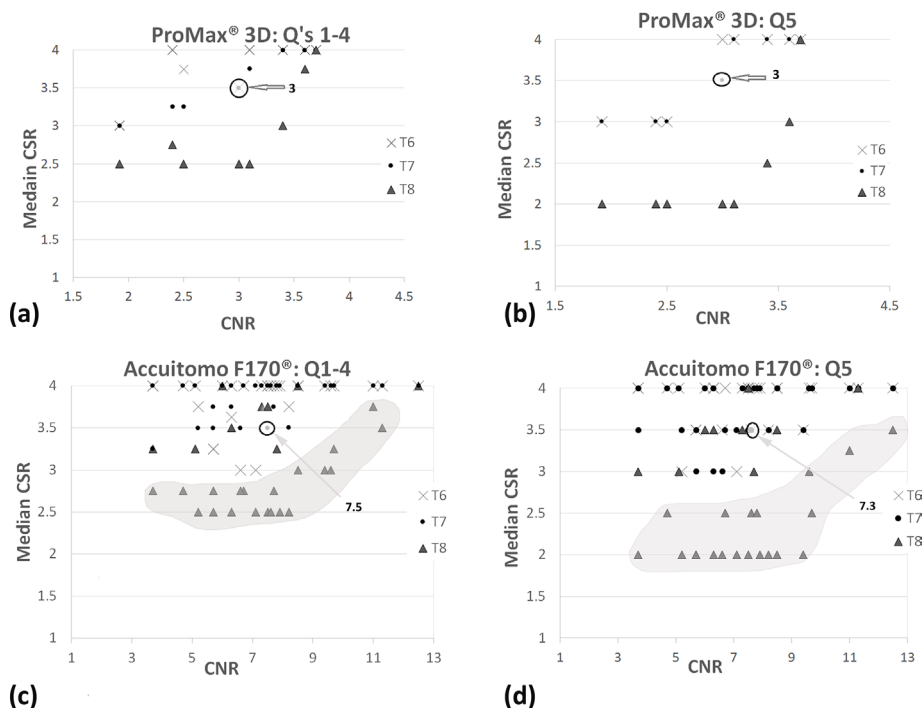
Figure 5 Median of the observer CSRs related to CNR for Qs 1–4 (a) and Q5 (b) for ProMax® 3D and Q1-4 (c) and Q5 (d) for Accuitomo F170®. Regarding simple-moderate anatomy, achievement of the second subjective task (median CSRs of ≥3.5) was possible at a CNR of 3 for the ProMax® 3D for both Qs 1–4 and Q5 and 7.5 and 7.3 respectively for the Accuitomo F170®. Shaded areas outlined in (c, d) highlight the trend of markedly lower median CSRs scored with complex anatomy compared to simple-moderate anatomy. CNR, contrast-to-noise ratio; CSR, confidence scale rating.

a range of protocols (Table 2b). Only three 180° scan protocol at the higher range of the kV and mA protocols were identified as achieving these combined "target subjective image quality tasks." Conversely, all high resolution Accuitomo F170® scans reached this level of subjective image quality, except at the lowest kV and mA experimental selection. These tables do not include complex anatomy (T8) as the combined subjective task was not achieved at any experimental DAP value.

Discussion

This purpose of this study was to ascertain whether a threshold level of image quality, and hence an optimised dose level, could be established for the accurate identification of root canal anatomy using CBCT imaging, a diagnostic task which is believed to necessitate high image detail and an associated increase in patient dose compared with less demanding diagnostic tasks.[30,31] By measuring DAP values at a range of exposure protocols and carrying out parallel subjective and objective image quality assessments, it was anticipated that the impact of varying exposure settings could lead to the identification of a threshold dose and CNR value as well as identification of a practical strategy for the reduction and optimisation of radiographic exposures within endodontics. Furthermore, by carrying out the investigations using two commercial CBCT scanners, an analysis

of whether the threshold level of objective image quality for this specific diagnostic task could be transferred to a different scanner was carried out. Protocols achieving significant dose reductions for specific dental diagnostic tasks have been established,[11–15] involving dose measurement, objective and subjective assessment, but not in an endodontic context and none of these has investigated the transferability of objective image quality measurements between scanners. Additionally, this study also examined the impact of anatomy complexity on establishing a threshold dose for this diagnostic task and the effect of operator experience on diagnostic efficacy. One previous study has investigated the relationship between objective and subjective image quality and the potential for transferability of findings between different CBCT scanners, recording observer findings of various anatomical features in a human skull phantom. These included "pulp canal" assessments, but were in the form of a general overview of all teeth in a skull phantom rather than a detailed endodontic assessment. They did not find evidence that minimally acceptable image quality values were applicable to multiple CBCT models, but did not specifically consider the root canal visualisation, focusing on implant planning, root pathology and sinus pathology.

CBCT imaging of root canal systems prior to endodontic management is indicated in cases in which anatomically challenging morphology is predicted and

for which a combination of conventional radiography and potential clinical investigation with a dental operating microscope cannot indicate the orifice, portals of exit or extent/continuity of the canal.[5] Identification and negotiation of more complex anatomy is important, as failure to locate anatomy reduces chemomechanical debridement and results in excessive dentine removal, which can lead to potential clinical complications including root fracture and perforation,[32] as well as an increased risk of root canal treatment failure and possible tooth loss.[33] The mesiobuccal root of a maxillary first molar is recognised as having the most predictably complex root canal anatomy in adult teeth[17,18] and therefore was used within the current study as a "model" to investigate the effect of reducing dose on the diagnostic task of root canal identification in teeth with a range of root complexities.

The need for dose reduction strategies within the discipline of endodontics and specifically canal anatomy identification is particularly pertinent. While it is difficult to currently ascertain the incidence of CBCT use for this indication, it appears that routine endodontic preoperative CBCT scans of teeth are being suggested for a more accurate assessment of root canal anatomy[34] which is not in keeping with current guidelines on dental CBCT imaging.[3]

This diagnostic task-based study ultimately relied on subjective analysis of the CBCT images. In order to reproduce the clinical situation as accurately as possible, the skull and cervical spine set up was used to replicate the normal attenuation and scatter by a human head.[27] However, like other optimisation studies in the literature,[11–15] it does not replicate the impact of patient movement on image quality, which can be particularly pertinent for high resolution settings with extended scan times.[35] Similarly, in this study the first molar and adjacent teeth had not been restored with metal restorations and were not previously root canal treated, which can both produce artefacts throughout the FOV that can negatively impact on image quality and thus on canal visualisation.[36,37]

Assessing the impact of differing exposure protocols on root canal anatomy identification necessitated selection of maxillary first molars with differing root canal anatomies, reflecting a spectrum of both complexity and difficulty with respect to diagnosis and treatment. To exclude the impact of MB2 canal width, it was ensured that all MB2 canals exceeded 100 μm at their narrowest point, this figure was extrapolated from the literature on CBCT detection of vertical fractures,[38,39] which has shown that defects above a minimum width of ≥100 μm could be predictably appreciated and diagnosed with CBCT imaging.

Anatomical variations in the MB root canal system vary in both incidence and complexity,[20,22] with recognised variations considered in this study encompassing additional, accessory and connecting canals, anastomoses and canal divisions. The three selected molars in this study all displayed a MB2 canal, but with variations in origin, length, anastomoses, divisions and as a result, complexity of the MB2 canal. T6 was classed as having simple anatomy as this canal variation (Type II Vertucci) is the most common in the MB root.[40] T7 was classed as representing a simple-moderate complexity, being Type II Vertucci, with an incidence of 25–45%,[22,41] but with an added anastomosis between MB1 and MB2, which is reported to occur in 2.9% of cases.[22] Although these anastomoses cannot be instrumented, their visualisation is relevant to alert the clinician regarding potential reservoirs of bacteria and need for enhanced irrigation. T8, possessing several variations and classified as complex (a variation of Type VIII Vertucci), has a reported incidence of 1.3% and 0.2–12%.[42,43] Obviously the selected sample of MB2 root anatomical configurations is not exhaustive; however, in combination with two CBCT scanners and range of exposure protocols it was not considered feasible to include a greater selection of teeth, not least because of observer time commitment requirements.

No validated tool for subjective assessment of root canal identification at a range of exposure protocols exists; the development of the 7-part questionnaire and subsequent assessment of the results took into account methodology from other previously published studies reporting on the measurement of image quality in diagnostic radiology.[12,14,44] This design approach was used in conjunction with a discussion amongst the researchers and the pilot study results. Use of a 5-point rating scale for observer assessments is a validated tool for assessing image quality in diagnostic radiology. This scale permits the observers to have a wider scope in which to record their answer, rather than being limited only to a positive/negative response, an approach utilised/validated in other subjective image quality studies.[12,29] This facilitates assessment of the degree of certainty and uncertainty and the option of being unsure to be reflected in elements of the analysis (median CSR responses). Additionally, dichotomisation of the data was necessary for other aspects (identification of diagnostic/undiagnostic data) with 0, 1, 2 responses being classified as a negative response and 3, 4 as a positive response. Unsure (=2) was noted as a negative response leaving just two positive options (=3, 4) ensuring that a positive response was documented only when the observer recorded as such.

Nine observers (three radiologists, three endodontists and three junior hospital dentists) were enlisted to perform subjective image quality assessments under standardised conditions in order to reflect the varying experience and skill set of a range of operators, who would realistically be carrying out this diagnostic task in primary/tertiary clinical/referral practice. Although, the number of observers was in keeping with other image quality assessment studies, there is no clear guidance on how many observers are needed in imaging studies.[45] Larger numbers of observers would reduce the impact

of subjectivity; however, recruiting greater number of observers was not possible.

Identifying a "target subjective image task" involved analysing the endodontists opinion of the volume of root canal identification necessary to fulfil the diagnostic task, balanced with clinical relevance. A consensus of opinion between the three endodontists established that the position of the MB2 orifice relative to the floor of the pulp chamber was particularly important, as this would dictate the volume of dentine required to be removed prior to potential canal location. Additionally, whether the canal was readily visible in the coronal third of the root was also clinically relevant, as it would be unlikely that the operator would search for a canal beyond the coronal third of the root, due to the potential complication of perforation and weakening of the root structure.[32] Percentage of root canal identified was assessed from tracing over the microCT "truth" and not from being asked to simply draw that part of the MB2 canal that they could definitively identify. It is of course possible that the availability of the "diagnostic truth" might have led to higher proportions of root canal length by observers than were genuinely seen by them, but the strategy was considered to be the only practicable way forward.

After analysis of the pilot study results and discussion with three "study" endodontists, a provisional figure of 95% of the MB2 canal identified was chosen as a "target subjective image task." It was observed from the pilot study data that that when the observers identified ≥95% canal anatomy, that the MB2 canal was also <u>always</u> successfully identifed at the level of the pulp floor and in the coronal third of the MB root, these two objectives being deemed by endodontists to be particularly clinically relevant to this diagnostic task. The target subjective image task of 95% was reassessed after analysis of the completed study results and it was identified that this same pattern was evident. Similarly, analysis of the pilot study results also elicited a further subjective image target of achieving median CSRs ≥ 3.5 (questionnaire scale 0–4), which reflected the observer's confidence in continuously identifying the canal in all thirds of the tooth and was established with 95% canal identification as the combined "target subjective image tasks."

Randomly selecting and randomly repeating 20% of data sets within the study sample was used as the method to assess intraobserver reliability, resulting in 54 of data sets (including duplicates). It could be argued that a means of reducing recall bias further would be to include a greater number of teeth but this would have increased the number of datasets and time required from observers to an impractical level. For the three junior hospital dentists, although statistically significantly lower than those of the specialists, intraobserver reliability was still classifiable as "moderate" for all questions except for one observer for the question (relating to overall image quality, not specific to root canal visualisation), which was only "fair." It might be argued that the lower intra observer reliability of the junior clinicians was not sufficient for a research study. Their inclusion was, however, considered worthwhile in being representative of the real world, in which use of CBCT is not limited to specialists.

Although pairwise comparison of observer results for questions relating to root canal identification and diagnostic acceptability (Q's 2–5 and 6) revealed moderate to good interobserver agreement, agreement was only 'fair' for identification of the MB2 canal at the level of the pulp chamber floor (Q1) . Differing perceptions as to whether this referred to a common orifice for MB and MB2 or a separate orifice for MB2 could potentially explain this as would observer perception of the pulpal floor.

Undiagnostic scans were removed prior to analysis, being identified as those scans which at least six out of the nine observers did not record as diagnostic (67%). This was keeping with majority based image quality acceptance that been utilised in optimisation studies.[12] The percentage of scans identified as undiagnostic by junior hospital dentists was significantly greater than that by the senior hospital staff ($p = 0.043$). This is likely to be due to the influence of experience and training that radiologists and endodontists possess with regard to diagnostic skills compared with recently qualified graduates. Notably, it has been suggested that the inexperienced operator is also more likely to request a CBCT scan,[46] highlighting less confidence with diagnostic skills in general and perhaps a familiarity and reliance on new technologies.

DAP was used to establish dose of each of the scanning protocols for both scanners; it is practically easy to achieve, relates relatively well to effective dose and has been recommended for establishing diagnostic reference levels (DRL's).[3] It is understood that DAP has the potential limitation of being over or underestimated[47]; nonetheless, DAP is still advocated and utilised for comparing dose between machines and assessing dose reduction strategies.[14,15,47]

A range of physical phantoms has been employed to facilitate dental CBCT objective image quality assessment.[48–50] The SedentexCT phantom was used in the current study, as it was designed specifically for dental CBCT and is successful in assessing basic image quality parameters.[51,52] The SedentexCT phantom is the size of an adult human head and is constructed from PMMA on the basis that this material simulates the average attenuation of the soft tissues of the human head, taking into account that there are also high attenuation structures (*e.g.* mandibular cortical bone and tooth enamel) in addition to the low attenuating contribution of air cavities (sinuses and oral cavity); this is reported to result in detector photon fluences similar to the human head.[51,53] Therefore, the objective image parameters measured using the selected inserts can be related to the scanners' clinical performance.

CNR is an objective measure of technical image quality and an effective means of assessing performance and constancy of a CBCT device.[51] CNR can be easily interpreted and has been widely used to assess the impact of tube voltage and tube current-exposure time product on image quality and therefore is considered an appropriate tool in optimisation strategies.[12,54–56] CNR was assessed using a PTFE insert (this particular insert approximating bone density), with previous related clinical diagnostic studies confirming that the PTFE insert generated CNR values which had a significant relationship with bone tissue.[12,14] While other software exists for evaluation of physical parameters on IQ phantoms for dental CBCT, Image J was employed in this study as it is readily accessible and its effectiveness has been validated in several similar studies.[12,14,51,53]

The results demonstrated that CNR increased with increasing DAP and hence with tube voltage and tube current (Figure 3b). Differences in CNR have been identified as largely influenced by the noise element of the equation.[23, 58] Increasing mAs decreases the image noise by increasing signal at the detector but, since the beam penetration remains the same, contrast is unaffected. Higher kV values increase the detector signal due to the increased photon count and energy, resulting in a proportional fall in photoelectric effects and an increase in Compton scatter. In 2D radiography, reducing tube voltage within diagnostic range leads to an increased difference in attenuation between tissues of varying density and therefore increased image contrast, the opposite being the case when tube voltage is increased. In contrast, with CBCT imaging, the pure signal that reaches the detector does not solely determine contrast due to the additional information from the projectional data at many angles. Therefore, for CBCT imaging in this otherwise fixed scanning set up, contrast over the range of exposures exhibited relatively little variation (as could be identified from the pixel/grey value data) whereas noise varied with exposure protocol (as identified from the SD of grey values consistently decreasing with increased tube voltage and tube current) causing noise to be the major contributor to CNR.

When compared to standard protocols, 180° scans resulted in CNR values at the lower end of the range (Figure 3b), this being related to decreased basis images and a concomitant increase in noise. For each kV and mA protocol, high resolution setting selection delivered CNR values only marginally greater than 180° scans and markedly lower than standard protocols. Moreover, when considering equivalent DAP, CNR values of high resolution settings were distinctly lower than both standard and 180° protocols. This can be attributed to the fact at high resolution setting the pixel array changes from a 2×2 array (*i.e.* four for standard setting) to an individual pixel (*i.e.* one for high resolution setting), thereby reducing the signal by one quarter, increasing noise and resulting in a decreased CNR values. Additionally, the small FOV (4×4 cm) reduces photon

fluence further, allowing noise to dominate. Accuitomo F170® CNR values for standard protocols were considerably higher than for the equivalent protocols using the ProMax® 3D scanner. This may be related to the differing voxel size and/or differing technologies, *e.g* detector efficiency

The evaluation of clinical image quality by observers is unavoidably subjective, as can be seen from interobserver agreement levels, whereas physical parameters can largely be measured in a reliable and repeatable manner; however, there is no direct way of translating these physical parameters to clinical image quality. This study defined a combination of subjective image tasks for the diagnostic task of root canal identification and identified the objective image quality, in this case CNR, that achieved these tasks for two different scanners. Regarding the ProMax® 3D, achieving all components of the combined "target subjective image task" elicited identical CNR values (3) and similar CNR values for the Accuitomo F170® (7.3, 7.5, 7.6), this being for maxillary first molars exhibiting simple-moderate root canal complexity. This indicates that for the same scanner, these clinically relevant and necessary tasks to achieve root canal identification all demanded the same or similar CNR level, indicating that CNR is a relevant measure of objective image quality in the task of canal identification. For both CBCT models, on relating CNR to the subjective measurements of image quality, similar patterns of improved subjective image quality with increased CNR were evidenced in the scatter plots (Figures 4a, b and 5a–d), albeit the relationship between CSRs and CNR for the Accuitomo F170 was less clear cut/evident (Figure 5c–d). However, it has to be concluded that in this study the CNR values identified to achieve the diagnostic task were not the same, or even similar, for the two CBCT models and therefore indicates that a reference CNR value for this diagnostic task cannot be applied between CBCT models. This can likely be attributed to differing technologies such as tube filtration, detector efficiency, FOV, filtering or voxel size of both scanners. Relating CNR alone to subjective image quality has some limitations in that it does not account for spatial resolution and, as can be seen from Figure 4b, focusing on the complex anatomy, there is a pattern of lower CNR high resolution scans achieving similar levels of canal identification to CNR standard protocols, which perhaps may be attributable to enhanced spatial resolution of these high resolution protocols. Therefore, in agreement with other studies, the relationship between objective measurements of image quality (in this case CNR) and subjective image quality is complex, with it being difficult to definitively relate one to the other in order to devise optimisation strategies.[11,12,14,57,58]

For maxillary first molars exhibiting simple-moderate root canal complexity, the threshold DAP values necessary to achieve the combined subjective image tasks were similar for both scanners (209.3 and 203.2 mGy

cm² for Promax® 3D and Accuitomo F170® scanners respectively) and lower than the recently published National Diagnostic Reference Level (NDRL) for adult CBCT (based on maxillary molar preoperative implant assessment) in the UK of 265mGy cm²[59] and much lower than the Finnish NDRL (specifically for CBCT examination aimed at assessment of tooth's periapical region and root canal morphology) of 550 mGy.cm².[60] This study suggests that there is scope for optimisation of patient dose in CBCT used in endodontic practice. Nonetheless, it is recognised that these study data are not clinical data and exclude the impact of movement and restoration artefact and that clinical studies would still be required. Furthermore, Table 2b highlights that standard protocols, except at the lower mA settings, achieved the diagnostic task while avoiding large DAP values that can be associated with high resolution scans.

The tables do not include complex anatomy (T8), as the target of 95% canal identification was not achieved at any experimental DAP value. This study suggests that factors other than diameter of a structure can impact on its visibility on CBCT scans. Rotating the 3D reconstructions of the MB2 canals of the selected molars, identified T8 as exhibiting the most curved MB2 canal structure, resulting in the canal "weaving in and out" of a coronal and sagittal slices and altering position in axial slices. These features were complicated further by the presence of isthmuses and reduced observer ability to confidently identify its path. It could be concluded that in perceived complex cases, as judged from clinical perception or preoperative 2D radiography, increasing kV and mAs and resultant patient dose [maximum experimental DAP values achieving canal identification of 65% (ProMax® 3D) and 77% (Accuitomo F170®)] could not be justified on the basis that it seemed probable that there was no likelihood of potentially improving diagnostic or clinical outcome.

Conclusions

This study found that for the diagnostic task of root canal anatomy identification as "modelled" by the maxillary first molar MB2 canal, a representative threshold dose of just over 200mGy cm² was identified for the ProMax® 3D and Accuitomo F170®, lower than published NDRLs. While achieving the individual subjective image tasks for root canal identification required a consistent CNR value within each scanner, the markedly different CNR values identified for the two CBCT models suggest that it not possible to determine a single threshold level of objective image quality that could be universally applicable to other CBCT models. Experience and expertise was shown to have a significant impact on the diagnostic efficacy of observers in the diagnostic task of root canal identification. Ultimately all dose reduction strategies are scanner specific and in practice needs to be achieved with the advice of a medical physics expert. The results suggested that selection of standard protocols instead of high resolution scans is a practical means of reducing patient dose and that increasing dose to enhance visualisation of the most complex anatomy was ineffective. As with all *ex-vivo* optimisation studies, these findings must be interpreted with caution. The *ex vivo* design, with a limited number of teeth, without patient movement or the presence of restorations, along with the subjective criteria for image quality and the complex inter relationship between subjective and objective image quality, all mean that there are significant limitations. Clinical studies are still required, presenting considerable challenges to researchers in terms of testing different exposure protocols.

REFERENCES

1. AAE and AAOMR Joint Position Statement Use of cone beam computed tomography in Endodontics 2015 update. *Oral Surg Oral Med Oral Pathol Oral Radiol Endod* 2015; **120**: 508–12.
2. Harris D, Horner K, Gröndahl K, Jacobs R, Helmrot E, Benic GI, et al. E.A.O. guidelines for the use of diagnostic imaging in implant dentistry 2011. A consensus workshop organized by the European association for osseointegration at the medical University of Warsaw. *Clin Oral Implants Res* 2012;; **23**: 1243–53Res. doi: https://doi.org/10.1111/j.1600-0501.2012.02441.x
3. European Commission. *Radiation protection 172: Evidence based guidelines on cone beam CT for dental and maxillofacial radiology*. Luxembourg: Office for Official publications of the European Communities; 2012.
4. Faculty of General Dental Practice (UK)In: Horner K, Eaton ka, EDS. selection criteria for dental radiography. 3rd EDN. London, UK. *Faculty of General Dental Practice (UK) Royal College of Surgeons of Surgeons of England* 2018;.
5. European Society of Endodontology: Patel S, brown J, semper M, Abella F, Manocci f. European Society of Endodontology posi-

tion statement: use of cone beam computed tomography in Endodontics. *Int Endod J* 2019; **52**: 1675–8.
6. Jacobs R, Levring Jäghagen E, Levring Jäghagen E, Lindh C, Baksi G, Schulze D, et al. Basic training requirements for the use of dental CBCT by dentists: a position paper prepared by the European Academy of DentoMaxilloFacial radiology. *Dentomaxillofac Radiol* 2014; **43**: 20130291. doi: https://doi.org/10.1259/dmfr.20130291
7. Körner M, Weber CH, Wirth S, Pfeifer K-J, Reiser MF, Treitl M. Advances in digital radiography: physical principles and system overview. *Radiographics* 2007; **27**: 675–86. doi: https://doi.org/10.1148/rg.273065075
8. Oenning AC, Jacobs R. Pauwels R Stratis a, Hedesiu M, salmon B: cone-beam CT in paediatric dentistry: DIMITRA project position statement. *Pediatr Radiol* 2018; **48**: 308–16.
9. Health protection agency: guidance on the safe use of dental cone beam CT (computed tomography) equipment Chilton Report No.: : HPA-CRCE-010.. UK: Health Protection Agency;. 2010.
10. Yeung AWK, Jacobs R, Bornstein MM, Reinhilde J. Novel low-dose protocols using cone beam computed tomography in dental

medicine: a review focusing on indications, limitations, and future possibilities. *Clin Oral Investig* 2019; **23**: 2573–81. doi: https://doi.org/10.1007/s00784-019-02907-y

11. Oenning AC, Pauwels R, De Faria Vasconcelos K, De Faria Vasconcelos K, Tijskens E, De Grauwe A, et al. Halve the dose while maintaining image quality in paediatric cone beam CT. *Sci Rep* 2019; **9**: 5521. doi: https://doi.org/10.1038/s41598-019-41949-w

12. Hidalgo Rivas JA, Horner K, Thiruvenkatachari B, Davies J, Theodorakou C. Development of a low-dose protocol for cone beam CT examinations of the anterior maxilla in children. *Br J Radiol* 2015; **88**: 20150559. doi: https://doi.org/10.1259/bjr.20150559

13. EzEldeen M, Stratis A, Coucke W, Codari M, Politis C, Jacobs R. As low dose as sufficient quality: optimization of cone-beam computed tomographic scanning protocol for tooth autotransplantation planning and follow-up in children. *J Endod* 2017; **43**: 210–7. doi: https://doi.org/10.1016/j.joen.2016.10.022

14. Al-Okshi A, Theodorakou C, Lindh C. Dose optimization for assessment of periodontal structures in cone beam CT examinations. *Dentomaxillofac Radiol* 2017; **46**: 20160311. doi: https://doi.org/10.1259/dmfr.20160311

15. Alawaji Y, MacDonald DS, Giannelis G, Ford NL, Nl F. Optimization of cone beam computed tomography image quality in implant dentistry. *Clin Exp Dent Res* 2018; **4**; : 268–78Res**4**:. doi: https://doi.org/10.1002/cre2.141

16. Lofthag-Hansen S, Thilander-Klang A, Gröndahl K. Evaluation of subjective image quality in relation to diagnostic task for cone beam computed tomography with different fields of view. *Eur J Radiol* 2011; **80**: 483–8. doi: https://doi.org/10.1016/j.ejrad.2010.09.018

17. Chang S-W, Lee J-K, Lee Y, Kum K-Y. In-Depth morphological study of mesiobuccal root canal systems in maxillary first molars: review. *Restor Dent Endod* 2013; **38**: 2–10. doi: https://doi.org/10.5395/rde.2013.38.1.2

18. Wolcott J, Ishley D, Kennedy W, Johnson S, Minnich S, Meyers J. A 5 yr clinical investigation of second mesiobuccal canals in endodontically treated and retreated maxillary molars. *J Endod* 2005; **31**: 262–4. doi: https://doi.org/10.1097/01.don.0000140581.38492.8b

19. Weine FS, Healey HJ, Gerstein H, Evanson L. Canal configuration in the mesiobuccal root of the maxillary first molar and its endodontic significance. *Oral Surg Oral Med Oral Pathol* 1969; **28**: 419–25. doi: https://doi.org/10.1016/0030-4220(69)90237-0

20. Vertucci FJ. Root canal anatomy of the human permanent teeth. *Oral Surg Oral Med Oral Pathol* 1984; **58**: 589–99. doi: https://doi.org/10.1016/0030-4220(84)90085-9

21. Cleghorn BM, Christie WH, Dong CCS. Root and root canal morphology of the human permanent maxillary first molar: a literature review. *J Endod* 2006; **32**: 813–21. doi: https://doi.org/10.1016/j.joen.2006.04.014

22. Briseño-Marroquín B, Paqué F, Maier K, Willershausen B, Wolf TG. Root canal morphology and configuration of 179 maxillary first molars by means of Micro-computed tomography: an ex vivo study. *J Endod* 2015; **41**: 2008–13. doi: https://doi.org/10.1016/j.joen.2015.09.007

23. Pauwels R, Silkosessak O, Jacobs R, Bogaerts R, Bosmans H, Panmekiate S. A pragmatic approach to determine the optimal kVp in cone beam CT: balancing contrast-to-noise ratio and radiation dose. *Dentomaxillofac Radiol* 2014; **43**: 20140059. doi: https://doi.org/10.1259/dmfr.20140059

24. Jordan RE, Abrams L, Kraus BS. Kraus dental anatomy and occlusion. ST Louia Mosby year book. 1992;.

25. Ahmed HMA, Versiani MA, De-Deus G, Dummer PMH. A new system for classifying root and root canal morphology. *Int Endod J* 2017; **50**: 761–70. doi: https://doi.org/10.1111/iej.12685

26. AAE: American Association of Endodontics. Endodontic Case Difficulty Assessment Form and Guidelines. 2006. Available from: www.aae.org.

27. Shelley AM, Brunton P, Horner K. Subjective image quality assessment of cross sectional imaging methods for the symphyseal region of the mandible prior to dental implant placement. *J Dent* 2011; **39**: 764–70. doi: https://doi.org/10.1016/j.jdent.2011.08.008

28. Altman DG. Practical statistics for medical research. London, UK: Chapman and Hall/CRC Texts in statistical science. 1990;.

29. Gijbels F, Sanderink G, Bou Serhal C, Pauwels H, Jacobs R. Organ doses and subjective image quality of indirect digital panoramic radiography. *Dentomaxillofac Radiol* 2001; **30**: 308–13. doi: https://doi.org/10.1038/sj.dmfr.4600640

30. Bauman R, Scarfe W, Clark S, Morelli J, Scheetz J, Farman A. Ex vivo detection of mesiobuccal canals in maxillary molars using CBCT at four different isotropic voxel dimensions. *Int Endod J* 2011; **44**: 752–8. doi: https://doi.org/10.1111/j.1365-2591.2011.01882.x

31. Maloul A, Fialkov J, Whyne C. The impact of voxel size-based inaccuracies on the mechanical behavior of thin bone structures. *Ann Biomed Eng* 2011; **39**: 1092–100. doi: https://doi.org/10.1007/s10439-010-0215-z

32. Tsesis I, Fuss ZVI. Diagnosis and treatment of accidental root perforations. *Endodontic Topics* 2006; **13**: 95–107. doi: https://doi.org/10.1111/j.1601-1546.2006.00213.x

33. de Chevigny C, Dao TT, Basrani BR, Marquis V, Farzaneh M, Abitbol S, et al. Treatment outcome in endodontics: the Toronto study--phases 3 and 4: orthograde retreatment. *J Endod* 2008; **34**: 131–7. doi: https://doi.org/10.1016/j.joen.2007.11.003

34. Patel S, Patel R, Foschi F, Mannocci F. The impact of different diagnostic imaging modalities on the evaluation of root canal anatomy and endodontic residents' stress levels: a clinical study. *J Endod* 2019; **45**: 406–13. doi: https://doi.org/10.1016/j.joen.2018.12.001

35. Spin-Neto R, Wenzel A. Patient movement and motion artefacts in cone beam computed tomography of the dentomaxillofacial region: a systematic literature review. *Oral Surg Oral Med Oral Pathol Oral Radiol* 2016; **121**: 425–33. doi: https://doi.org/10.1016/j.oooo.2015.11.019

36. Bechara BB, Moore WS, McMahan CA, Noujeim M. Metal artefact reduction with cone beam CT: an in vitro study. *Dentomaxillofac Radiol* 2012a; **41**: 248–53. doi: https://doi.org/10.1259/dmfr/80899839

37. Bechara B, McMahan CA, Geha H, Noujeim M, Moore WS, Ca M. Evaluation of a cone beam CT artefact reduction algorithm. *Dentomaxillofac Radiol* 2012b; **41**: 422–8. doi: https://doi.org/10.1259/dmfr/43691321

38. Brady E, Mannocci F, Brown J, Wilson R, Patel S. A comparison of cone beam computed tomography and periapical radiography for the detection of vertical root fractures in nonendodontically treated teeth. *Int Endod J* 2014; **47**: 735–46. doi: https://doi.org/10.1111/iej.12209

39. Guo XL, Li G, Zheng JQ, Ma RH, Liu FC, Yuan FS, et al. Accuracy of detecting vertical root fractures in non-root filled teeth using cone beam computed tomography: effect of voxel size and fracture width. *Int Endod J* 2019; **52**: 887–98. doi: https://doi.org/10.1111/iej.13076

40. Martins JNR, Marques D, Silva EJNL, Caramês J, Versiani MA. Prevalence studies on root canal anatomy using cone-beam computed tomographic imaging: a systematic review. *J Endod* 2019; **45**: 372–86. doi: https://doi.org/10.1016/j.joen.2018.12.016

41. Guo J, Vahidnia A, Sedghizadeh P, Enciso R. Evaluation of root and canal morphology of maxillary permanent first molars in a North American population by cone-beam computed tomography. *J Endod* 2014; **40**: 635–9. doi: https://doi.org/10.1016/j.joen.2014.02.002

42. Sert S, Bayirli GS. Evaluation of the root canal configurations of the mandibular and maxillary permanent teeth by gender in the Turkish population. *J Endod* 2004; **30**: 391–8. doi: https://doi.org/10.1097/00004770-200406000-00004

43. Ahmad IA, Al-Jadaa A. Three root canals in the mesiobuccal root of maxillary molars: case reports and literature review. *J Endod* 2014; **40**: 2087–94. doi: https://doi.org/10.1016/j.joen.2014.07.034

44. Martin CJ, Sharp PF, Sutton DG. Measurement of image quality in diagnostic radiology. *Appl Radiat Isot* 1999; **50**: 21–38. doi: https://doi.org/10.1016/S0969-8043(98)00022-0

45. Obuchowski NA. How many observers are needed in clinical studies of medical imaging? *AJR Am J Roentgenol* 2004; **182**: 867–9. doi: https://doi.org/10.2214/ajr.182.4.1820867

46. Matzen LH, Wenzel A. Efficacy of CBCT for assessment of impacted mandibular third molars: a review - based on a hierarchical model of evidence. *Dentomaxillofac Radiol* 2015; **44**: 20140189. doi: https://doi.org/10.1259/dmfr.20140189

47. Lofthag-Hansen S. Cone beam computed tomography radiation dose and image quality assessments. *Swed Dent J Suppl* 2010; **209**: 4–55.

48. Loubele M, Maes F, Jacobs R, van Steenberghe D, White SC, Suetens P. Comparative study of image quality for MSCT and CBCT scanners for dentomaxillofacial radiology applications. *Radiat Prot Dosimetry* 2008; **129**(1-3): 222–6. doi: https://doi.org/10.1093/rpd/ncn154

49. Suomalainen A, Kiljunen T, Käser Y, Peltola J, Kortesniemi M. Dosimetry and image quality of four dental cone beam computed tomography scanners compared with multislice computed tomography scanners. *Dentomaxillofac Radiol* 2009; **38**: 367–78. doi: https://doi.org/10.1259/dmfr/15779208

50. Watanabe H, Honda E, Tetsumura A, Kurabayashi T. A comparative study for spatial resolution and subjective image characteristics of a multi-slice CT and a cone-beam CT for dental use. *Eur J Radiol* 2011; **77**: 397–402. doi: https://doi.org/10.1016/j.ejrad.2009.09.023

51. Pauwels R, Stamatakis H, Manousaridis G, Walker A, Michielsen K, Bosmans H, et al. Sedentexct project Consortium development and applicability of a quality control phantom for dental cone beam CT. *J Appl Clin Med Phys* 2011; **12**: 245–60.

52. Bamba J, Araki K, Endo A, Okano T. Image quality assessment of three cone beam CT machines using the SEDENTEXCT CT phantom. *Dentomaxillofac Radiol* 2013; **42**: 20120445. doi: https://doi.org/10.1259/dmfr.20120445

53. Pauwels R, Stamatakis H, Bosmans H, Bogaerts R, Jacobs R, Horner K, et al. SedentexCT project Consortium: quantification of metal artefacts on cone beam computed tomography images. *Clin Oral Implants Res* 2013; **A100**: 91–4.

54. Kalender WA, Deak P, Kellermeier M, van Straten M, Vollmar SV. Application- and patient size-dependent optimization of x-ray spectra for CT. *Med Phys* 2009; **36**: 993–1000. doi: https://doi.org/10.1118/1.3075901

55. Yu L, Liu X, Leng S, Kofler JM, Ramirez-Giraldo JC, Qu M, et al. Radiation dose reduction in computed tomography: techniques and future perspective. *Imaging Med* 2009; **1**: 65–84. doi: https://doi.org/10.2217/iim.09.5

56. Klintström E, Smedby O, Klintström B, Brismar TB, Moreno R. Trabecular bone histomorphometric measurements and contrast-to-noise ratio in CBCT. *Dentomaxillofac Radiol* 2014; **43**: 20140196. doi: https://doi.org/10.1259/dmfr.20140196

57. Pauwels R, Seynaeve L, Henriques JCG, de Oliveira-Santos C, Souza PC, Westphalen FH, Guimarães Heriques JC, Couto Souza P, et al. Optimization of dental CBCT exposures through mAs reduction. *Dentomaxillofac Radiol* 2015; **44**: 20150108. doi: https://doi.org/10.1259/dmfr.20150108

58. Bechara B, McMahan CA, Moore WS, Noujeim M, Geha H, Teixeira FB. Contrast-to-noise ratio difference in small field of view cone beam computed tomography machines. *J Oral Sci* 2012c; **54**: 227–32. doi: https://doi.org/10.2334/josnusd.54.227

59. Public Health England PHE-CRCE: dose to patients from dental radiographic X-ray imaging procedures in the UK -2017 review. 2019;.

60. STRÅLSÄKERHETSCENTRALEN, STUK. Reference levels for patient radiation exposure in cone-beam computed tomography examinations of adults' head region. *STUK, Decision 12/3020/* 2016;.